

**This dissertation has been  
microfilmed exactly as received**

**69-8022**

**MENG, Ching-I, 1940-  
POLAR AURORAL AND MAGNETIC SUBSTORMS:  
THEIR MORPHOLOGY AND RELATION TO THE  
RING CURRENT.**

**University of Alaska, Ph.D., 1968  
Physics, general**

**University Microfilms, Inc., Ann Arbor, Michigan**

**POLAR AURORAL AND MAGNETIC SUBSTORMS:  
THEIR MORPHOLOGY AND RELATION TO THE RING CURRENT**

**A  
DISSERTATION**

**Presented to the Faculty of the  
University of Alaska in Partial Fulfillment  
of the Requirements  
for the Degree of  
DOCTOR OF PHILOSOPHY**

**by**

**Ching-I Meng, B.S., M.S.**

**College, Alaska**

**May 1968**

POLAR AURORAL AND MAGNETIC SUBSTORMS:  
THEIR MORPHOLOGY AND RELATION TO THE RING CURRENT

APPROVED:

T. Neil Davis

Charles R. Wilson

Daniel W. Swift

Joseph H. Mearns  
Chairman

Roger Sheridan  
Department Head

APPROVED: C. R. Wilson DATE: 4/24/68

Dean of the College of Mathematics, Physical  
Sciences and Engineering

H. J. Davis  
Vice President for Research and Advanced Study

## FOREWORD

The candidate has participated in my various research activities, so that the majority of the analyses reported in this thesis was done jointly with me and has been published under joint authorship. The candidate has played an important role in carrying out the vast amount of analyses. The compilation and organization of these materials, as well as the concluding Chapter entitled "Conclusion and Discussion", were done entirely by the candidate.



Syun-ichi Akasofu

## ABSTRACT

- I. There are four topics in this work, 1) magnetic storms in low latitudes, 2) polar substorms, 3) the relation between polar substorms and the growth of the ring current and 4) the polar cap aurora during magnetic storm sudden commencement.
- II. The growth and decay of the geomagnetic storm of April 17-18, 1965 and Sept. 13, 1957 is studied by using world wide magnetic records. In particular, the asymmetric growth of the main phase decrease is studied in detail. For the storm of April 17-18, 1965 results from simultaneous satellite observations are also discussed.
- III. It is shown that the polar electrojet which causes polar magnetic substorms in high latitudes usually flows westward in all longitudes along a closed oval curve (the auroral oval). The strength of the polar electrojet is not uniform along the oval; some of the excess current flows across the polar cap; the remainder departs from the afternoon sector and crosses the midnight meridian to complete its circuit by joining the main westward flow in the morning sector. Since the auroral oval is poleward of the auroral zone in the evening sector, a typical auroral zone station, situated in a transition belt between the region of intense negative bays on the poleward side of

the auroral zone and the region of positive bays on the equatorward side, thus experiences a great variety of types of the disturbance field.

From the study of the polar substorm conjugacy, it is found that the magnitude of positive bays is mainly controlled by the ionization produced by solar radiation and not by the intense auroral particle bombardment which is the major phenomenon during negative bays. Also the pattern of the polar electrojet with respect to the dipole pole is different in the two polar caps. The electrojet appears further toward the pole in the winter polar cap than in the summer one.

IV. The study of magnetic disturbances in the evening sector, during polar substorm shows that the 'negative bay' in middle and low latitudes, which had been thought to be due to the westward return current of the SD current system, is caused by the growth of the asymmetric storm-time radiation belt (the ring current), simultaneously with the polar substorm. This suggests a very close relationship between the onset of the polar substorm and the development of the storm-time radiation belt.

V A study of all-sky camera data from polar cap stations reveals the occurrence of two kinds of auroras in the polar cap: sun-aligned arcs which appear during magnetically quiet times, and active auroras which seem to be a part of the poleward expansion of the auroral substorm. A similar dichotomy exists for auroras that occur near the dipole pole in association with magnetic storm sudden commencements or sudden impulses, where the presence or absence of a polar magnetic substorm at the auroral oval determines the kind of aurora that appears.

VI. Based on the morphology of polar substorms and the development of the ring current, models and mechanisms related to the energy transfer into the magnetosphere and the development of the polar substorm are discussed. The interchange instability of the ring current is a favorable mechanism for producing the polar substorm.

## ACKNOWLEDGEMENTS

I wish to express my sincere thanks to Dr. Syun-Ichi Akasofu to whom I am deeply indebted for helpful guidance, advice, assistance and strong encouragement in completing this manuscript. Many thanks must also go to Prof. Daniel W. Swift for reviewing the manuscript and many useful discussions during the preparation of the last chapter of this thesis.

Special thanks also go to Mr. Robert Porter and Mrs. Constance Burnett of the Data Processing Group of the Geophysical Institute.

Many thanks are due to Mrs. Helen Linde for typing this thesis, and Mrs. Carolyn Abney for improving my English.

My gratitude also goes to Mrs. Jean Lipscomb whose general help and typing must be acknowledged.

My thanks to Mr. Koji Kawasaki who assisted me in many small details of thesis writing.

My ultimate gratitude must go to my dear wife, Martha, and lovely daughter, Margaret, who suffered more than I.

This research was supported by the Atmospheric Sciences Section of the National Science Foundation through Grants GA-505, GA-953 and also through the Grant from the National Aeronautics and Space Administration, NSG 201-62.



# TABLE OF CONTENTS

	Page
ABSTRACT	iii
ACKNOWLEDGEMENTS	vi
TABLE OF CONTENTS	vii
LIST OF ILLUSTRATIONS	ix
LIST OF TABLES	xx
CHAPTER I INTRODUCTION	1
1. Historic Background of Geomagnetism	1
2. The Geometric and Physical Analyses of Magnetic Disturbances	3
3. Outline of Following Chapters	6
CHAPTER II MAGNETIC STORMS	9
1. Introduction	9
2. Individual Study of Two Storms	11
1) April 17-18, 1965 Storm	11
2) September 13, 1957 Storm	39
CHAPTER III HIGH LATITUDE POLAR SUBSTORM	47
1. Introduction	47
2. Polar Substorms	60
1) Polar magnetic disturbances (polar magnetic substorm) and its revised equivalent current	61
2) The polar magnetic substorm and the auroral substorm	78
3) Polar substorms inside the auroral zone	110
3. Conjugacy of the Polar Substorm	138
1) Introduction	138
2) Auroral zone conjugate pairs	143
3) Polar cap conjugate pairs	153
CHAPTER IV LOW LATITUDE NEGATIVE BAYS AND THE POLAR SUBSTORM	162
1. Introduction	162
2. Low Latitude Negative Bays	165
3. A World-wide Magnetic Disturbance During a Simple Intense Polar Substorm	180

## TABLE OF CONTENTS (Con't.)

	Page
CHAPTER V      AURORAL ACTIVITY OVER THE POLAR CAP ASSOCIATED WITH MAGNETIC DISTURBANCES	225
1. Daytime Auroras	225
2. Polar Cap Auroras	230
3. Auroral Activity Near the Dipole Pole and Storm Sudden Commencement	234
1) Sudden commencements followed by polar magnetic substorms	234
2) Sudden impulses followed by quiet periods	238
3) Unclassified example	240
CHAPTER VI      CONCLUSION AND DISCUSSION	245
1. The Important Morphological Features of Magnetic Storms and Polar Substorms	245
2. Energy Requirement for the Magnetic Storm and the Polar Substorm	250
3. Magnetic Storm and Polar Substorm Theories	252
4. The Relationship between the Polar Substorm and the Growth of the Ring Current	264
5. Eastward Current in the Afternoon Sector of the Auroral Zone	273
APPENDIX I	282
APPENDIX II	287
REFERENCES	291

## LIST OF FIGURES

Figure		Page
II-1	Idealized overhead electric current-system that could produce (A) Dst field, (B) DS part and (C) total field of the average disturbance field during the main phase of magnetic storms of moderate intensity.	10
II-2	Solar flare activity in April 1965.	18
II-3a	The variation of D(H) between 1200 UT, April 17, 2400 UT, April 18, at 38 stations between dipole latitude $\pm 45^\circ$ in four sectors.	19
II-3b	The variation of D(H) between 1200 UT, April 17, 2400 UT, April 18, at 38 stations between dipole latitude $\pm 45^\circ$ in four sectors.	20
II-4	The variation of D(H) at five stations distributed evenly in longitude approximately along the dp lat $25^\circ$ circle. Local midnight at each station is indicated by a triangle.	23
II-5a	The variation of D(H), between 1200 UT, April 17, and 1200 UT, April 18, at 19 middle latitude stations between $45^\circ\text{N}$ and $59^\circ\text{N}$ in Europe.	24
II-5b	The locations of stations used in Fig. II-5a and four auroral-zone stations (A, Leirvogur; B, Abisko; C, Sodankyla, and D, Dombas). The numbers corresponding to the stations are 1, Lovo; 2, Nurmijarvi; 3, Stonyhurst; 4, Valentia; 5, Rude Skov; 6, Hartland; 7, Witteveen; 8, Gottingen; 9, Dourbes; 10, Minsk; 11, Moscow; 12, Swider; 13, Chambon-La-Foret; 14, Pruhonice; 15, Furstenfeldbruck; 16, Sverdlovsk; 17, Wien-Kobenzl; 18, Hurbanovo; and 19, Logrono.	25
II-6a	The development of the main phase of the April 17-18, 1965 storm. Approximate iso-intensity contours of D(H) are drawn at each UT hour, between 0500 and 1000 UT, April 18, 1965.	27
II-6b	The development of the main phase of the April 17-18 1965 storm. Approximate iso-intensity contours of D(H) are drawn at each UT hour, between 0500 and 1000 UT, April 18, 1965.	28

Figure		Page
II-7	Top: The D-component records from Irkutsk and Tashkent; the solid lines show the D-component variation on the storm day and the dashed curves show the $S_q$ variation (April 16-17, 1965). Bottom: The iso-intensity contour of D(H) at 0800 UT on April 18, 1965. Irkutsk and Tashkent are marked.	32
II-8	The variation of D(H) between 1200 UT, April 17, and 1200 UT, April 18, at high latitude. The first column shows the five major stations along the northern auroral zones; the second column shows five other northern auroral zone stations; the third column shows three southern auroral zone stations, and the fourth column shows both northern and southern polar cap stations.	34
II-9	The combined high-latitude records (between dp lat $76.1^\circ\text{N}$ and $78.5^\circ\text{S}$ ) to examine global activity of the polar electrojet. This method was first used by Davis and Sugiura [1966].	35
II-10	Magnetic disturbances of H component between dp lat $20^\circ$ and $55^\circ$ and that of D (Declination) component between dp lat $45^\circ$ and $55^\circ$ in the American sector.	37
II-11	The magnetic storm of September 13, 1957 recorded at Koror.	40
II-12	The variation of D(H) at middle and low latitudes (between dp lat $\pm 50^\circ$ ) during the September 13, 1967 magnetic storm.	42
II-13a	The development of the main phase of the September 13, 1957, storm. Approximate iso-intensity contours of D(H) are drawn at each UT hour, between 01 and 12.	43
II-13b	The development of the main phase of the September 13, 1957, storm. Approximate iso-intensity contours of D(H) are drawn at each UT hour, between 01 and 12.	44
II-14	The variation of D(H) for Sept. 13, 1957 storm at five stations distributed evenly in longitude approximately along the dp lat $25^\circ$ circle. Local midnight at each station is indicated by a triangle. The AE index is also shown.	46
III-1	Idealized equivalent current systems for the DS field; view from above dp north pole; the direction of the sun is indicated (after Chapman (1935)).	49

Figure		Page
III-2	Idealized equivalent current systems for the $D=Dst + DS$ field; view from above dp north pole; the direction of the sun is indicated (after Chapman, 1935).	50
III-3	Mean hourly disturbance vectors and corresponding equivalent current system at 24 UT, 1 May 1933; view from above dp north pole; the direction of the sun is indicated (after Vestine, 1940).	52
III-4	Disturbance vectors and corresponding equivalent current system at 2115 UT, 30 April 1933; view from above dp, north pole; the direction of the sun is indicated (after Fukushima, 1953).	54
III-5	Earlier model current system (schematic) for polar magnetic substorm; view from above dp north pole; the direction of the sun is indicated.	56
III-6	Isoaurores in the northern hemisphere. (After Feldstein, Y.L., and E. K. Solomatina, 1961 [18].)	58
III-7	Average curve of auroral incidence versus geomagnetic latitude ( $60^{\circ}$ - $90^{\circ}$ ). (After Davis, T. N., 1962.)	59
III-8	Revised model current system (schematic) for polar magnetic substorm; view from above dp north pole; the direction of the sun is indicated.	62
III-9	Magnetic records (H) on 26 Sept. 1958 (UT) from ten Alaskan Stations, Cape Wellen (Siberia) and Macquarie (New Zealand). (After Wescott and Mather, 1965).	64
III-10	Location of the ten Alaskan magnetic stations and of Cape Wellen (Siberia), whose records are used in Fig. III-9, together with McIlwain's curves $L = 2.5, 3, 4, 5$ and $6$ , [after Wescott and Mather (1965)].	65
III-11	Locations of magnetic stations in the dp coordinate system, whose records are used in this section.	67
III-12	Simultaneous magnetic records from Murchison Bay, Kiruna and Tixie Bay between 1500 and 1900 UT on 30 April 1958; the local time at 1700 UT at each station is indicated.	68

Figure		Page
III-13	Simultaneous magnetic records from Murchinson Bay, Kiruna and Tixie Bay between 1200 and 1600 UT on 19 January 1958; the local time at 1400 UT at each station is indicated.	70
III-14	Simultaneous magnetic records from Murchison Bay, Kiruna, Lovo, Chambon-La-Forêt, Logrono and M'Bour between 1200 and 0600 UT on 17/18 April 1958. All the stations are located approximately in the same sector (see Fig.III-11), so that their local times do not differ much from UT.	71
III-15	Average disturbance vectors obtained by subtracting the quiet day hourly mean values from the all-day mean daily variation values, in the IGY winter months; view from above dp north pole (after Feldstein, 1963).	73
III-16	Simultaneous magnetic records between 1600 and 2100 UT on 16 Dec. 1957 from a number of stations in the northern hemisphere; view from above dp north pole; the direction of the sun at 1600, 1800 and 2100 UT is indicated, and also the local time at each station at 1800 UT; scale = 200 $\gamma$ .	74
III-17	Revised model current system for an intense polar magnetic substorm; view from above dp north pole; the direction of the sun is indicated at the maximum epoch.	77
III-18	Schematic diagram to illustrate the development of the auroral substorm (dp coordinates). The sun is toward the top of the figure.	79
III-19a	Successive all-sky camera photographs to illustrate the westward traveling surge recorded at Fort Yukon on 10 February 1958 (150°WMT). The direction to the north dp pole is upward.	84
III-19b	Successive all-sky camera photographs to illustrate the westward traveling surge recorded at Barrow on 10 February 1958 (150°WMT). The direction to the north dp pole is upward.	85
III-19c	Successive ground projections of the surge illustrated in Figures III-19a and 19b. The locations of the Barrow, Bettles and College all-sky camera stations are indicated by cross-marks.	86
III-19d	Magnetic records from College during the passage of the westward traveling surge illustrated in Figure III-19a-c.	87
III-19e	Magnetic records from Barrow during the passage of the westward traveling surge illustrated in Figure III-19a-c.	88

Figure		Page
III-20	Successive all-sky photographs from Pyramida on Dec. 13, 1957 (UT) illustrating a westward traveling surge seen in the afternoon sector (L.T. = U.T. + 1). The direction to the north dp pole is upward.	90
III-21	Schematic diagram to show the development of both the auroral and polar magnetic substorms, from (a) a quiet situation, (b) an early epoch of the expansive phase, (c) the maximum epoch of the substorm to (d) an early epoch of the recovery phase. The region where a negative bay is observed is indicated by the lined shade, and the region of a positive bay by the dotted shade.	91
III-22	Typical H-component variations at different longitudes along the dp latitude circles of 65° and 72°. For the first column (local time) and the second column (A,B,C...), see Figure 1a.	93
III-23	The College (H) magnetic record and Ft. Yukon all-sky camera photographs (in negative) in evening of February 17/18, 1958. The hours shown refer to 150°W.	97
III-24	Top: The most common types of magnetic variations at Barter Island, College and Anchorage in the evening sector. Bottom: The most common combinations of the types at three stations.	99
III-25	The locations of the four Alaskan north-chain stations, Barter Island, Ft. Yukon, College and Anchorage. The magnetic meridian which passed College is indicated.	100
III-26	Examples of the combination (A) in Figure III-24. The hours shown refer to UT.	101
III-27	Examples of the combination (B) in Figure III-24. The hours shown refer to UT.	103
III-28	Examples of the combination (B) in Figure III-24. The hours shown refer to UT.	104
III-29a	The all-sky camera photographs (in positive) taken from Ft. Yukon (Feb. 12, 1958, UT) during the event shown in the first example of Figure III-28. The hours shown refer to 150°W.	105
III-29b	The all-sky camera photographs (in negative) taken from Ft. Yukon (March 25, 1958 UT) during the event shown in the second example of Figure III-28.	106
III-30	Example of the combination (C) in Figure III-24.	107

Figure		Page
III-31	Proposed latitudinal variation of the field of the polar magnetic substorm in the evening sector.	108
III-32	Examples which do not seem to fit into the proposed profile.	109
III-33	The locations of the M and N 'spirals' and of the auroral oval.	112
III-34	The locations of three Canadian magnetic stations, Baker Lake, Churchill and Meanook.	113
III-35	The H-component magnetic records from Baker Lake for five successive moderately active days in 1964. The corresponding $K_p$ indices are shown at the bottom.	115
III-36	The example of an intense negative bay recorded at Baker Lake and the corresponding geomagnetic changes at Churchill and Meanook. An intense negative bay was in progress in the morning sector of the auroral oval (Reykjavik, Iceland) at the time of the events.	116
III-37	The example of an intense negative bay recorded at Baker Lake and the corresponding geomagnetic changes at Churchill and Meanook. An intense bay was in progress in the morning sector of the auroral oval (Reykjavik, Iceland) at the time of the events.	117
III-38	The example of an intense negative bay recorded at Baker Lake and the corresponding geomagnetic changes at Churchill and Meanook. An intense negative bay was in progress in the morning sector of the auroral oval (Reykjavik, Iceland) at the time of the events.	118
III-39	The Baker Lake all-sky photographs (in negative) and corresponding geomagnetic changes at Baker Lake and Churchill.	119
III-40	The simultaneous magnetic records from the N-S Alaskan Chain of magnetic stations (Wescott and Mather, 1965).	123
III-41	The location of the two magnetic stations, Mould Bay and College, whose data are used in this paper, together with the location of the auroral oval (obtained by Feldstein (1963)) at 0600 UT; the geomagnetic pole and the meridian passing through College are indicated.	125



Figure		Page
III-42	(a), (b), Examples of positive bay recorded at Mould Bay indicated by M and the corresponding geomagnetic changes at College indicated by C. (c), (d), (e) Examples of positive bay with negative indentation recorded at Mould Bay and the corresponding geomagnetic changes at College.	126
III-43	Examples of indented positive bays recorded at Mould Bay.	128
III-44a	Examples of the all-sky photographs of the expanding auroral bulge and associated magnetic records. Mould Bay, Canada, November 5, 1965. (Photographs in negative.)	130
III-44b	Examples of the all-sky photographs of the expanding auroral bulge and associated magnetic records. Scott Base, Antarctica, July 5, 1957. (Photographs in negative.)	131
III-44c	Examples of the all-sky photographs of the expanding auroral bulge and associated magnetic records. Mould Bay, Canada, December 1, 1965. (Photographs in negative.)	133
III-45	Poleward expansion of the aurora from the midnight sector of the auroral oval (photographs in negative). In this case the expansion reaches the south geomagnetic pole. The direction of the sun is marked by a dot next to the photographs.	136
III-46	Poleward expansion to the south geomagnetic pole of the aurorally active region at the dawn sector of the auroral oval, (photographs in negative). The direction of the sun is marked by a dot next to the photographs.	137
III-47	Magnetic records from the post midnight quadrant of the auroral zone for nine consecutive days. Times when the Vostok all-sky camera was operating are marked by a line below the magnetograms. The occurrence of sun-aligned arcs (S.A.) is marked by solid bars and triangles, and of substorm associated auroras (S.S.), by open bars.	139
III-47	(Continued)	140
III-48	Typical example of magnetic records (the horizontal component) from the near conjugate pair stations College and Macquarie.	144
III-49	Relative magnitude ratio (R) for the associated bays for the College-Macquarie pair: a) Northern Winter, January 1958 b) Northern Summer, June 1958.	146

Figure		Page
III-50	Exceptional case to show that the positive bay at College was larger than that at Macquarie (January 29, 1958).	147
III-51	Relative magnitude ratio (R) for associated bays for the Reykjavik-Syowa pair: a) Northern Winter, December 1959 b) Northern Summer, June 1959	149
III-52a	Simultaneous H component and riometer records from College; January 23, 1958.	151
III-52b	Simultaneous H component and riometer records from College; June 24, 1958.	152
III-53	Examples of non-associated bays from the Shepherd Bay-Scott Base pair (after Wescott and Mather, 1965).	154
III-54	The seasonal variation of the occurrence frequency of well-defined positive and negative bays at Mould Bay and Godhavn.	155
III-55	The simultaneous magnetic records of H component from a pair of high latitude conjugate stations (Murchison Bay and Mirny) in northern winter.	157
III-56	The simultaneous magnetic records of H component from a pair of high latitude conjugate stations (Murchison Bay and Mirny) in northern summer.	158
III-57	The schematical configuration of geomagnetic field lines in the magnetosphere for the northern summer.	160
IV-1	The simultaneous magnetic records from College (dp lat 64.7°N) and Honolulu (dp lat 21.0°N).	164
IV-2	Vector-diagrams of the mean horizontal disturbing force of geomagnetic bays observed at Honolulu. (After N. Fukushima and H. Ōno).	166
IV-3	The N-S chain stations in the Europe-Africa sector whose records are used in this paper.	167
IV-4a	The DR type: an example of geomagnetic changes in middle and low latitudes when the corresponding AP bay in the auroral zone is weak, (Dec. 26, 1958).	168
IV-4b	The DR type: an example of geomagnetic changes in middle and low latitudes when the corresponding AP bay in the auroral zone is weak, (Dec. 13, 1957).	171

Figure		Page
IV-5a	The DP type: an example of geomagnetic changes in middle and low latitudes when the corresponding AP bay in the auroral zone is intense, (Sept. 9, 1958).	172
IV-5b	The DP type: an example of geomagnetic changes in middle and low latitudes when the corresponding AP bay in the auroral zone is intense, (Mar. 19, 1958).	173
IV-6	The (DR $\sim$ DR) type: an example of geomagnetic changes when both the DR and DP fields grow strongly.	175
IV-7	The (DR $\sim$ DP) type: an example of geomagnetic changes when both the DR and DP fields grow strongly.	177
IV-8	The (DP + DR) type: an example of geomagnetic changes when the growth of the DP field appears to precede that of the DR field.	179
IV-9	Hourly values of AE index from Dec. 11 to Dec. 30, 1964.	182
IV-10	Variations of the magnetic field (both H and D components) between 1000 UT and 1700 UT, Dec. 16, 1964 at stations above +60° in the midnight and morning sector.	183
IV-11	Hourly AE index for Dec. 16, 1964.	187
IV-12	Magnetic disturbance recorded above +60° in the afternoon and noon sectors between 1000 UT and 1700 UT, Dec. 16, 1964.	188
IV-13	Magnetic disturbances recorded in the polar cap between 1000 UT and 1700 UT, Dec. 16, 1964.	190
IV-14	Locations of magnetic stations above +60° used in this analysis together with the location of auroral oval at 1400 UT.	191
IV-15	Magnetic disturbances recorded below +60° in the afternoon sector (at 1400 UT) between 1000 UT and 1700 UT, Dec. 16, 1964.	192
IV-16	Magnetic disturbances recorded below +60° in the noon and early afternoon sectors (at 1400 UT) between 1000 UT and 1700 UT, Dec. 16, 1964.	194
IV-17	Magnetic disturbances recorded below +60° in the morning sector (at 1400 UT) between 1000 UT and 1700 UT, Dec. 16, 1964.	195

Figure		Page
IV-18	Magnetic disturbances recorded below $+60^\circ$ in the mid-night sectors (at 1400 UT) between 1000 UT and 1700 UT, Dec. 16, 1964.	196
IV-19	The location of 73 stations used in the study of a simple polar substorm on the polar plot. The code number of these stations can be found in Table IV-1.	199
IV-20a to 20v	Polar plots of the magnetic disturbance vectors during a simple polar substorm of Dec. 16, 1964. The length of the disturbance vector is reduced five times for stations higher than $dp$ lat $70^\circ$ . The interval between each plot is 5 minutes, with the first one at 1200 UT and the last one at 1535 UT.	200
V-1	Example (in negative) of the midday auroras observed at Pyramida; the upper three photographs were taken at about the magnetic midday and the lower three at about the local midday.	226
V-2	The Dst curves for three days in Figure V-1.	228
V-3	The orientation of auroral arcs observed at Pyramida; MN, LN, LM refer to the magnetic noon, the local noon and midnight, respectively.	229
V-4	Examples (in negative) of the midday auroras; except the first one (Dec. 20, 1959), they are multiple.	231
V-5	Magnetic records from the post midnight quadrant of the auroral zone for nine consecutive days. Times when the Vostok all-sky camera was operating are marked by a line below the magnetograms. The occurrence of sun-aligned arcs (S.A.) is marked by solid bars and triangles, and of substorm associated auroras (S.S.), by open bars.	232
V-6	Sudden commencement magnetic storms accompanied by bright substorm type auroras (Group I). The times at which sun-aligned arcs appeared are marked by triangles, and the intervals during which substorm type auroras appeared are marked by black bars. Magnetic midnight at the auroral zone stations whose magnetograms were shown is indicated by an upward pointing arrow.	236
V-7	All-sky camera pictures (in negative) taken at Vostok following the ssc at about 1630 UT, July 11, 1959. Cinematic projection of the data indicates that the motion of the auroral forms was in the direction away from the sunward horizon. (The sunward direction is marked by a dot next to the photographs).	237

Figure		Page
V-8	Sudden commencements and sudden impulses accompanied by sun-aligned auroras (Group II). In this figure both triangles and black bars indicate times at which sun-aligned arcs appeared. The upward pointing arrow indicates magnetic midnight at the auroral zone station.	239
V-9	Sudden commencement immediately followed by a polar magnetic substorm, but not immediately accompanied by substorm type aurora. The black bar indicates an interval during which diffuse patches could be seen at Scott Base and Vostok in the Antarctic. The upward pointing arrow marks magnetic midnight at the auroral zone station.	241
VI-1a	A sketch of the Equatorial section of the earth's magnetosphere looking from above the North Pole. Streamlines of the solar wind are shown on the exterior, and the internal streamlines refer to the circulation which it is proposed is set up by viscous interaction between the solar wind and the surface of the magnetosphere. The internal streamlines are also equipotentials of an associated electric field which may be regarded as being due to accumulations of positive and negative charges as indicated at A and B.	255
b.	A sketch of the circulation at ionospheric levels in the North Polar Cap corresponding to the internal circulation in the magnetosphere shown in (a). (Axford, 1964).	
VI-2	The simultaneous H components at Honolulu and ATS-I Satellite.	261
VI-3	The maximum decrease of H along the $dp$ lat $25^\circ$ circle and the envelope of the negative change of H in the high latitude for April 17-18, 1965 magnetic storm.	266
VI-4	Changes of H component in the middle latitude for different sectors; together with the hourly AE index (Davis, Echols and Wong, 1968), for September 13, 1957 magnetic storm.	268
VI-5	The hourly value of H component at College from 1957 to 1965.	271
VI-6	A. Earlier model current system (schematic) for polar magnetic substorms. B. New model current systems (schematic) for polar magnetic substorms.	275

## LIST OF TABLES

	Page
Table II-1. Low Latitude Stations Used in April 17/18, 1965 Storm Study	13
Table II-2. Middle Latitude Stations Used in April 17/18, 1965 Storm Study	15
Table II-3. High Latitude Stations Used in April 17/18, 1965 Storm Study	16
Table III-1. Table of Auroral Activity	57
Table III-2. Stations Used in the Study of Conjugacy of the Polar Substorm	142
Table IV-1. Magnetic Observatories Used in the Study of a Simple Polar Substorm	184

## CHAPTER I

### INTRODUCTION

#### 1. Historical Background of Geomagnetism

The study of geomagnetism began around 1600 A.D., when Gilbert (1600) announced that the earth is a magnet. A few years later Galileo observed the sunspots and deduced from their motions that the sun rotates. The transient changes of the earth's magnetic field were discovered by Graham (1724) in 1722. Later Celsius (1740) and Graham reported that irregular magnetic disturbances were observed simultaneously at both Uppsala, Sweden and London, England while the aurora was also observed at the same time at Uppsala. De Mairan, in 1733, published the first book about the aurora in which the aurora was suggested to be a planetary phenomenon related to the sun. The first morphological connection between auroras and geomagnetism was made in 1770 by Wilcke (1777) who found that auroral rays lie along the magnetic lines of force.

In the nineteenth century, a very useful analytical method of mathematics was applied to the study of geomagnetism, and it was during this century that magnetic observatories were set up in several places. It became possible to make global synoptic studies of the magnetic regular as well as irregular changes. The study of sun-spot activity was also started. The periodicity of magnetic variations and the sun-spot cycle was found to be similar by Lamont in 1851 and by Sabine in 1852.

Based on auroral reports in the northern hemisphere, the American scientist Loomis (1860) drew the first map of the auroral zone. Thirteen years later, Fritz (1873) published the first map of isochasms, i.e.

lines of equal frequency of visibility of auroras. Before the twentieth century, it was already known that magnetic storms were world-wide phenomena and also that they began almost simultaneously all over the earth. Morphologically, it was also known that the initial phase, main phase decrease and recovery phase were typical features of a storm and that near and within the auroral zone the magnetic disturbance was exceptionally intense during magnetic storms.

Extensive research in magnetic storm and aurora began in the early part of the twentieth century. It was Birkeland (1911) who first attempted experimental and theoretical explanations of the aurora and magnetic storms. Stormer carried out the mathematical development of Birkeland's work and developed the well known Birkeland-Stormer solar corpuscular theory. In 1923, Chapman developed a theory of aurora and magnetic storms based on the idea of Lindemann (1919) that the solar stream may be electrically neutral. Later Chapman and Ferraro (1930, 1931, 1932) completed the so-called neutral solar-corpuscular theory. Another classical theory is the ultraviolet light theory which suggests that auroral phenomena and magnetic disturbances may be caused by charged corpuscles of terrestrial origin produced by the action of ultraviolet rays of the sun on the upper atmosphere. Stormer's work on the motion of solar-corpuscles, namely the motions of single charges in a dipole field, was not successful in explaining the aurora and the magnetic storm but has been successfully applied to cosmic ray trajectories. Chapman and Ferraro's study on the interaction of a dipole field and the solar plasma has recently been extended by a number of workers. It rather successfully explains the



formation of the magnetosphere, but auroral phenomena still can not be well explained.

## 2. The Geometric and Physical Analyses of Magnetic Disturbances

The morphological study of the average features of the disturbance field was first conducted by an Indian scientist Moos (1910) mainly by using the long series of Bombay, India magnetic data. Later Chapman (1918, 1927, 1935, 1952) studied the average features of moderate storms at many stations in different latitudes. The method is to separate the average storm field geometrically into a part Dst symmetrical about the earth's dipole axis, while the remaining part is denoted by DS. In this notation D denotes disturbance and st denotes storm time; in DS, S denotes solar. To this latter part Chapman first gave the name "disturbances daily variation" and the symbol SD which signified the variation superposed on the quiet-day daily variation Sq during magnetic storm, so that the whole daily variation S is  $Sq + SD$ . This choice was made because the part of the D variations and the field which is asymmetrical relative to the earth dipole axis was averaged over whole days. Later Chapman (1952) determined this part for several epochs in the storm, separated by intervals of one or a few hours only; thus SD is a field which varies with storm-time and has pattern which is found to be fairly constant as viewed from the sun; therefore, it is a function of dp (dipole) latitude, dp local time (relative to the dp meridian half-plane containing the sun) and storm time. This part of the field was then re-named the "disturbance local-time inequality", with the symbol DS. Thus, SD signifies the average of the DS field over a day. Therefore  $D = Dst + DS$ .

This geometrical analysis is equivalent to a Fourier analysis of the D field

$$D = C_0 + \sum_n C_n \sin(n\lambda + \epsilon_n)$$

where  $\lambda$  denotes dp longitude and  $\epsilon_n$  the phase angle. The first term is the d.c. component (namely, the Dst component) and the second term the harmonic a.c. components (namely, the DS component). By definition, the DS component has both positive and negative changes of the same magnitude. Clearly the DS variation is mainly diurnal, i.e.  $C_1 \gg C_2, C_3$ .

Akasofu and Chapman (1961) suggested another way of dividing the disturbance field according to the physical sources of disturbances.

There are at least five major sources and D can be described as

$$D = DCF + DR + DP + DT + DG.$$

The letters have the following significance: D for disturbance; CF for corpuscular flux; R for ring current; P for polar; T for tail; G for ground. The definitions of these fields are as follows:

#### 1) DCF Field:

The neutral ionized gas ejected from the (sun solar corpuscular flux) toward the earth interacts with the earth dipole field and forms the magnetosphere. At the front of the solar stream, i.e. at the surface of the magnetosphere, (magnetopause) the protons and electrons are deflected in opposite directions. Looking towards the earth from the sun, the protons move to the right and the electrons to the left. This produces eastward electric current flow in the region near the solar ecliptic plane. The magnetic field produced by this eastward current will increase the magnetic field inside the magnetosphere. It corresponds to the sudden commencement of the magnetic storm. If the stream flow continues for hours, the currents and their magnetic field will similarly persist and

also will change the size of the magnetosphere. Since this additional magnetic field depends essentially on the continuance of the corpuscular flux; it is denoted by DCF.

## 2) DR Field:

The existence of a ring current which corresponds to a decrease of the field during the main phase of the magnetic storm was suggested by Stormer (1911, 1912, 1955) and later developed by Chapman and Ferraro (1941), Singer (1957) and many other workers (cf. Akasofu 1966). This ring current located at a few earth radii away from the center of the earth, with protons and electrons flowing with different speeds, is westward. During a storm, this DR field grows and decays during the developing phase and recovery phase, respectively; it produces most of the Dst field.

## 3) DP Field:

During the magnetic storm, the auroral activities near the polar regions are extremely violent and frequent. Accompanying the auroral activity, intense magnetic disturbances are also observed near the auroral zone. This field is thought to be related to the so-called polar electrojet which is concentrated in the polar region, thus is called DP.

## 4) DT Field:

Based on satellite observations (Behannon and Ness, 1966) it has been found that the magnetic field in the magnetospheric tail increases during magnetic storms. The magnetic field change in the magnetospheric tail is due to the change of the tail current on the neutral sheet (Speiser and Ness, 1967). Thus, a small portion of the magnetic disturbance on the earth's surface can be attributed to the change of the tail current denoted by DT. The increase of the magnetospheric tail current is also associated with the equatorward shift of the auroral oval during the storm (cf. Akasofu 1966).

### 5) DG Field:

The above four disturbance fields all have their primary origin above the earth's surface, partially beyond and partly in the ionosphere. The changes of these primary external parts induce electric currents within the earth. The field due to these currents flowing in the ground is denoted by DG.

Only the first three of the above five fields, are considered to be important in the study of the morphology of magnetic disturbances. In actuality the effect of the induced ground current is very large, especially for DP, but due to our limited knowledge of the distribution of the induced current, in effect the conductivity of the earth, the influence of the induced ground current is either neglected or it is assumed that the ratio between the primary fields and that of their induced currents is taken to be constant.

### 3. Outline of Following Chapters

The above brief review serves as the introduction to our problem, namely the relationship between magnetic storms and auroral phenomenon. Even though geomagnetism has a long history, more than three hundred years, our understanding of magnetic storms, auroral phenomenon and other related geophysical phenomena is rather limited. This is due to the inaccessibility of the polar regions and the lack of simultaneous worldwide recording of these phenomena. In other words, basic morphological facts of these phenomena are not completely known. The International Geophysical Year (1957-1958) and International Geophysical Cooperation

(1958-1959) has produced a vast amount of data in which some has already been analyzed by a number of workers and has greatly improved our knowledge of various geophysical phenomena, for example the auroral oval. The purpose of this work is to present some morphological features of magnetic storms and polar substorms by using the IGY/C and post IGY/C world-wide magnetic and all-sky camera data filed in the Geophysical Institute Archives, University of Alaska. These morphological features and the Interpretation of the observations are based on some post-IGY concepts of geophysical phenomena; for example, the auroral substorm model, the auroral oval and the asymmetry of the storm time radiation belt.

Since the morphology of geophysical phenomena--the geographical distribution and characteristic sequence of time changes--cannot be obtained from studies of the records of one or a few observatories, the effort is concentrated in the study of simultaneous world-wide data. In other words, a world-wide study of single events is adopted rather than a statistical one.

There are three main topics in this study: magnetic storms, polar magnetic substorms and auroral substorms. The interrelations among these three topics are also studied. In Chapter II, a very brief review of early morphological studies is given first. This is then followed by an extensive study of two magnetic storms, April 17-18, 1965, and September 13, 1957, by using the above mentioned method. Polar substorms, including both magnetic and auroral substorms, particularly their equivalent current system, development and conjugacy, are discussed in Chapter IV. Based on Chapters II and III, the relationship between the polar substorm and the

simultaneous low latitude negative bays is discussed in Chapter IV.

Auroral activity near the dipole pole is not only related to the development of the auroral substorms but also to the onset of the magnetic storm.

This is discussed in Chapter V. Summary and conclusion of the present work will be found in Chapter VI.

## CHAPTER II

### MAGNETIC STORMS

#### 1. Introduction

Since the disturbance magnetic field can be conveniently indicated by diagrams of current systems flowing at a constant height above the earth which could produce the Dst and DS variations, Chapman (1935) first drew idealized current diagrams corresponding to the Dst, DS parts of the disturbance field as well as the total field. His idealized overhead equivalent current system is shown in Figure II-1. After the equivalent current system was introduced, many workers were confused about the equivalent and real current systems. Although the diagrams show current systems which could produce the disturbance field, these are not necessarily the currents that do produce the field. Without further consideration, the diagrams must be regarded as only a convenient geometric mode of indicating the distribution of the surface disturbance field. The true distribution of the external currents which produce the primary part of the disturbance field can only be inferred from additional physical data or inferences.

The most extensive study of the average properties of the storm time disturbance field was made by Sugiura and Chapman (1960). A sum of 346 storms with recognizable times of storm sudden commencement was studied by using 43 years of records from 19 observatories. In their analysis, the storms were divided into three groups according to their intensities--weak, moderate and great. Even in this most extensive study, they concluded "Though the material used in this work is extensive, the storm morphology

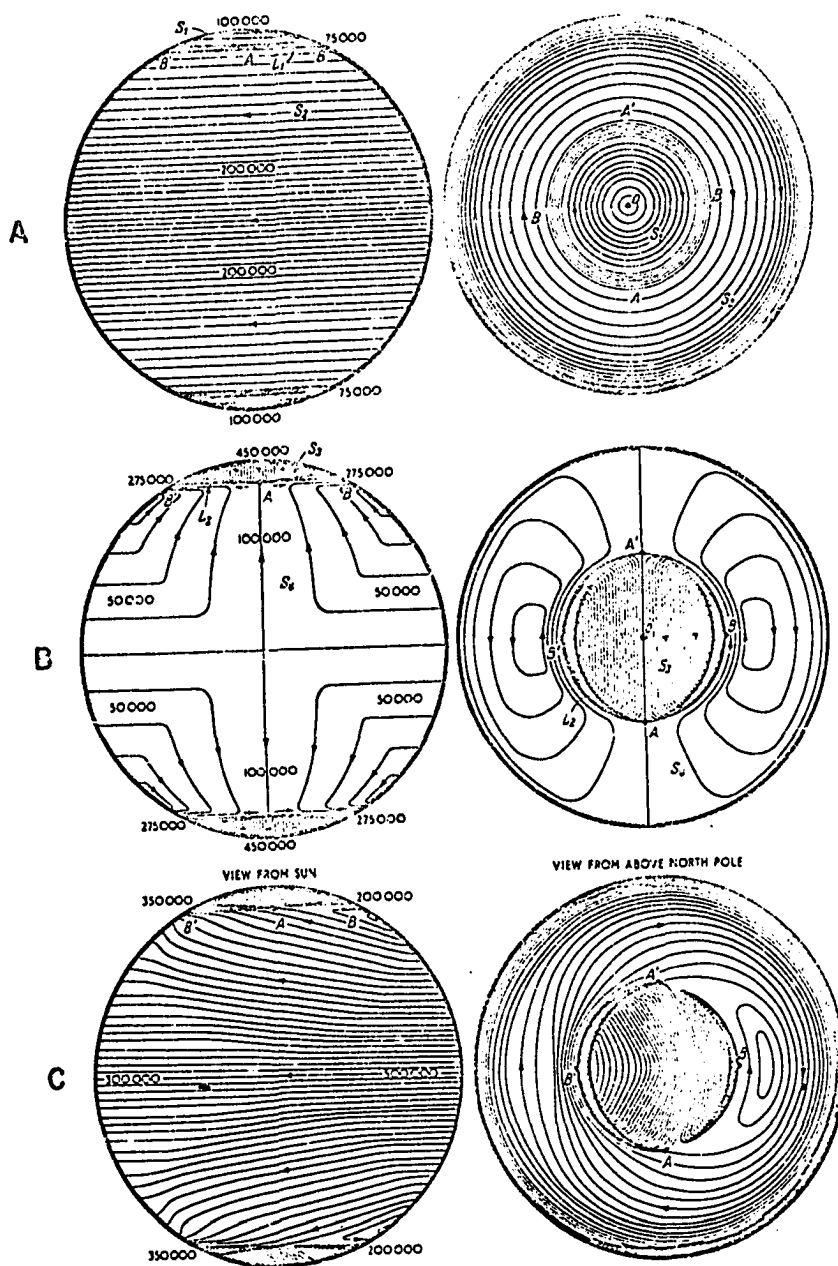


Fig: II-1. Idealized overhead electric current-system that could produce (A) Dst field, (B) DS part and (C) total field of the average disturbance field during the main phase of magnetic storms of moderate intensity.



derived from it for high latitudes is not enough to enable reliable current systems to be drawn for the polar regions". This shows the need for further studies of magnetic storms and polar substorms.

## 2. Individual Study of Two Storms

The studies of geomagnetic storms and of related phenomena have long relied on the concept of the average magnetic storm. It is believed that further progress in geomagnetism depends in part on a detailed analysis of individual storms on the basis of records collected from all over the world. This is because the development of storms varies considerably for individual cases and because any correlative studies of geomagnetic disturbance fields with quantities in related fields require precise knowledge of the characteristics of the storm fields. On the other hand, it has become evident that we need additional and much more accurate knowledge of geomagnetic activity in terms of the storm-field components, such as the field of the storm-time radiation belt (DR), the field caused by the compression or decompression of the magnetospheric boundary (DCF) and the field of the polar electrojet (DP).

During the past several years, Akasofu (cf. 1966) analyzed a number of individual magnetic storms and obtained the distribution of disturbance fields on an instantaneous basis. Indeed, it is this type of study which has definitely established that the storm-time radiation belt is asymmetric (Akasofu and Chapman 1964).

### 1) April 17-18, 1965 Storm:

The development of standard type magnetic storms can be described as follows. The onset of magnetic storms is characterized by a sudden increase in the horizontal component. After this storm

sudden commencement (ssc), the horizontal component remains above the initial undisturbed value and is called the initial phase which is followed by a main phase characterized by a large decrease in H. When H reaches the minimum value, there is a slow recovery toward its undisturbed value and is called the recovery phase. The most characteristic feature of magnetic storms is their main phase decrease. A large world-wide decrease of H in low and middle latitudes during geomagnetic storms has long been ascribed to a westward ring current (DR) encircling the earth. The direct detection of ring current particles by satellites was not successful until OGO-3 (Frank, 1967). The first conclusive evidence of the existence of the ring current was obtained during the observations of the April 17-18, 1965 storm by Explorer 26 (Cahill, 1966). During this storm, besides the direct ring current measurements, there were charged particle observations in the radiation belts and also a complete interplanetary solar wind measurement. Thus, a world-wide morphological study of this storm is useful for a better understanding of the storm and it is discussed in the following.

Magnetograms from a total of 88 stations were used. They were divided into three groups according to their latitude; low latitude stations of dp latitudes less than  $45^{\circ}$  (see table II-1), middle latitude stations of geomagnetic latitudes between  $45^{\circ}$  and  $59^{\circ}$  (see table II-2), auroral zone and polar cap stations of dp latitudes higher than  $59^{\circ}$  (see table II-3). They are classified into four sectors according to longitude; the Europe-Africa sector (between dp long  $45^{\circ}\text{E}$  and  $100^{\circ}\text{E}$ ), the Middle East-India sector (between dp long  $100^{\circ}\text{E}$  and  $165^{\circ}\text{E}$ ), the Pacific sector (between dp long  $165^{\circ}\text{E}$  and  $285^{\circ}\text{E}$ ), and the American sector (between dp long  $285^{\circ}\text{E}$

TABLE II-1. Low Latitude Stations Used in April 17/18, 1965 Storm Study

SECTOR	STATION	GEOMAGNETIC		GEOGRAPHIC	
		LATITUDE	LONGITUDE	LATITUDE	LONGITUDE
1	L'Aquila	42.9	92.9'	42 23N	13 19E
	San Fernando	41.0	71.3	36 28N	6 12W
	Gibilmanna	38.5	92.2	37 59N	14 01E
	Tamanrasset	25.4	79.6	22 48N	5 32E
	Ibadan	10.7	74.7	7 26N	3 54E
	Bangui	4.8	88.5	4 26N	18 34E
	Binza	-3.1	83.6	4 16S	15 22E
	Luanda	-7.2	80.6	8 55S	13 10E
	Hermanus	-33.3	80.5	34 25S	19 14E
2	Odessa	43.7	111.1	46 47N	30 53E
	Grocka	43.6	100.9	44 38N	20 46E
	Tashkent	32.3	144.0	41 20N	69 37E
	Tehran	29.4	126.5	35 44N	51 23E
	Quetta	21.6	139.7	30 11N	66 57E
	Alibag	9.5	143.6	18 38N	72 52E
	Addis Ababa	5.4	109.2	9 02N	38 46E
	Annamalainagar	1.5	149.4	11 24N	79 41E
	Kodaikanal	0.6	147.1	10 14N	77 28E
	Trivandrum	-1.1	146.4	8 29N	76 57E
	Nairobi	-4.4	105.3	1 19S	36 49E

TABLE II-1. Low Latitude Stations Used in April 17/18, 1965 Storm Study

SECTOR	STATION	GEOMAGNETIC		GEOGRAPHIC	
		LATITUDE	LONGITUDE	LATITUDE	LONGITUDE
3	Irkutsk	40.7	174.8	52 10N	104 27E
	Kakioka	26.0	206.0	36 14N	140 11E
	Simosato	23.0	202.4	33 34N	135 56E
	Honolulu	21.1	266.5	21 19N	158 00W
	Guam	4.0	212.9	13 35N	144 52E
	Banguio	5.1	189.2	16 25N	120 36E
	Muntinlupa	3.0	189.7	14 22N	121 01E
	Apia	-16.1	260.2	13 48S	171 47W
	Kuyper	-17.5	175.6	6 02S	106 44E
	Port Moresby	-18.6	217.9	9 24S	147 09E
	Gnangara	-43.2	185.8	31 47S	115 57E
4	Dallas	43.0	327.7	32 59N	96 45W
	Tucson	40.4	312.2	32 15N	110 50W
	San Juan	29.6	3.1	18 07N	66 09W
	Paramaribo	17.0	14.3	5 49N	55 13W
	Fuquene	16.9	355.1	5 28N	73 44W
	Huancayo	-0.6	353.8	12 03S	75 20W
	La Quiaca	-10.6	3.2	20 06S	65 36W
	Pilar	-20.2	4.6	31 40S	63 53W
	Trelew	-31.8	3.2	43 15S	65 19W

TABLE II-2. Middle Latitude Stations Used in April 17/18, 1965 Storm Study

SECTOR	STATION	GEOMAGNETIC		GEOGRAPHIC	
		LATITUDE	LONGITUDE	LATITUDE	LONGITUDE
1	Lovo	58.1	105.8	59 21N	17 50E
	Nurmijarvi	57.9	112.6	60 31N	24 39E
	Stonyhurst	56.9	82.7	53 51N	2 28W
	Valentia	56.6	73.5	51 56N	10 15W
	Rude Skov	55.9	98.5	55 51N	12 27E
	Hartland	54.6	79.0	51 00N	4 29W
	Witteveen	54.1	91.2	52 49N	6 40E
	Gottingen	52.3	93.7	51 32N	9 58E
	Dourbes	52.0	87.7	50 06N	4 36E
	Minsk	51.5	110.4	54 06N	26 31E
	Moscow	50.9	120.5	55 29N	37 19E
	Swider	50.6	104.6	52 07N	21 15E
	Chambon-La-Foret	50.5	84.4	48 01N	2 16E
	Pruhonice	49.9	97.3	49 59N	14 33E
	Furstenfeldbruck	48.8	93.3	48 10N	11 17E
	Sverdlovsk	48.5	140.7	56 44N	61 04E
	Wein-Kobenzl	47.9	98.2	48 16N	16 19E
	Hurbanovo	47.2	99.8	47 52N	18 11E
	Logrono	46.1	77.2	42 27N	2 30W
2	Yakutsk	51.0	193.8	62 01N	129 43E
	Toolangi	-46.7	220.8	37 32S	145 28E
	Amberley	-47.7	252.5	43 09S	172 43E
3	Agincourt	55.1	347.0	43 47N	79 16W
	Victoria	54.2	293.0	48 31N	123 25W
	Fredericksburg	49.6	349.8	38 12N	77 22W
	Boulder	49.0	316.5	40 08N	105 14W

TABLE II-3. High Latitude Stations Used in April 17/18, 1965 Storm Study

STATION	GEOMAGNETIC		GEOGRAPHIC	
	LATITUDE	LONGITUDE	LATITUDE	LONGITUDE
Thule	89.0	358.0	77 29N	69 10W
Alert	85.9	168.2	82 30N	62 30W
Resolute Bay	83.0	289.3	74 42N	94 54W
Godhavn	79.9	32.5	69 14N	53 31W
Mould Bay	79.1	256.4	76 12N	119 24W
Sukkertoppen	76.1	28.7	65 25N	52 54W
Baker Lake	73.8	315.2	64 20N	96 02W
Julianehaab	70.8	35.5	60 43N	46 02W
Leirvogur	70.2	71.0	64 11N	21 42W
Ft. Churchill	68.7	322.8	58 48N	94 06W
Barrow	68.5	241.1	71 18N	156 45W
Abisko	66.0	115.0	68 21N	18 49E
College	64.6	256.5	64 52N	147 50W
Sodankyla	63.8	120.0	67 22N	26 38E
Dombas	62.3	100.1	62 04N	9 07E
Meanook	61.8	301.0	54 37N	113 20W
Sitka	60.0	275.3	57 04N	135 20W
Sanae Station	-63.6	44.2	70 18S	2 21W
Byrd	-70.6	336.3	80 00S	119 30W
Wilkes	-77.7	179.2	66 15S	110 35E
South Pole	-78.5	0.3	89 57S	13 19W
Scott Base	-79.0	294.4	77 51S	166 47E

and  $45^\circ$  E). Since the low latitude magnetic field does not have sharp variations, data from low latitude stations were scaled at 15 minute intervals between 1200 UT, April 17 and 2400 UT, April 18, 1965 by using a semi-automatic Benson Lehner OSCAR machine and the first value at 1200 UT, April 17 was normalized. For the purpose of obtaining an accurate disturbance field, the solar quiet daily variation field (Sq) was subtracted from the normalized values. The solar quiet daily variation field used here was obtained from IGY with a modification factor 0.6 which was calculated by comparing Sq of April 16, 1965 with the result of Matsushita and Maeda (1965).

A complex series of solar-terrestrial events began on April 11, 1965, after a period of very low solar activity that had lasted from April 1, Figure II-2. The events seem to be associated with an active region that appeared near the eastern limb on April 11 and in which a number of solar flares with low intensities occurred. The activity reached its maximum on April 15-16 and then gradually subsided to the preceding level. During this period, there were two distinct peaks of solar activity, namely on April 11 and April 16. An intense geomagnetic storm began suddenly at 1312 UT on April 16, with a typical step-function type of commencement (ssc) in the horizontal component (H); this was reported by 62 observatories (Lincoln, 1966).

Figures II-3 a and b present the H-component records, between 1200 UT, April 17, and 2400 UT, April 18, from 38 stations between dipole latitude (dp lat)  $\pm 45^\circ$ .

Several obvious features are common in all records, namely the ssc at 1312 UT on April 17, a negative sudden impulse (si) at 1730 UT, an

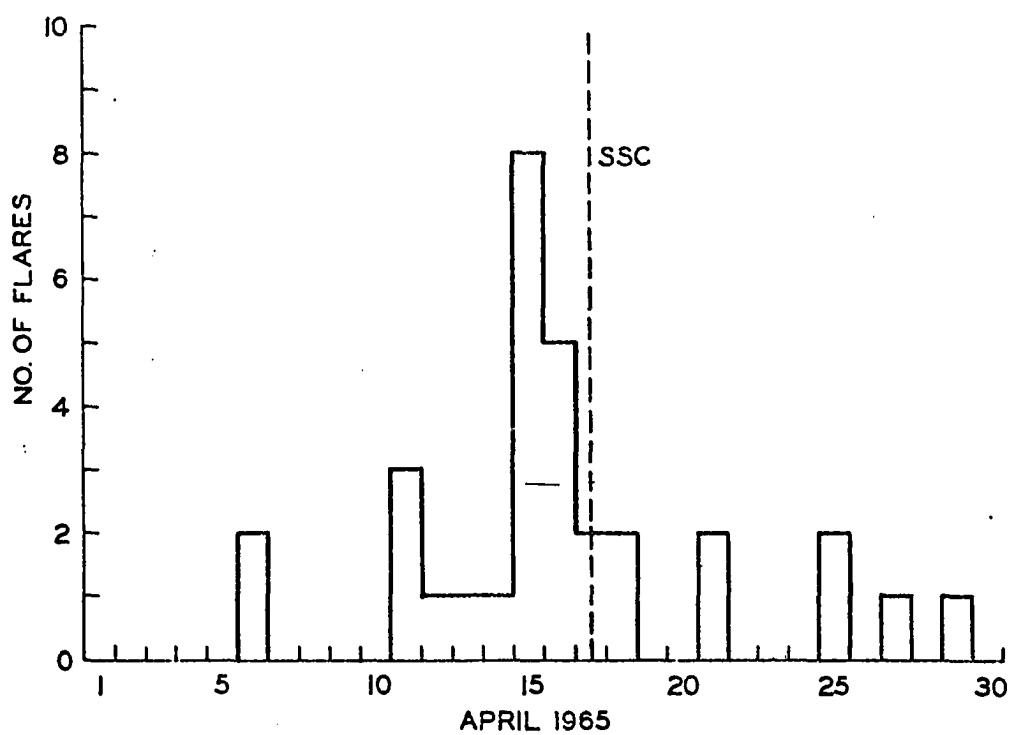
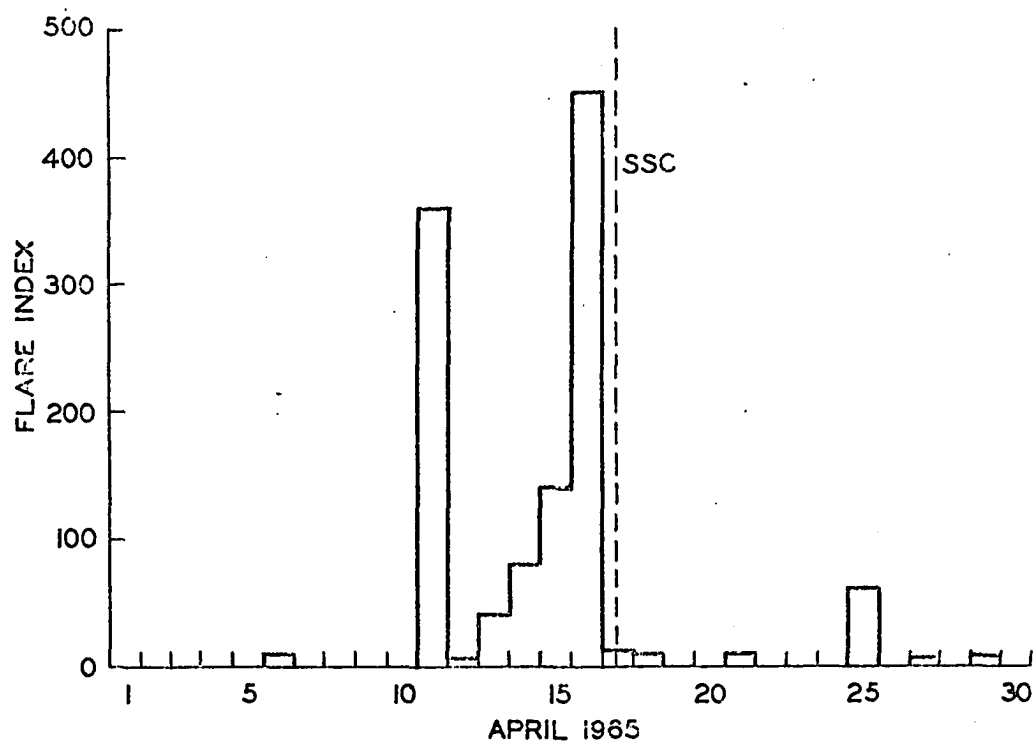


Fig. II-2. Solar flare activity in April 1965.



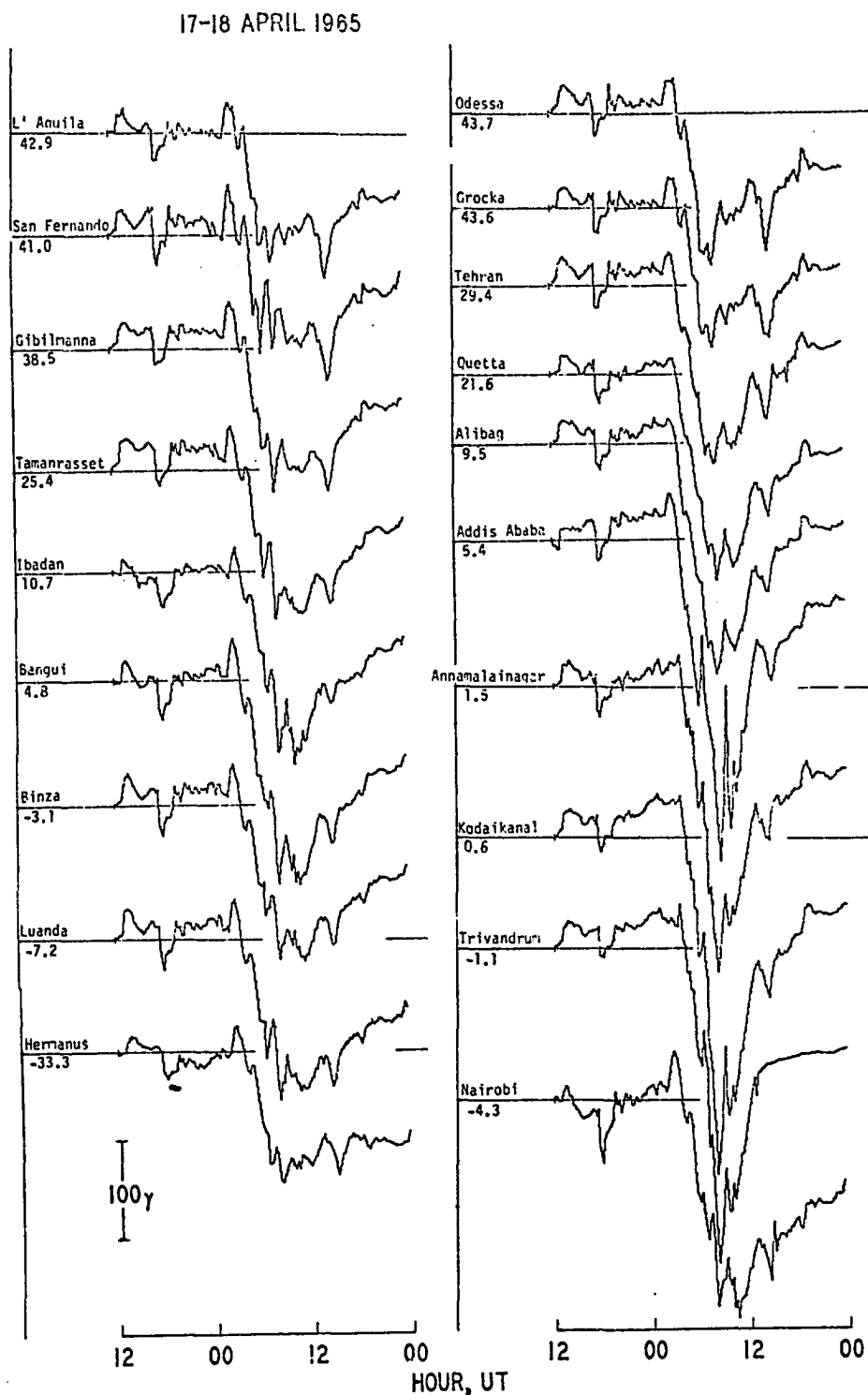


Fig. II-3a. The variation of  $D(H)$  between 1200 UT, April 17, 2400 UT, April 18, at 38 stations between dipole latitude  $\pm 45^\circ$  in four sectors.

17-18 APRIL 1965

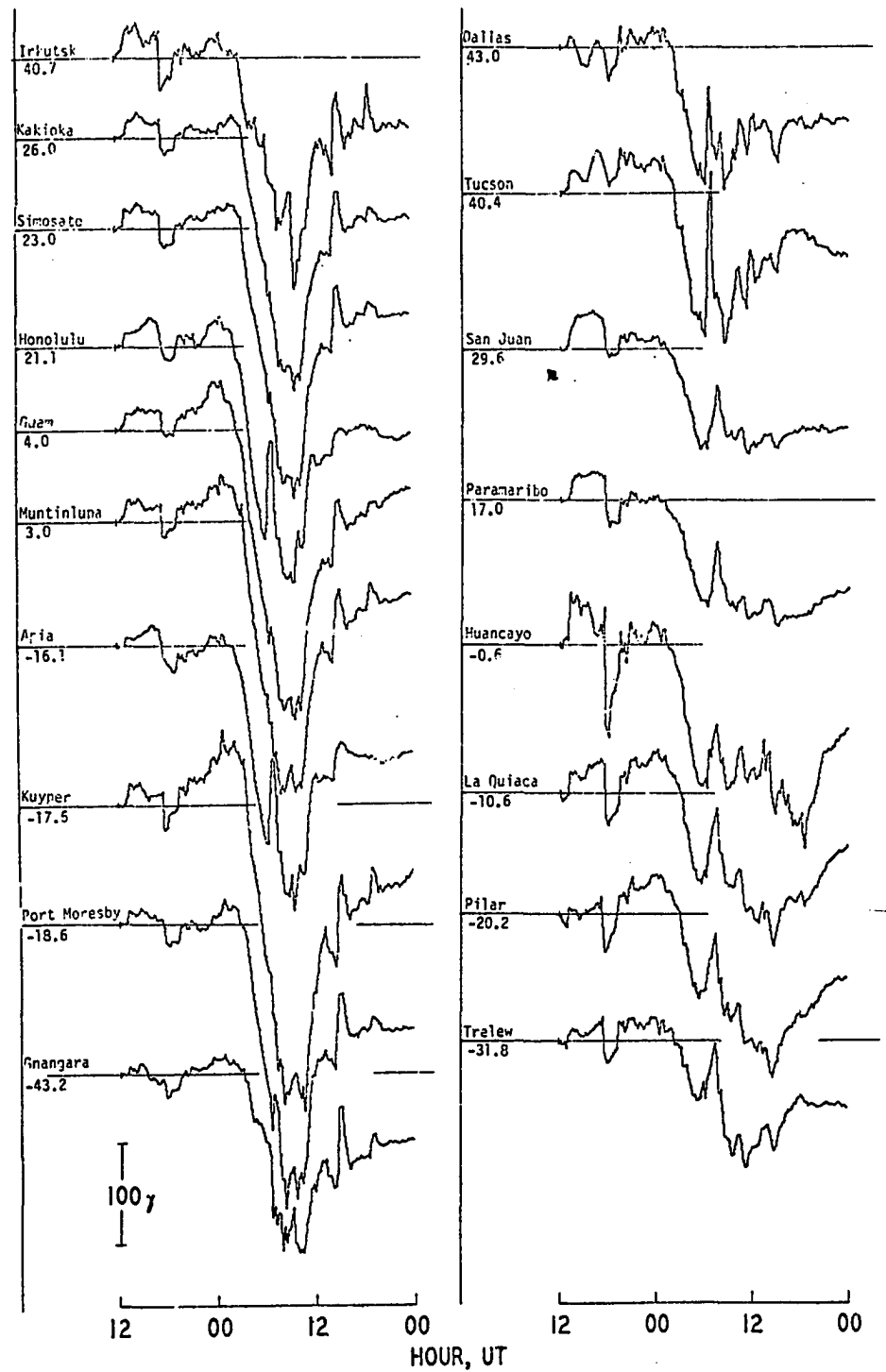


Fig. II-3b. The variation of  $D(H)$  between 1200 UT, April 17, 2400 UT, April 18, at 38 stations between dipole latitude  $\pm 45^\circ$  in four sectors.

ssc-like increase at about 1930 UT on the same day, and the onset of the main phase in the early morning of April 18. However, when examined in detail, different stations show significant differences. For example, Huancayo shows the well-known enhancement of ssc and si (Sugiura, 1953).

Gosling et al. (1967) inferred that the magnetosphere expanded at the time of the si (1730 UT) and enveloped the Vela 2B satellite, which happened to be moving outward near the boundary. At the time of the increase at 1930 UT, the satellite began to detect solar wind particles; this was ascribed to increased solar wind pressure and the compression of the magnetosphere.

Thus it appears that the first enhancement of the solar wind, associated with ssc, subsided suddenly at 1730 UT, without producing a significant main phase decrease, and that the main phase which began in the early morning of April 18 was related to the second enhancement of the solar wind at 1930 UT.

Geomagnetic variations during the main phase decrease show certain similarities in each sector but differ significantly for different sectors. The magnitude of the decrease in low latitudes was much larger in the second and third sectors than in the first and fourth sectors. In the fourth sector there was a large positive impulsive change at about 0600 UT, superposed on the main phase decrease. The same change was also seen in the western part of the Pacific (the third) sector, Honolulu and Apia; a careful inspection shows that it was also seen in all the stations in the first sector and at least at Addis Ababa, Annamalainagar, Kodaikanal, and Trivandrum in the second sector. There were also many other positive changes during the main phase. Such impulsive changes were closely

associated with the polar electrojet that grew in the polar region at that time. Our main concern here is the asymmetric growth of the main phase decrease.

Figure II-4 illustrates the different modes of onset of the main phase decrease; it shows the records from five stations distributed fairly evenly in longitude approximately along the  $dp$  lat  $25^{\circ}N$  circle; for comparison, the San Juan record was superposed on the Simosato (Japan) and the Tamanrasset (Algeria) records; local midnight at each station is indicated by a triangle. It is obvious from Figure II-4 that the main phase decrease began at San Juan at about 0100 UT (2100 LT at San Juan), whereas the onset appeared to be delayed at the other stations.

An early onset of the main phase in the evening sector has long been attributed to the westward return current from an eastward electrojet that was thought to flow along the auroral zone. Akasofu and Chapman (1964) showed, however, that such an interpretation is untenable. Cummings (1966) also made a detailed model study.

The apparent delay of the onset in the European sector (see Figures II-3a and b or the Tamanrasset record in Figure II-4) is partly caused by a positive change that began at about 0200 UT. The positive change was seen at all the stations in the first sector and also at most of those in the second sector. Figure II-5a illustrates the nature of this positive change; it shows simultaneous records from 19 stations in Europe. The stations are divided into two groups; one east, the other west of the  $95^{\circ}E$  meridian (Figure II-5b). Clearly, all the stations except Moscow (11) and Sverdlovsk (16), recorded the positive change. It is usually inferred that such a longitudinally limited change has an ionospheric origin, namely

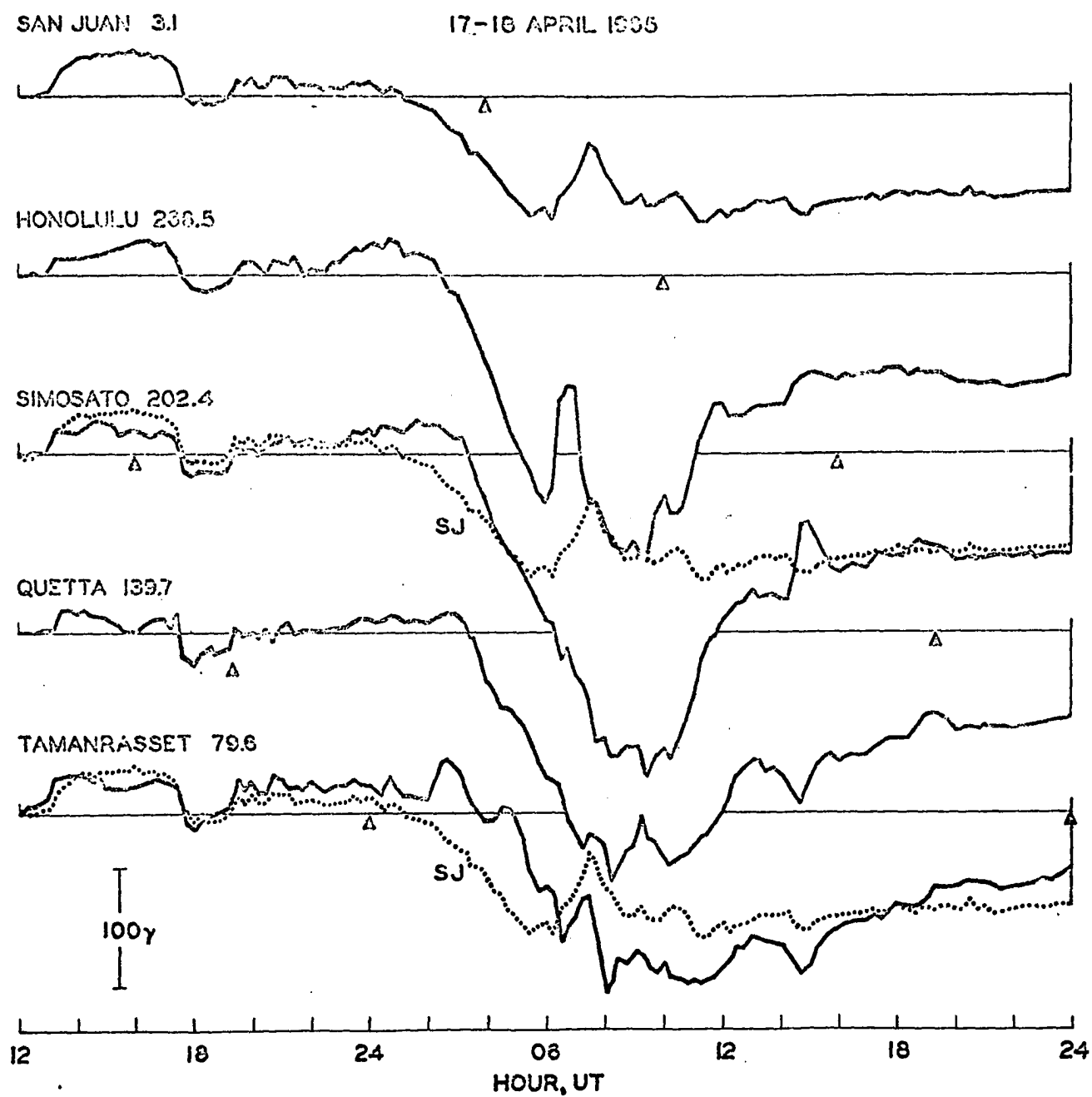


Fig. II-4. The variation of  $D(H)$  at five stations distributed evenly in longitude approximately along the  $dp$  lat  $25^\circ$  circle. Local midnight at each station is indicated by a triangle.

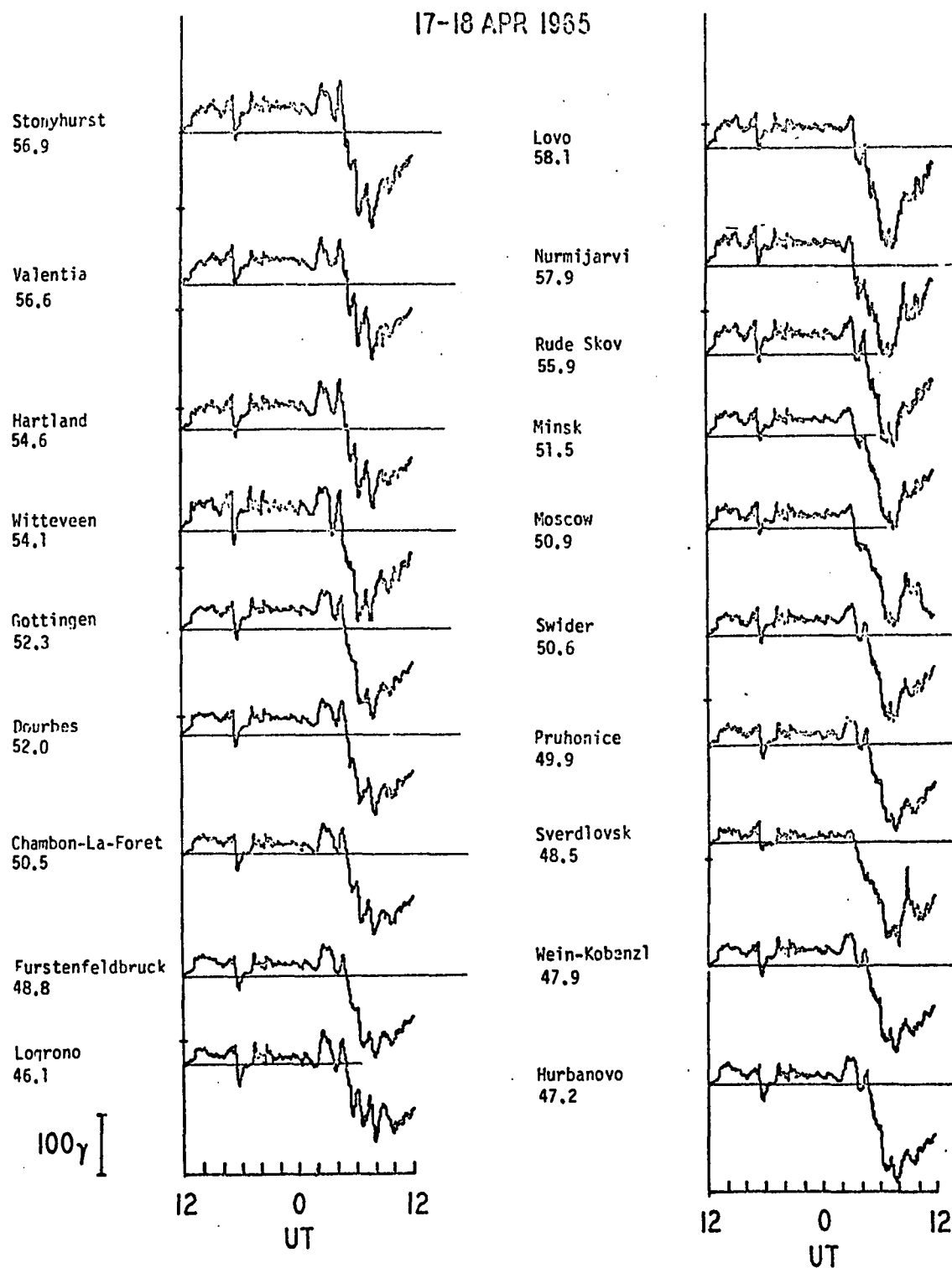


Fig. II-5a. The variation of  $D(H)$ , between 1200 UT, April 17, and 1200 UT, April 18, at 19 middle latitude stations between  $45^{\circ}\text{N}$  and  $59^{\circ}\text{N}$  in Europe.

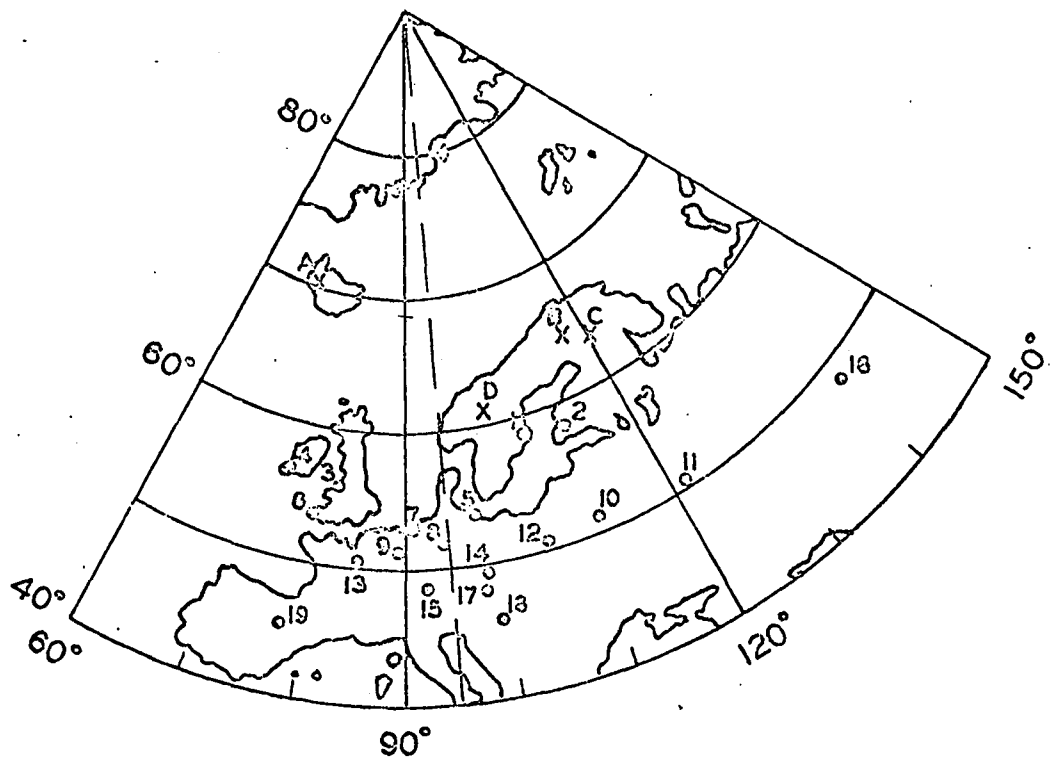


Fig. II-5b. The locations of stations used in Fig. II-5a and four auroral-zone stations (A, Leirvogur; B, Abisko; C, Sodankyla, and D Dombas). The numbers corresponding to the stations are 1, Lovo; 2, Nurmijarvi; 3, Stonyhurst; 4, Valentia; 5, Rude Skov; 6, Hartland; 7, Witteveen; 8, Gottingen; 9, Dourbes; 10, Minsk; 11, Moscow; 12, Swider; 13, Chambon-La-Foret; 14, Pruhonice; 15, Furstenfeldbruck; 16, Sverdlovsk; 17, Wien-Kobenzl; 18, Hurbanovo; and 19, Logrono.

the return current from a polar electrojet; indeed, a polar jet grew and became intense at that time in the auroral zone. But the rather constant magnitude of the positive change over a wide range of latitude ( $0-60^\circ$ ) is not at all compatible with the usual form of such a return current. This particular storm field has, thus, different characteristics from those of the known fields (DCF, DR, DP). Such a feature can be brought out only when the records from a large number of stations are put together as in Figures II-3a and b and II-5a and b.

Both Figures II-3a and b and II-4 clearly show a great difference in the magnitude of the main phase decrease in different sectors; compare particularly the records from Simosato and San Juan in Figure II-4. Figures II-6a and b illustrate the growth and decay of the main phase decrease between 0400 and 2000 UT on April 18 by showing approximate iso-intensity contours of  $D(H)$ , the deviation of the H component from the pre-storm level. The subsolar, antisolar, and sub-Explorer 26 points are marked by a dot, cross, and rayed dot, respectively. The general tendency is quite similar to that shown by Akasofu and Chapman (1964) for different storms during the IGY/C.

Because of the positive change mentioned above, the horizontal component decreased below the prestorm level at all stations only after 0500 UT. (At 0400 UT, two stations in India were registering a positive value, although this could be due to the fact that the  $S_q$  correction was not very accurate for such equatorial stations). In spite of such complications, however, it is not too difficult to draw a few iso-intensity contours of  $D(H)$  at 0500 UT. The center of the maximum main phase decrease appeared to be located in the central Pacific at that time; at Honolulu,



UT

18 APR 1965

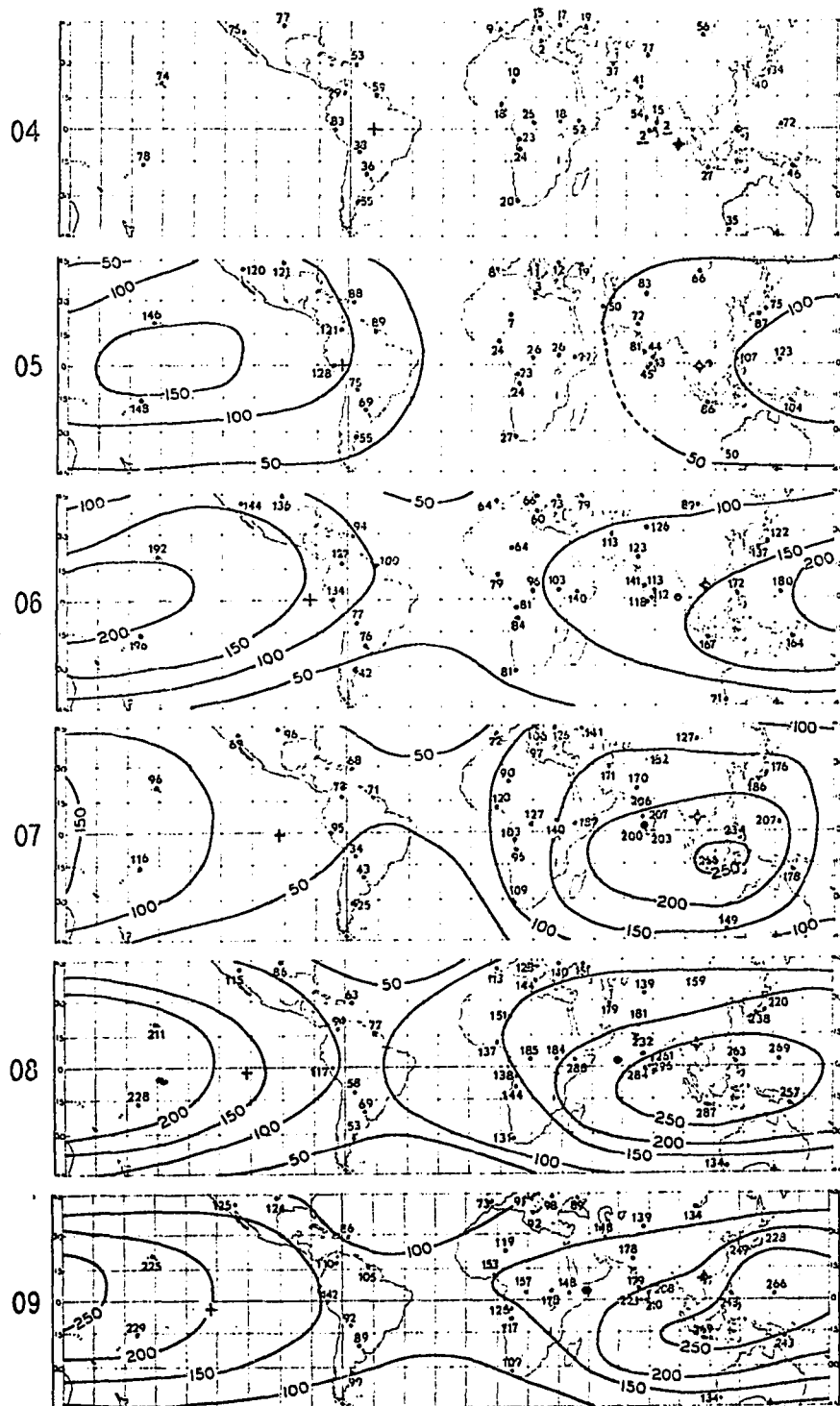


Fig. II-6a. The development of the main phase of the April 17-18, 1965, storm. Approximate iso-intensity contours of  $D(H)$  are drawn at each UT hour, between 0500 and 1000 UT, April 18, 1965.

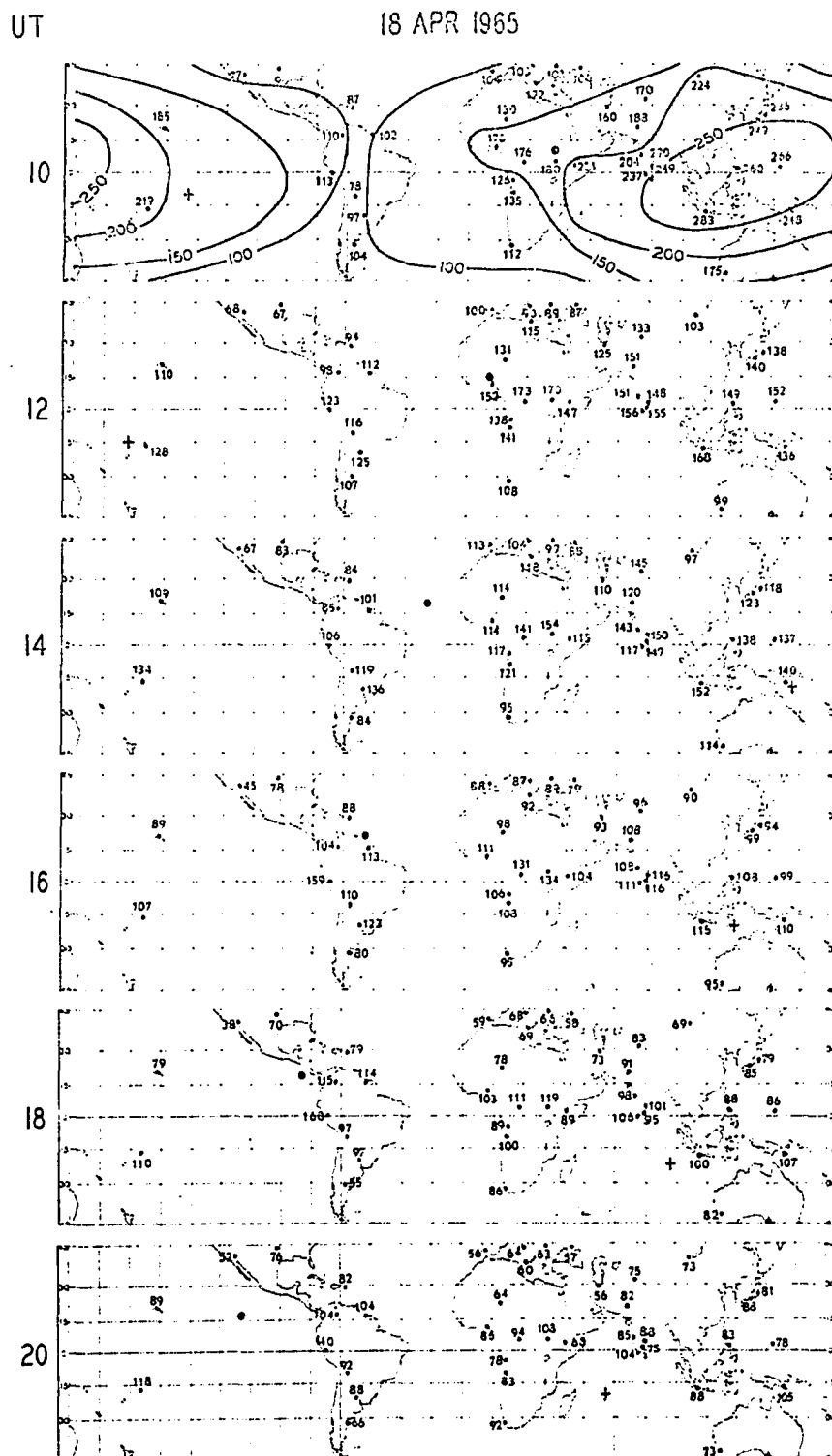


Fig. II-6b. The development of the main phase of the April 17-18, 1965, storm. Approximate iso-intensity contours of  $D(H)$  are drawn at each UT hour, between 0500 and 1000 UT, April 18, 1965.

the local time was 1800 hr. The maximum region of the main phase decrease followed the sun and appeared to move faster than the sun until 0700 UT. This fact was noted by Chapman (1952) in his statistical study of geomagnetic storms and was confirmed by Sugiura and Chapman (1960; see also Akasofu and Chapman, 1967).

During the growing stage of the main phase decrease, the Explorer 26 satellite was moving slowly eastward. The subsolar point and the subsatellite point coincided at almost 0500 UT. The satellite and the region of the maximum main phase decrease moved toward each other during the early growing state of the main phase decrease.

Comparing the results obtained by Cahill (1966, Figure 7) and Figures II-6a and b, a few important points may be noted. First, it is justifiable, to assume that between 0700 and 1000 UT the Explorer 26 sampled mainly the radial variation of the magnetic field produced by the storm-time radiation belt. This is because the satellite was located in the sector of the most intense region of the main phase decrease that remained fairly constant during that period. Second, between 0500 and 0600 UT, in spite of a large main phase decrease on the ground, the satellite observed only minor changes. It seems thus that the main region of the belt was located between the satellite and the earth in the midday sector or that the ground change was caused by a partial belt that did not occupy the midday sector. However, any partial storm-time belt will induce an ionospheric current system (Fejer, 1961; Akasofu and Chapman, 1964; Parker, 1966; Cummings, 1966; Swift, 1967). Suppose, for example, that as Cummings (1966) proposed, the greater main phase decrease in the Pacific region was caused by an additional distribution of the belt particles above that region. The additional 'cloud'

of the particles polarized by itself because of their differential motions, resulting in a positive space charge near the western end of the cloud and a negative space charge near the eastern end. The resulting space charges should be discharged through the ionosphere; the additional current should flow westward in the cloud and to the ionosphere along the field line from the eastern end of the cloud as an ionospheric current (the Pedersen current) and then back to the cloud along the field line. Therefore, we would expect an intense eastward current between the feet of the field lines from both ends of the cloud; the latitude of the feet should be about  $55^\circ$ , since the belt extends from  $L = 2.5$  to  $L = 4$ .

At 0800 UT, the additional main phase decrease over the Pacific sector was of order  $250 \gamma - 100 \gamma = 150 \gamma$  in low latitudes. Subtracting the induction effect, the current intensity associated with the additional main phase decrease ( $150 \gamma \times 2/3 = 100 \gamma$ ) is estimated to be of order  $10^6$  amperes for the above situation (Akasofu and Chapman, 1967). A part of this current should flow eastward in the Pacific sector. (A much weaker current should flow westward in the Atlantic region, since it was located in the early morning sector.)

Suppose that the ionospheric current spreads uniformly over  $5 \times 10^3$  km in width, the current intensity would be of order 100 amp/km and would cause  $D(H)$  of order  $+ 150 \gamma$  in the middle and high latitudes. This value is more than enough to cancel the additional main phase decrease along  $dp$  lat  $50^\circ$  belt; the additional decrease of  $D(H)$  at  $dp$  lat  $50^\circ$  is about one-half of the equatorial value,  $75 \gamma$ . Therefore, the observed distribution of  $D(H)$  between  $\pm 45^\circ$  does not support the existence of such a current. This can be seen also in Figure II-5a, which includes the records from

stations distributed between  $\text{dp lat } 58^\circ$  and  $46^\circ$ . On the other hand, intense positive 'bays' were observed at subauroral-zone stations in the American sector, including Sitka (see Figure II-8) and Meanook. Such a positive change has been interpreted as an indication of an eastward electrojet or a return current from the polar (westward) electrojet, but it is important to investigate further this change by choosing storms that have the growth period of the main phase during local evening in the European sector which has the closest network of stations in the subauroral zone.

It may be noted that the space charge should also induce an intense Hall current (Swift, 1967), which flows clockwise around the foot of the field line from the western end of the cloud and counterclockwise around the foot of the field line from the eastern end, resulting in an intense equatorward current across the line connecting the two feet. Since the Hall conductivity is at least three times greater than the Pedersen conductivity, we would expect an intense eastward (the D component) component change of order 500  $\gamma$  there. For this purpose, the D-component records from Irkutsk and Tashkent were examined and are shown in Figure II-7; these stations are located in the middle latitude zone in the Pacific sector. It is clear that there is no definite indication of such a current.

It is also possible to demonstrate that the asymmetry of D(H) cannot be due to a return current from the polar electrojet; one of the obvious reasons is that when the polar electrojet was greatly enhanced between 0600 and 0700 UT, both Honolulu and Apia recorded a positive change rather than a negative change. Since both stations were located in the region of

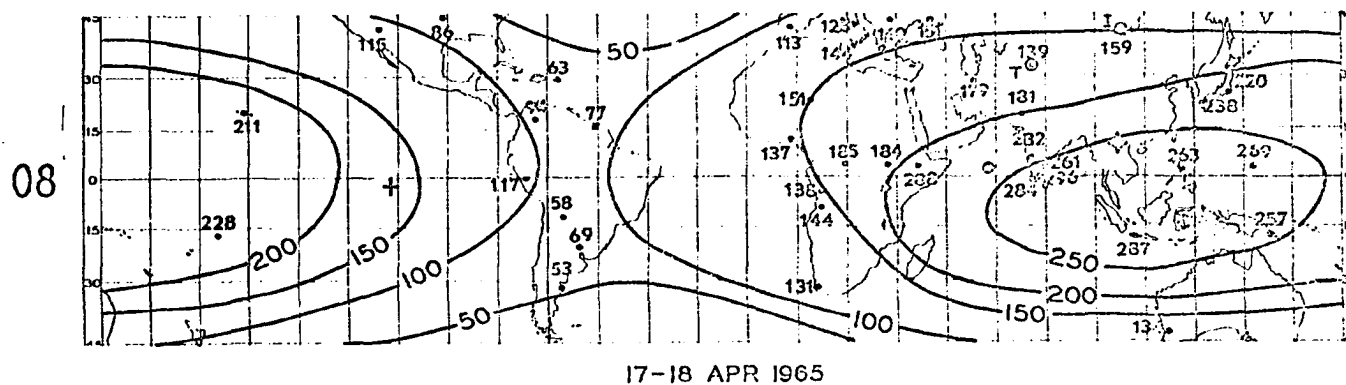
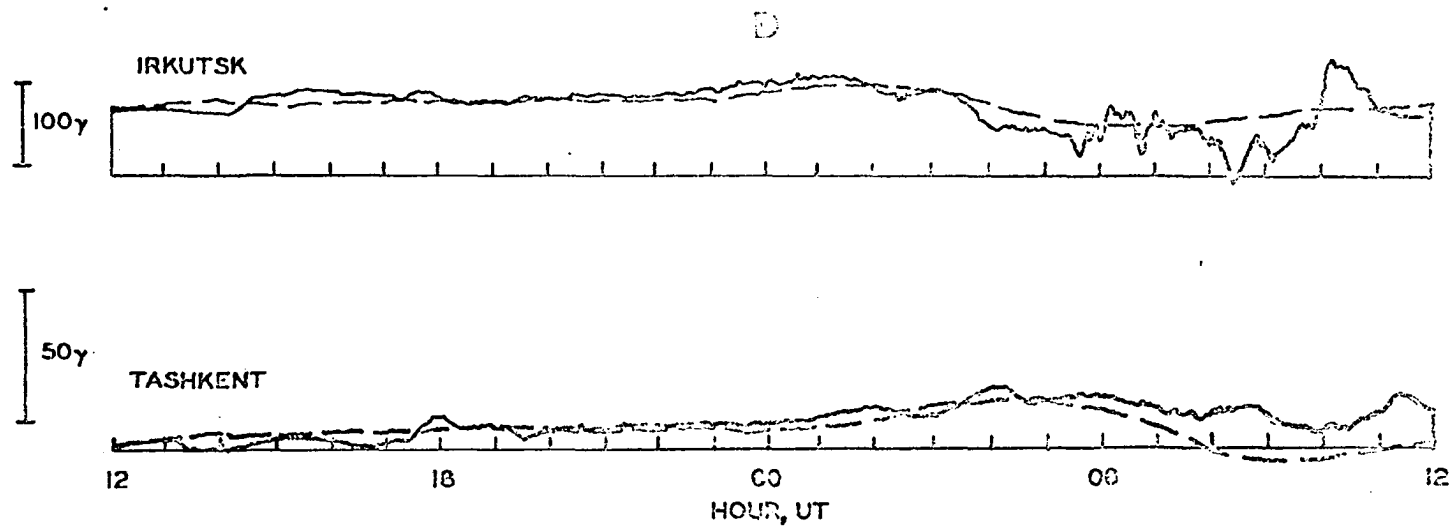


Fig. II-7. Top: The D-component records from Irkutsk and Tashkent; the solid lines show the D-component variation on the storm day and the dashed curves show the  $S_q$  variation (April 16-17, 1965).

Bottom: The iso-intensity contour of  $D(H)$  at 0800 UT on April 18, 1965. Irkutsk and Tashkent are marked.

the most intense main phase decrease at that time, an enhanced jet current would have to deepen the negative change, if the asymmetry were produced by the return current.

The main phase reached its maximum epoch at about 0900-1000 UT. Then the asymmetry, as well as the magnitude of the main phase decrease, became much less pronounced, although it is recognizable even at 2000 UT.

Figure II-8 shows a collection of magnetic records from high-latitude stations: in the first column, from five major stations along the northern auroral zone; in the second column, from five other northern auroral-zone stations; in the third column, from three southern auroral-zone stations, and in the fourth column, from both northern and southern polar cap stations. The time scale in the first column is more open than in the other columns. Local midnight at each station is indicated by a triangle.

During the first enhancement of the plasma flow, i.e., initial phase, there was one moderate substorm that began at about 1400 UT and ended at 1820 UT, with a maximum magnitude of about 200  $\gamma$  ; it was recorded as a negative bay at College, Barrow, and Baker Lake in the morning sector, and as a positive bay at Abisko, Julianehaab, Leirvogur, Sodankyla, and Sukkertoppen in the early afternoon sector. During the same substorm, the polar cap stations recorded smaller disturbances of about 100  $\gamma$  .

The major activity of polar substorms began at about the beginning of the main phase decrease, namely 0100-0200 UT, April 18, and continued until at least 0800 UT. This is clearly demonstrated in Figure II-9, which combines all the records between dp lat  $76.1^{\circ}$ - $60.0^{\circ}$ N and  $63.6^{\circ}$ - $78.5^{\circ}$ S in Figure II-8, together with that from Dombas (dp lat  $62.3^{\circ}$ N), in the way devised by Davis and Sugiura (1966) to obtain the AE index. This tendency

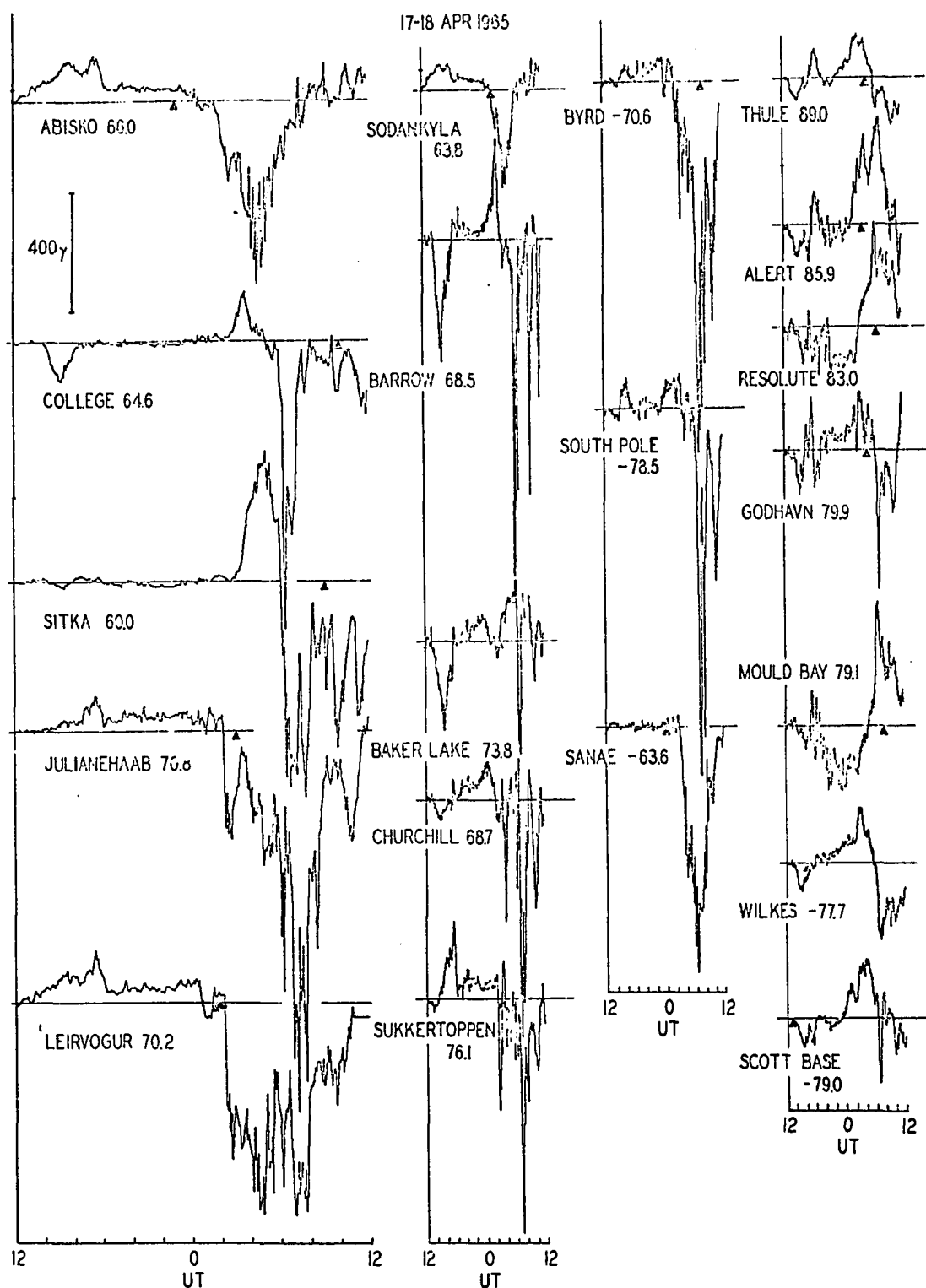


Fig. II-8. The variation of  $D(H)$  between 1200 UT, April 17, and 1200 UT, April 18, at high latitude. The first column shows the five major stations along the northern auroral zones; the second column shows five other northern auroral zone stations; the third column shows three southern auroral zone stations, and the fourth column shows both northern and southern polar cap stations.



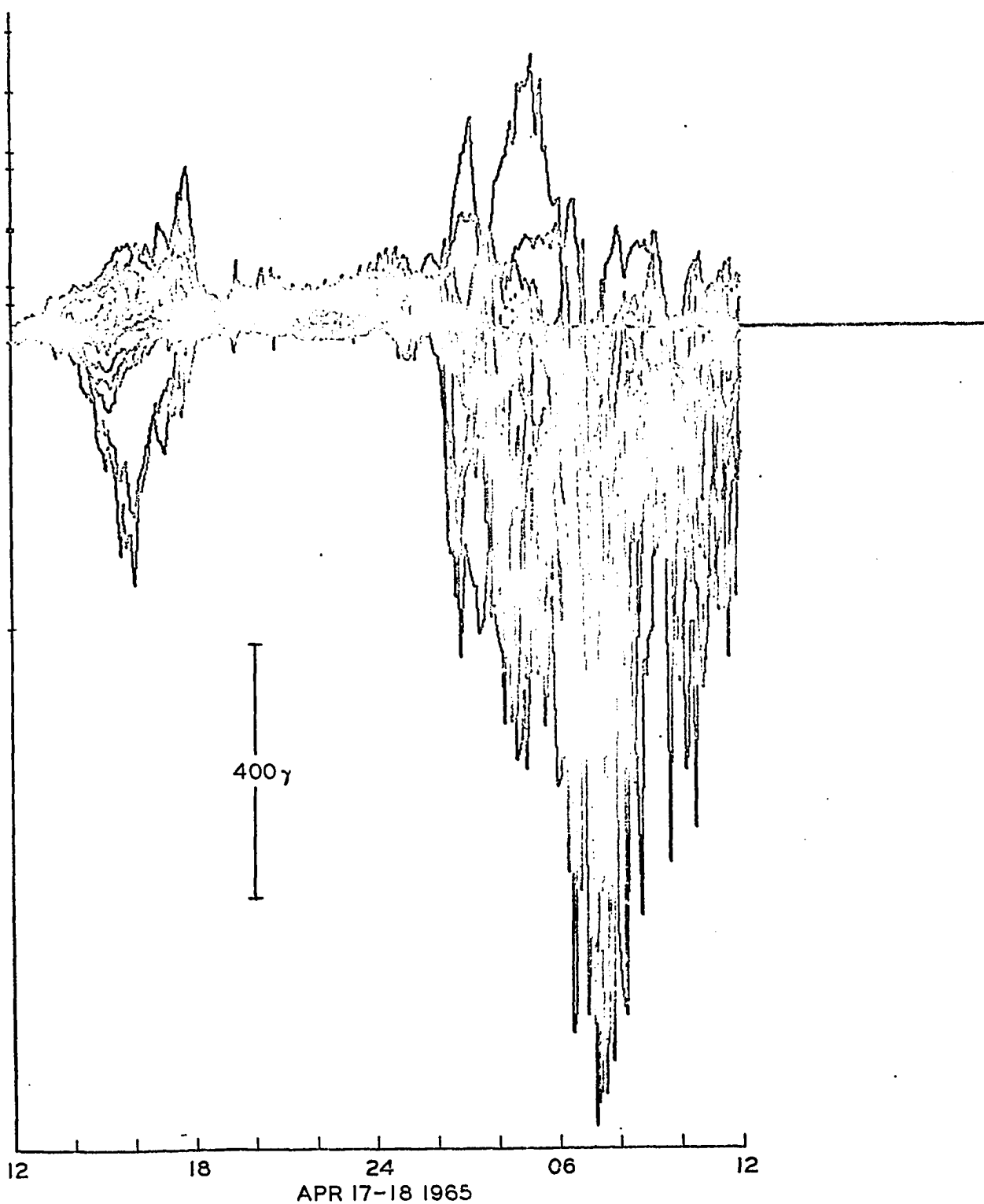


Fig. II-9. The combined high-latitude records (between dp lat  $76.1^{\circ}\text{N}$  and  $78.5^{\circ}\text{S}$ ) to examine global activity of the polar electrojet. This method was first used by Davis and Sugiura [1966].

was first noted by Akasofu and Chapman (1963). At the beginning of the series of polar substorms, Abisko, Leirvogur, Julianehaab, Sukkertoppen, and Sodankyla (located in the midnight sector) recorded substorms as negative bays of about 500  $\gamma$ ; but Barrow, College, and Sitka (located in the early evening sector) recorded only positive bays until 0600 UT. At 0600 UT, a very intense substorm began and reached its maximum intensity at about 0630 UT. During this substorm, the auroral-zone and subauroral-zone stations in the dark sector (such as Baker Lake, Churchill, and Julianehaab in the northern hemisphere and Byrd, Sanae, and South Pole in the southern hemisphere) recorded negative bays; its maximum magnitude was of order 1200  $\gamma$  at Julianehaab, Byrd, and South Pole. In the morning sector, the polar electrojet appeared to flow in the poleward side of the auroral zone, since the corresponding negative bay was recorded at Sukkertoppen (dp lat 76.1°N), but not at Abisko (dp lat 66.0°N). The corresponding negative bay appeared extensively in the evening sector (College, Sitka, Barrow) where positive bays are, in general, common features at that particular local hour. Akasofu and Meng (1967) have recently shown that this abnormally early appearance of the negative bays is caused by the expansion of the auroral oval along which the polar electrojet flows; the expansion of the oval is closely related to the intensity of the storm-time radiation belt (Akasofu and Chapman, 1964). The polar cap stations recorded the effect of the return current from the polar electrojet. During the maximum epoch of this storm, the American continent was in the night sector, thus the relationship between high latitude negative bays and low latitude positive bays can be observed there. (The detailed study of polar substorms is in Chapter III). Figure II-10 shows magnetic disturbances of H component between dp lat 20°

17-18 APR 1965

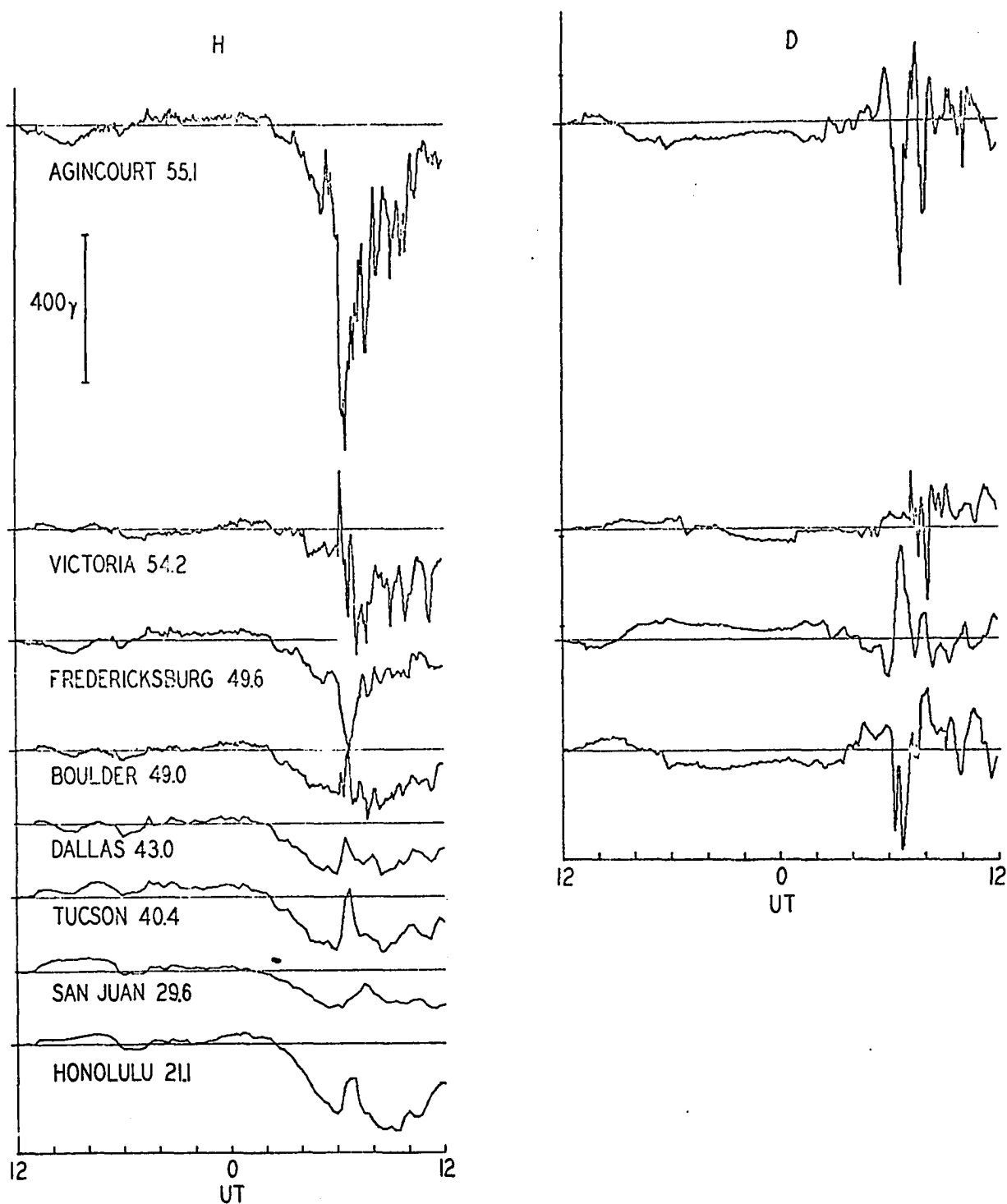


Fig. II-10. Magnetic disturbances of H component between dp lat 20° and 55° and that of D (Declination) component between dp lat 45° and 55° in the American sector.

and  $55^\circ$  and that of D (Declination) component between dp lat  $45^\circ$  and  $55^\circ$  in this sector. Between 0600 UT and 0700 UT, a negative bay of about 900 Y was observed at Agincourt (dp lat  $55^\circ$ ) and one of about 300 Y at Victoria (dp lat  $49.6$ ) which were located in the midnight sector (02-03 LT). Thus during this storm, the auroral oval extended to at least as low as dp lat  $55^\circ$  to  $50^\circ$ . At the same time, a sharp positive bay of about 100 Y was observed in all low latitude stations as has been pointed out previously. This phenomenon agrees with the revised polar electrojet current system which will be discussed in detail in the next chapter. During the recovery phase of the main phase, the activity of the polar substorm also was reduced and its activity subsided at about 1230 UT, April 18.

During this storm, the solar wind measurement by the Vela 2A satellite indicated no significant change in the speed, number density, and temperature of the solar wind corresponding to the development of the polar substorm. Thus, the onset of the polar magnetic substorm is not directly related to changes of the solar wind pressure (Akasofu, 1964; Gosling et al., 1967).

The geomagnetic storm of April 17-18, 1965, is an excellent example of the close relationship between the asymmetric storm-time radiation belt and intense polar magnetic substorms. Important unsolved problems are how the two phenomena are physically related and what is the true nature of the asymmetric radiation belt. Such problems are vital in understanding the way in which the storm-time belt is generated.

A further detailed study of the storm field distribution is required in order to investigate the nature of the asymmetric main phase decrease, in particular ionospheric current systems set up by a partial ring current.

It is suggested that a well-organized rocket study of ionospheric currents is quite important in understanding the nature of the asymmetric field.

The intense polar magnetic substorm that began at 0600 UT on April 18 indicates that the substorm is not directly related to changes of the solar wind intensity. As suggested earlier (Akasofu, 1964), it is more likely to be an internal process within the magnetosphere (such as an instability), although its energy must initially be introduced into the magnetosphere by the solar wind.

## 2) September 13, 1957 Storm:

One of the largest magnetic storms during the IGY is the storm of September 13, 1957 which began at 0040 UT of this day. According to "the new classification of geomagnetic storms and their source flares" by Yoshida (1965), the storm is related to a solar flare at 0239 UT, September 11, 1957. It was associated with type IV solar radio bursts as well as the polar cap absorption. In fact, the region of precipitation of solar high energy protons was extended from the dipole pole to  $dp\ lat\ 65^\circ$ .

Since this was an unusually intense storm and many observatories are not well-prepared for such intense storms, only magnetograms of 53 low and middle latitude stations between  $dp\ lat\ 50^\circ$  and  $dp\ lat\ -50^\circ$  were analyzed in the method described previously. The Sq variation was subtracted by using the IGY results obtained by Matsushita and Maeda (1965). Two very remarkable features of this storm can be easily recognized in the Koror magnetogram Figure II-11. One is the unusually large magnitude of ssc and the other is the unusually intense main phase decrease. The range of ssc is about 100 gammas in the low and some of the middle latitude stations. The

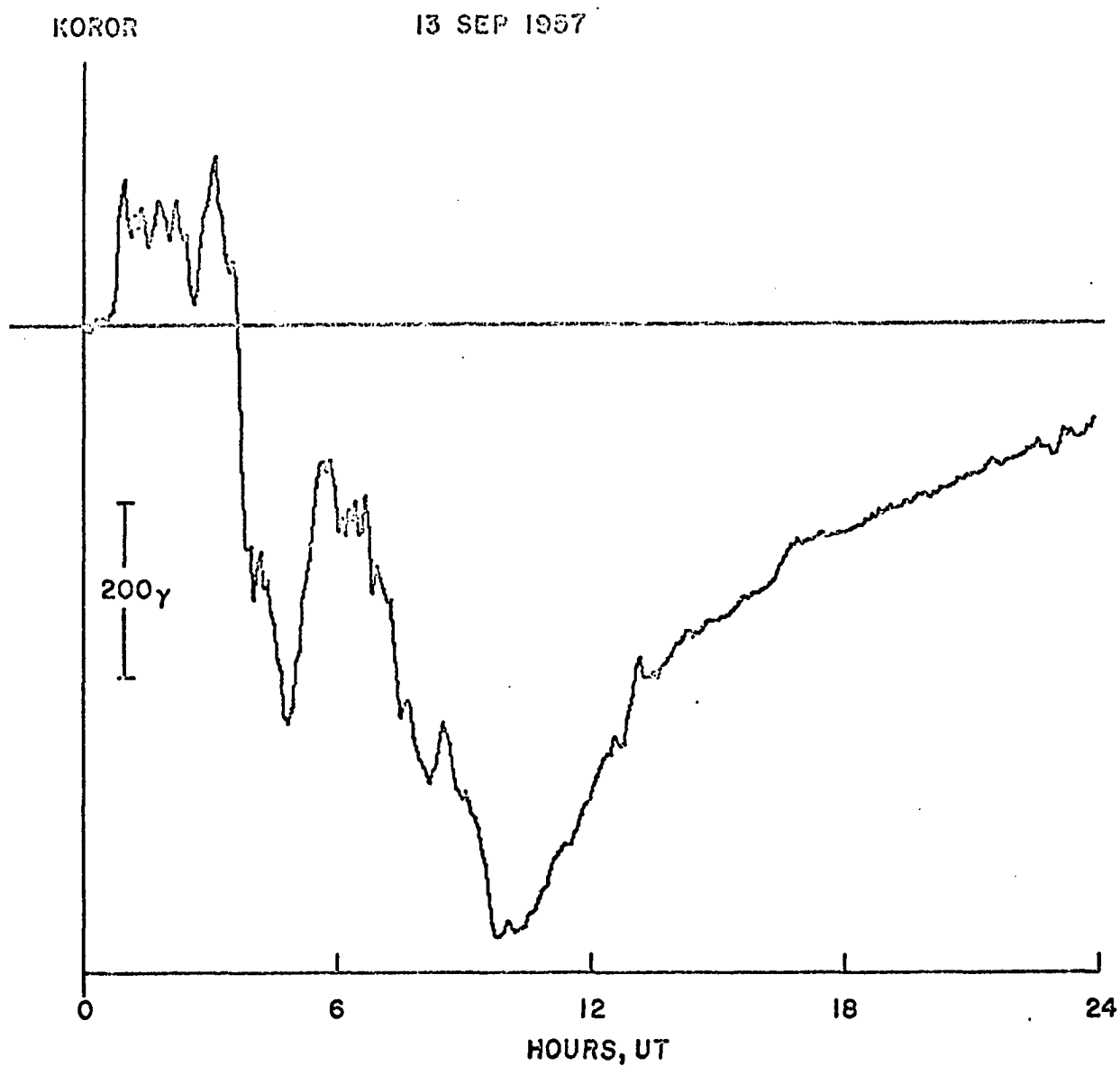


Fig. II-11. The magnetic storm of September 13, 1957 recorded at Koror.

distribution of the range of ssc is fairly uniform, in fact the well-known abnormal enhancement of ssc and initial phase along the dip equator and near the noon sector is not obvious during this storm, (see Fig. II-12).

The maximum main phase decrease at Koror occurred at about 1000 UT, Sept. 13, 1957, with a magnitude of almost 700  $\gamma$ . At some other low and middle latitude stations, its magnitude exceeded 400  $\gamma$  as shown in Figure II-12 which represents the H-component records, between 0000 UT and 2400 UT, September 13, 1957, from 46 stations between dp lat  $\pm 50^\circ$ .

As already pointed out in the study of April 17-18, 1965 storm, geomagnetic variations during the main phase have certain similarities in each sector but differ significantly for different sectors. The magnitude of the main phase decrease was larger in the Pacific and Middle East-India sectors than in the American and Europe-Africa sectors for this storm.

In order to see the growth and decay of the asymmetric main phase of a great storm, Figure II-13a, and b, show the development of the main phase. Approximate iso-intensity contours of D(H), the duration of the H component from the pre-storm level, are drawn between dp lat  $\pm 45^\circ$  both the subsolar and anti-solar points are marked by a rayed circle and dot, respectively. The first frame (0100 UT) shows the contours of the initial phase. The magnitude of the initial phase seemed to be fairly uniform, but with a tendency to be greater in the dark sector than in the day sector. During the next few hours, the main phase began to develop rapidly in the dark sector and also in the afternoon sector (Central Pacific). At 0400 UT, the main phase in the Central Pacific had already reached 200  $\gamma$ , but in the Far Eastern sector the initial phase was still in progress. The main phase reached its maximum at about 1000 UT.

13 SEPT 1957

H

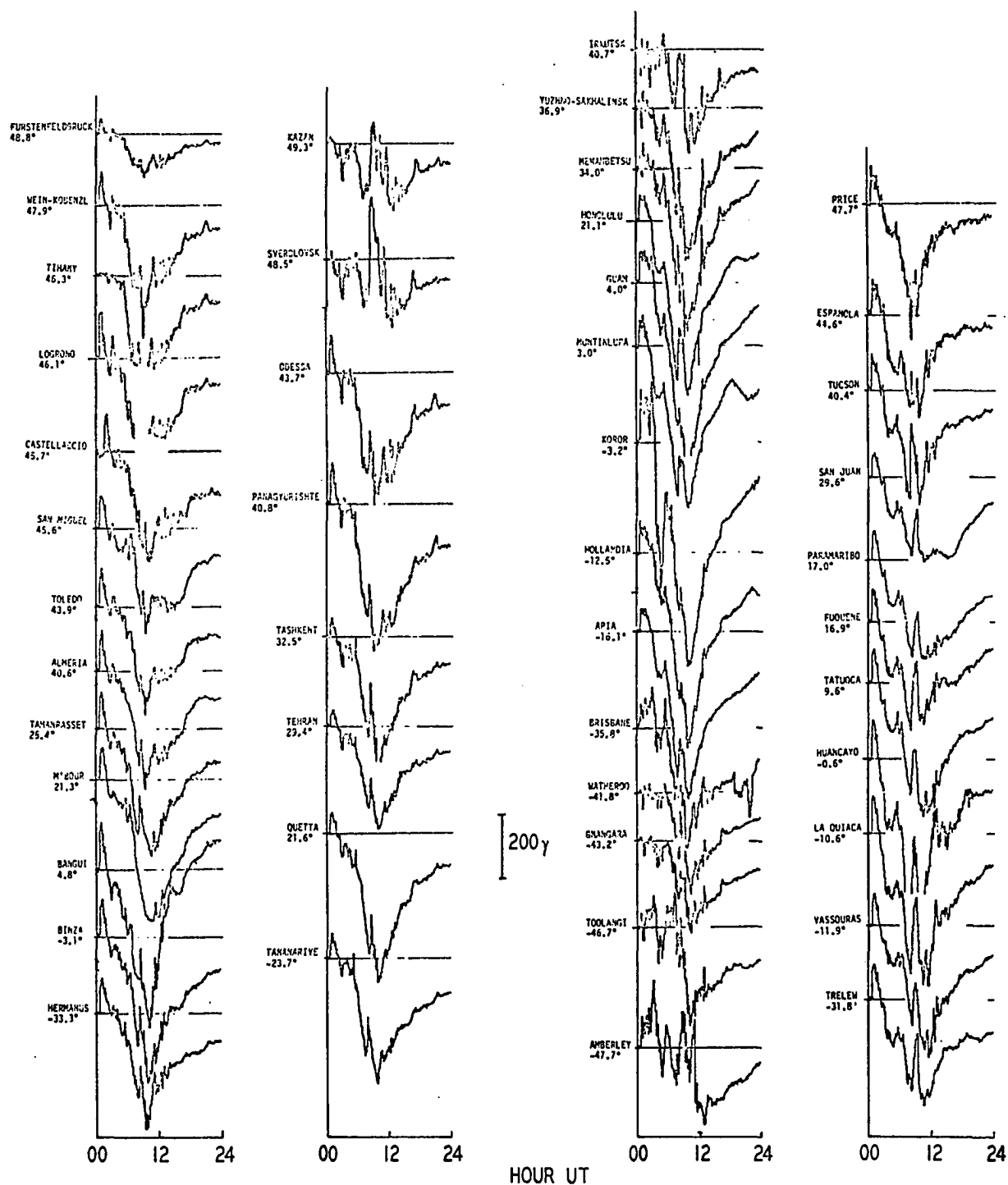


Fig. II-12. The variation of  $D(H)$  at middle and low latitudes (between  $\text{dp lat } \pm 50^\circ$ ) during the September 13, 1967 magnetic storm.



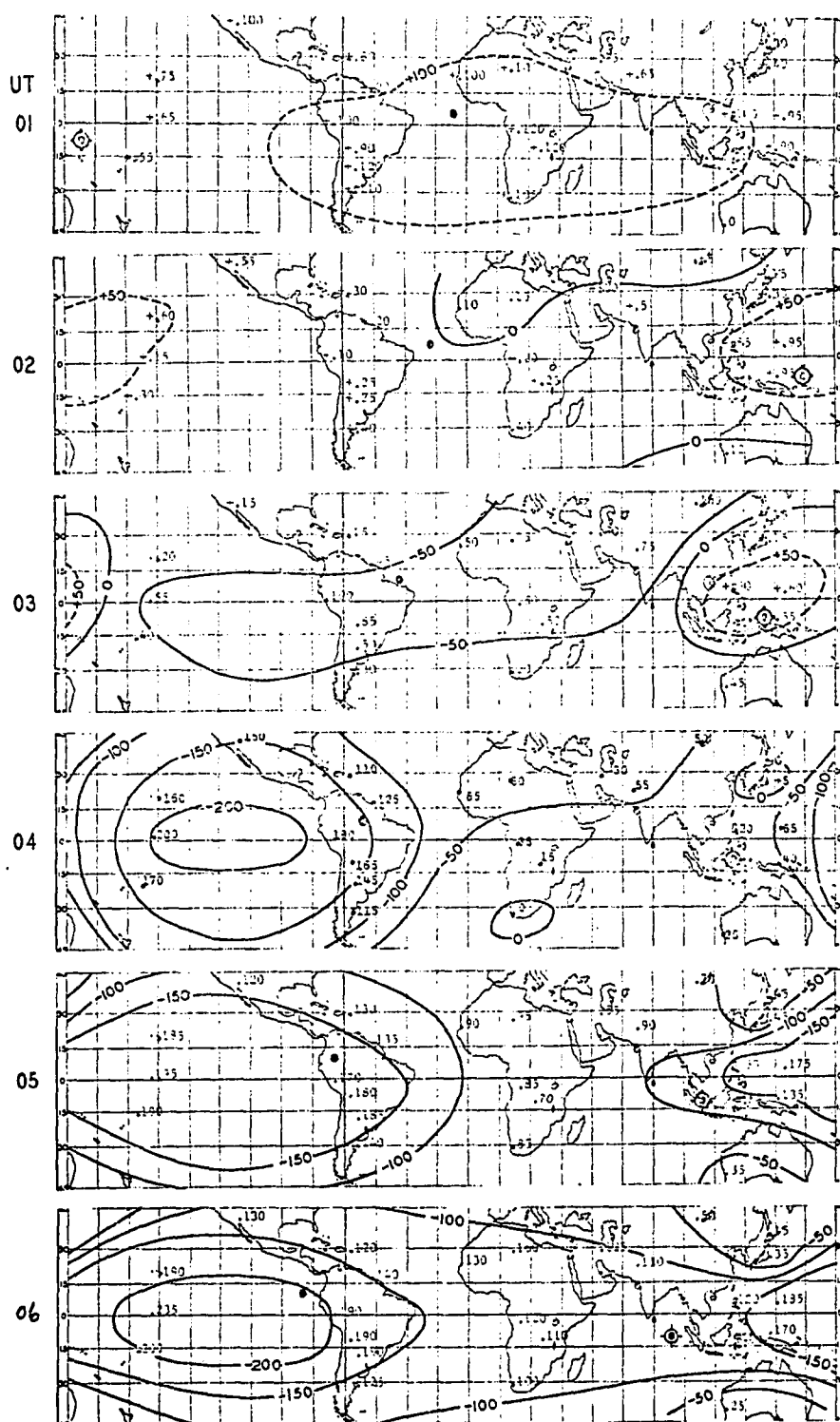


Fig. II-13a. The development of the main phase of the September 13, 1957, storm. Approximate iso-intensity contours of  $D(H)$  are drawn at each UT hour, between 01 and 12.

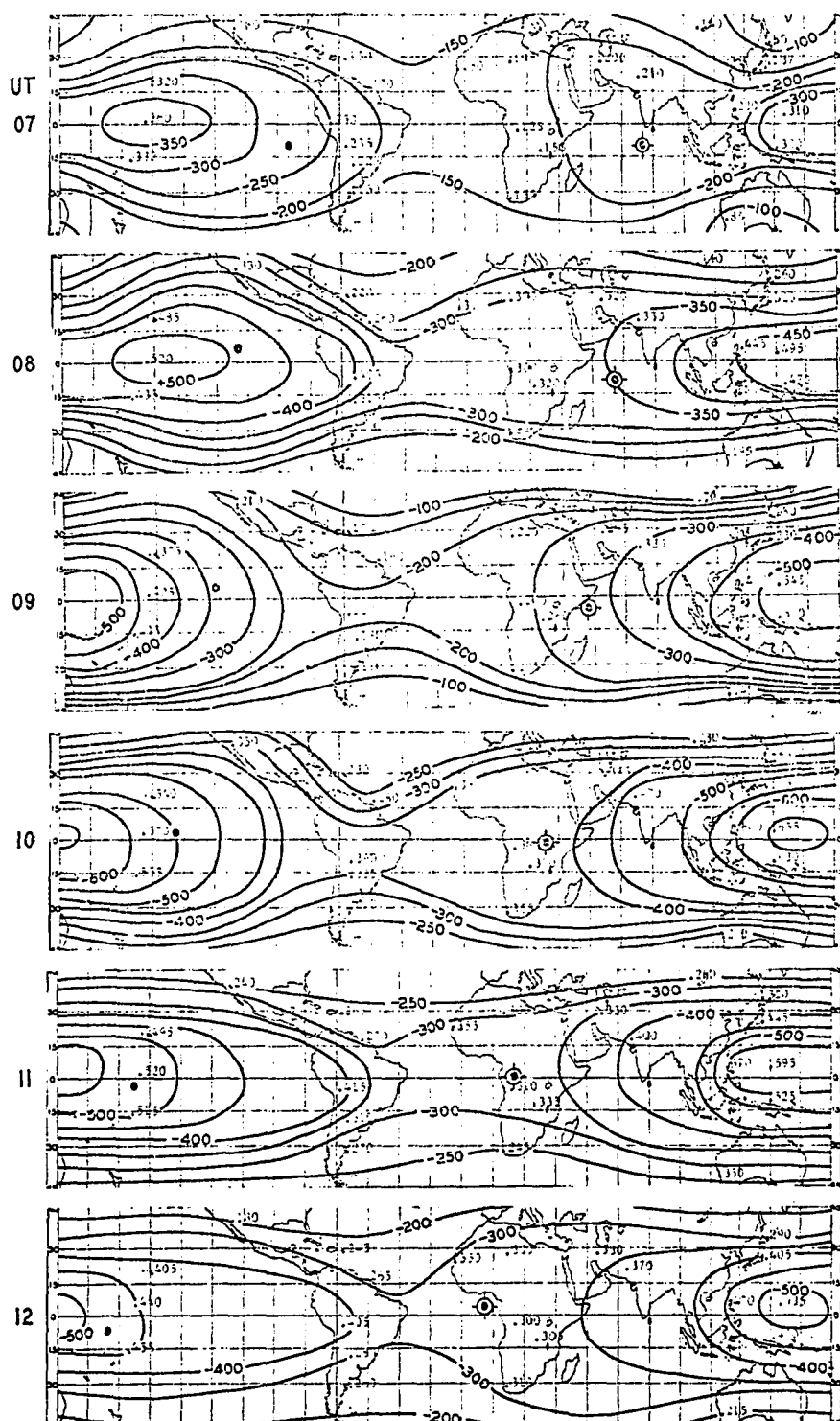


Fig. II-13b. The development of the main phase of the September 13, 1957, storm. Approximate iso-intensity contours of  $D(H)$  are drawn at each UT hour, between 01 and 12.

Figure II-14 illustrates the different modes of onset of the main phase decrease; it shows the records from five stations distributed fairly evenly in longitude approximately along the dp lat.  $25^{\circ}$  circle, except for Memambetsu (dp lat  $34^{\circ}$ ). The San Juan record was superposed on the Honolulu record for comparison and local midnight at each station is indicated by a triangle. The asymmetry of the main phase decrease is also very obvious. The hourly AE index which represents polar electrojet activity near the auroral zone is also shown on the bottom of this diagram. The relation between the positive impulses superposed on the main phase in the middle and low latitudes and the increase of the AE index is very similar to that seen in the storm of April 17-18, 1965.

From the study of the above two storms of different intensity and duration of initial phase, some interesting features which should improve our understanding of the nature of magnetic storms have been determined. They are:

1. The simultaneous growth of the main phase and the polar substorm,
2. The main phase decrease is larger in the afternoon sector than in any other sector. The ratio for this asymmetry is between  $1/2$  to  $1/3$ , but the relation between this ratio and the characteristics of the storm is not known.
3. The intense polar substorm which occurred during the magnetic storm is not directly related with the change of the characteristics of the solar wind. Thus, the onset of the polar substorm must be an internal process within the magnetosphere, but its energy source is initially introduced into the magnetosphere by the solar wind.

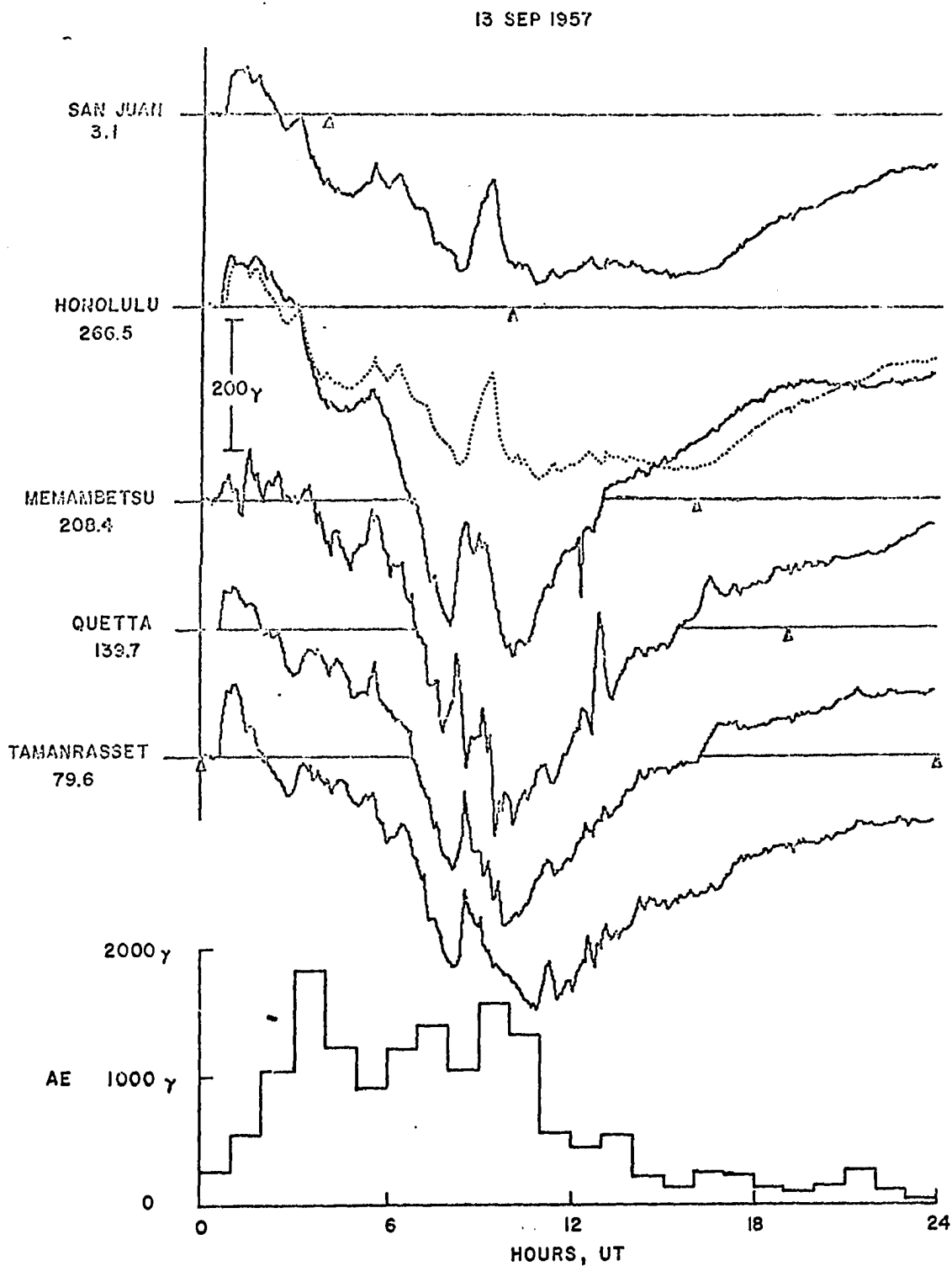


Fig. II-14. The variation of  $D(H)$  for Sept. 13, 1957 storm at five stations distributed evenly in longitude approximately along the  $dp$  lat  $25^\circ$  circle. Local midnight at each station is indicated by a triangle. The AE index is also shown.

## CHAPTER III

### HIGH LATITUDE POLAR SUBSTORM

#### 1. Introduction

The morphological studies of auroral display and high latitude magnetic disturbances were started during the first and second Polar Year 1882/85, 1932/33. From the small number of observatories in high latitudes and limited amount of data, results could only be obtained statistically. During the International Geophysical Year and International Geophysical Cooperation (1957-1959), a large number of magnetic observatories were established inside and near the Arctic Circle and numerous all-sky cameras were installed over both polar regions. These international cooperative efforts provided us with useful data not only for studies of gross character, but also for detailed simultaneous studies of individual events over the entire polar region. Therefore, our knowledge of auroral display and polar magnetic disturbance can be classified according to the two epochs, namely pre-IGY and post-IGY. The former is reviewed in this section and the latter will be discussed in the other sections.

#### 1) Magnetic Disturbances in High Latitudes

During his three Arctic expeditions, Birkeland (1908,1913) made magnetic and auroral observations for many months. He divided magnetic disturbances into five different types:

1. The positive equatorial storms
2. The negative equatorial storms
3. The positive polar storms
4. The negative polar storms
5. The cyclo-median storms

Of these five types, the positive and negative polar storms, and the positive equatorial storms are most frequently observed. Here, the two polar storms are considered under the new name magnetic substorm (Akasofu & Chapman 1961).

The average feature of the polar magnetic disturbance has been investigated by many scientists. Some of them introduced the overhead current equivalent to the disturbance produced by the substorm and are reviewed in the following:

(a) Chapman's equivalent current system

The average morphology of world-wide magnetic storms investigated by Chapman (1919, 1927, 1935, 1952) are reviewed in the last two chapters. The currents are especially intense along the auroral zone, a westward current in the forenoon sector and an eastward current in the afternoon sector (Fig.III-1). They were later named polar electrojets by Chapman (1951). The local time of the most intense current is 06 and 18 LT, respectively. In this model, the westward current is considered to produce a return current from the dark side to the sunlit side across the polar cap, and also an oval current system in the interzonal belt. Similarly, the eastward current produces a polar cap current from the darkside to the sunlit side, and also an oval current system in the interzonal belt. The plane of symmetry for the DS system is the noon meridian plane.

The complete equivalent current system representing the D field is the combination of the DS current system with the Dst current system. This combined system is reproduced in Figure III-2. The Dst system dominates in

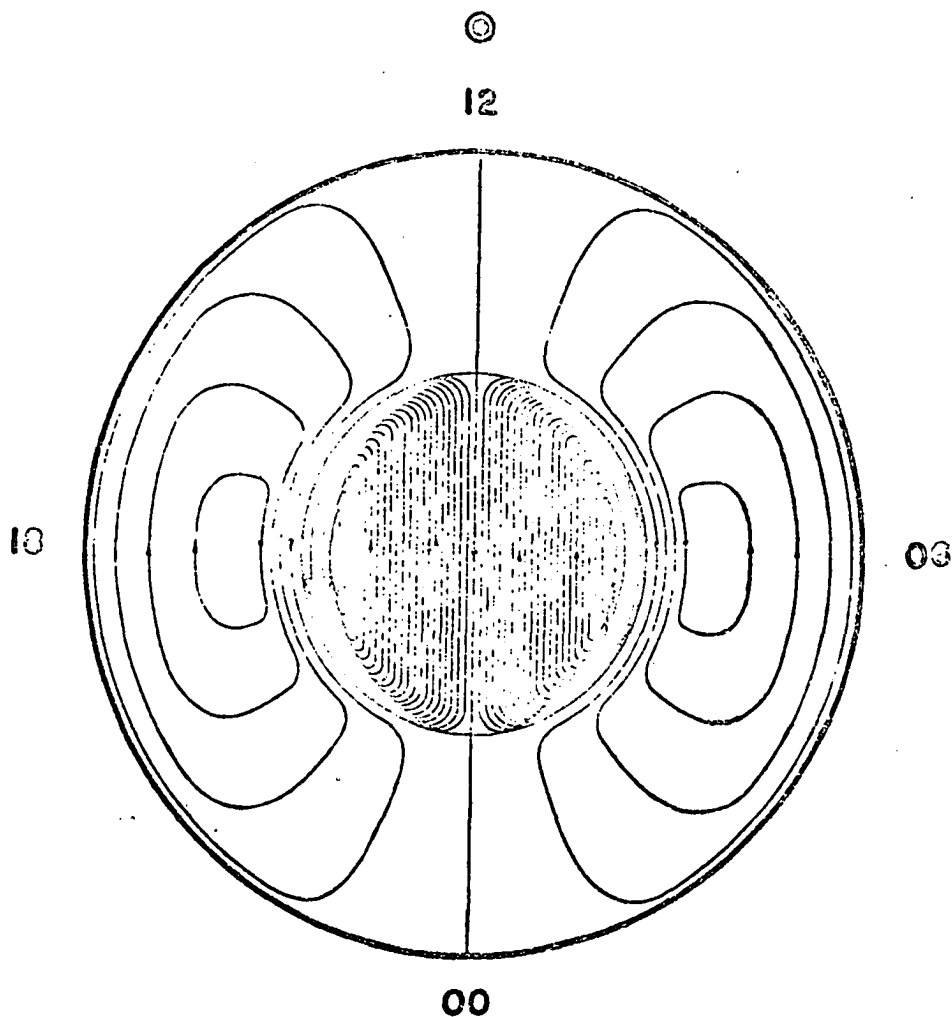


Fig. III-1. Idealized equivalent current systems for the DS field; view from above the north pole; the direction of the sun is indicated (after Chapman (1935)).

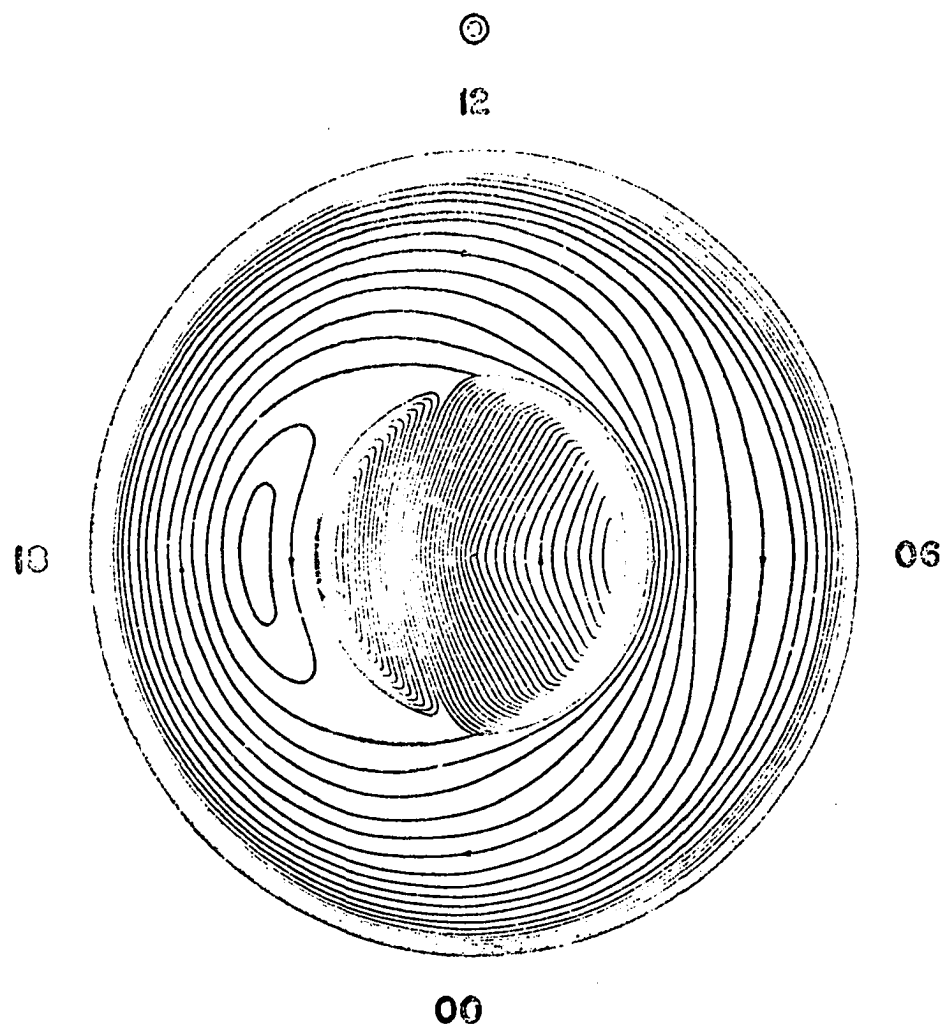


Fig. III-2. Idealized equivalent current systems for the  $D=D_{st} + D_S$  field; view from above dp north pole; the direction of the sun is indicated (after Chapman, 1935).



lower latitudes, indicating that the major contribution to the disturbance field D is produced by the ring current. However, in and near the auroral zone, and over the polar cap, the DS component dominates. The complete current system in the polar region is no longer symmetric with respect to the noon meridian. The westward current along the auroral zone in the forenoon sector is more intense than the eastward current in the afternoon sector.

#### (b) Vestine's equivalent current systems

Chapman's material for the strongest part of the current system in polar latitudes was scanty; it dated mainly from the First International Polar Year (1882/83). Using magnetic records obtained during the Second Polar Year (1932/33), Vestine (1940) deduced the equivalent current systems for several epochs during some individual magnetic storms by use of hourly mean values of the three components. He concluded that their general pattern resembles Chapman's D current system as in Figure III-2. The orientation, however, differed from that in Figure III-1; the local time of the most intense current was usually not at 6 AM; it fluctuated by about  $\pm 20^\circ$  around 2 AM or 3 AM. Further, there were certain epochs during which the eastward current in the afternoon sector was virtually absent; such an example is shown here in Figure III-3.

#### (c) Fukushima's equivalent current systems

Fukushima (1953) constructed a number of equivalent current systems at particular instants, not by using tables of hourly mean values, but by referring to the actual magnetic records collected world-wide during the Second International Polar Year.

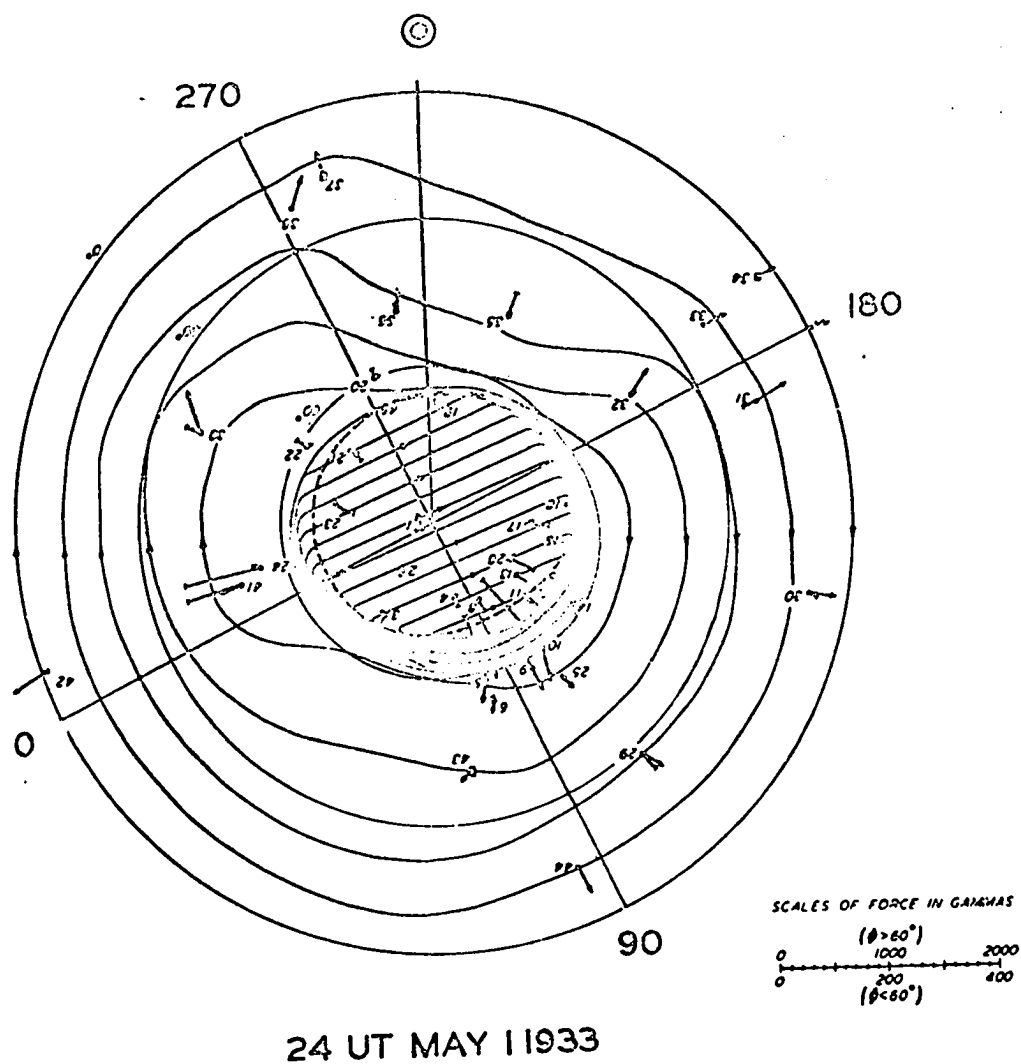


Fig. III-3. Mean hourly disturbance vectors and corresponding equivalent current system at 24 UT, 1 May 1933; view from above the north pole; the direction of the sun is indicated (after Vestine, 1940).

Fukushima chose instants when intense polar magnetic substorms were in progress and concluded that in general his current systems resembled those given by Chapman and Vestine. This means that although he dealt with polar magnetic substorms of life time of order a few hours, rather than with the daily disturbance variation DS of period 24 hours, their equivalent systems were essentially alike. Silsbee and Vestine (1942) had reached the same conclusion by studying statistically weak polar magnetic substorms. Thus, the DS variation has been regarded as representing an average condition of polar magnetic substorms.

However, Fukushima also showed a few examples in which the eastward current in the afternoon sector is very weak or not obvious; such an example is shown here in Figure III-4. Further, he compared the distribution of his instantaneous current vectors with the approximately corresponding equivalent current system obtained by Vestine, and indicated some significant discrepancies between them (Fukushima's Figs. 11 and 12).

The studies reviewed briefly in the above make it possible to construct a model current system for a typical polar magnetic substorm. Unlike the ring current producing the major part of the Dst variation in low latitudes, the current system for the polar magnetic substorms is likely to be located rather close to the earth, since the disturbance vectors differ greatly even at two points separated by a distance of only a few hundred kilometers. The ionosphere has been thought to be the most suitable layer for the current because of its rather high electrical conductivity transverse to the geomagnetic field.

The procedure of constructing such an ionospheric model current system from the equivalent current system is rather arbitrary; this is because

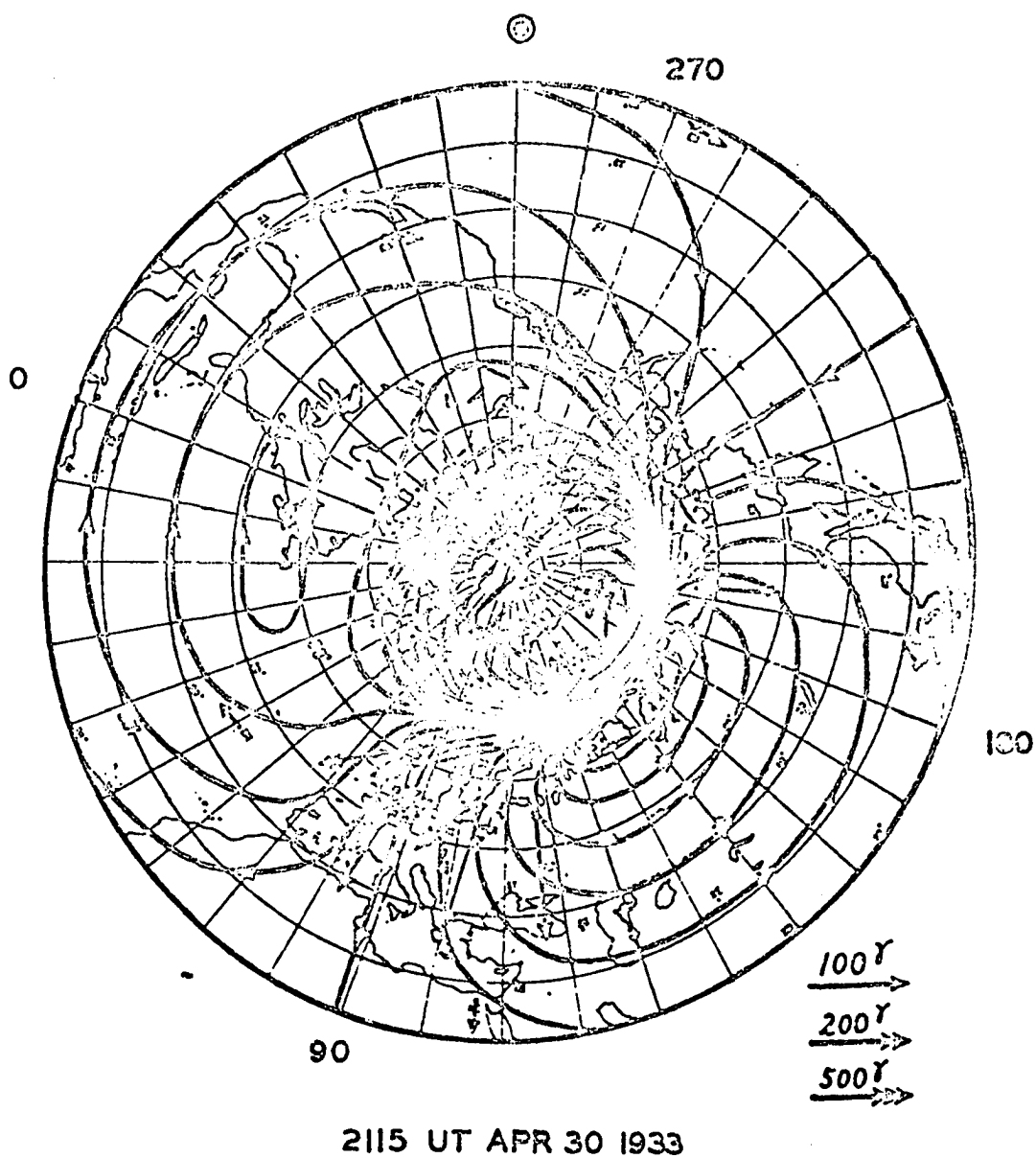


Fig. III-4. Disturbance vectors and corresponding equivalent current system at 2115 UT, 30 April 1933; view from above dp, north pole; the direction of the sun is indicated (after Fukushima, 1953).

surface magnetic observations cannot uniquely determine the actual distribution of the storm producing currents above the earth. In the earlier model, for additional physical reasons, the whole DS current, together with a part of the polar Dst current, was considered to be located in the ionosphere, although it was recognized that the result was, by choice, to some extent arbitrary. Figure III-5 shows schematically a model current system which includes the major features of the earlier model, having a certain resemblance to the diagram by Silsbee and Vestine (1942).

(d) Auroral display in high latitude

The auroral display is one of the complex polar geophysical phenomena. For the purpose of understanding the nature of this complicated phenomenon, its spatial and temporal characteristics had to be investigated first. From the result of this morphological study the earth's surface can be divided into five parts (Chapman 1953) according to the auroral occurrence frequency. They are:

- 1) Auroral regions: within the circles of dp lat  $60^\circ$  (N or S)
  - a) Auroral zone: a narrow band of about  $3^\circ$  wide lying approximately within the circle of dp lat  $67^\circ$  (N and S).
  - b) Auroral cap: the region enclosed by the auroral zone (N and S).
- 2) Subauroral zones: regions between  $45^\circ$  and  $60^\circ$  dp lat (N and S)
- 3) Minauroral belt: the region between the circles of dp lat  $45^\circ$  (N and S).

Loomis (1860) was the first to draw a zone, encircling the north geomagnetic pole. After making a great compilation of auroral data, Fritz (1881) determined the position and form of the zone more accurately. He drew lines of equal average number of nights of visible auroras per year. This work

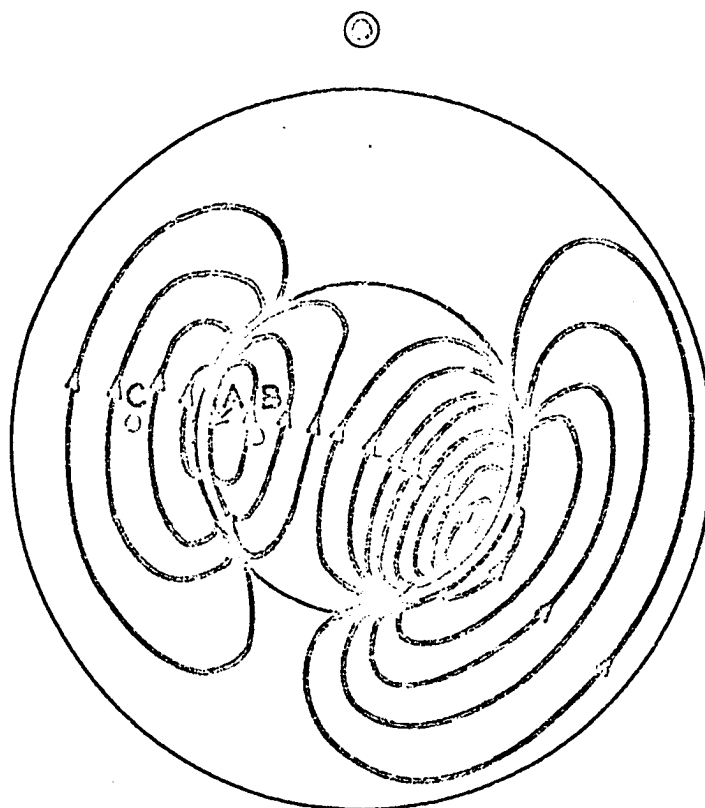


Fig. III-5. Earlier model current system (schematic) for polar magnetic substorm; view from above dp north pole; the direction of the sun is indicated.

was later extended by Vestine (1944). By use of all-sky camera photographs at 42 stations in the northern hemisphere obtained during the IGY, Feldstein and Solomatina (1961) obtained isoauroras, lines of equal frequency of the overhead appearance of auroras (Fig. III-6). Based on data from five Alaskan all-sky camera stations, Davis (1962) defined the term "incidence" signifying the total number of auroral lower borders appearing on the meridional segment  $60^\circ$  to  $70^\circ$  each hour as determined by counting the lower borders at 5-minute intervals, (Fig. III-7). According to this definition, the center line of the auroral zone is between dp lat  $66^\circ \sim 67^\circ$  over Alaska.

The geometric form of the aurora shows great variety. The simplest type of aurora is a band called the homogeneous arc, which appears as an east-west extended parallel arc with nearly homogeneous brightness along its horizontal extent. Any feature in addition to this simplest form is an indication of activity (Table III-1):

	<u>Additional Features:</u>	<u>Called:</u>
	Rays	Rayed arc
Homogeneous arc plus	Waves or folds	Homogeneous band
	Rays, waves or folds	Rayed band
	Pulsations	Pulsating arc or band

The typical auroral displays seen at a single station along and near the auroral zone can be summarized into a "cycle". Such a cycle consists of three phases which are typified by quiet homogeneous arcs, active rayed arcs and isolated cloud-like auroral patches, respectively. Before midnight an arc may be seen on the northern horizon and is gradually moving toward the station as night progresses. Near midnight, a sudden increase of brightness occurs, and the quiet arc breaks into irregular forms together with very

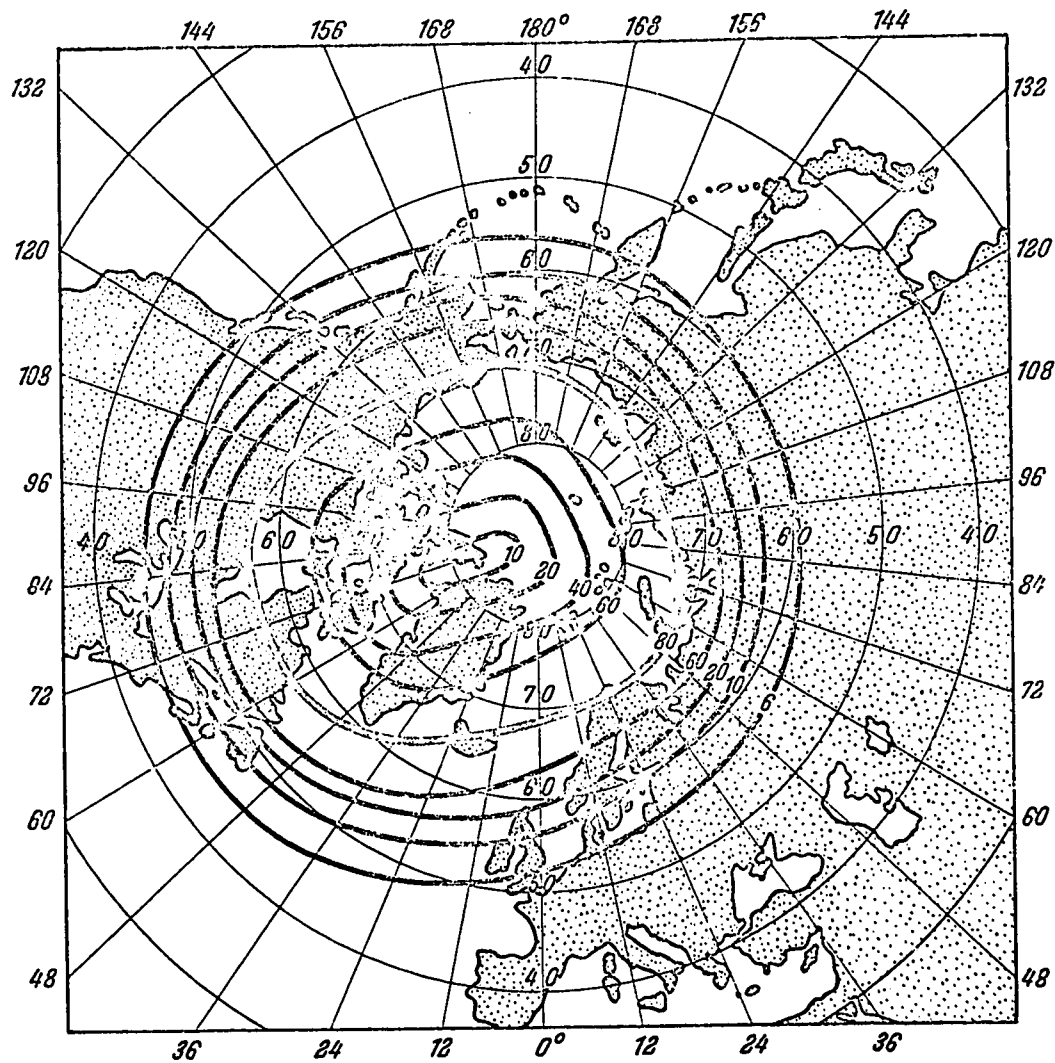


Fig. III-6. Isoaurores in the northern hemisphere. (After Feldstein, Y.L., and E. K. Solomatina, 1961 [18].)



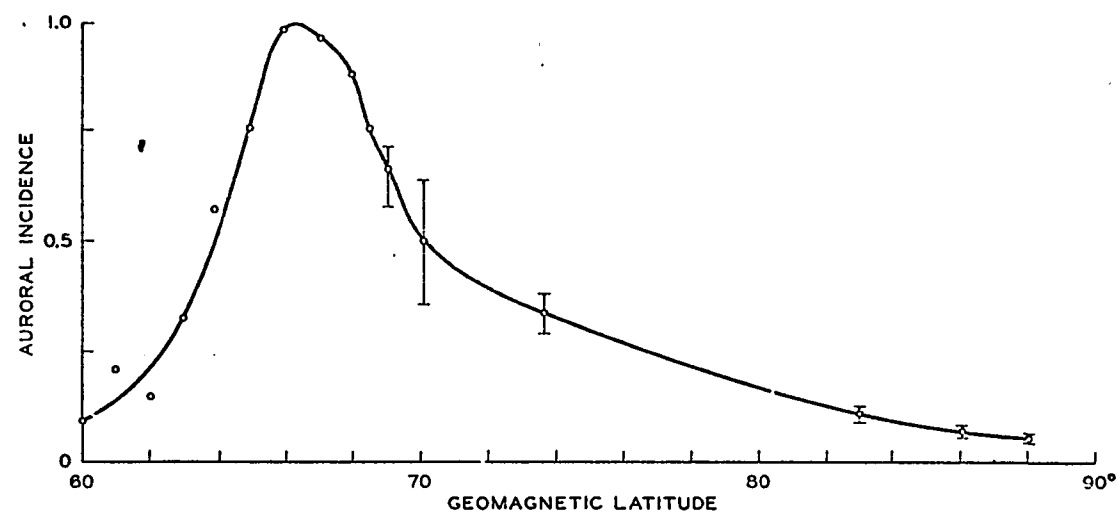


Fig. III-7. Average curve of auroral incidence versus geomagnetic latitude (60°-90°). (After Davis, T. N., 1962).

violent and complicated motion. After this break-up phase, in the morning hours, auroral patches cover the whole sky. This display can be thought of as an average pattern of auroral forms fixed in space above the auroral zone while the earth rotates under it once a day.

## 2. Polar Substorms

The auroral zone established in the last section should be understood as a statistical concept based on data spanning many decades. Thus, the instantaneous location of the auroras may greatly differ from the location of the auroral zone. Based on the IGY/C all-sky camera data, the studies of Feldstein (1960), Davis (1961) and Khorosheva (1962) clearly show that at a particular instant auroras tend to be distributed in a belt which does not coincide with the auroral zone. In order to avoid confusion between such an instantaneous location and the statistically determined auroral zone, the term auroral oval or auroral belt is used to signify the former. The center of the oval is appreciably displaced from the auroral zone towards the darkside, roughly along the midnight meridian. Individual arcs or bands do not necessarily extend all around the oval. On the average the largest number of arcs or bands are seen in the midnight sector; this, together with the fact that the average latitude of the oval in the midnight sector is about  $67^\circ$  dp, results statistically in the auroral zone lying approximately along the dp lat circle  $67^\circ$ . Thus, the auroral zone coincides approximately with the average location of this oval only in the midnight sector where the auroras appear most frequently; because of the rotation of the earth, the geographical locus of active aurora, which by definition is the auroral zone, has a nearly circular pattern. Based on this new natural frame of reference for the polar geophysical phenomena, namely the

auroral oval, the investigations of polar magnetic disturbances and auroral displays entered into a new era.

1) Polar magnetic disturbances (polar magnetic substorm) and its revised equivalent current

From more abundant polar magnetic records obtained during the IGY, an important revision of the pattern of polar magnetic substorms, namely that the polar electrojet is usually westward in all longitudes, and lies along a closed oval curve which is not concentric with the auroral zone, is discussed. Such a westward electrojet produces negative bays under it, and near it on either side, in all longitudes.

There is, however, also a significant current departing from the main westward jet, and flowing from the afternoon sector across the midnight meridian and rejoining the electrojet in the morning sector. Figure III-8 shows this situation schematically. Such a 'return' current produces positive bays over a large part of the earth's surface. Such positive bays observed in the afternoon sector near the auroral zone were previously taken to imply the presence of the eastward polar electrojet shown in Figures III-2 and III-5.

Thus, the main revision made here concerns the afternoon sector. There are at least two ways to examine the two models shown in Figure III-5 and Figure III-8, respectively. In the early model current system (Fig. III-5), the positive bay observed during polar magnetic substorms in the afternoon and evening sectors not far outside the auroral zone, was supposed to complete its circuit by the westward return current over the polar cap and in subauroral latitudes. Thus, when a positive bay is observed in the auroral zone, say at point A in Figure III-5, a less intense negative bay should be

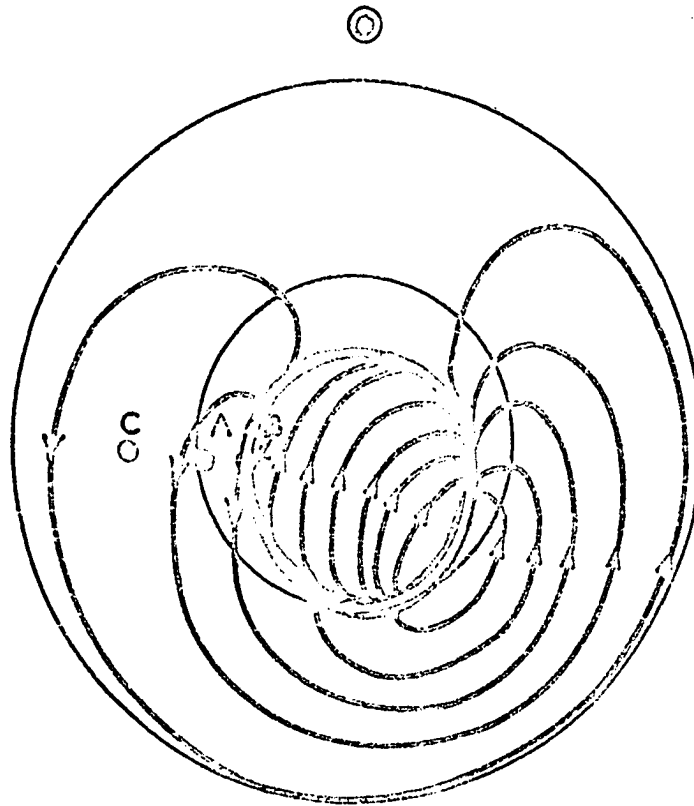


Fig. III-8. Revised model current system (schematic) for polar magnetic substorm; view from above dp north pole; the direction of the sun is indicated.

observed at the points B and C in Figure III-5. But according to the revised model, a more intense negative bay should be observed at B and a less intense positive bay at C.

(a) Negative bay at point B

The IGY data show many cases in which there was a more intense negative bay on the adjacent poleward side of the auroral zone when positive bays were recorded near the auroral zone. Figure III-9 shows one example of this by magnetic records from ten stations in Alaska, from Cape Wellen (Siberia) and from Macquarie Island (New Zealand) on September 26, 1958 (Wescott and Mather (1965)). At the Alaskan stations between dp latitudes  $66^{\circ}$  and  $60^{\circ}$  (Fig. III-10), outside the auroral zone, there were positive bays of order 100  $\gamma$  during the local evening hours from 0200 UT (= 1600 LT) onward; but between 0440 and 0900 UT the records at Barter Island (dp lat  $70^{\circ}$ ) showed larger negative changes. We interpret this as indicating a westward electrojet lying within the zone. Consistent with this, the records of the intervening stations Fort Yukon (dp lat  $66.7^{\circ}$ ) and Barrow (dp lat  $68.6^{\circ}$ ), in the region where the current changes sign, are neither definitely positive or negative. Positive bays which occurred a little after 0200 UT are seen at most of the Alaskan stations, including Barter Island. We interpret this to be due to the eccentricity of the flow pattern with respect to the auroral zone; this will be discussed later.

The existence of such a westward electrojet, has been confirmed by such evidence in about a hundred individual polar magnetic substorms. They were examined by records from two groups of magnetic stations: (i) Murchison Bay (dp lat  $75.3^{\circ}$ ), Kiruna (dp lat  $65.3^{\circ}$ ), and Tixie Bay (dp lat  $60.5^{\circ}$ ), (ii) Baker Lake (dp lat  $73.8^{\circ}$ ), Churchill (dp lat  $86.6^{\circ}$ ) and Kiruna.

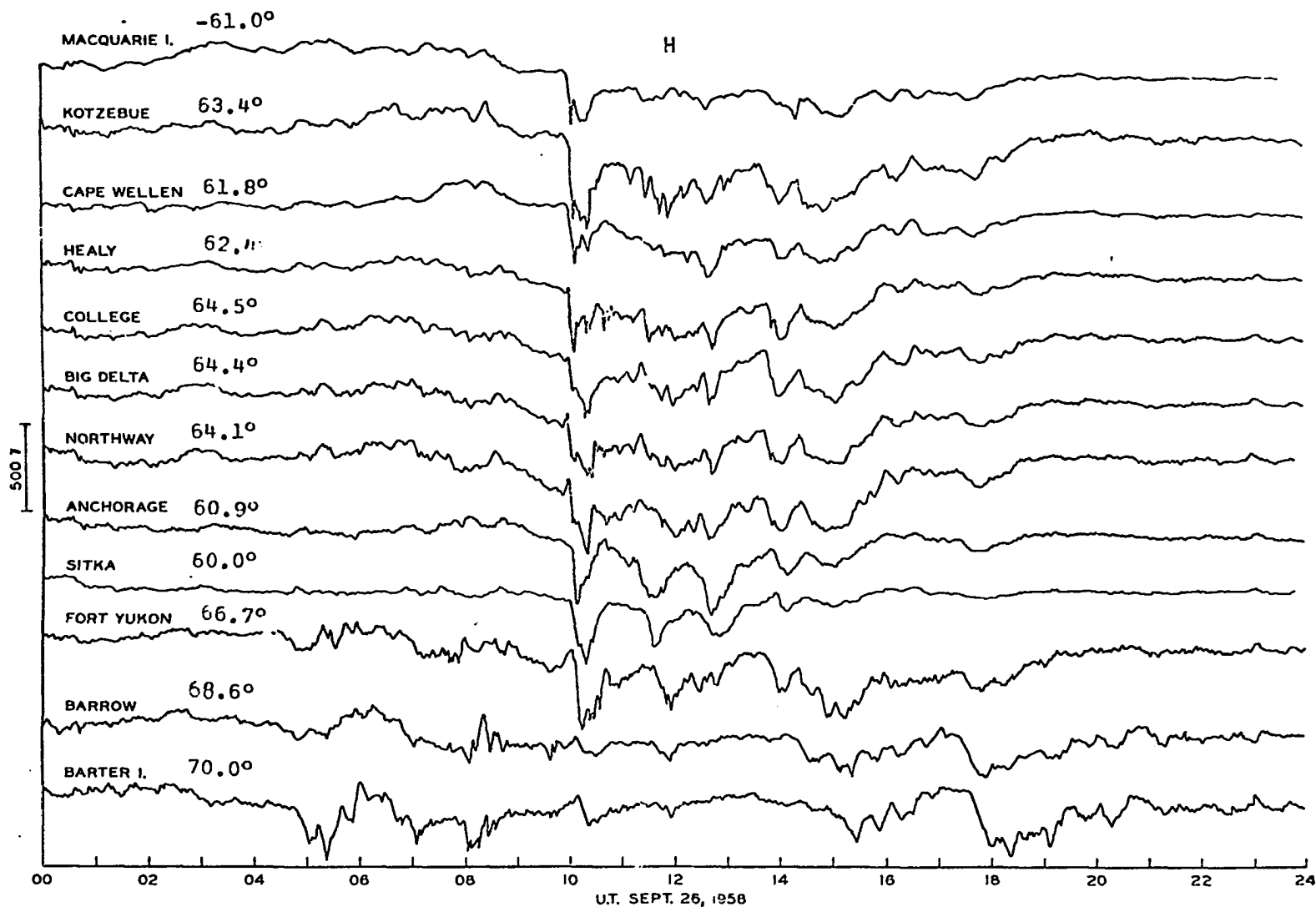


Fig. III-9. Magnetic records (H) on 26 Sept. 1958 (UT) from ten Alaskan Stations, Cape Wellen (Siberia) and Macquarie (New Zealand) (After Wescott and Mather, 1965).

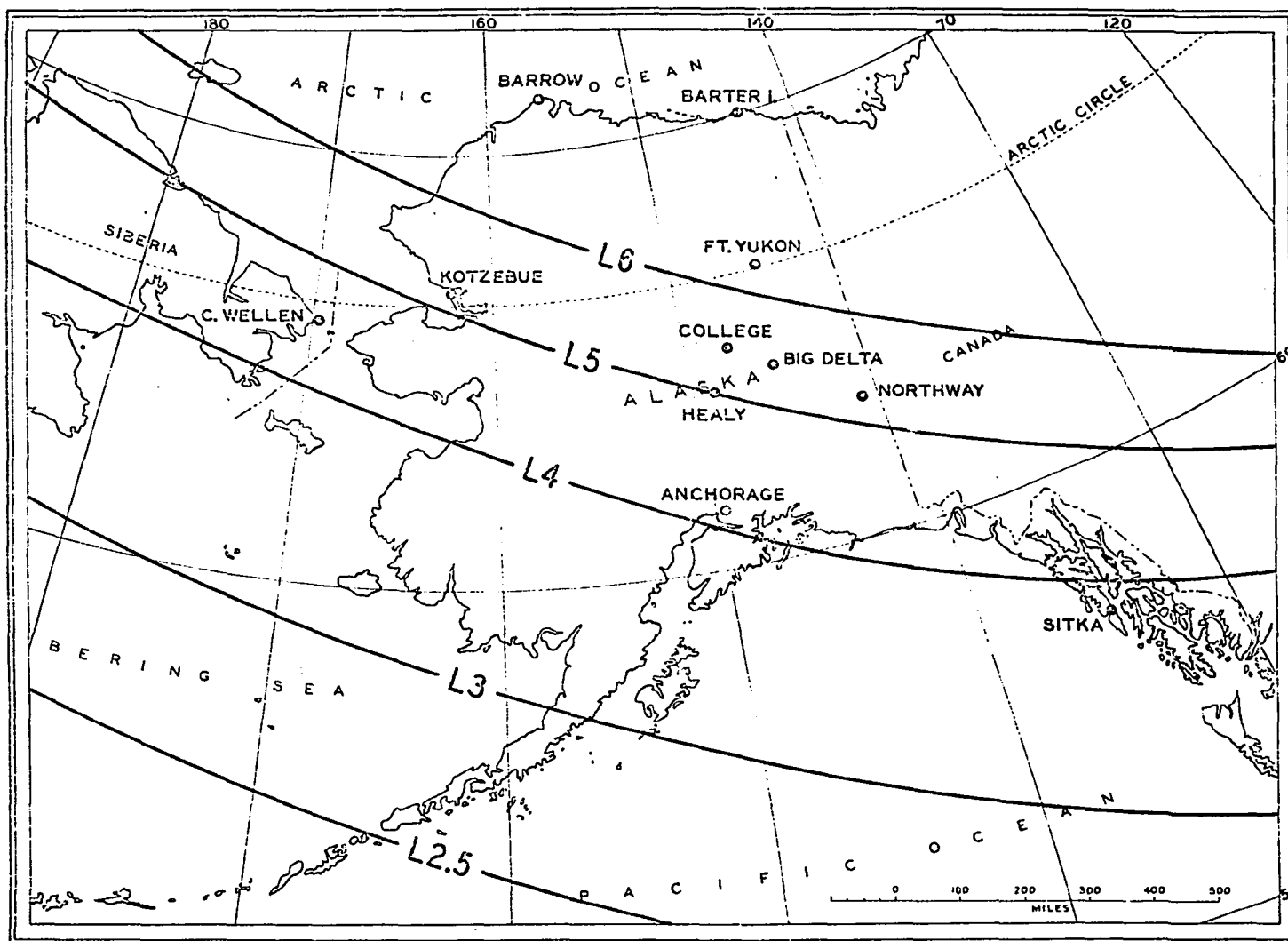


Fig. III-10. Location of the ten Alaskan magnetic stations and of Cape Wellen (Siberia), whose records are used in Fig. III-9, together with McIlwain's curves  $L = 2.5; 3, 4, 5$  and  $6$ , [after Wescott and Mather (1965)].

A third group, Godhavn (dp lat  $79.9^\circ$ ), Reykjavik (dp lat  $70.2^\circ$ ) and Kiruna, was also used to supplement the study. The distribution of the magnetic stations whose data are used here is shown in Figure III-11.

In each group the first station is located well inside the polar cap, the second station is near the same dipole meridian and a little south of the auroral zone. The records were examined at the hours of UT when the first two stations (corresponding to the points B and A in Figure III-8, respectively) were located in the afternoon sector, while the third station was in the late evening or the midnight sector; this choice made it possible to confirm the simultaneous presence of westward electrojets in the midnight and afternoon sectors.

Two examples from this large number of substorms are illustrated here. The first, between 1500 and 1900 UT on April 30, 1958 (Fig. III-12), showed as a negative bay at Murchison (at 1750 LT;  $\sim 450 \gamma$ ) and at Tixie (at 0045 LT;  $\sim 550 \gamma$ ). Its maximum intensity at Tixie Bay was at 1645 UT, but at Murchison Bay it was at 1650 UT; such a delay, up to 10 to 15 min, is common between the two stations in this particular situation. At Kiruna, however, the substorm showed as a positive bay with its peak ( $\sim 350 \gamma$ ) at 1745 LT. Such time differences indicate that the magnetic substorm does not grow uniformly over the entire polar region. This will be discussed later in connection with the growth of the auroral substorm. This conclusion also indicates that at least several equivalent current diagrams should be obtained with a time interval of a few minutes in order to follow the full development of a single polar magnetic substorm. Such a polar substorm is investigated in the next chapter in conjunction with low latitude negative bays. An equivalent current diagram obtained by hourly mean values,



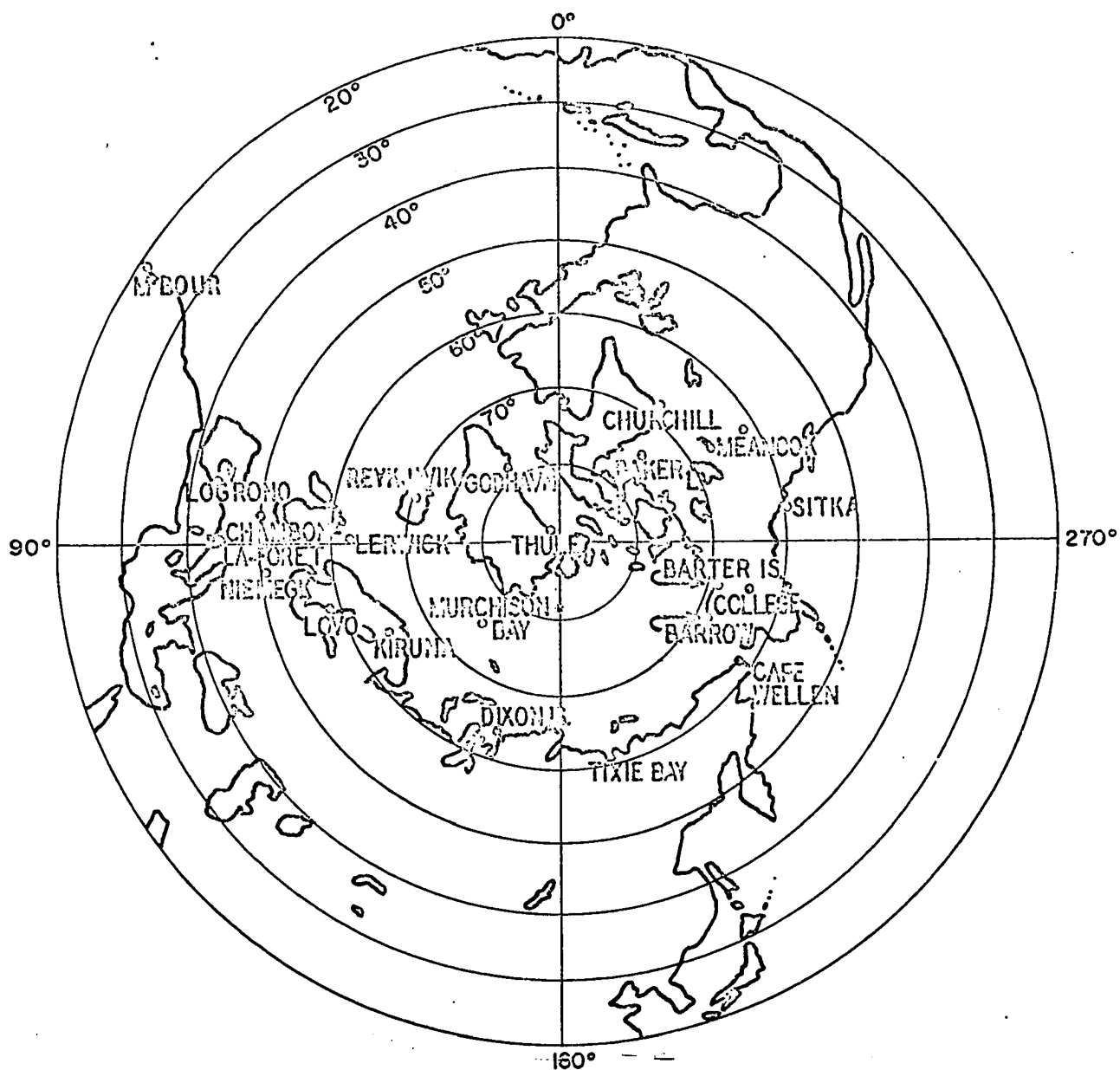


Fig. III-11. Locations of magnetic stations in the dp coordinate system, whose records are used in this section.

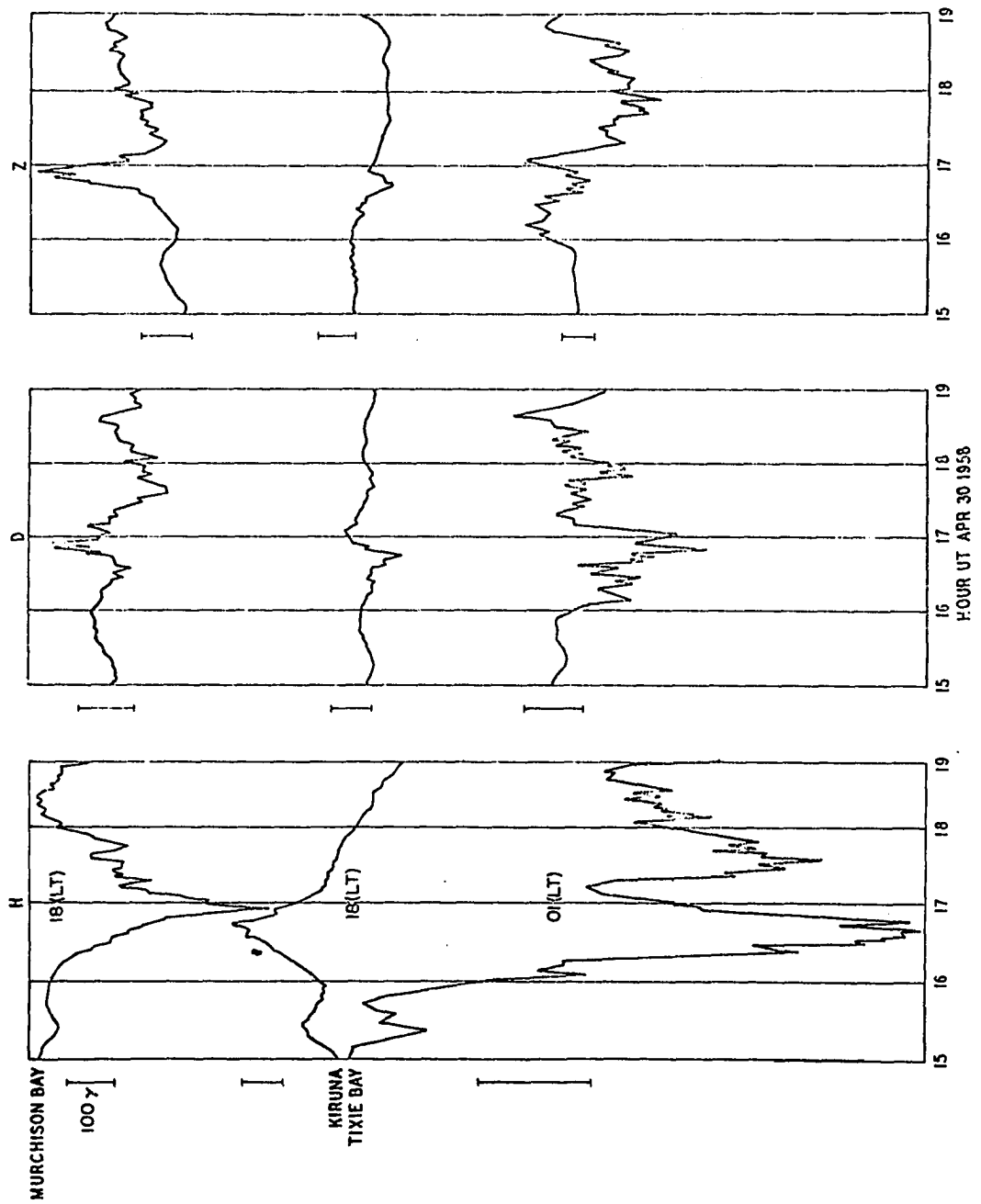


Fig. III-12. Simultaneous magnetic records from Murchison Bay, Kiruna and Tixie Bay between 1500 and 1900 UT on 30 April 1958; the local time at 1700 UT at

or only a single current diagram to represent the whole polar magnetic substorm, may sometimes be misleading.

The second substorm, at about 14 UT on January 19, 1958 (Fig. III-13), showed as a negative bay at Murchison (15 LT;  $\sim 300 \gamma$ ) and at Tixie (22 LT;  $\sim 500 \gamma$ ), but as a positive bay at Kiruna (15 LT;  $\sim 150 \gamma$ ).

(b) Positive bays at point C

According to the earlier model, the return current from the eastward jet should be westward and hence should produce a negative bay in the interzonal belt in the same sector, at such a point as C in Figure III-8. However, if the positive afternoon and evening bays in the auroral zone are caused by the return current of a westward jet somewhat farther north, the stations south of C should also record positive afternoon bays of less intensity. This agrees with Figure III-14 which shows simultaneous H records from Murchison Bay, Kiruna, Lovö (dp lat  $58.1^\circ$ ), Chambon-la-Forêt (dp lat  $50.4^\circ$ ), Logrono (dp lat  $45.4^\circ$ ) and M'Bour (dp lat  $21.3^\circ$ ) from 1200 UT April 17 to 0600 UT April 18, 1958; all the stations are located approximately in the same sector (Fig. III-11). The intense negative bay ( $\sim 600 \gamma$ ) recorded at Murchison Bay at about 1545 UT cannot be due to a return current from the weaker eastward current causing the positive bay ( $\sim 250 \gamma$ ) at Kiruna. Also, the positive bays observed at the same time at Lovö, Chambon-la-Forêt, Logrono and M'Bour, indicate an extensive eastward return current existing as far south as dp lat  $20^\circ$ . After 1700 UT the intermittent westward jet moved somewhat southward and produced successive negative bays at Kiruna. At Chambon-la-Forêt, Logrono and M'Bour, the corresponding changes were mostly positive bays and Lovö then lay in the intervening region of current reversal.

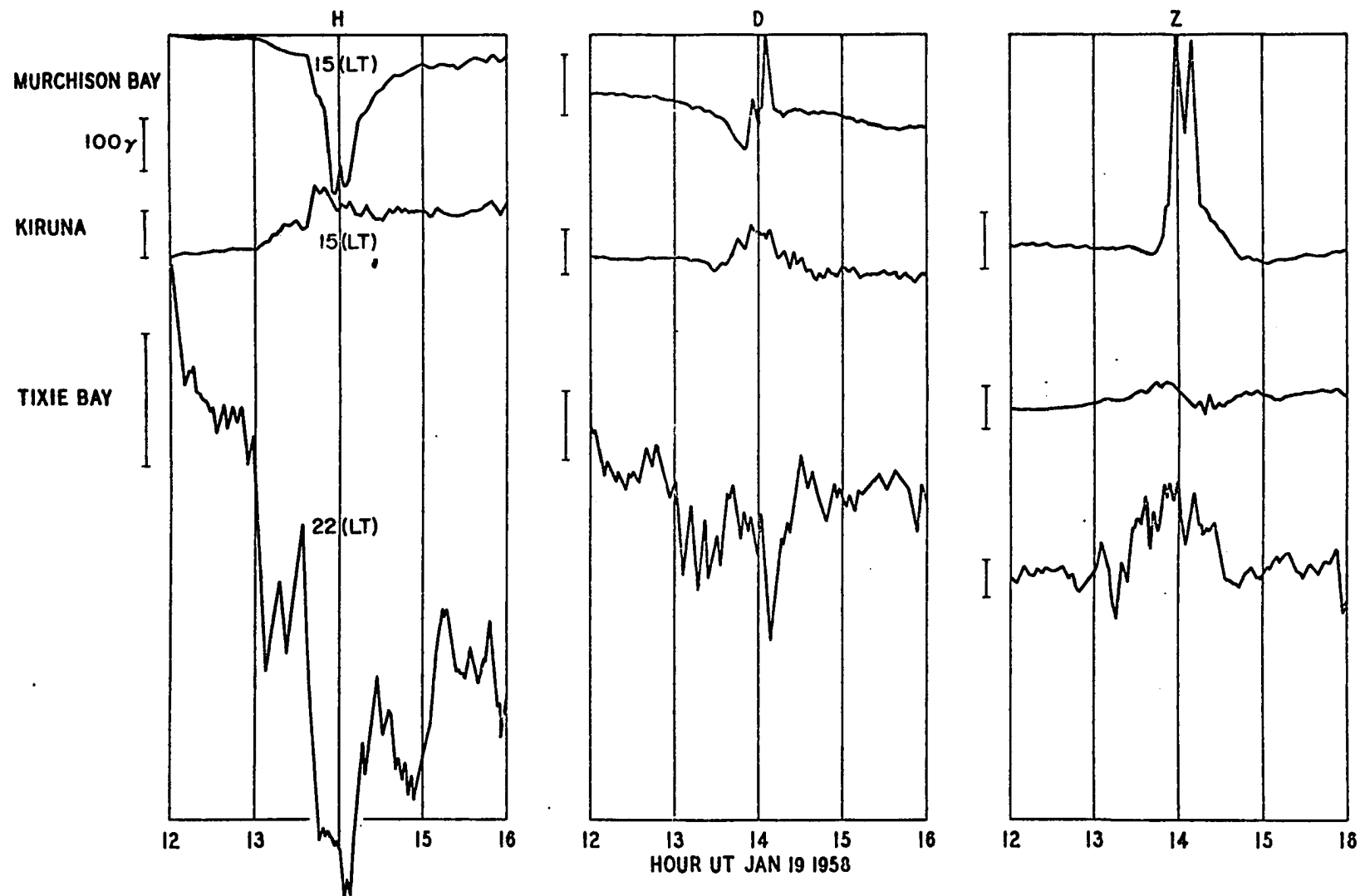


Fig. III-13. Simultaneous magnetic records from Murchinson Bay, Kiruna and Tixie Bay between 1200 and 1600 UT on 19 January 1958; the local time at 1400 UT at each station is indicated.

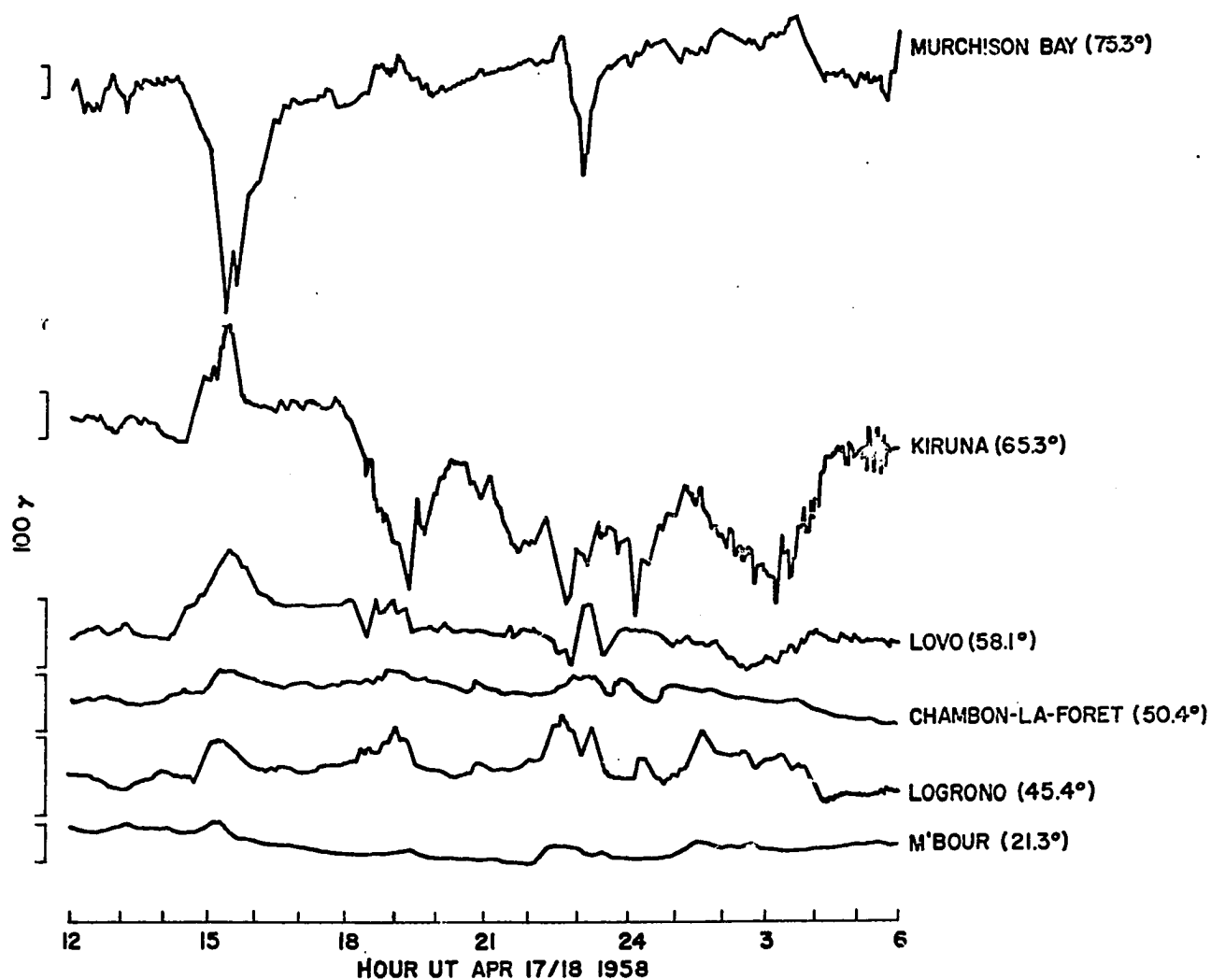


Fig. III-14. Simultaneous magnetic records from Murchison Bay, Kiruna, Lovo, Chambon-La-Foret, Logrono and M'Bour between 1200 and 0600 UT on 17/18 April 1958. All the stations are located approximately in the same sector (see Fig.III-11), so that their local times do not differ much from UT.

A few cases were found of positive bays at Kiruna more intense than simultaneous negative bays at Murchison. This can occur, consistent with the model of Figure III-8, if the jet is not located close to B. In those cases the Z component at Murchison Bay shows a large change whose sign indicates that the westward jet lies still farther to the north or south. Such complexity of the geometry of the jet is discussed later in connection with the associated auroral motions. However, the stations in lower latitudes are well removed from such a complexity, and such cases support the model in Figure III-8 particularly clearly.

(c) Feldstein's equivalent current system

Feldstein (1963, 1964) has studied the extensive IGY magnetic records to ascertain the average distribution of geomagnetic disturbance over the polar cap. From Thule (dp lat  $88.9^\circ$ ), Resolute Bay (dp lat  $83.0^\circ$ ), Godhavn, Murchison Bay, Baker Lake, Tikhaya Bay (dp lat  $71.5^\circ$ ), Chelyuskin (dp lat  $65.9^\circ$ ), Dixon (dp lat  $63.0^\circ$ ), Tromso (dp lat  $67.0^\circ$ ), College and Lerwick (dp lat  $62.5^\circ$ ), he obtained average disturbance vectors by subtracting the quiet day hourly mean values from the all-days mean daily variation values in the IGY winter months (Fig. III-15). His diagram clearly indicates larger disturbance vectors directed equatorward between dp lat  $70^\circ$  and  $80^\circ$  than those directed poleward in the auroral zone in the afternoon sector. However, he drew current lines similar to those in the earlier model, although his material is more consistent with the revised model of Figure III-8.

(d) The westward electrojet in the noon sector

Feldstein's diagram (Fig. III-15) also shows a moderate westward current flowing between dp lat  $70^\circ$  and  $80^\circ$  in the noon sector, but surprisingly only a weak current in the auroral zone. As an example, Figure III-16 shows

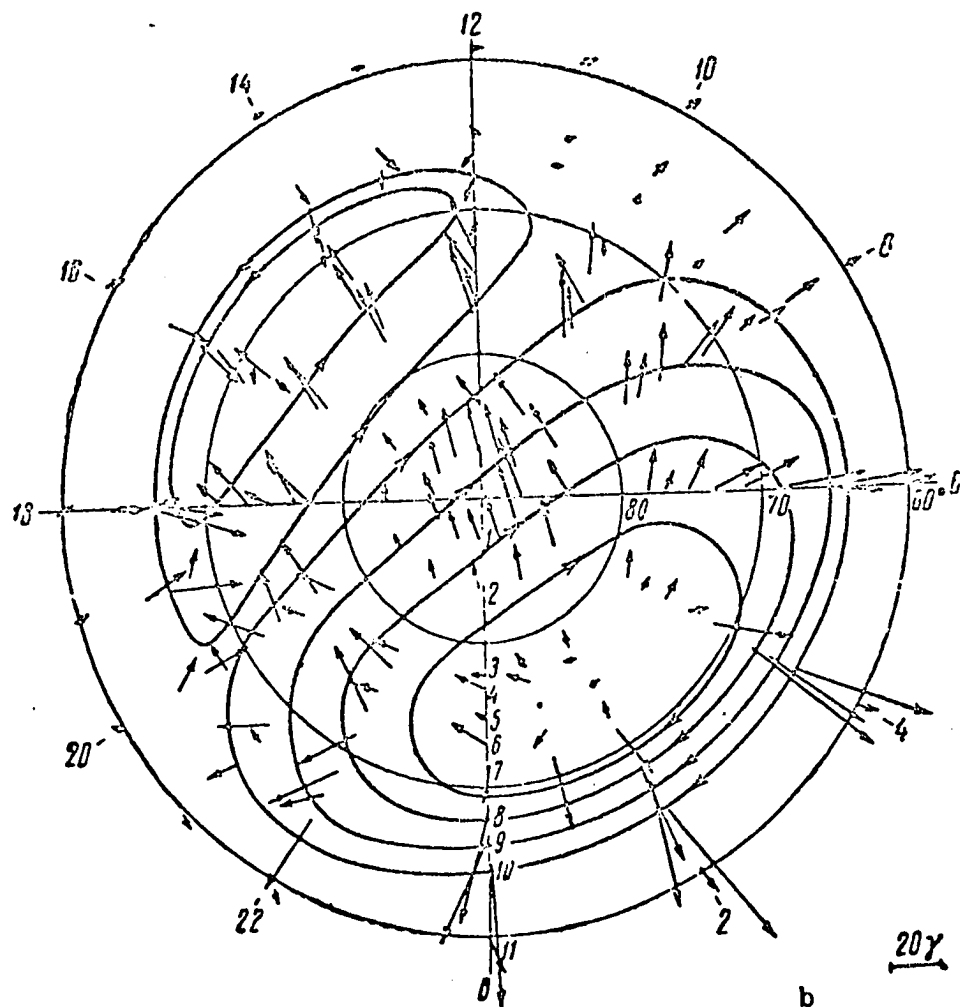


Fig. III-15. Average disturbance vectors obtained by subtracting the quiet day hourly mean values from the all-day mean daily variation values, in the IGY winter months; view from above dp north pole (after Feldstein, 1963).

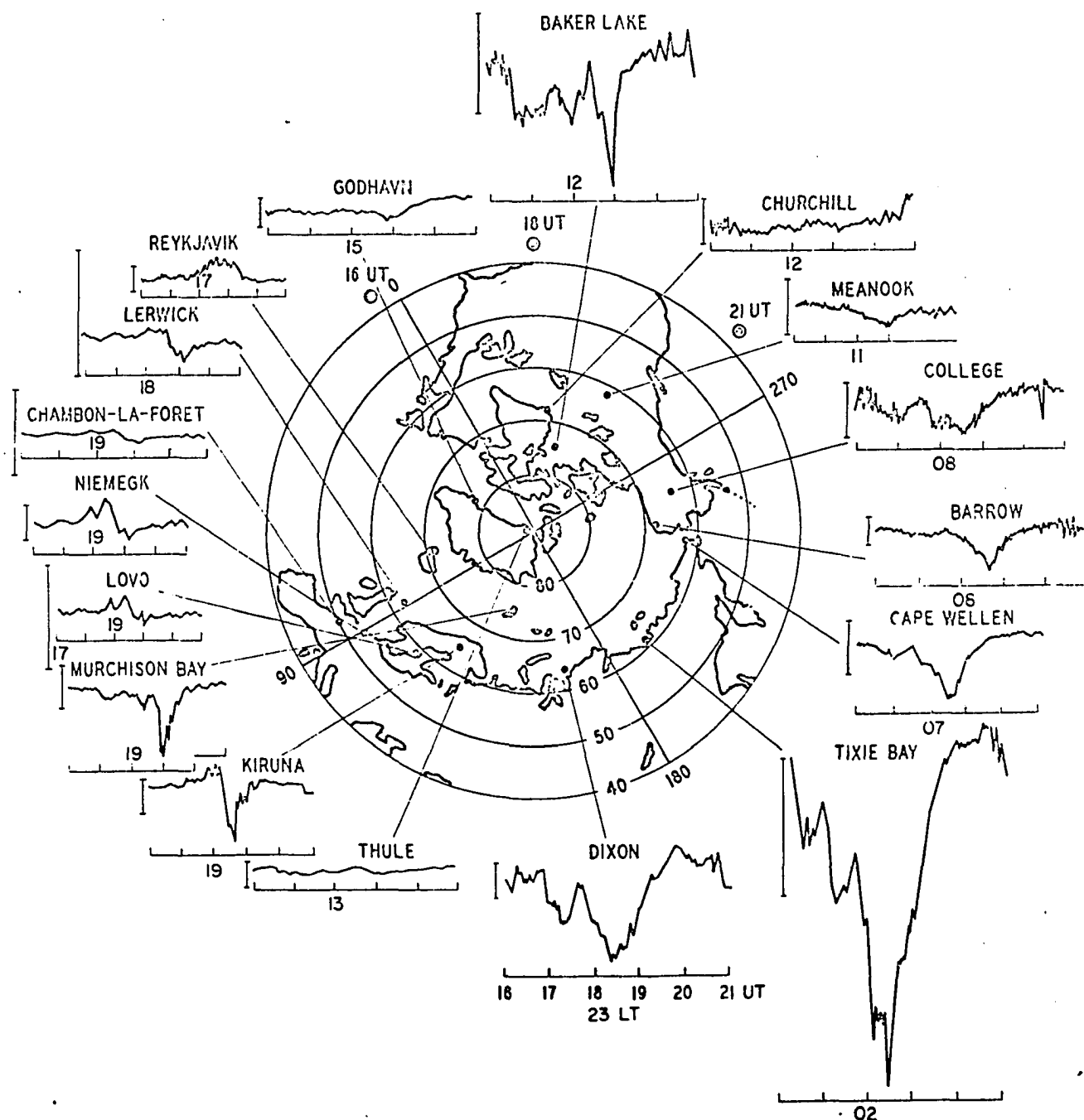


Fig. III-16. Simultaneous magnetic records between 1600 and 2100 UT on 16 Dec. 1957 from a number of stations in the northern hemisphere; view from above the north pole; the direction of the sun at 1600, 1800 and 2100 UT is indicated, and also the local time at each station at 1800 UT; scale = 200 Y.



simultaneous H or X records of a polar magnetic substorm that occurred between 1800 and 2100 UT, on December 16, 1957 from a number of stations. In the midnight sector (Dixon and Tixie Bay), it showed as a negative bay of order 500  $\gamma$ , most intense at about 1830 UT. In the early morning sector, it showed as a less intense negative bay in the auroral zone at Cape Wellen, College, Barrow and Meanook. In the afternoon sector of the auroral zone, it showed as a positive bay of order 100  $\gamma$  at Reykjavik, and as a combination of a positive and negative bay at Kiruna. At Murchison Bay, it appeared as a negative bay of more than 300  $\gamma$ , although there was a delay of almost 30 minutes in the epoch of its maximum intensity there, as compared with that in the midnight sector. In the noon sector of the auroral zone (Churchill), there was very little systematic variation. However, at Baker Lake the disturbance was strikingly similar to that at Murchison Bay (note the difference in the sensitivity of their records). This is a common feature in this latitude, suggesting that the westward jet in the afternoon sector extends to the noon sector. Since Thule and Godhaven, both of them well inside the auroral cap, show no comparable disturbance, it would seem that most of the westward jet flows roughly along  $dp$  latitude circles in the noon sector, instead of returning over the  $dp$  pole. This is borne out by the corresponding changes in the Y component, which at Baker Lake show no systematic change; also Feldstein's disturbance vectors between  $dp$  lat  $70^\circ$  and  $80^\circ$  are roughly radial.

(e) The revised model of the equivalent current systems

Based on these studies, it is proposed that the westward current, which flows between  $dp$  lat  $70^\circ$  and  $80^\circ$  in the evening and afternoon sectors and which produces an eastward return current and thus a positive bay in the

auroral zone and also in the interzonal zone in the same sectors, is an extension of the westward auroral electrojet flowing along the auroral zone in the midnight sector; furthermore the westward jet causing negative bays between  $dp$  lat  $70^\circ$  and  $80^\circ$  in the noon sector is a further extension of this jet. A significant portion of the westward jet should thus circulate along an oval belt encircling the  $dp$  pole, although its center is appreciably shifted from the geomagnetic pole towards the dark hemisphere approximately along the sun-earth line. The proposed model current system is schematically shown in Figure III-17.

Figure III-17 is to be taken as showing only a gross average pattern of the current system for the polar magnetic substorm. A more detailed quantitative study of the distribution of the intensity of both the jet and its return current is obviously necessary. This requires one or more close N-S chains of magnetic stations. The polar magnetic substorm does not grow uniformly and simultaneously over the entire polar cap; particularly in the early growing state of the substorm the current pattern may change considerably even in a few minutes. The westward jet may shift rapidly poleward or equatorward even during a single event. This is one of the remarkable features of the jet in the midnight sector; Akasofu (1960) showed that in some cases the jet moved northward or southward with a speed of order 1 km/sec, in accordance with the corresponding motions of the aurora.

In Figure III-16 a somewhat different appearance of the same polar magnetic substorm can be seen along the flow lines of the jet. In the midnight sector, the negative bays have the largest magnitude and a well-defined beginning; in the morning sector, it is much less intense and is not well defined; rapid fluctuations of the disturbance field are superposed on it.

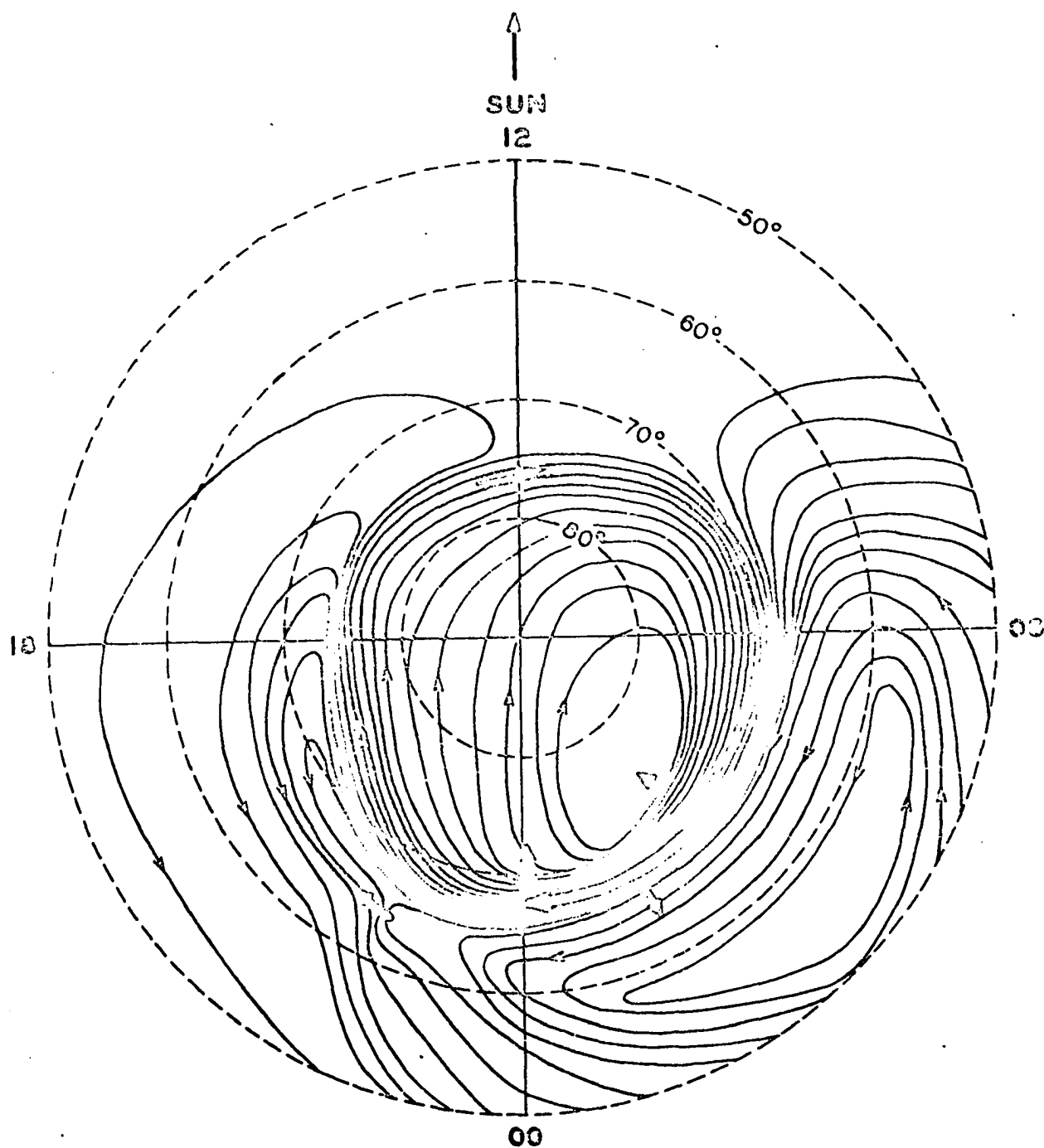


Fig. III-17. Revised model current system for an intense polar magnetic substorm; view from above dp north pole; the direction of the sun is indicated at the maximum epoch.

In the afternoon and evening sector, it is also less intense, but often well-defined; however, some records show a combination of positive and negative changes. Such complexity can be understood, when the simultaneous development of the auroral substorm and its different appearance at different locations are discussed together.

## 2) The Polar Magnetic Substorm and the Auroral Substorm

### (a) The auroral substorm

During the last few years, a great effort has been made to analyze all-sky camera films obtained simultaneously at a number of stations distributed over the entire polar region (Akasofu (1964)). It is found that the auroral system in the midnight sector of the auroral zone repeatedly undergoes large-scale expansions and contractions, which extend far beyond the field of view of a single station. Such large-scale auroral activity occurs in single events which are called auroral substorms.

Each auroral substorm has a life time of order  $1 \sim 3$  hr, and consists of two phases. It always originates in the midnight sector at the place where quiet arcs exist. The first phase is characterized by a sudden increase in the brightness of the part of a quiet arc that is near the midnight meridian and by subsequent rapid motion of the arc toward the dp pole (Fig.III-18). This expansive phase is rapid, taking place within only about 10-30 min. Within the expanding bulge, except perhaps near its western border, violent eastward motions of auroras are seen.

After a certain lapse of time such abrupt and violent activity affects the aurora in various ways in both the evening and morning sectors. In the evening sector, the expanding bulge is seen as a surge which travels rapidly westward along auroral arcs (the westward traveling surge). In the morning

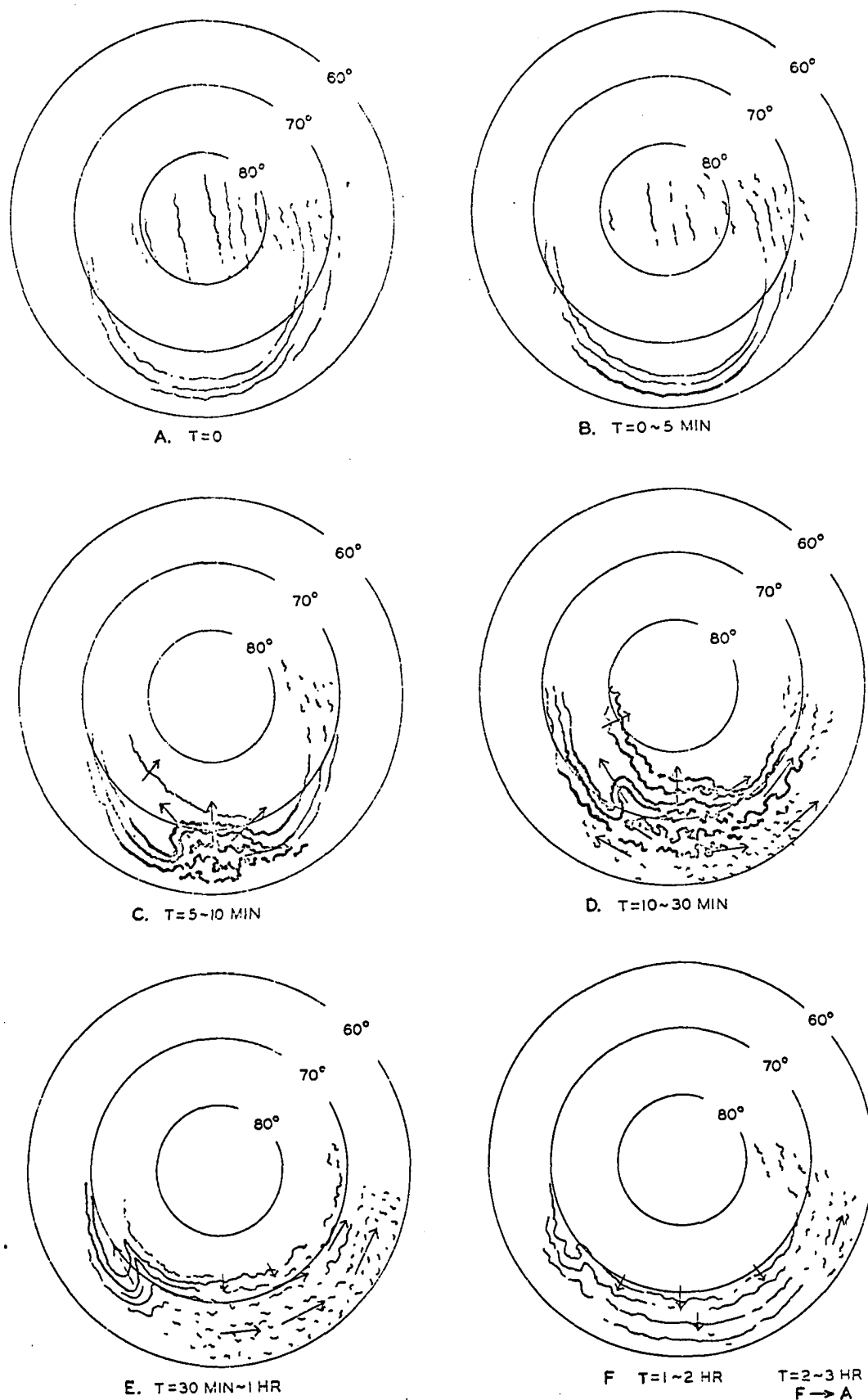


Fig. III-18. Schematic diagram to illustrate the development of the auroral substorm (dp coordinates). The sun is toward the top of the figure.

sector, most of the auroral arcs or bands break up into cloud-like patches, and these patches drift as a whole eastward, like a group of drifting cumulus clouds.

When bands moving rapidly poleward attain their northernmost latitude (in the northern hemisphere) they begin to return to their original location. This is the beginning of the second or recovery phase. During this phase various after effects of the first expansive phase travel toward both the evening and morning sectors. The second phase may last more than two hours; at its end there may be a few quiet arcs in the region where the arcs were originally located just before the auroral substorm began.

(b) The polar magnetic substorm and the auroral substorm

A great number of works have been devoted to a study of the close association of auroral and geomagnetic activity [cf. Heppner (1954)]; they have been reviewed by Akasofu (1965). The progress of the morphological studies of auroral activity, which is now described in terms of the auroral substorm, is a considerable help in understanding the complexity of polar magnetic substorms. This is because the luminosity and the structure of the aurora can be a certain guide to infer the distribution of the ionization, particularly in the E region where the conductivity is highest.

Furthermore, some of the auroral motions can be used to infer the approximate velocity of ionospheric electrons causing the electrojet. Consider an equatorward electric field  $\underline{E}$  is introduced into the auroral ionosphere from outside. In the upper F region of the ionosphere, both positive ions and electrons are gyro-free, so that they drift eastward approximately with a velocity  $\underline{v}$  of

$$\underline{v} = \underline{E} \times \underline{B}/B^2$$

where  $\underline{B}$  denotes the geomagnetic field vector. In the polar region,  $\underline{B}$  is approximately vertical, nearly perpendicular to the ionospheric layer. In this simple situation, both the ions and electrons drift eastward with a speed of  $v \sim E/B$ . The current generated in this situation is small, since there is very little relative velocity between the ions and electrons. But, in the E region, the electrons drift eastward with the above velocity, while the drift motion of the ion is impeded by frequent collisions with neutral particles. The result is a large difference in their relative velocity, an eastward drift motion of the electrons and thus a westward (jet) current (cf. Akasofu (1960)).

Consider two geomagnetic field lines in the midnight meridian separated by a few hundred kilometers at their foot in the auroral zone. Because polar magnetic substorms are strikingly similar at geomagnetic conjugate points [Nagata and Kokobun (1960); Wescott (1962)], and because the conductivity along geomagnetic field lines embedded in the body of the magnetosphere is very high, each field line is likely to be nearly equipotential, with different potentials for the two field lines. The equatorward electric field shown above which is able to produce the westward electrojet implies that the electrostatic potential of the outer field line is less than for the other line. This implies also that the magnetospheric plasma located between the two field lines will have an  $(\underline{E} \times \underline{B})$  drift like the plasma in the plasma in the upper F region. Therefore the eastward drift motion of auroras that is closely associated with the negative bay and thus with the westward electrojet strongly suggests that any magnetospheric source causing auroral electrons participates in the same  $(\underline{E} \times \underline{B})$  drift. Further, recalling that the westward electrojet is essentially due to the  $(\underline{E} \times \underline{B})$  drift motion of the

electrons in the E region, the flow pattern of the westward electrojet should be anti-parallel to that of the associated magnetospheric plasma motion [cf. Hines (1964); Piddington (1964)]. The auroral oval suggests thus an intermittent eastward motion of the plasma shell near the boundary of the co-rotating region of the magnetosphere.

In the central region of an auroral substorm bulge, the eastward drift motion of the aurora is particularly violent, suggesting an intense westward electrojet in this region. Further, Meng (1965) has shown that the jet is likely to be greatly concentrated in the bright auroral bands near the leading edge of the expanding bulge. An explosive growth of the auroral substorm in the midnight sector, together with the existence of highly conductive regions along bright bands, is likely to be associated with the well-defined beginning of an intense negative bay in the midnight sector.

This violent auroral activity travels rapidly towards the morning sector, with diminishing intensity. Auroral arcs or bands in this sector tend to break up into cloud-like patches soon after the onset of the auroral substorm. In a typical case, when the substorm is observed in the morning sector, an auroral band starts to break up into patches from its western 'end' and the resulting patches drift eastward as a whole. In this region, there cannot be a well-defined beginning and a great concentration of westward current, as in the midnight sector.

The onset of the auroral substorm in the midnight sector is immediately recognized in the evening sector, first as a great increase of brightness of the auroral arcs and bands that lie there. Then, the western leading edge of the expanding bulge appears as the westward traveling surge, rapidly and violently folding the brightened arcs or bands. The distribution of the



current in and near the surge seems to be extremely complicated. However, this has an important bearing on the proposed revision of the model current system. Thus, in the next subsection, the surges and associated geomagnetic field changes are discussed in detail.

- (c) The development of the polar magnetic substorm in connection with the growth of simultaneous auroral substorms.

Akasofu (1964) and Akasofu, Kimball and Meng (1965) have shown that the surges traveling westward in the evening sector approximately along the center line of the auroral zone (see Fig. III-10,  $L = 6$  line), are associated with positive bays of order  $100 \gamma$ , at the southern border of the auroral zone, e.g. College ( $64.5^\circ \text{N}$  dp) and more intense negative bays at the northern border of the auroral zone, e.g. Barrow. Figures III-19a and b show an example of a westward traveling surge observed at Fort Yukon and Barrow, respectively, on February 10, 1958. The successive ground projections of the surge recorded at Barrow, Fort Yukon and College are also shown in Figures III-19c, III-19d, III-19e show the geomagnetic field changes recorded at College and Barrow during the surge. The H, Z and D geomagnetic changes are shown in the upper left part of the diagram. From them disturbance magnetic vectors  $d\mathbf{H}$  are determined, for particular instants indicated by numbers, (1, 2,...) along the time-line below the three traces. The disturbance vectors, marked by the corresponding numbers, are shown relative to geomagnetic north (indicated by the mark N) for these parts of the interval. The arms of the cross in each figure all correspond to a magnitude of  $20 \gamma$ . At College the disturbance vectors  $d\mathbf{H}$  associated with the auroral surge all swung rapidly, first counter-clockwise, then clockwise; their greatest magnitude was about  $110 \gamma$ . At Barrow, during the sharp negative bay observed at that time, the maximum

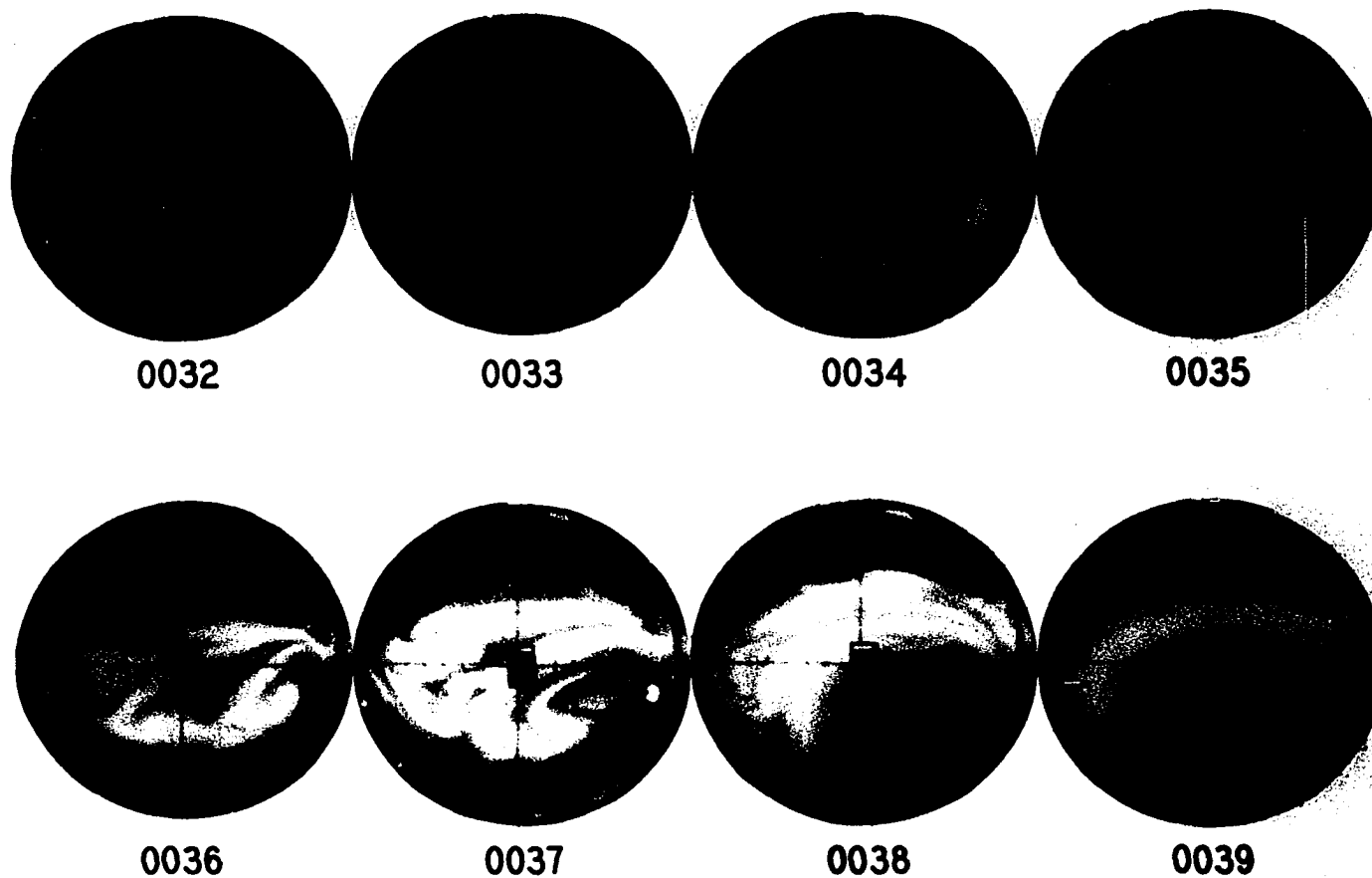
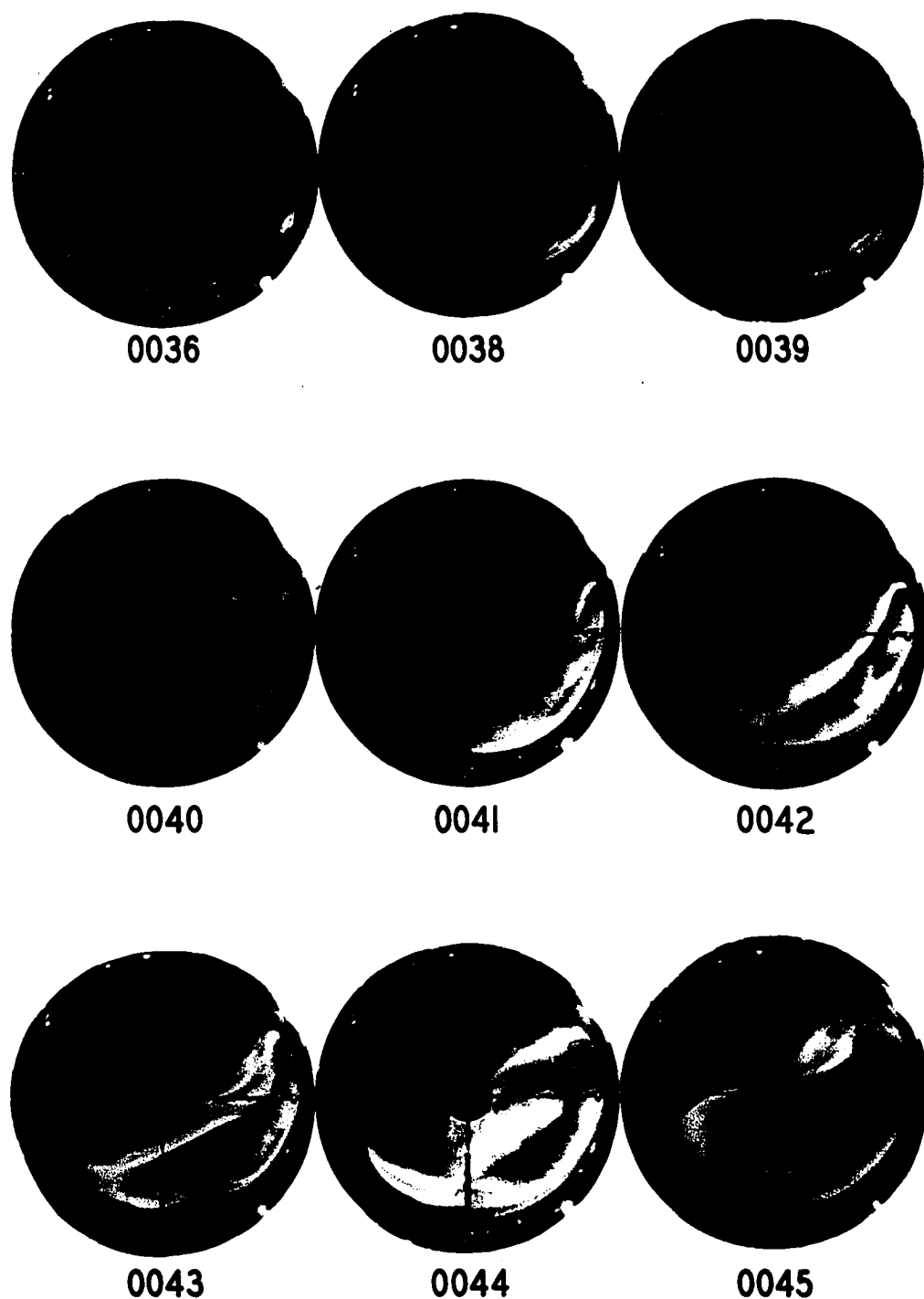


Fig. III-19a. Successive all-sky camera photographs to illustrate the westward traveling surge recorded at Fort Yukon on 10 February 1958 (150°WMT). The direction to the north dp pole is upward.



**Fig. III-19b. Successive all-sky camera photographs to illustrate the westward traveling surge recorded at Barrow on 10 February 1958 (150°WMT). The direction to the north dp pole is upward.**

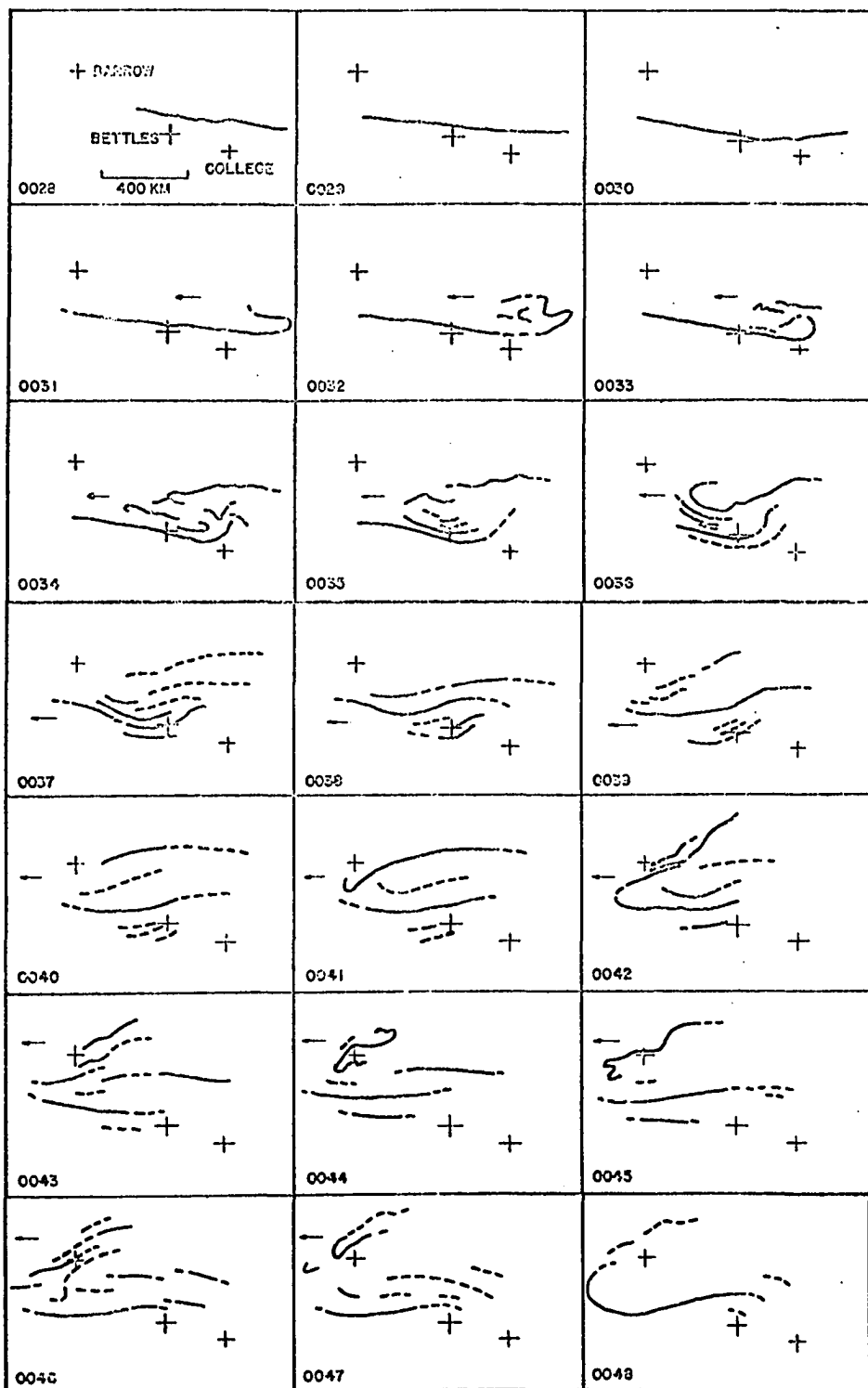


Fig. III-19c. Successive ground projections of the surge illustrated in Figures III-19a and 19b. The locations of the Barrow, Bettles and College all-sky camera stations are indicated by cross-marks.

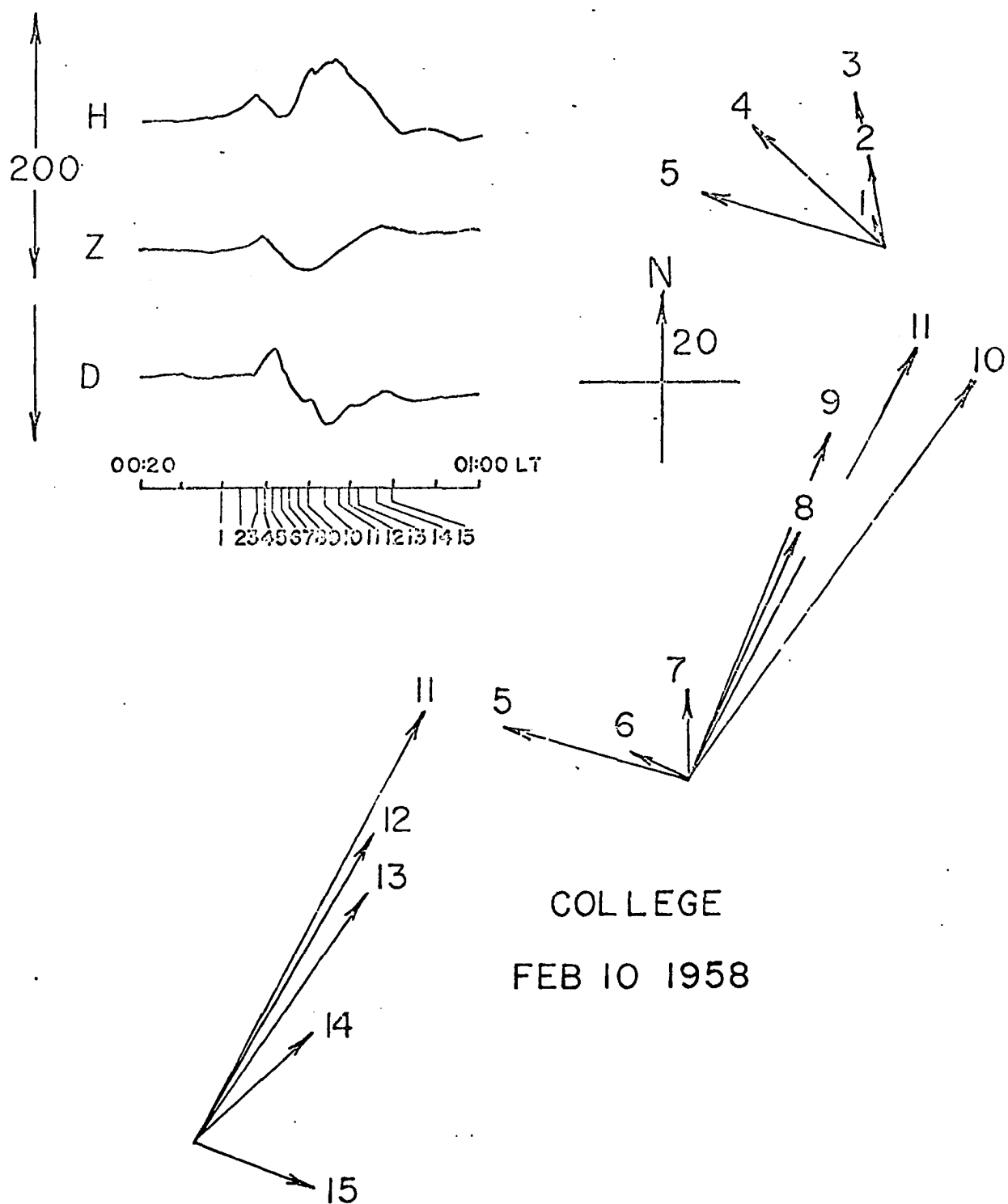


Fig. III-19d. Magnetic records from College during the passage of the westward traveling surge illustrated in Figure III-19a-c).

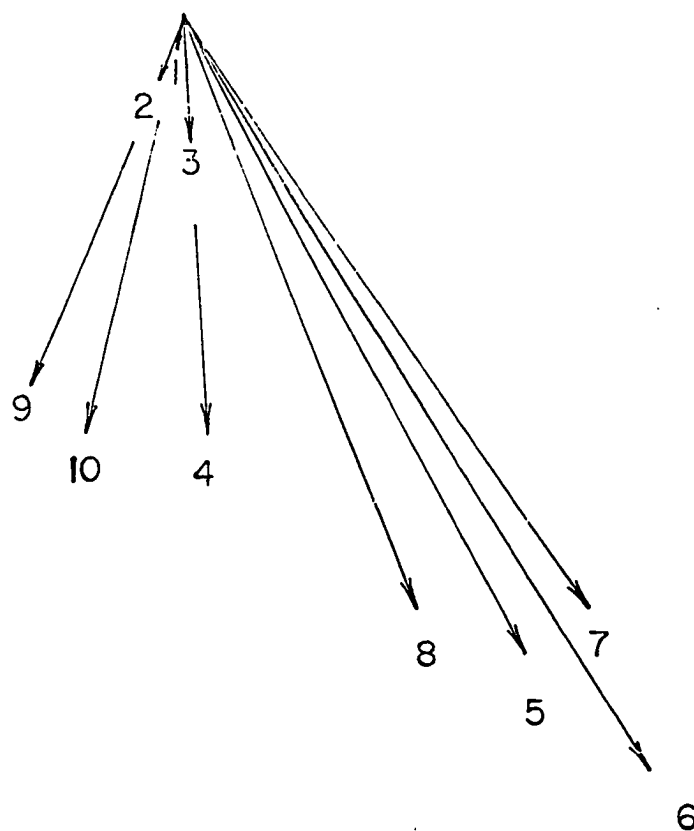
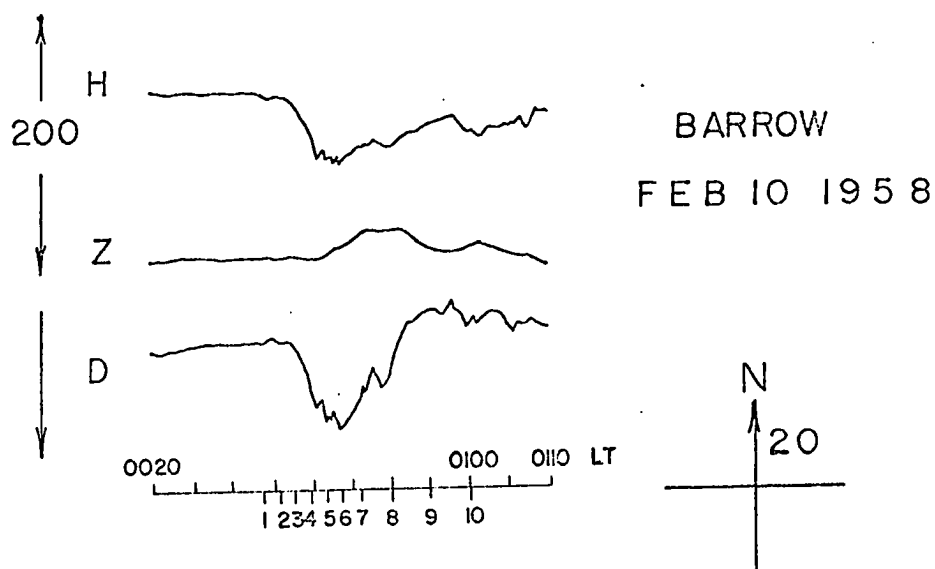


Fig. III-19e. Magnetic records from Barrow during the passage of the westward traveling surge illustrated in Figure III-19a-c.

(negative)  $dH$  was about 220  $\gamma$ , twice as large as the positive  $dH$  at College. The Barrow minimum was delayed by about 5 min after the maximum  $dH$  at College. The successive ground projections of the auroral surges suggest that the delay corresponds to the finite velocity of the surge. A number of similar examples are discussed by Akasofu, Kimball and Meng (1965) and Meng (1965).

Pyramida (dp lat  $74.5^\circ$ ) is an ideal station from which to observe the westward surge, which travels to as far as the early afternoon sector, because its geographic latitude ( $78.2^\circ N$ ) is high enough to enable auroras to be seen there throughout the whole 24 hours, during a few weeks around the winter solstice. The station is located only 200 km SSW of Murchison Bay. Figure III-20 shows all-sky camera photographs (in negative) showing a westward surge during the afternoon of December 13, 1957; it is similar to the surge at Barrow illustrated in Figure III-19b. The associated magnetic change at about 1545 UT at Murchison Bay was a negative bay of order 300  $\gamma$ , and at Kiruna it was a positive bay of order 200  $\gamma$ . A comparison of the above two examples (the first one (Fig. III-19) in the late evening sector and the second one (Fig. III-20) in the afternoon sector) indicated that the westward traveling surge which originated in the midnight sector produced the same type of geomagnetic disturbances along its course, to as far as the afternoon sector; the delay of the peak time of the negative bays at Tixie and at Murchison can be attributed to the finite velocity of the surge.

The development of both auroral and polar magnetic substorms is schematically shown by Figure III-21. The expansion of the bulge is rapid in the morning sector. Even in the dawn sector the same negative bay is

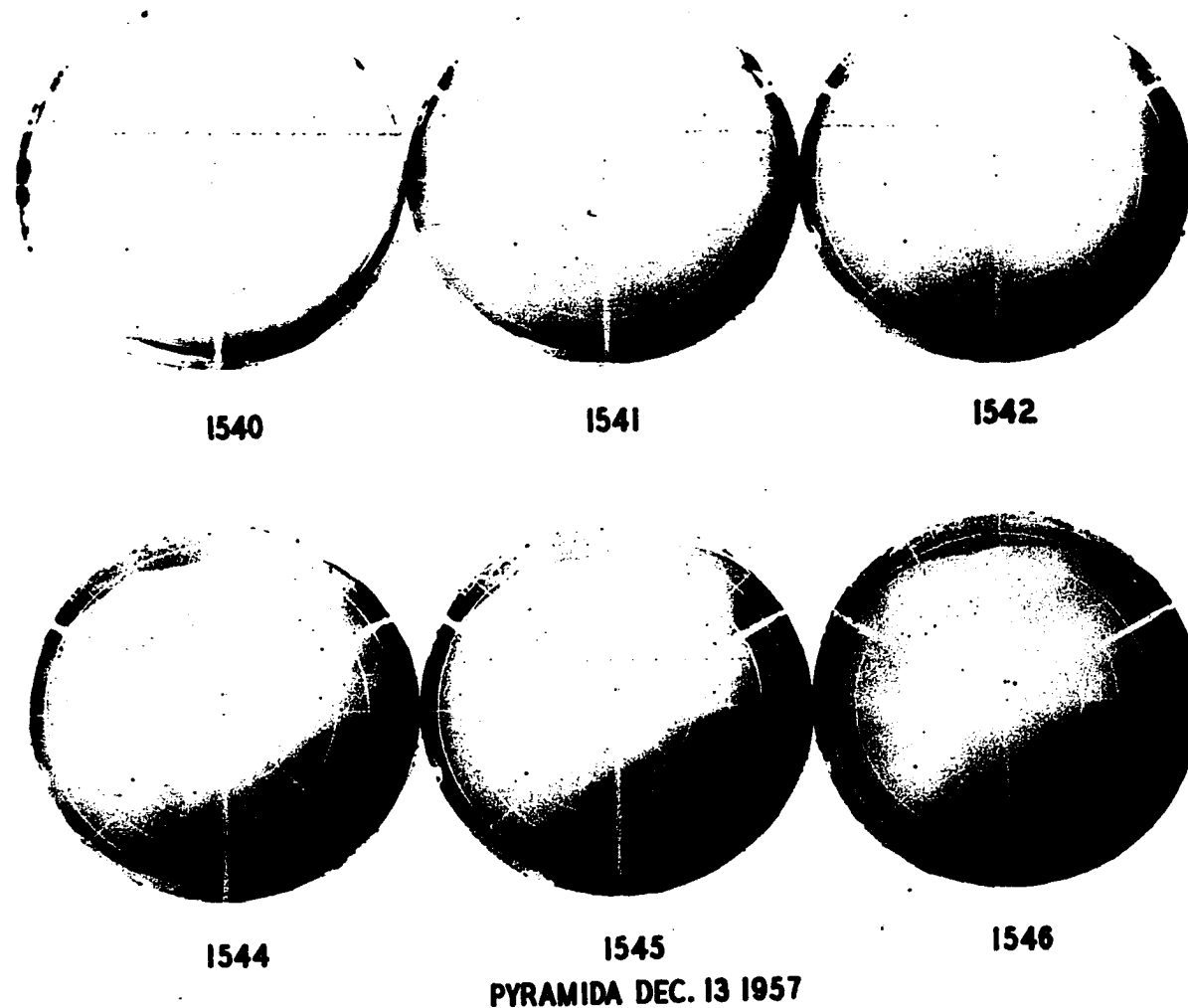


Fig. III-20. Successive all-sky photographs from Pyramida on Dec. 13, 1957 (UT) illustrating a westward traveling surge seen in the afternoon sector (L.T. = U.T. + 1). The direction to the north dp pole is upward.



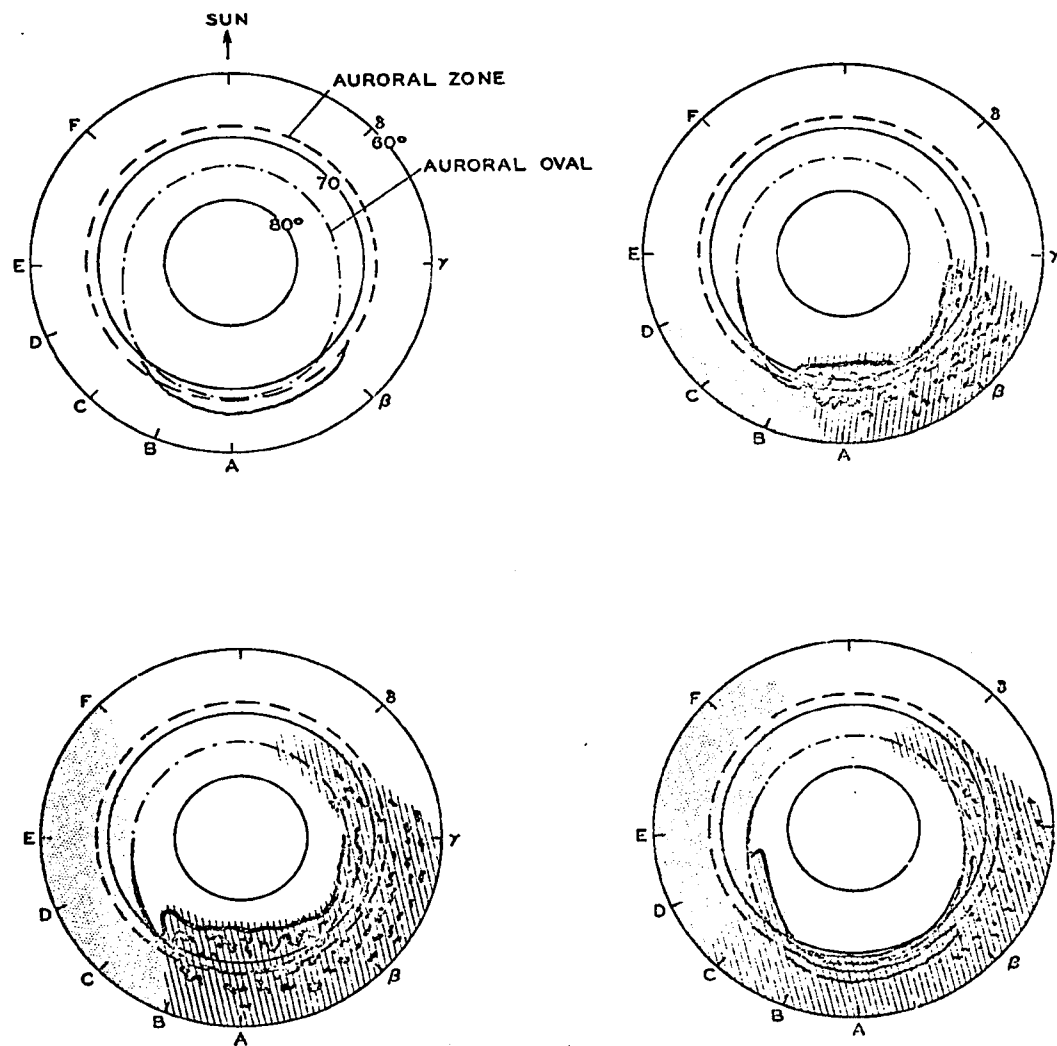


Fig. III-21. Schematic diagram to show the development of both the auroral and polar magnetic substorms, from (a) a quiet situation, (b) an early epoch of the expansive phase, (c) the maximum epoch of the substorm to (d) an early epoch of the recovery phase. The region where a negative bay is observed is indicated by the lined shade, and the region of a positive bay by the dotted shade.

observed without much delay, only of order  $5 \sim 15$  minutes, although it tends to be less intense than that observed in the midnight sector.

In the evening sector, when the bulge is expanding, the surge may be considered to be the westward leading edge of the bulge. Thus, the westward motion of the surge indicates a westward expansion of the region in which a negative bay is observed. At the same time, a positive change in the horizontal component, namely the so-called 'positive bay', is observed to the west of the surge in the equatorward side of the oval; in Figure III-21, the region where a positive bay is observed is indicated by the dotted shade. Therefore, a station located a little to the equatorward side of the path of the surge, observes first a positive change when the surge is seen in the northeastern sky (in the northern hemisphere), and then a negative change when the surge passes to the northwestern sky. The speed of the surge is of order  $1 \text{ km/sec}$ , so that the region of the negative bay expands with this speed which is much less than the expansion speed in the morning ( $\sim 10 \text{ km/sec}$ ).

This situation is also schematically shown in Figure III-22. It shows typical changes in the H component at two stations, whose dp latitudes are  $65^\circ$  and  $72^\circ$  respectively, at different local times (the first column), indicated in Figure III-21(a).

A station whose dp lat is about  $60 \sim 65^\circ$ , like College (Alaska) and Kiruna (Sweden), will observe a sharp negative bay only when it happens to be located near the midnight meridian (A). When this station is located in the late evening sector (B and C), a positive bay will be observed first as a westward surge appears in the north-eastern sky, and then a negative bay after the surge advances to the northwestern sky. When the

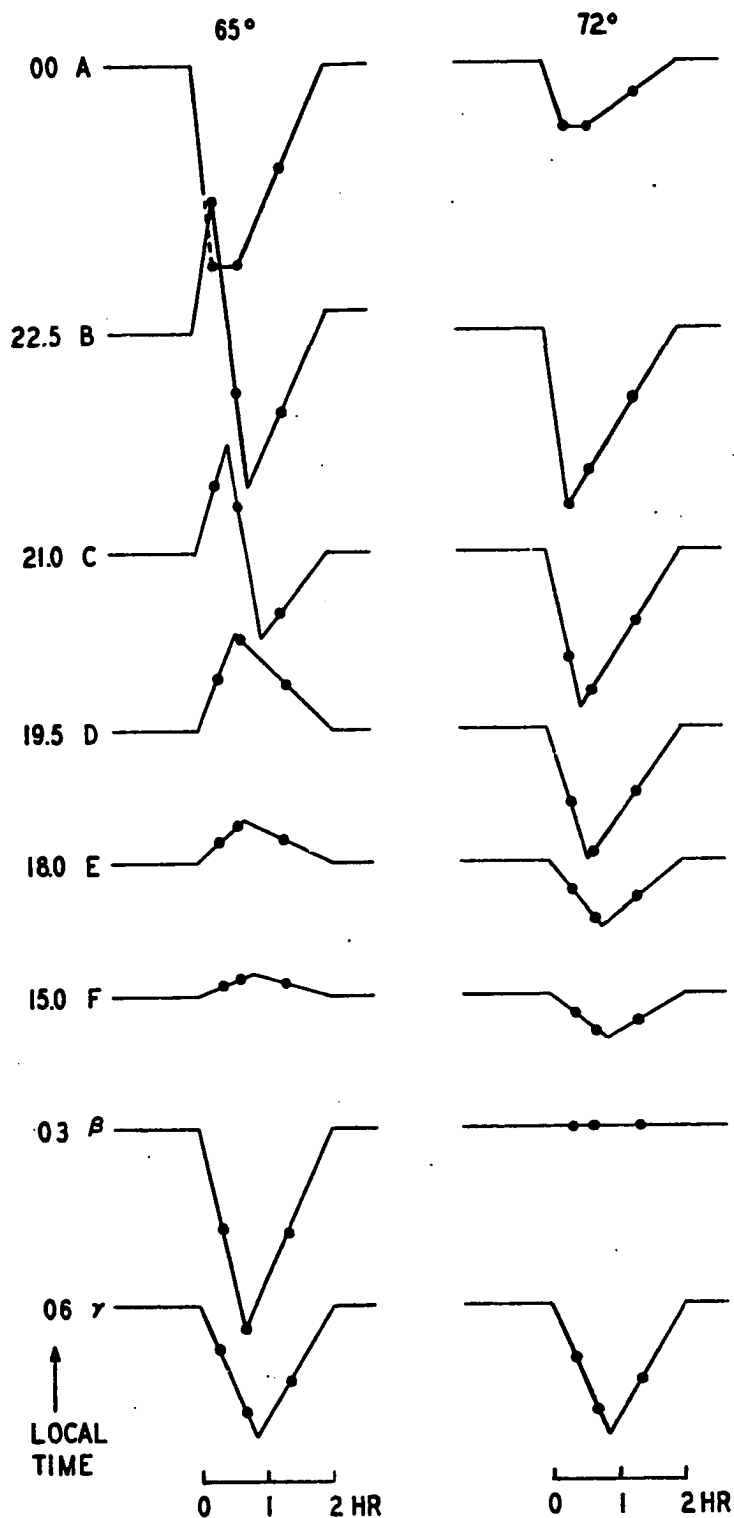


Fig. III-22. Typical H-component variations at different longitudes along the dp latitude circles of 65° and 72°. For the first column (local time) and the second column (A,B,C...), see Figure III-21.

station happens to be located further to the west (in the early evening or afternoon sectors, namely D, E, and F), it will observe, however, only a positive bay. For such locations the surge will be passing too far north to be seen or the sky may not be dark enough.

Since the surge (in the evening sector) travels along the pre-existing arcs that lie along the auroral oval, it travels poleward of the auroral zone. It can often propagate as far as the early afternoon sector and reach a latitude of about  $\text{dp lat } 75^\circ$  (as shown in Figure III-20). However, since the speed of the surge is only of order 1 km/sec and the typical duration of the expansive phase is of order 30 min or less, the maximum epoch of the auroral substorm (or the expansive phase) in the midnight sector will be over by the time the surge travels a distance of about 1000 ~ 2000 km along the oval. After this epoch, the surge ceases to be the western leading edge of the bulge and travels as a sort of wave without leading the region of negative bay (Figure III-21 (d)). However, such a degenerated surge is still associated with an intense westward current near its polar boundary and a less intense eastward current in an extensive area to its equatorward side (Figure III-22, a  $65^\circ$  station at D, E, and F).

A station whose  $\text{dp lat}$  is  $72^\circ$  will not observe a sharp negative bay in the midnight sector unless the poleward expansive motion reaches that far. In the evening sector, a surge advances along the oval and passes over the station, and an intense negative bay will be recorded when it is passing nearly overhead. Because of the finite speed of the surge, however, there is a slight delay in the time at which the positive and negative bays peak at different longitudes in the evening sector (see Fig. III-22).

It should be stressed that the schematic diagrams presented in Figures III-21 and 22 will vary greatly, depending on the over-all storm conditions in the magnetosphere. During magnetic storms with an intense main phase, the oval shifts toward the equator, sometimes to dp lat  $50^\circ$ , and the situation will be quite different from the above average condition. Such a great complication can, however, be greatly reduced by taking the auroral oval as a natural frame of reference. The important thing is the relative location of a station with respect to the oval (namely, inside, within, or outside), rather than its dp lat. When the oval shifts equatorward from its average location, College (dp lat  $64.5^\circ$ ) becomes temporarily similar to a polar cap station whose dp lat is  $70 \sim 72^\circ$ , and thus westward traveling surges and negative bays appear abnormally early in the evening. During quiet periods the auroral oval contracts poleward, and College becomes temporarily a sub-auroral station (Stringer, Belon and Akasofu, 1965).

The intensity of the substorm is another factor to be considered in understanding the complexity of the substorm. When substorms are intense, the region in which the poleward expansive motion takes place (the bulge) will be much larger than that which is shown in Figure III-21 (b). Thus, a station of dp lat  $65^\circ$  at local time 2230 (B) and even 2100 (C) sometimes observes a negative bay, rather than a combination of positive and negative bays.

The development of the magnetic and auroral polar substorms along the oval has already been discussed. Since the auroral bulge is not only expanding along the auroral oval, but also poleward and equatorward, the morphology of the polar magnetic substorm in the evening sector both to

the north and south of the auroral oval is also studied by using a chain of four Alaskan north-south stations distributed between dp lat  $61^{\circ}$  and  $70^{\circ}$ . Figure III-23 shows an example of geomagnetic disturbances, recorded at College (dp lat  $64.7^{\circ}\text{N}$ ), which occurred when an intense westward surge was traveling westward in the northern sky of Ft. Yukon (dp lat  $67.8^{\circ}$ ), located at about 200 km dp north of College. In the magnetic record a rather sharp positive change of the horizontal component at 1915 LT ( $150^{\circ}$  WMT) is followed by both negative and positive irregular changes. In the lower part of the figure all-sky camera photographs from Ft. Yukon (in negative) are shown; in the upper row, the photographs taken at each hour (with some additions) are shown, and in the second row the photographs during three selected periods, A, B and C. Period A corresponds to the time when intense irregular variations were observed. The three photographs in period A indicate typical features of the westward traveling surge described in detail by Akasofu, Kimball and Meng (1965).

As indicated later, College was located in a transition belt between the region of a very intense negative bay ( $\sim 800 \gamma$ ) to the north and the region of a weak positive bay ( $\sim 100 \gamma$ ) to the south. A typical auroral zone station, like College, tends to be located in the transition region in the late evening sector, since the auroral oval (which is the path of the extending westward jet current) lies a few hundred kilometers on the poleward side of the station. The example indicates that one cannot infer the distribution of the equivalent current system over an area as small as Alaska (compared with the whole polar cap) by using the record from a single station like College. In particular, without having a station along the auroral oval it is impossible to obtain a complete knowledge of the morphology of the disturbances in the evening sector. It also shows

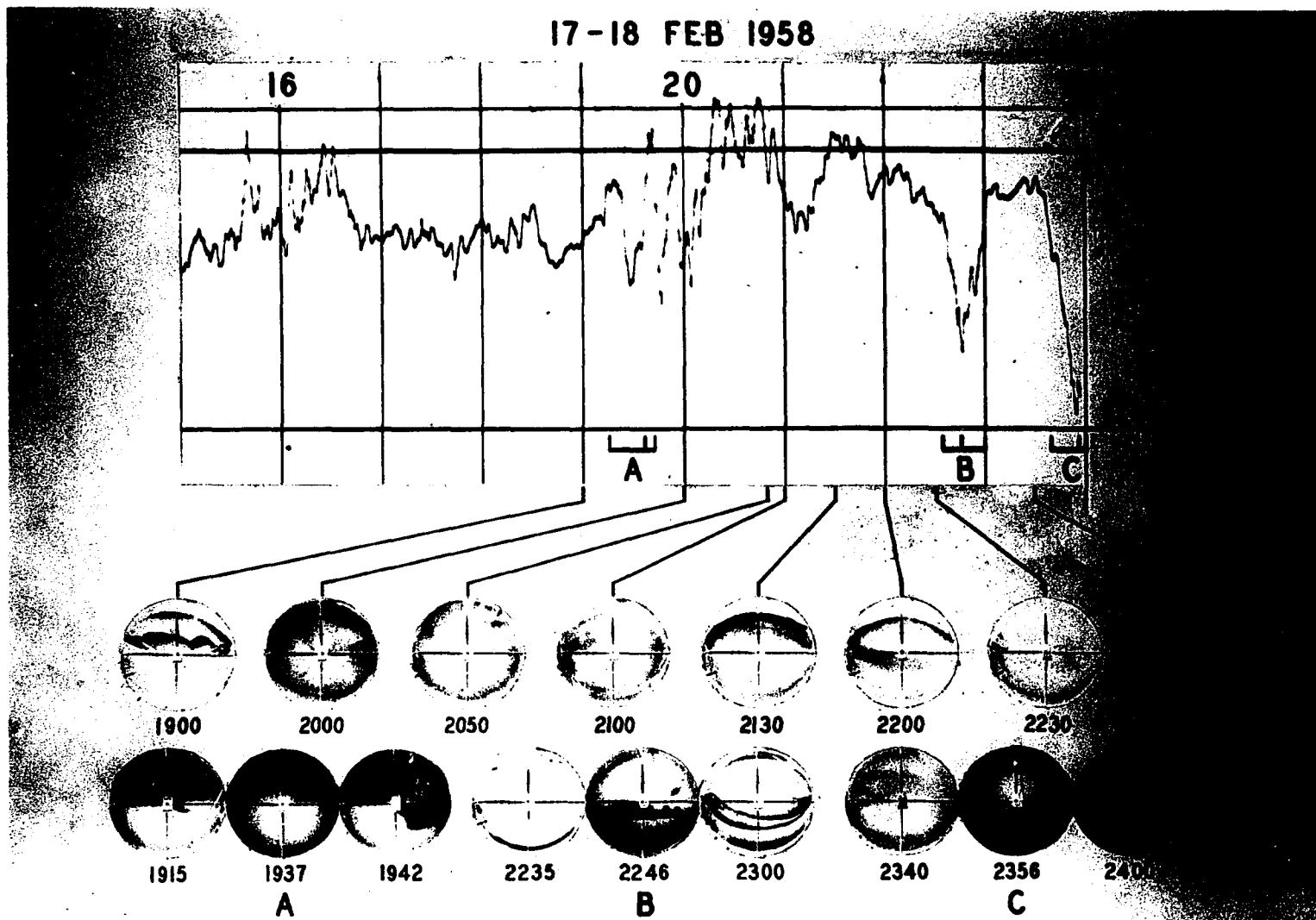


**Fig. III-23. The College (H) magnetic record and Ft. Yukon all-sky camera photographs (in negative) in evening of February 17/18, 1958. The hours shown refer to 150°W.**

that hourly mean values are inadequate for the study of the polar magnetic substorms (they smooth out such transient changes as are shown in Figure III-23). As night progresses, geomagnetic changes at College tend toward a simpler form, namely negative bays; see periods B and C in Figure III-23.

The most common types of horizontal force change at Barter Island, College and Anchorage are shown schematically in the upper part of Figure III-24. Though there is a great variety in appearance of the sets of simultaneous records from these three stations, they can be approximately resolved into five types symbolized in the following table and in the lower part of Figure III-24.

Type	Barter Island	College	Anchorage
A	-	+	+
B	-	+ <sub>-</sub>	+
B'	-	+ <sub>-</sub>	+ <sub>-</sub>
C	-	- <sub>+</sub>	+
C'	-	- <sub>+</sub>	+ <sub>-</sub>

The location of the four Alaskan stations used here are shown in Figure III-25.

Figure III-26 shows three sets of disturbance records of type A events which were obtained on the evenings of February 7, March 8 and May 2, 1958. In the last two cases records from Ft. Yukon are also shown. The times shown are UT: 10 hours must be subtracted to give the local (150°W meridian) time, so that 04, 05, 06 and 07 UT correspond to 18, 19, 20 and 21 LT, respectively. The first and simplest case corresponds to a moderate bay at Barter Island. In general, the intensity of the changes decreases from



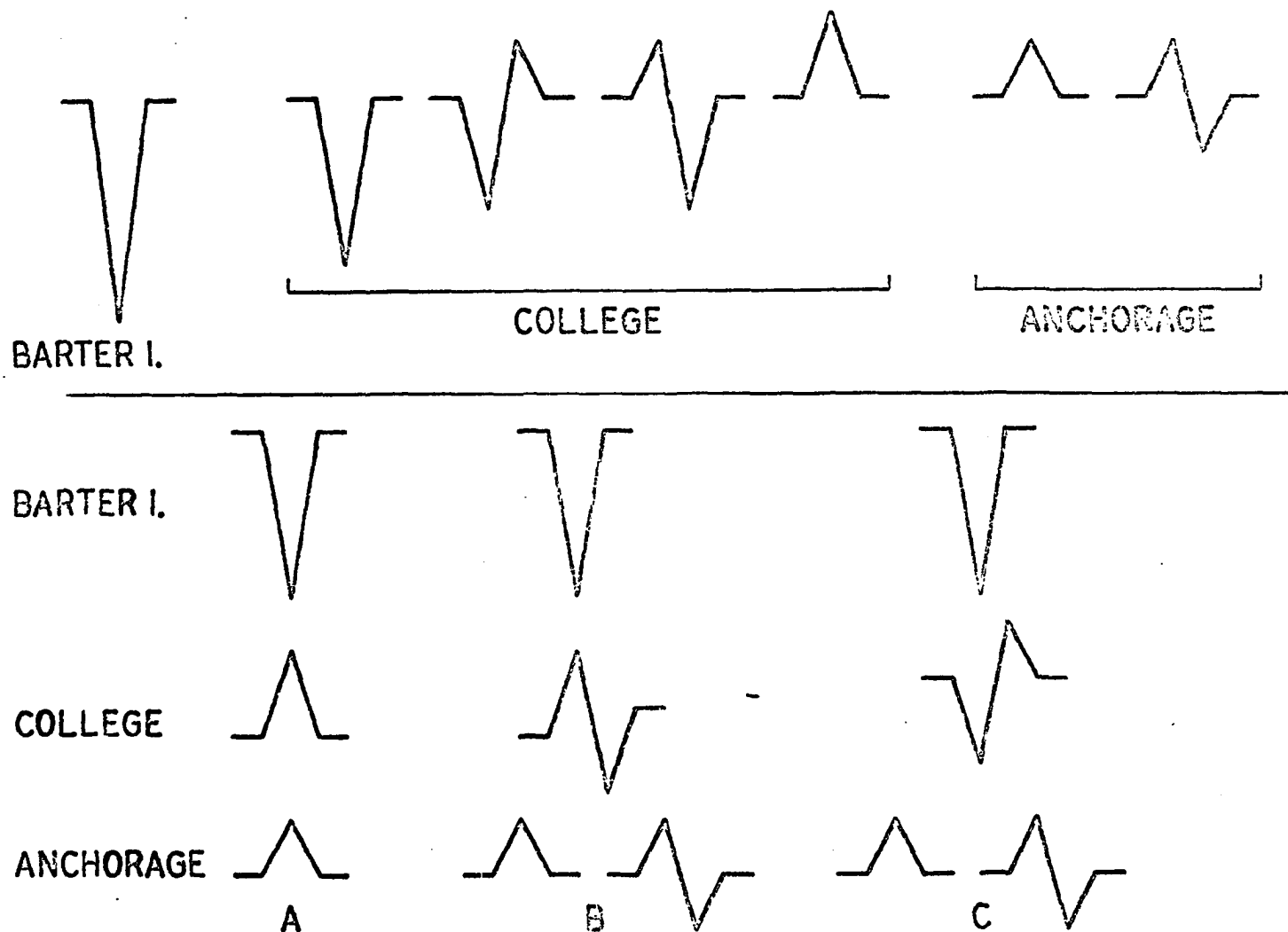


Fig. III-24. Top: The most common types of magnetic variations at Barter Island, College and Anchorage in the evening sector.

Bottom: The most common combinations of the types at three stations.

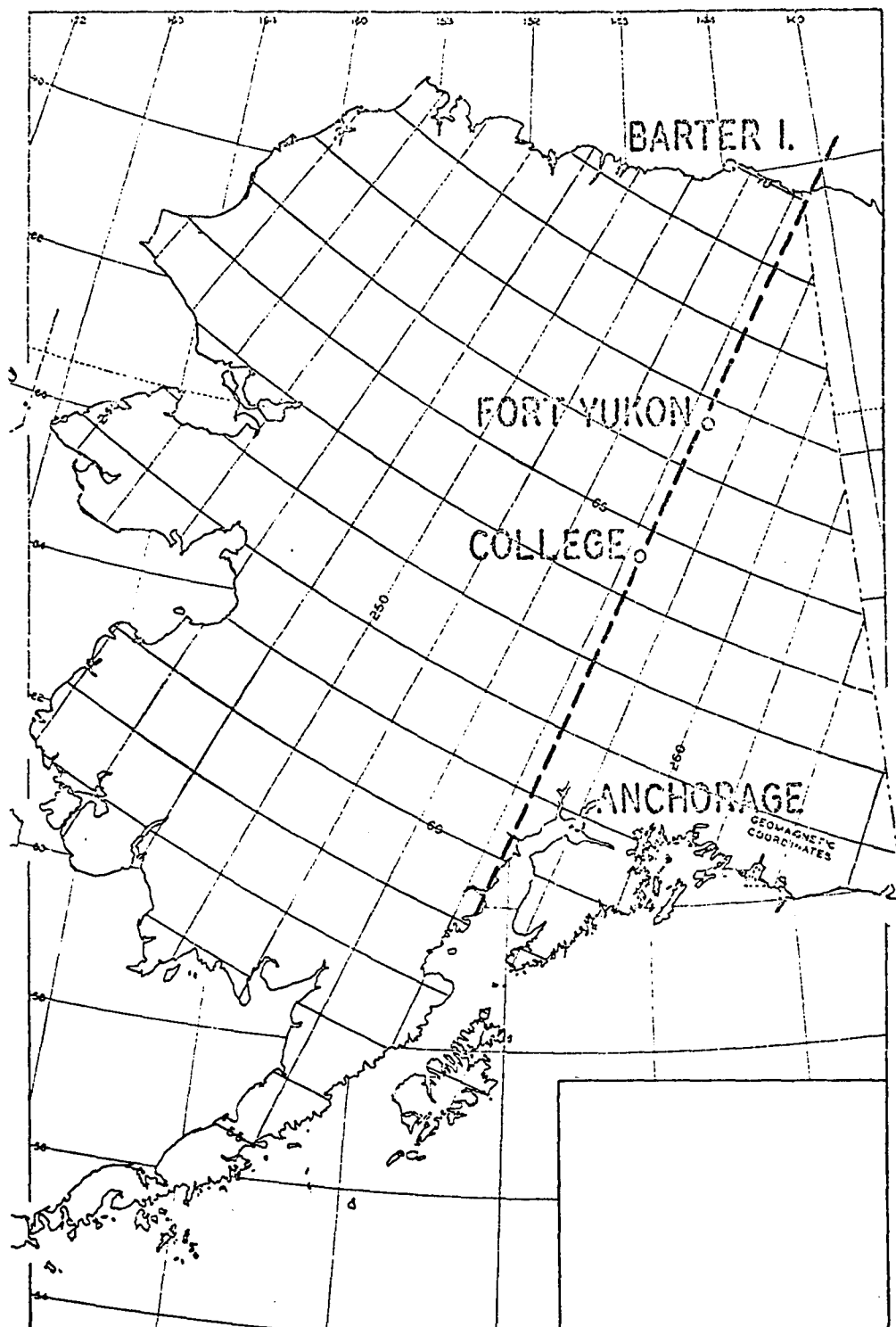


Fig. III-25. The locations of the four Alaskan north-chain stations, Barter Island, Ft. Yukon, College and Anchorage. The magnetic meridian which passed College is indicated.

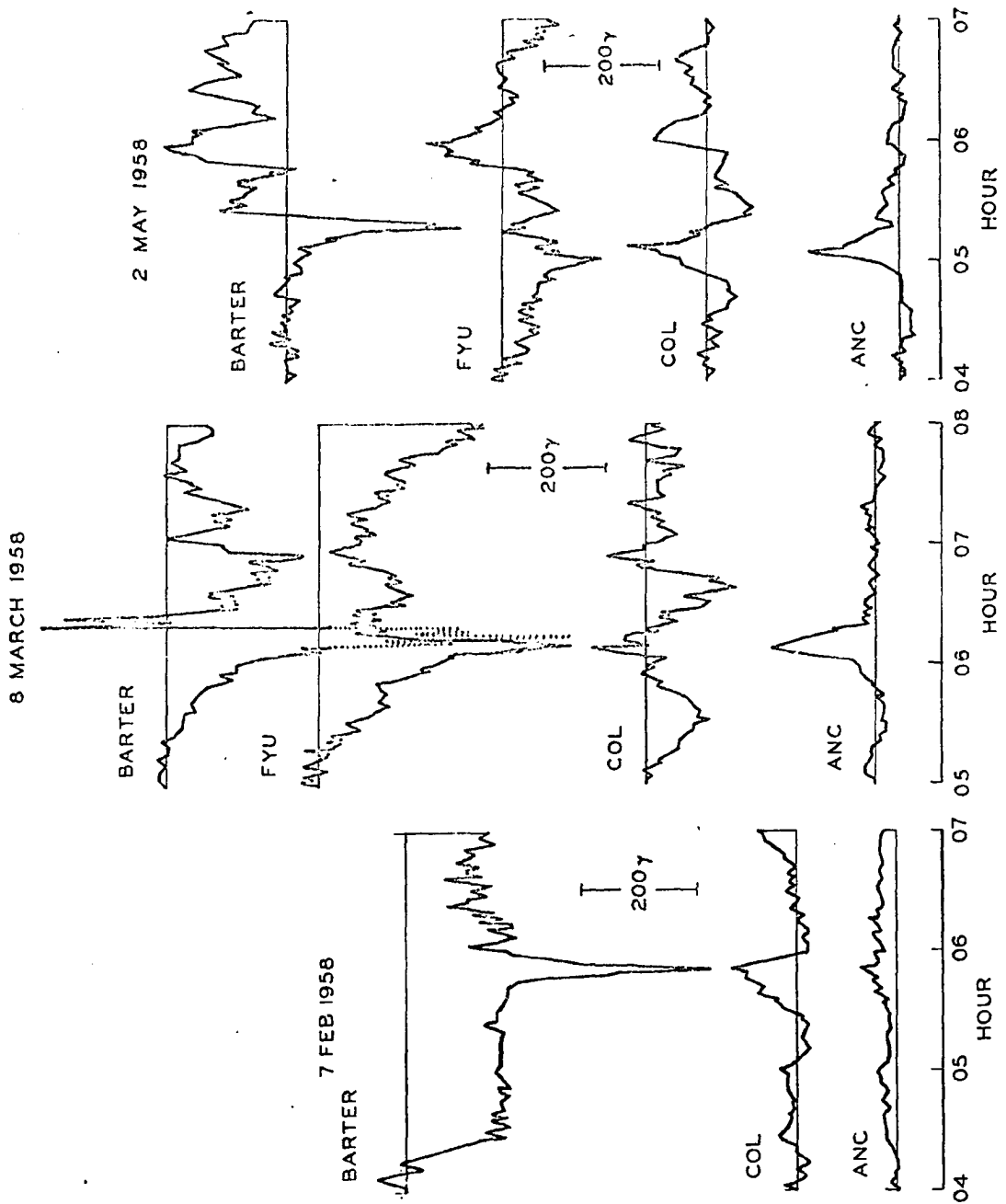


Fig. III-26. Examples of the combination (A) in Figure III-24. The hours shown refer to UT.

Barter Island to Anchorage ---- in most cases the magnitude of the negative bay at Barter Island exceeds the range of the College and Anchorage changes. Minor irregularities may be superposed on the main bay-type changes.

Figure III-27 shows three cases of type B events. In the first and third, there are two negative bays at Barter Island; they are treated here as single events. The second case is the one already illustrated in Figure III-23.

Figure III-28 shows two cases of type B' events with similar intensity at Barter Island. The (+ -) nature of the Anchorage record is very clear in the second. The Ft. Yukon all-sky auroral records for these two cases, given in Figure III-29, show strong westward traveling surges passing overhead. Figure III-30 shows one example of each type of C and C' event.

Thus, the longitudinal morphology of the polar magnetic substorms in the evening sector can be summarized by Figure III-31 which is a schematic series of types of records from 70° to 60° dp latitude. The transitional form observed at any one station will depend on the linear scale of the oval at the time (or on the oval midnight latitude), so that the whole pattern of Figure III-31 may be shifted to north or south, depending on the intensity of the main phase decrease during geomagnetic storms. However, the extremes on the inner and outer sides of the oval are typically negative bays and positive bays, respectively.

There are obviously some cases which cannot be classified easily either as type (B) or type (C) and also which do not seem to fit into Figure III-31. Figure III-32 shows a few such examples. In the first example (February 14), the first negative bay at Barter Island was associated with less intense positive bays at both College and Anchorage. However, at College, there was

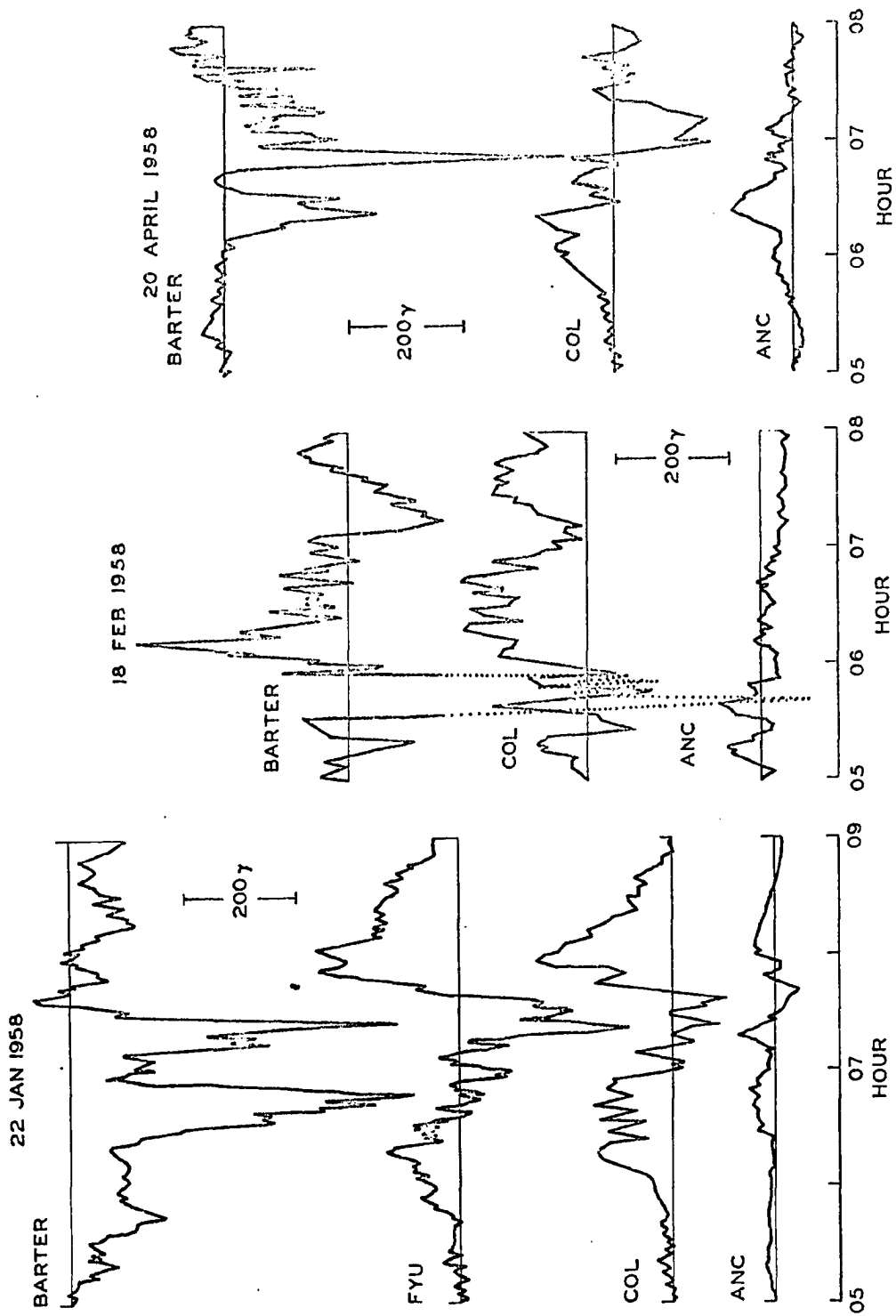


Fig. III-27. Examples of the combination (B) in Figure III-24. The hours shown refer to UT.

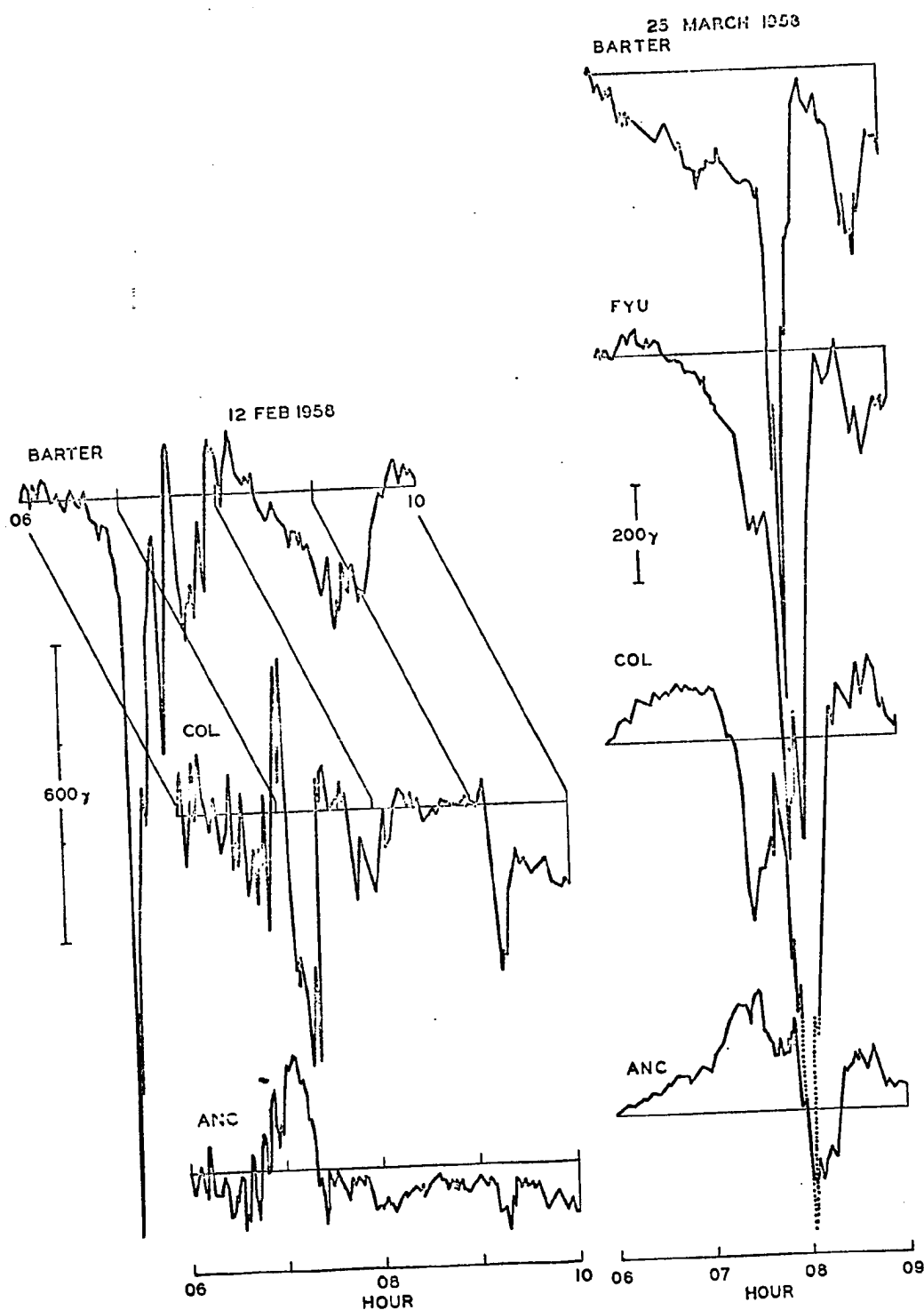
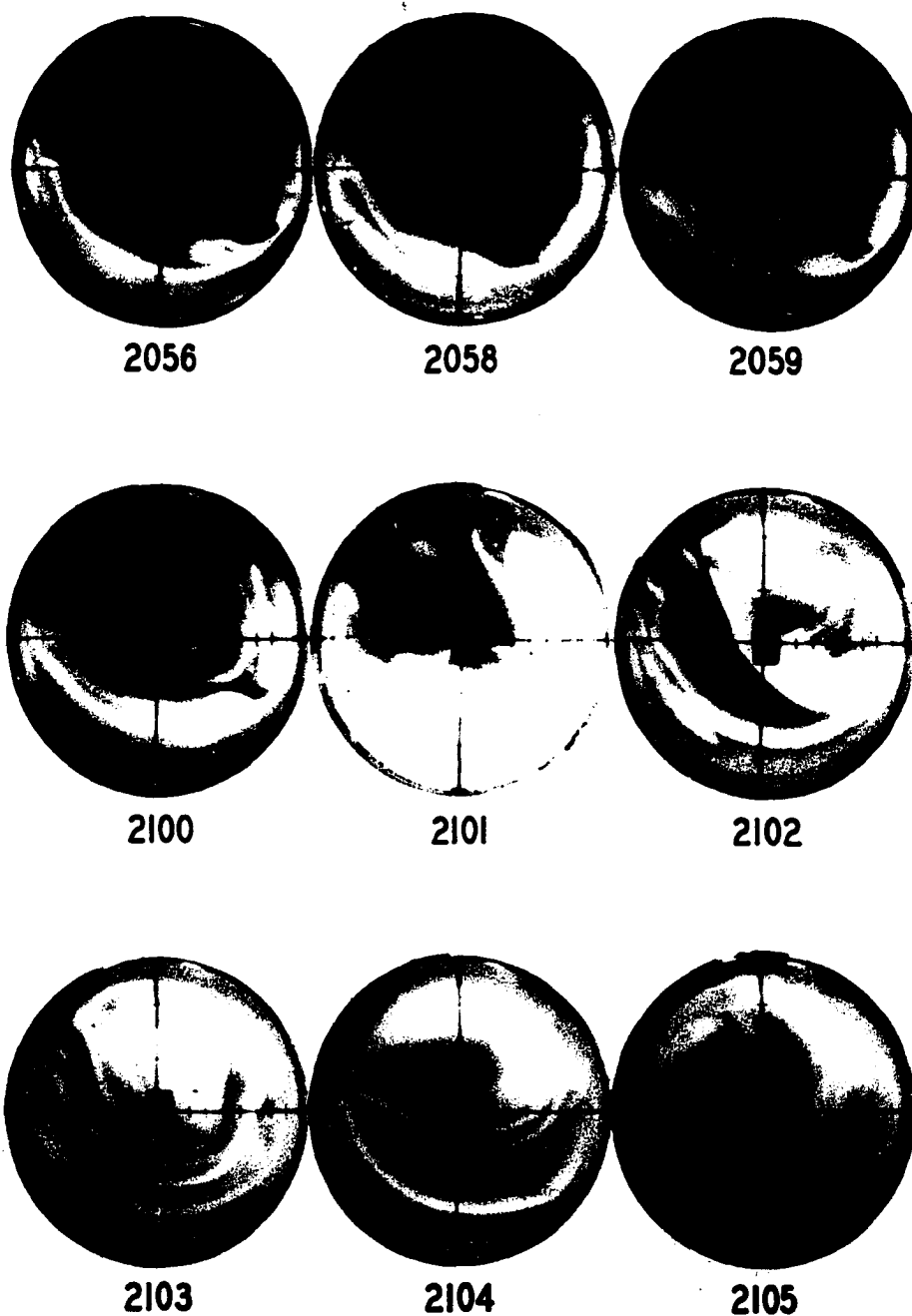


Fig. III-28. Examples of the combination (B) in Figure III-24. The hours shown refer to UT.



**Fig. III-29a.** The all-sky camera photographs (in positive) taken from Ft. Yukon (Feb. 12, 1958 UT) during the event shown in the first example of Figure III-28. The hours shown refer to 150°W.

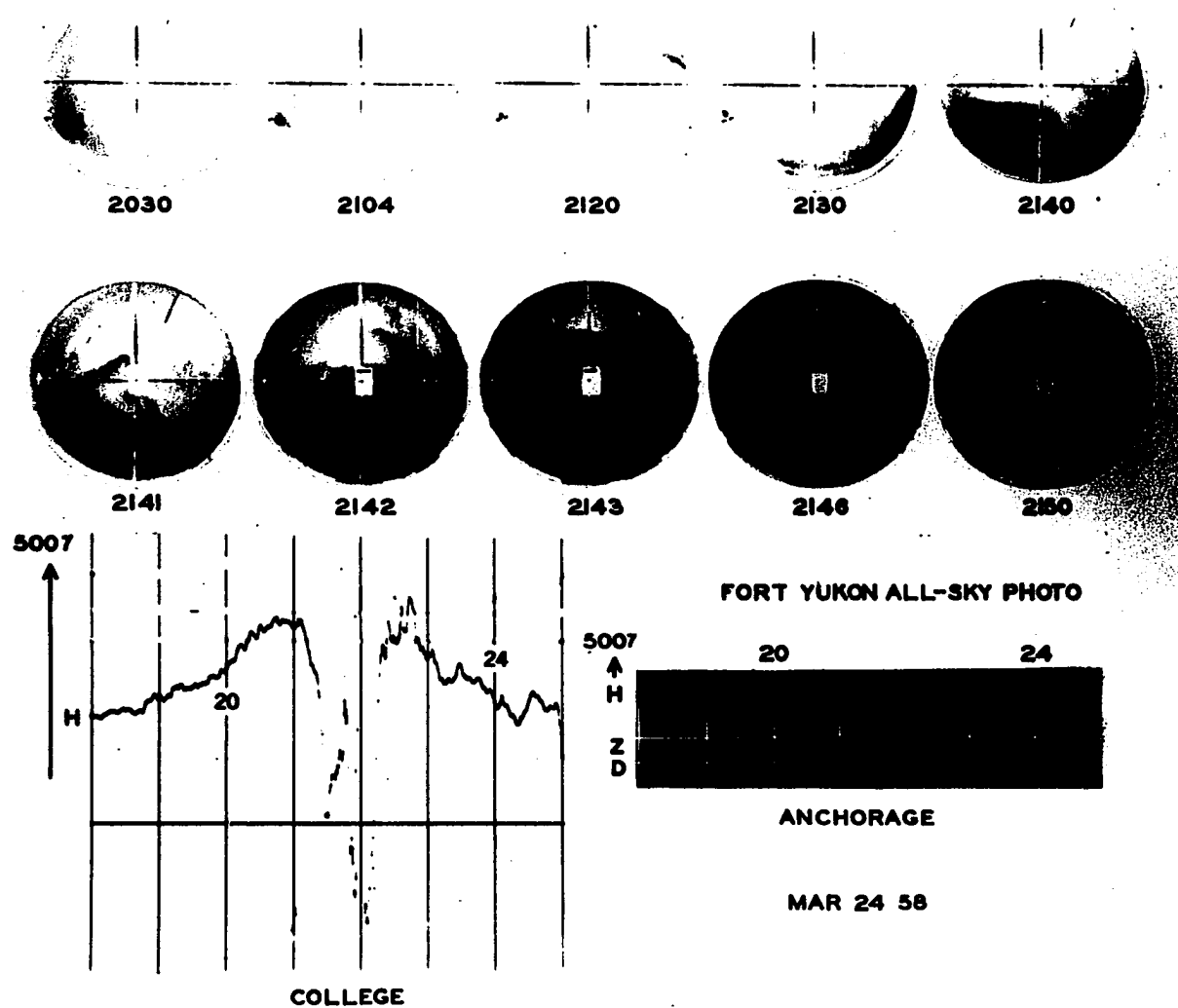


Fig. III-29b. The all-sky camera photographs (in negative) taken from Ft. Yukon (March 25, 1958 UT) during the event shown in the second example of Figure III-28.



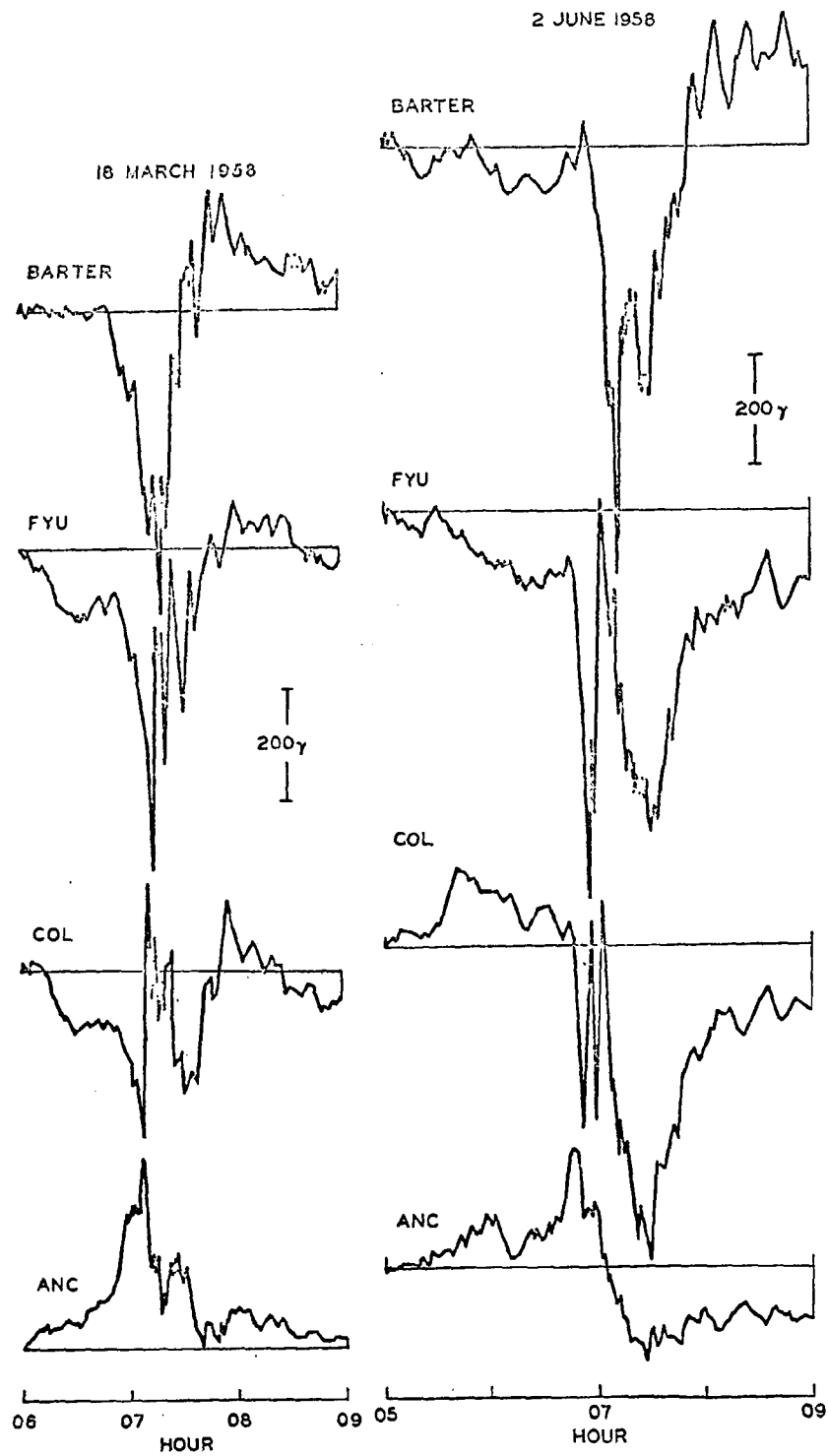


Fig. III-30. Example of the combination (C) in Figure III-24.

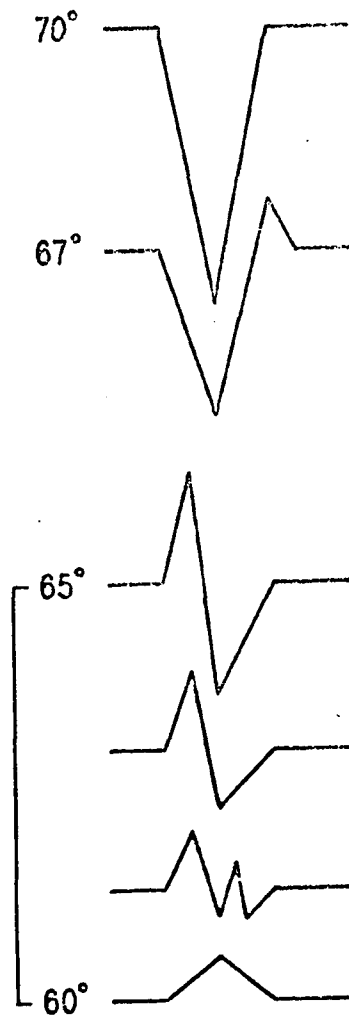


Fig. III-31. Proposed latitudinal variation of the field of the polar magnetic substorm in the evening sector.

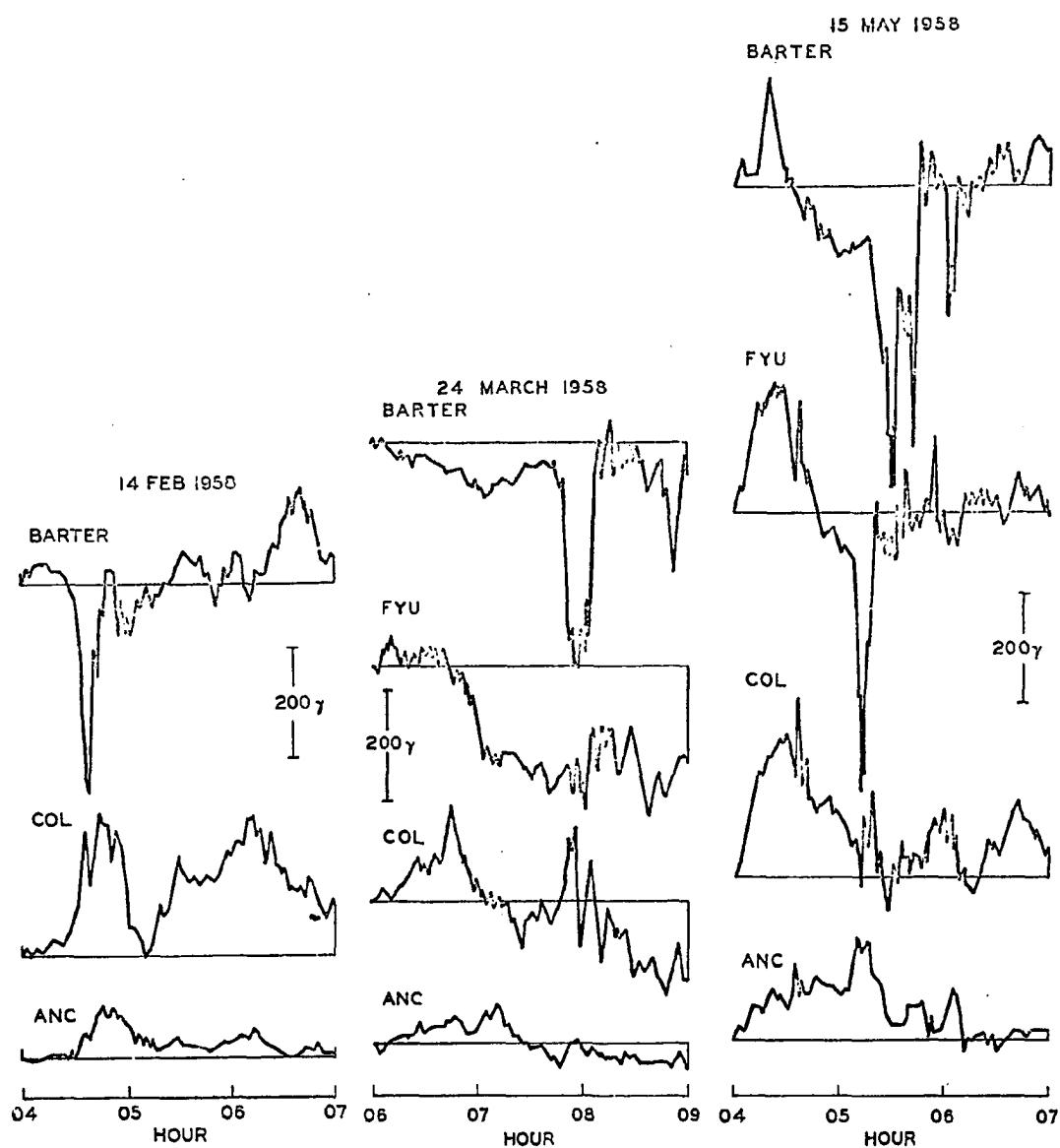


Fig. III-32. Examples which do not seem to fit into the proposed profile.

a significant positive change after 0510 UT, which did not seem to have the corresponding change at Barter Island. Unfortunately, the malfunction of the Ft. Yukon magnetometer prevented further investigation. In the second example (March 24), a positive bay at about 0650 UT was also associated with a more intense negative bay. At Ft. Yukon, however, there was a significant negative change which began at about the peak time of the positive bay. Note, however, that the negative bay which occurred at Barter Island at about 0750 UT agrees with the proposed profile. In the third example, a distinct positive bay at about 0430 UT recorded at College was also seen at all the other stations. At 0430 UT (1830, 150° WMT), the oval lies at about  $\text{dp lat } 73^\circ$ , so that even Barter Island could be located equatorward side of the oval at such an early evening hour; in other words, all four Alaskan stations were well outside the oval. From the above examples, we can state that the relative location of a station with respect to the auroral oval is more meaningful than the dipole latitude.

### 3) Polar Substorms Inside the Auroral Zone

The magnetic disturbance of the substorm near the auroral zone was discussed in the last subsection. Here the magnetic disturbances observed well inside the auroral zone are investigated.

#### (a) Intense Negative Bays

The occurrence of intense negative bays at very high latitudes has been noted by several workers. Harang (1946) was one of the first to realize that negative bays occur not only in the midnight and the early morning sector of the auroral zone, but also well poleward inside the auroral zone in the early evening and late morning hours.

Nikolsky (1947) examined the occurrence of intense geomagnetic disturbances inside the auroral zone. He plotted the time of the maximum occurrence of negative bays on a polar map and found that the points align along two curves, emanating from the midnight sector of the auroral zone and extending to higher latitudes in the evening sector and morning sector, respectively. These curves are called the N 'spiral' (evening curve) and the M 'spiral' (morning curve) respectively. His results were later confirmed by other workers, including Burdo (1957) and Feldstein (1963). Figure III-33 shows the N and M spirals obtained by Feldstein (1963); they are indicated by 'Mag. N' and 'Mag. M', respectively.

It is important to note that when these two curves were combined, they gave essentially the same results that Harang obtained. However, these studies were based on statistical analyses, so that it was rather difficult to infer an instantaneous pattern of the current system over the polar region. In fact, there has been much discussion on the problem as to whether or not the M and N curves should be considered a single one or independent ones. Hope (1961) made an extensive review on these matters. Furthermore, this morphological feature of geomagnetic disturbances in the polar region does not seem to agree with the DS current system, in which the westward current is well confined in the forenoon sector of the auroral zone.

In order to better understand the nature of these negative bays, three Canadian magnetic stations, Baker Lake (dp lat  $73.8^{\circ}$ ), Churchill (dp lat  $68.7^{\circ}$ ) and Meanook (dp lat  $61.8^{\circ}$ ) were chosen for this study. Baker Lake is located well inside the auroral zone, Churchill and Meanook are respectively near its poleward boundary and its southern boundary. Figure III-34 shows the location of these three stations; 1964 magnetic records were used;

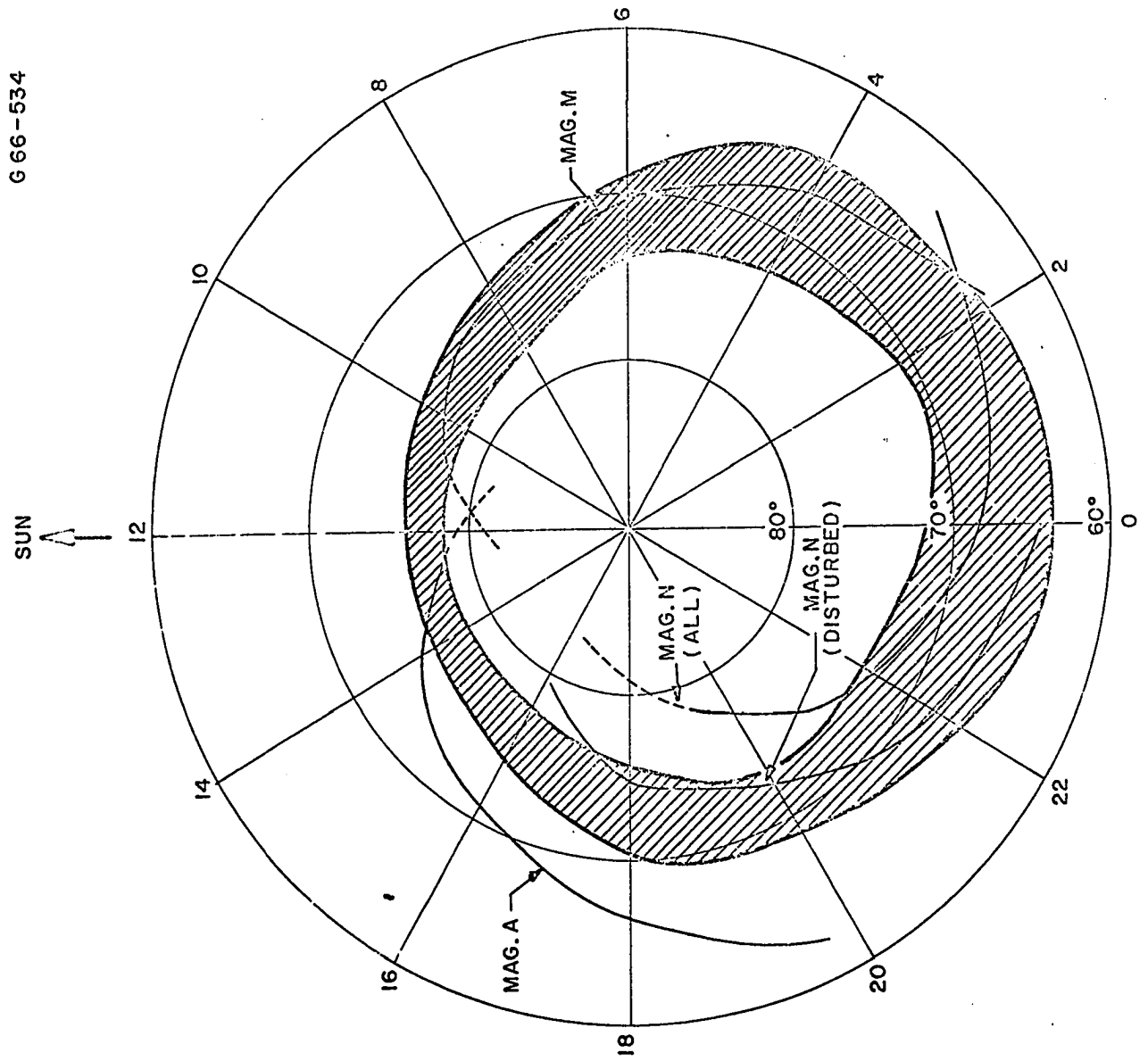


Fig. III-33. The locations of the M and N 'spirals' and of the auroral oval.

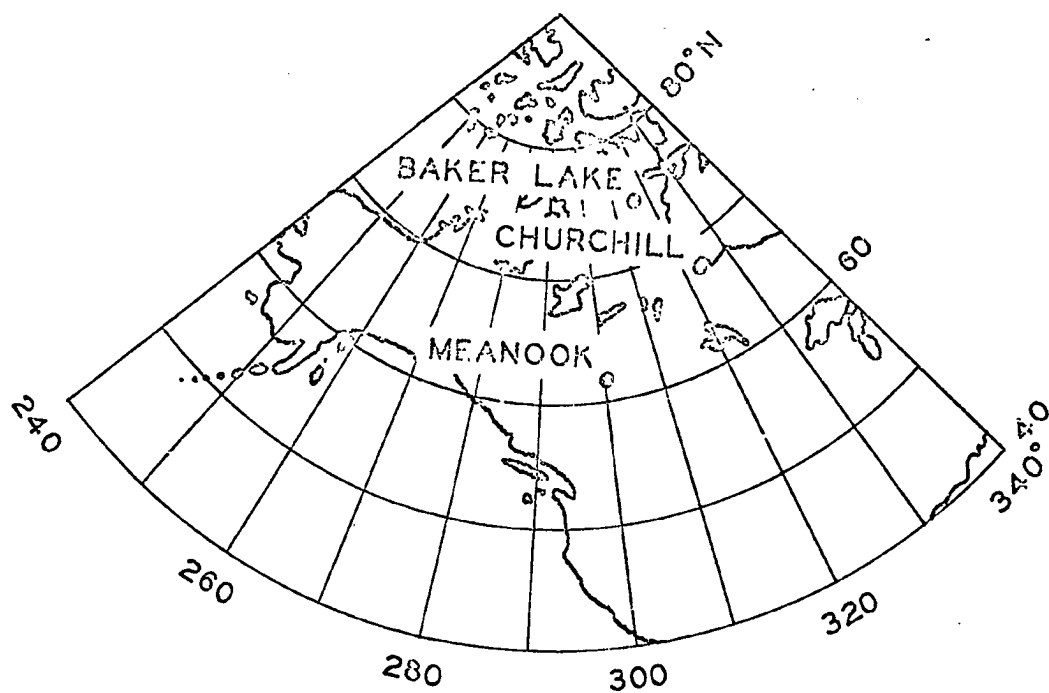


Fig. III-34. The locations of three Canadian magnetic stations, Baker Lake, Churchill and Meenook.

however, in order to examine the simultaneous auroral activity, IGY records were also studied.

As expected from earlier studies by Harang (1946), Nikolsky (1947) and others, the occurrence of an intense negative bay at Baker Lake in the evening hours was very common during the IGY period and during 1964. This tendency is clearly shown by Figure III-35, which gives the horizontal component (H) records for eight series, each consisting of five successive moderately active days from January, February, March, April, August, September, October and December, 1964; the Kp indices for each period are also shown.

Figures III-36, III-37 and III-38 give several examples of the simultaneous magnetic records (X or H component) from the three stations. We have chosen here only rather simple events, so that individual negative bays can be clearly recognized. Magnetic midnight at Baker Lake is at 0710 UT in midwinter and 0730 UT in midsummer. Figures III-36 and III-37 clearly show that the negative bays are far better defined and more intense westward current flows near or over Baker Lake, namely in the early evening as high as  $\text{dp lat } 74^\circ$ .

There is, however, almost constantly a delay of the onset of the maximum epoch of negative bays at Baker Lake as compared with Churchill. Therefore, it may be argued that the negative bays observed at Baker Lake and Churchill are independent events. To investigate this point, we have examined some of the events during the IGY for which all-sky camera photographs from Baker Lake are available.

Figure III-39 shows that rapid and irregular magnetic changes began at Churchill at 0225 UT, the maximum negative excursion being at 0240 UT.



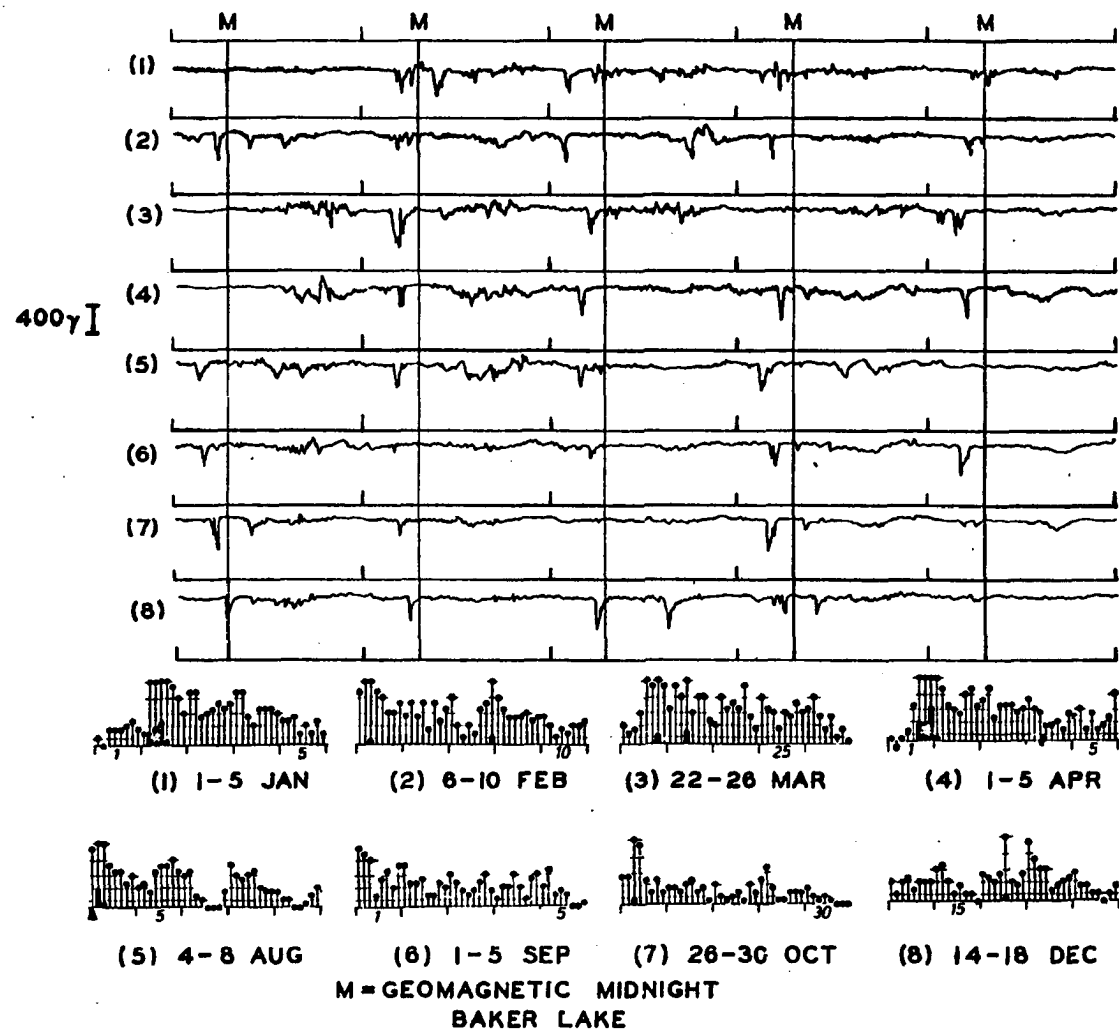


Fig. III-35. The H-component magnetic records from Baker Lake for eight groups of five successive moderately active days in 1964. The corresponding  $K_p$  indices are shown at the bottom.

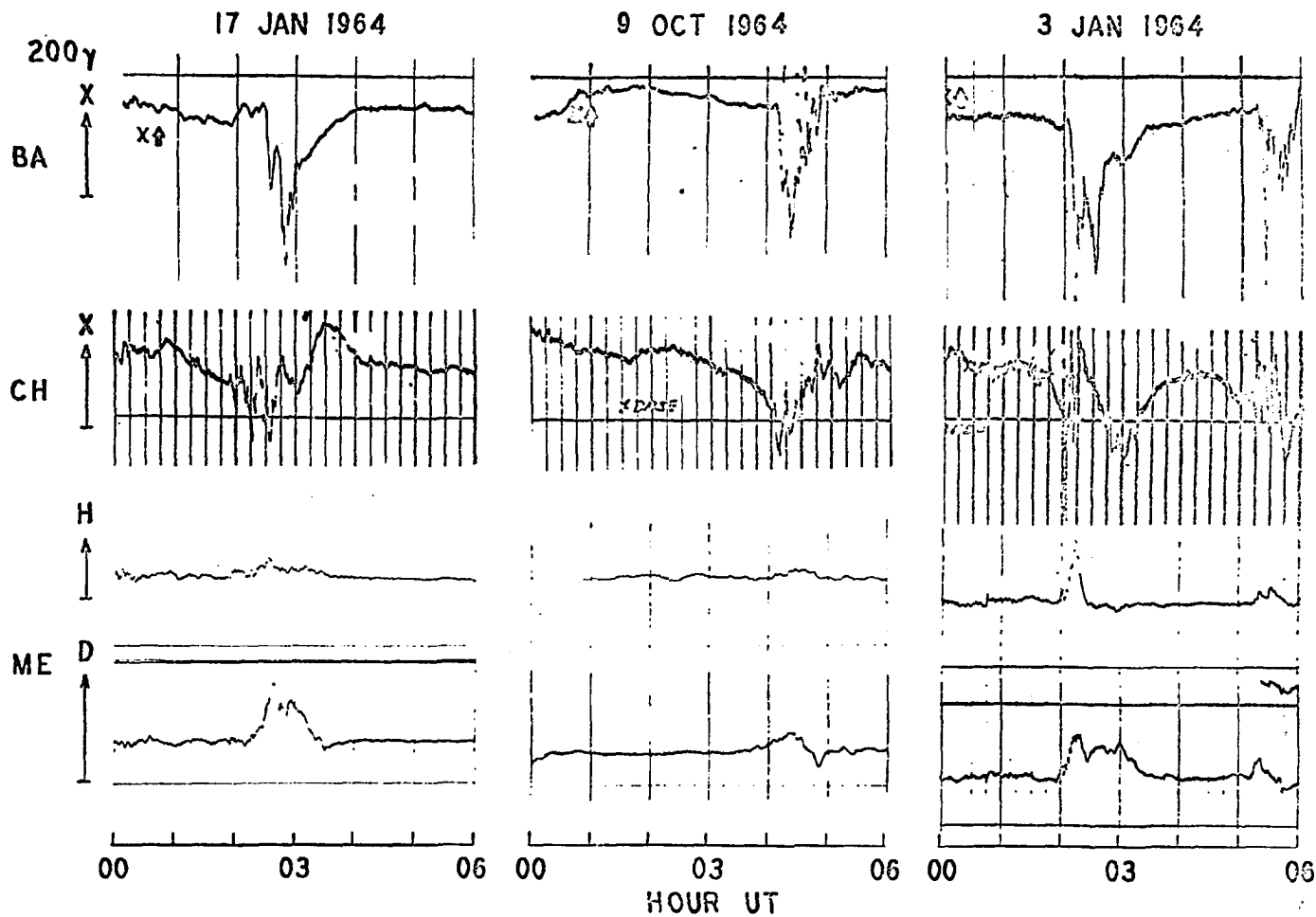


Fig. III-36. The example of an intense negative bay recorded at Baker Lake and the corresponding geomagnetic changes at Churchill and Meanook. An intense negative bay was in progress in the morning sector of the auroral oval (Reykjavik, Iceland) at the time of the events.

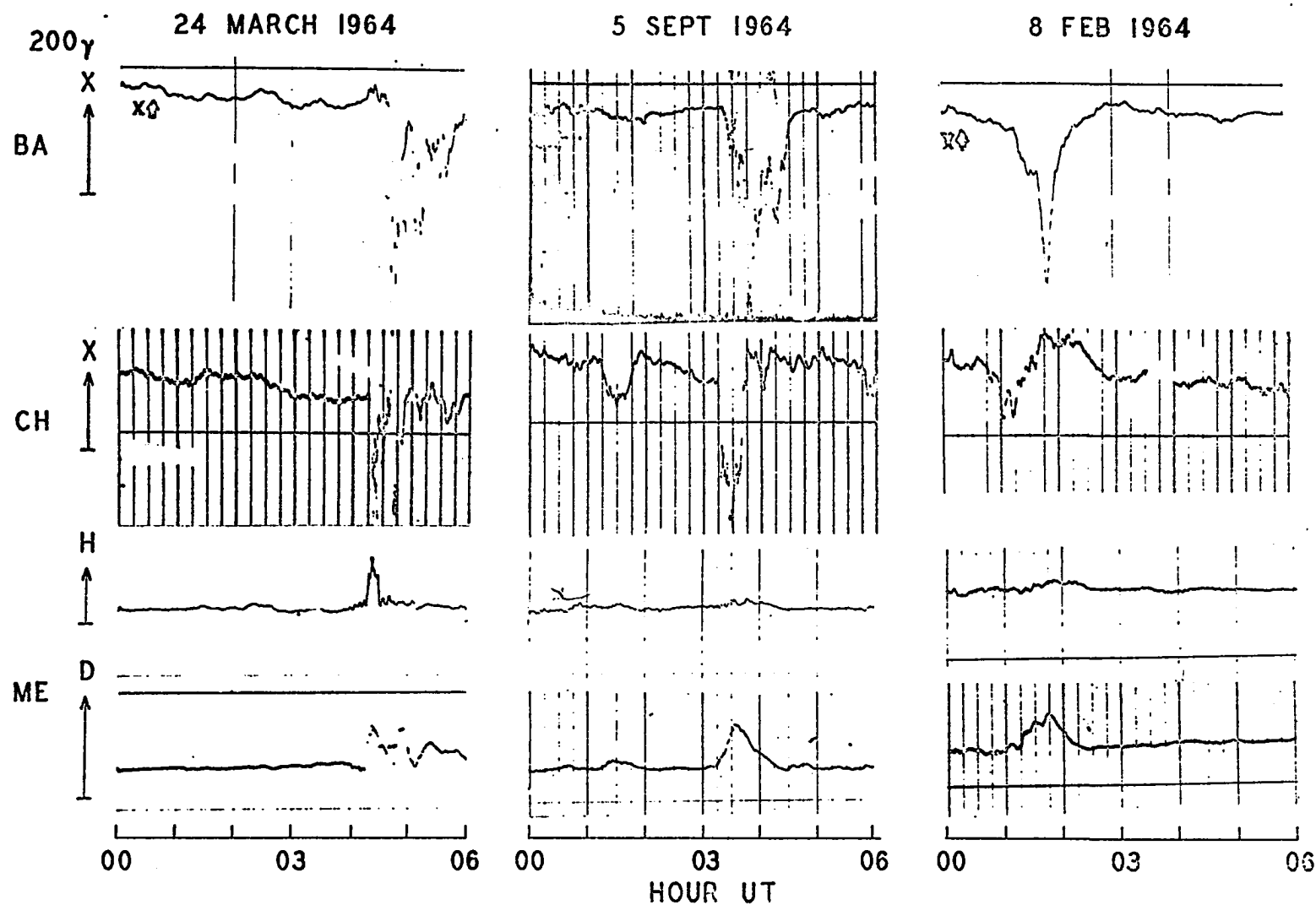


Fig. III-37. The example of an intense negative bay recorded at Baker Lake and the corresponding geomagnetic changes at Churchill and Meanook. An intense bay was in progress in the morning sector of the auroral oval (Reykjavik, Iceland) at the time of the events.

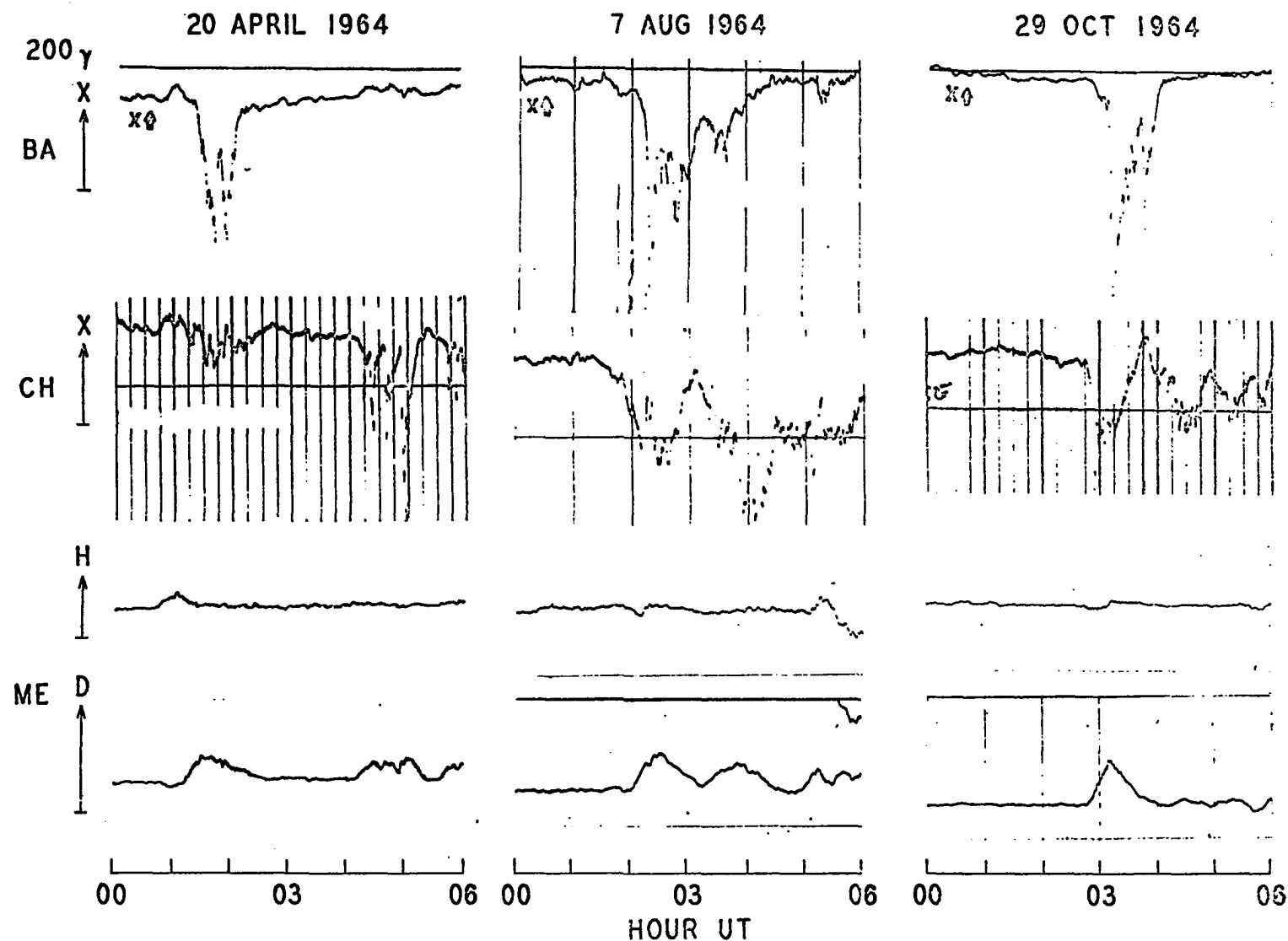


Fig. III-38. The example of an intense negative bay recorded at Baker Lake and the corresponding geomagnetic changes at Churchill and Meanook. An intense negative bay was in progress in the morning sector of the auroral oval (Reykjavik, Iceland) at the time of the events.

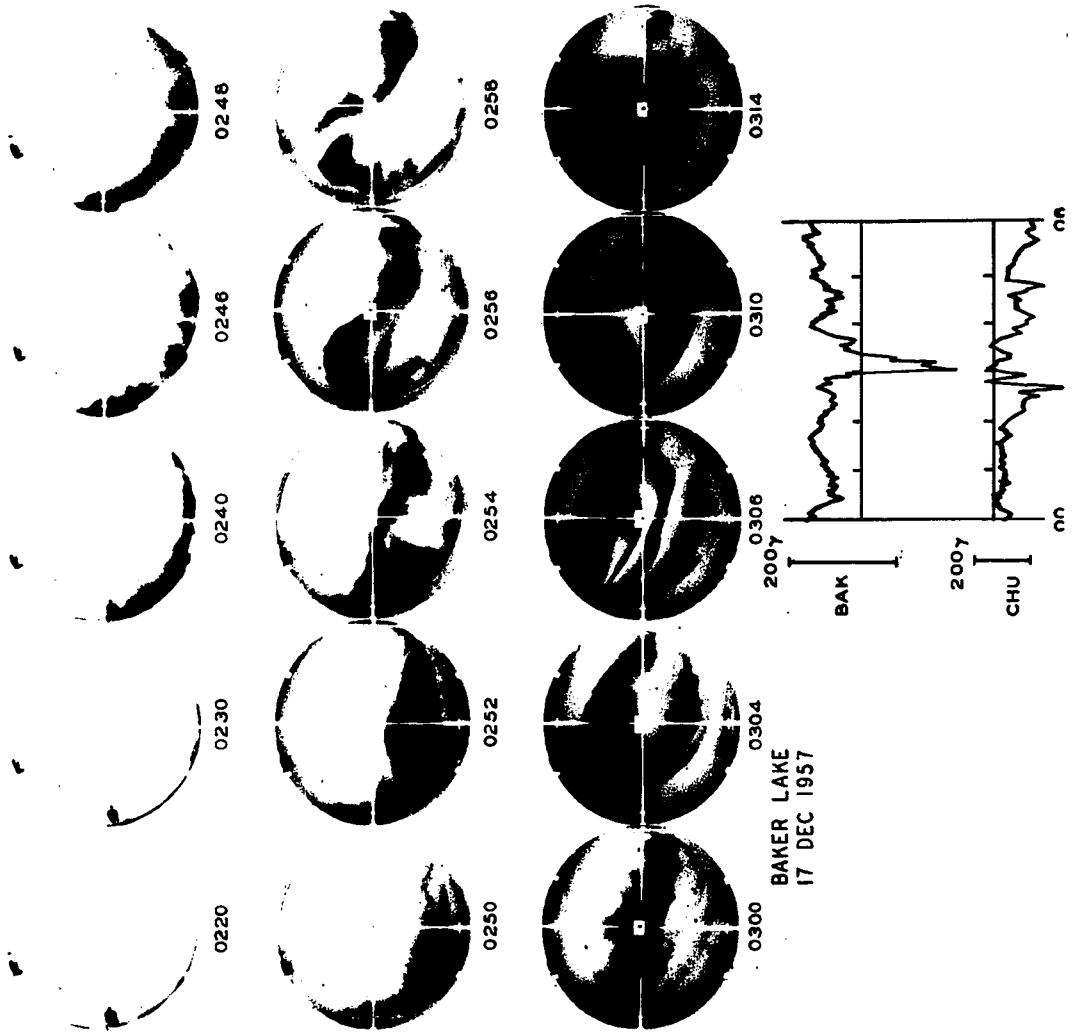


Fig. III-39. The Baker Lake all-sky photographs (in negative) and corresponding geomagnetic changes at Baker Lake and Churchill.

However, by 0300 UT they were essentially over. On the other hand, at Baker Lake a sharp negative bay began at about 0245 UT and reached maximum intensity at about 0300 UT. Figure III-39 also shows the all-sky camera photographs (in negative) taken from Baker Lake during this period. At 0200 UT, a faint arc was barely visible near the dp southern horizon. The arc became suddenly bright a few minutes later. At Baker Lake its poleward motion became obvious at about 0234 UT, and the activated band reached the zenith at 0254 UT. Therefore the event began well south of Baker Lake and spread poleward. The successive photographs show the poleward expansion of the auroral system. Note particularly a large scale fold structure in the western sky, which traveled along the band. This is a typical feature of the westward traveling surge described previously. All-sky photographs are, as in this case, of great help in understanding complicated spatial and time structures of geomagnetic variations. Indeed the negative bays seen at Churchill and Baker Lake are merely a part of the same auroral (and polar magnetic) substorm. A number of IGY examples show essentially the same results.

It was also pointed out that the electrojet does not grow instantly over a large area, but rather its development in the evening sector is very closely associated with the growth of the westward traveling surge. The westward surge travels along the pre-existing arcs or bands, namely along the auroral oval, and is accompanied by a strong westward current. Since the auroral oval extends from the midnight sector of the auroral zone to higher latitudes (Feldstein, 1966), both the surge and the westward current advance along the oval. With the useful aid of all-sky photographs it seems

clear that Harang's findings are essentially a statistical result of the magnetic disturbances associated with the westward traveling surges.

Further, it is reasonable to infer that there will be a return current from the extended jet to both the polar cap and the middle-low latitude regions. Figures III-36, III-37 and III-38 show also the H and D component records from Meanook. All the examples in Figures III-36 and III-38 show a positive change in the H component; they are the so-called 'positive bays'. Further, the magnitude of the H component (or even the total horizontal disturbance  $= \sqrt{(H^2 + D^2)}$ ) is less than the magnitude of the X component at Baker Lake. In Figure III-38 the H component changes at Meanook are not very clear. Both the August 7 and October 28 examples show a slight negative change. However, the D component shows consistently a positive (eastward) change in all the examples discussed here. This complexity was already discussed in detail in the last section.

Though we do not wholly exclude the possibility of the existence of an eastward jet, there is no obvious reason why the extended westward electrojet cannot produce a return current to lower latitude regions, including the auroral zone. Thus not all the positive bays in the auroral zone can be attributed to an eastward electrojet. Nikolsky (1947) also found the curve which lies outside the auroral oval, namely the A 'spiral' in Figure III-33 (the curve denoted by 'Mag A'). We suggest that the A spiral delineates the region where a strong eastward 'leakage' current (from the westward jet flowing along the oval) flows.

The claimed relation of geomagnetic disturbances at Baker Lake and Churchill tends to break down late in the evening or when successive polar magnetic substorms occur. In Figure III-38, all the examples show a single

well-defined negative bay. The corresponding negative bays at Churchill are weaker than those at Baker Lake (indeed there is a slight positive change there at that time). The second and third examples show similar results.

This is a natural consequence of the current pattern of flow along the auroral oval. Each magnetic station rotates under the (westward) polar electrojet with its varying intensity. The oval is eccentric with respect to the dipole pole. A high latitude station, like Baker Lake, 'crosses' the oval in the early evening sector from outside to inside. Intense negative bays are observed when the station is within the oval. But, in the late evening and midnight sector, it is well inside the auroral oval, and an auroral zone station, like Churchill, then observes an intense negative bay, but Baker Lake does not.

This is well illustrated by Figure III-40, which gives simultaneous magnetic records from six stations of a N-S Alaskan chain (1000 UT = 0000 LT, 150°WMT); see Figure III-34. The diagram is part of one originally produced by Wescott and Mather (1965) for their study of magnetic variations at conjugate points; Figure III-40 gives only the Alaskan part. In the early evening hours, between 1900 LT (0700 UT) and 2300 LT (0900 UT), intense negative bays were observed at Barter Island, while weaker positive changes were observed at College, Healy and Anchorage; both Barrow and Ft. Yukon were in the transition region. However, between 2300 LT and 0400 LT (0900 UT and 1400 UT), the records of both Barter Island and Barrow were fairly quiet while very intense negative bays were observed at Ft. Yukon and to the south. Obviously the regions of intense magnetic activity shifted toward lower latitudes.



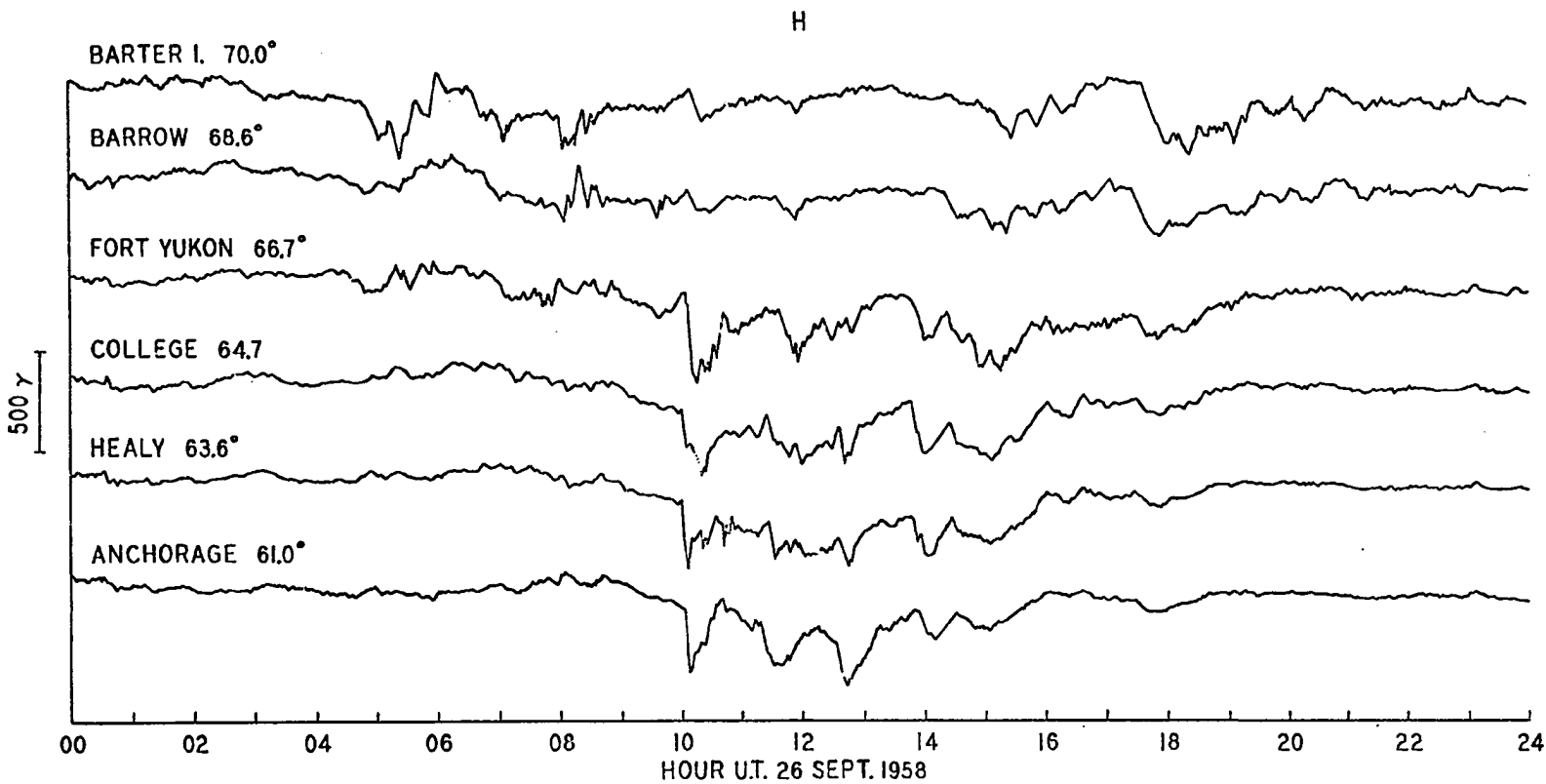


Fig. III-40. The simultaneous magnetic records from the N-S Alaskan Chain of magnetic station (Wescott and Mather, 1965).

As morning progressed, both Barter Island and Barrow again began to record intense negative bays, much more intense than those observed in the lower latitudes. This indicates that Barter Island and Barrow were 'crossing' the oval from inside to outside at that time. After 1000 LT (2000 UT) all Alaskan stations were outside the oval. This sequence is repeated daily; see other examples produced by Wescott and Mather (1965). Statistical studies have clearly confirmed this, since both the M and N spirals indicate the time when a station crosses the oval.

(b) Indented Positive Bay

Besides the simple intense negative bay, the intense negative bay superposed on a gradual positive change of the horizontal component (H or X) of the earth field, as the positive change is indented by negative bay, is also frequently observed at a dipole latitude as high as  $78^\circ$ . At such a high latitude region, the gradual positive change at the time of the polar magnetic substorm has been interpreted as due to the fact that the return current has an eastward component (cf. Silsbee and Vestine, 1942). The superposition of an intense negative bay on it indicates thus a large-scale change of the polar electrojet current system during the course of the development of the polar magnetic substorm.

Here a pair of stations, Mould Bay (dp lat  $79.1^\circ\text{N}$ ) and College ( $64.7^\circ\text{N}$ ) were chosen. They are located in the same geomagnetic meridian and are indicated in Figure III-41 together with an approximate location of the auroral oval at 0600 UT (corresponding to 2000 LT,  $150^\circ\text{WMT}$ ). Figures III-42 (a) and (b) show two examples of rather simple positive changes observed at Mould Bay (X), and the simultaneous College magnetic records (H). The College records show a complex change which is typical in the late evening hours during the substorm.

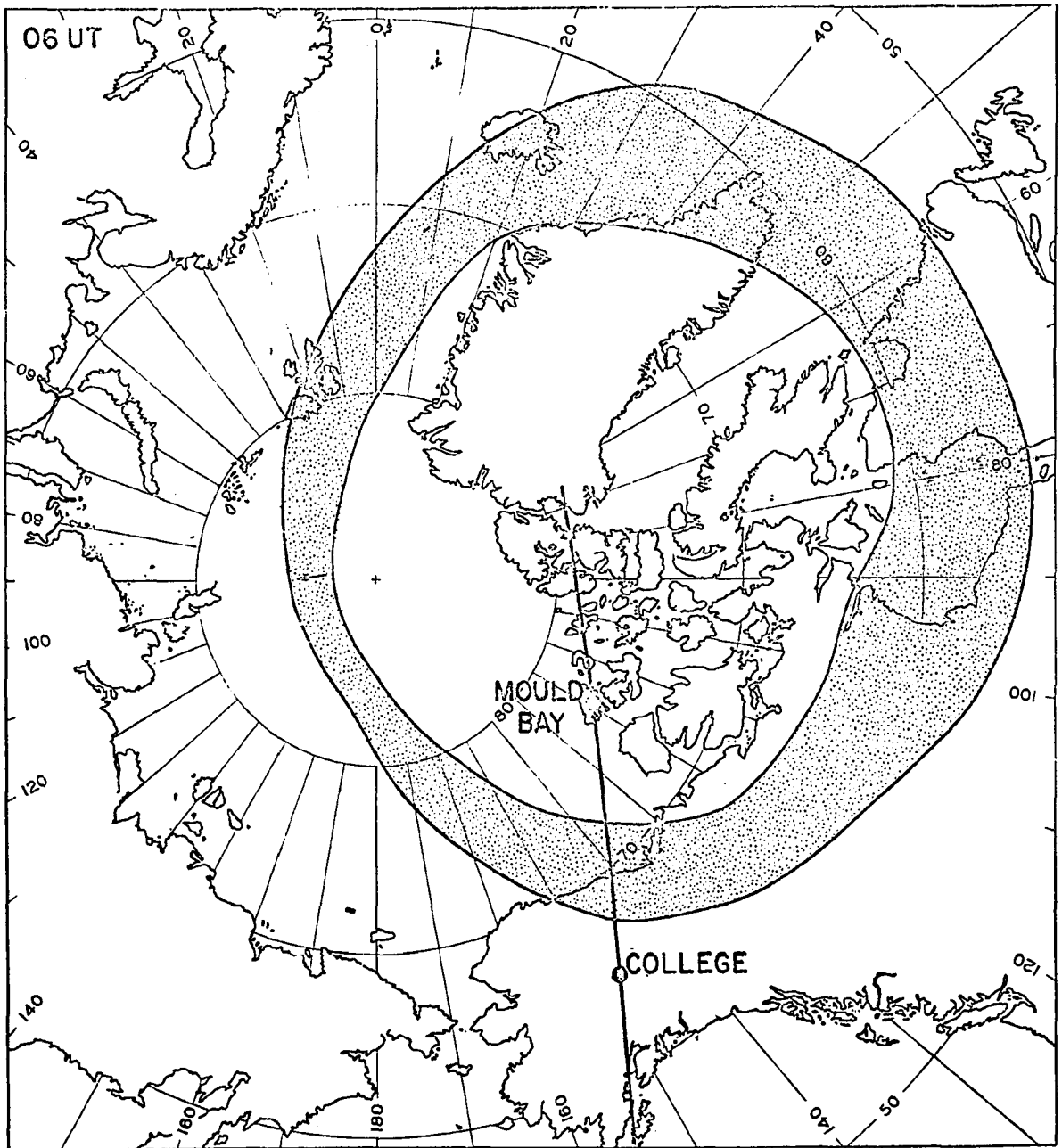


Fig. III-41. The location of the two magnetic stations, Mould Bay and College, whose data are used in this paper, together with the location of the auroral oval (obtained by Feldstein (1963)) at 0600 UT; the geomagnetic pole and the meridian passing through College are indicated.

H

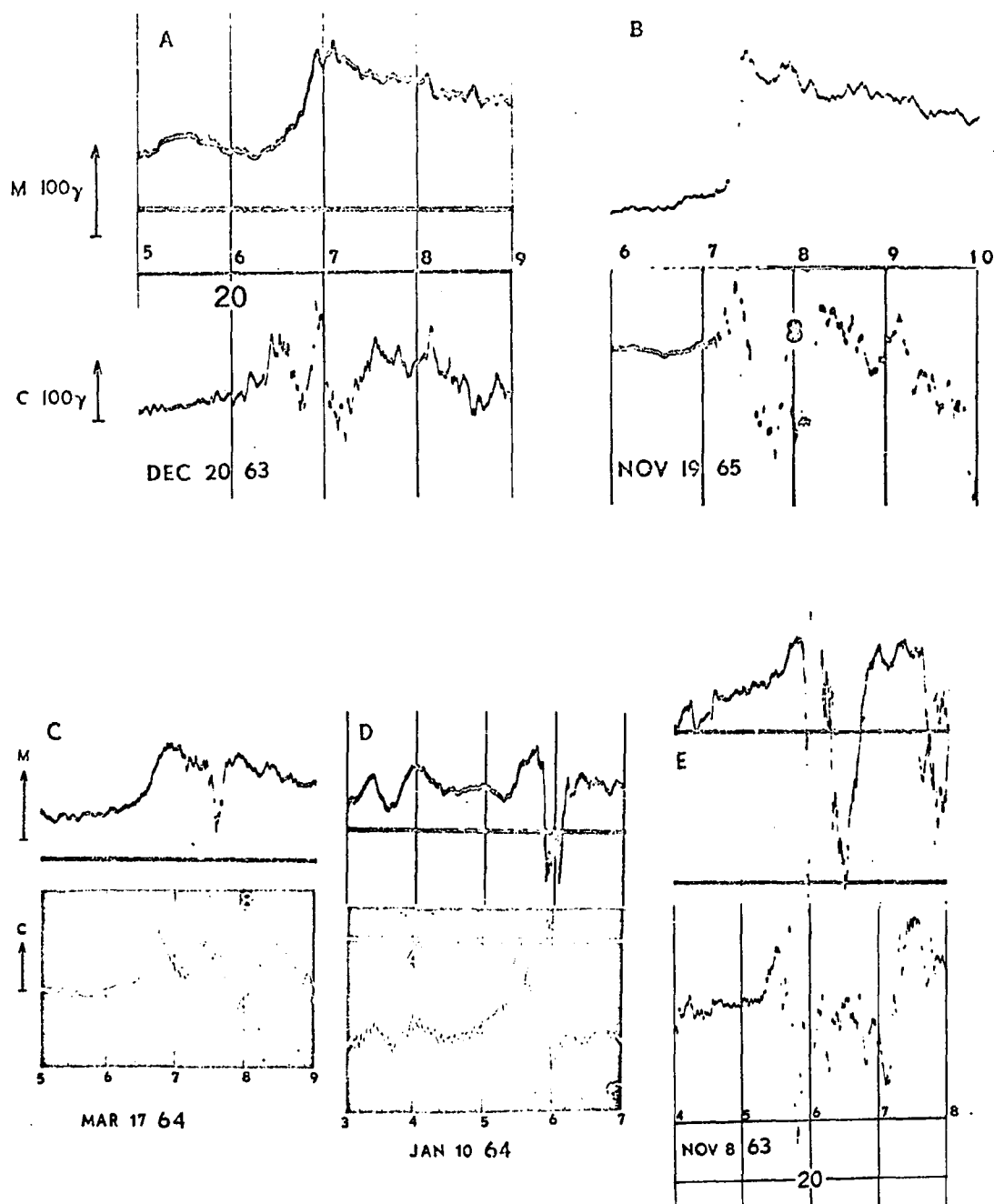


Fig. III-42. (a), (b), Examples of positive bay recorded at Mould Bay indicated by M and the corresponding geomagnetic changes at College indicated by C. (c), (d), (e) Examples of positive bay with negative indentation recorded at Mould Bay and the corresponding geomagnetic changes at College.

However, magnetic records from Mould Bay are, in general, more complicated than the above two examples and often show a sharp negative indentation on the slow positive change. Figures III-42 (c), (d) and (e) show three such examples, together with the simultaneous College magnetic records. In all three cases the positive change began at about the same time at both Mould Bay and College, namely at about 0630, 0515 and 0520 UT respectively; this particular phenomenon will be discussed later. However, the negative indentation is clearly seen to be superposed on the positive change in each case in the Mould Bay records. Figure III-43 shows several other examples of such negative indentations recorded at Mould Bay. The magnitude of the negative indentation frequently exceeds that of the slow increase.

The negative indentation at Mould Bay indicates that an intense polar (westward) electrojet can appear near Mould Bay.

It has already been shown that intense negative bays are observed near and within the expanding auroral bulge during the auroral substorm; the expanding bulge can be roughly visualized as an expansion of the auroral oval on the night side. Therefore, the occurrence of the indented positive bays at Mould Bay suggests that Mould Bay is located well outside of the expanding bulge in the early phase of the substorm (and thus is in the region of the eastward return current), as is indicated in Figure III-41. As the substorm progresses, the width of the oval rapidly increases, particularly to the poleward side of the oval. Thus, the expanding oval can reach near Mould Bay at about the maximum stage of the substorm. In fact, at Churchill (which was located in the midnight sector), intense substorms were observed at those times.

H

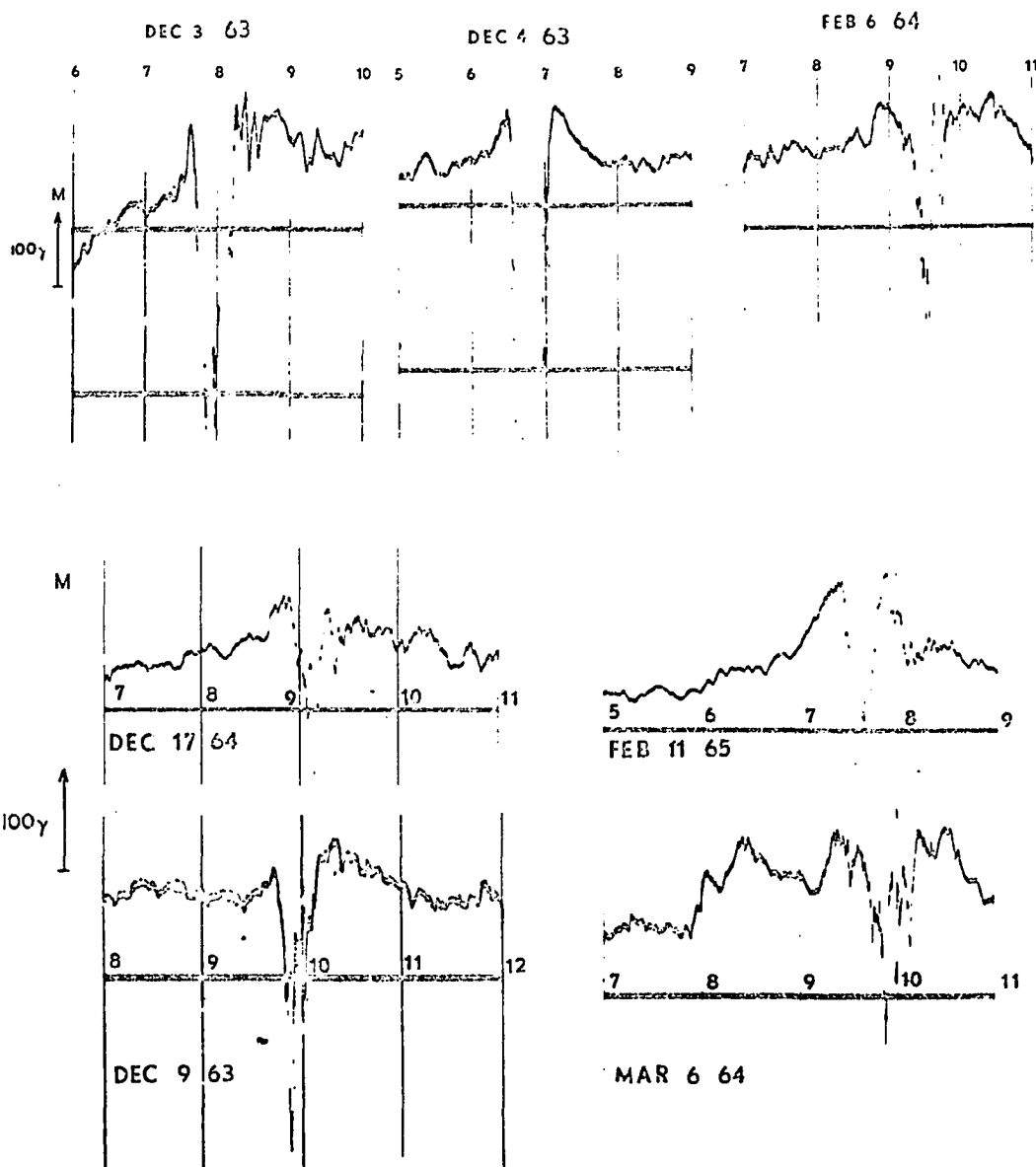
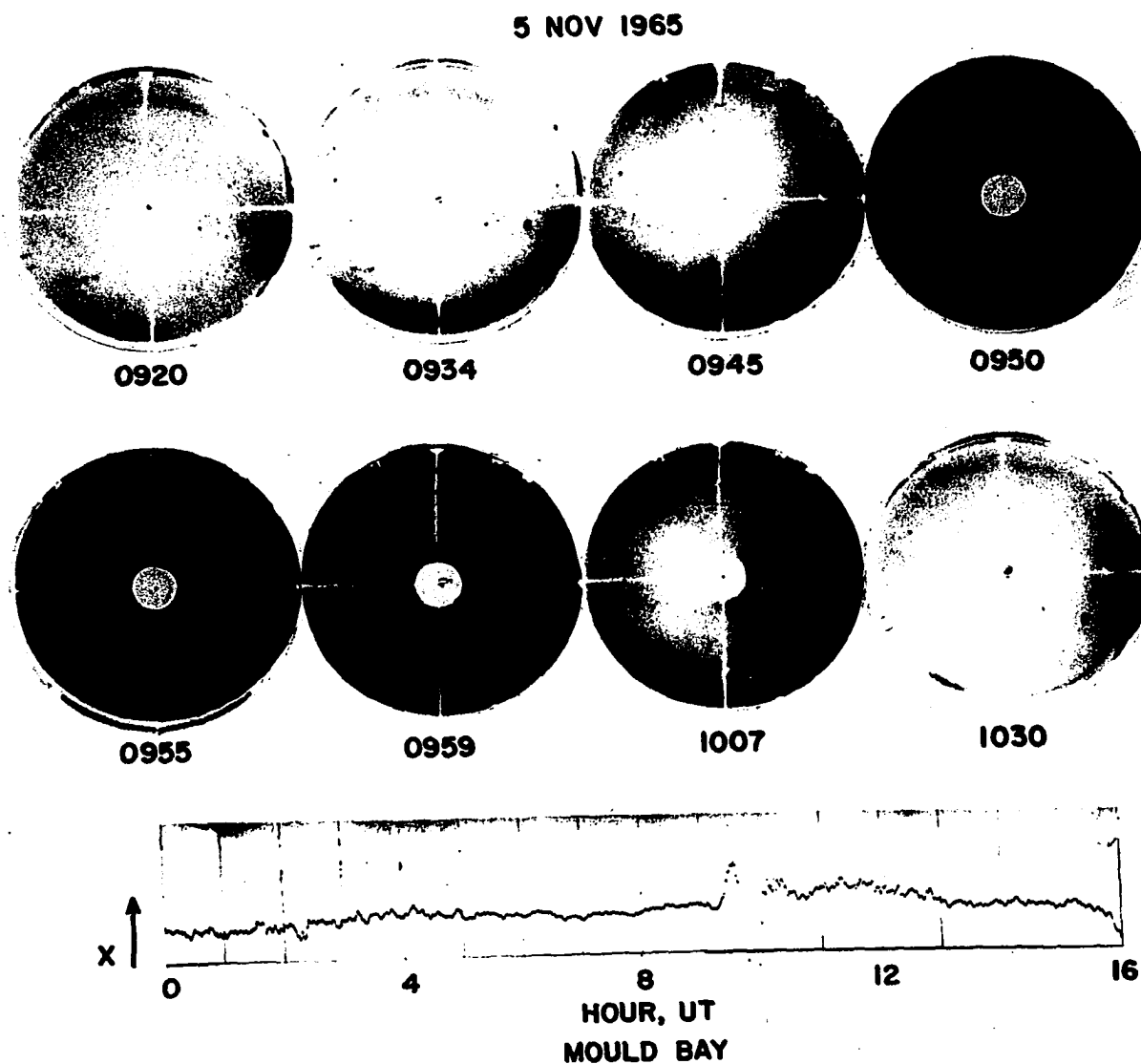


Fig. III-43. Examples of indented positive bays recorded at Mould Bay.

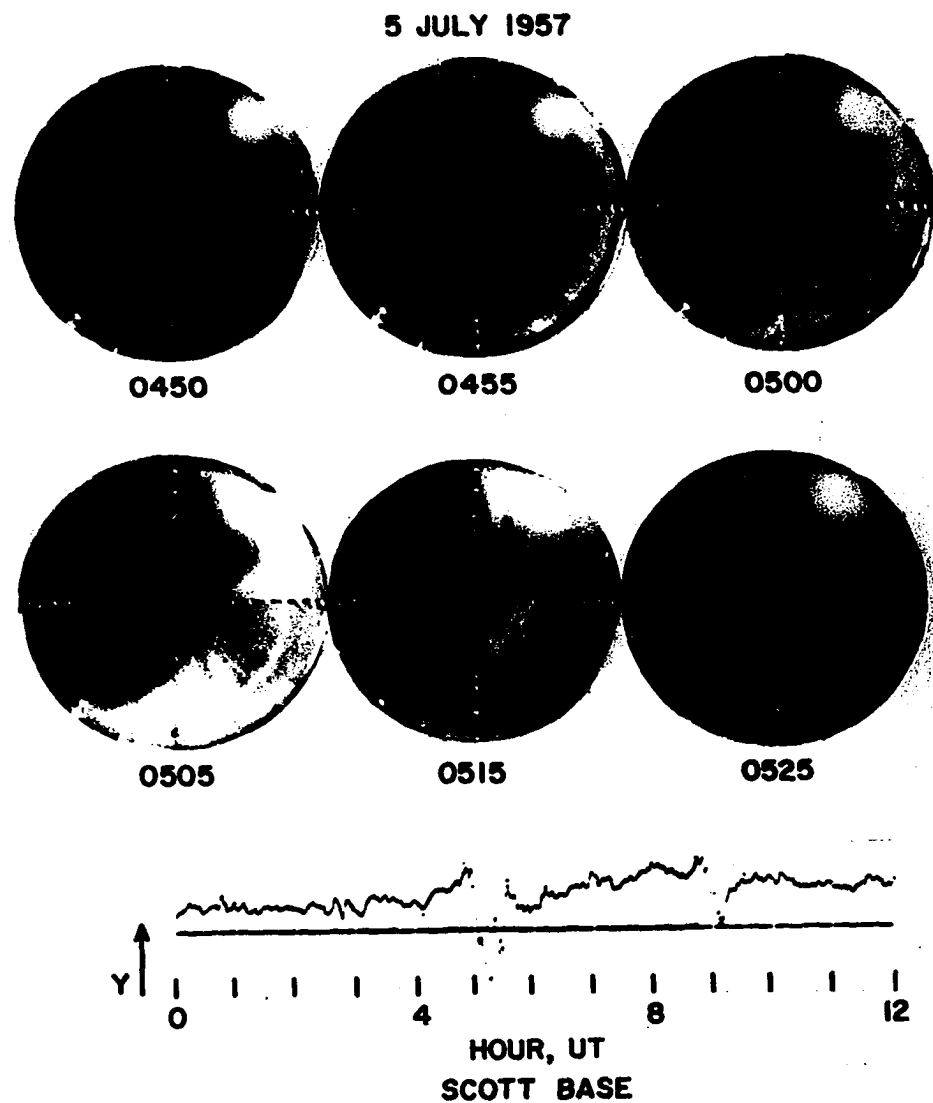
In Figure III-44 we show a few examples of the expanding auroral bulge and associated magnetic records. Figure III-44 (a) shows a series of all-sky camera photographs and the simultaneous magnetic records taken at Mould Bay, Canada, on November 5, 1965. At 0920 UT, Mould Bay was well inside the auroral oval, so that auroras were located too far south to be clearly seen. At that time auroras were seen at about 200 km dipole north of College, which is located approximately along the same dipole meridian as Mould Bay. The College all-sky camera records, though not shown here, indicate the onset of an auroral substorm at about 0830 UT. The poleward expanding bulge at Mould Bay can be seen in the photographs between 0934 and 0955 UT. The bulge reached the zenith there at 0955. The X component magnetic record shows a gradual increase which began at 0920 UT. This was followed by a brief intense negative bay at about 0935 UT when the bulge was about 200 km south of the zenith. The maximum intensity of the negative bay was reached at about 0955 UT when the bulge reached the zenith. It appears that the main part of the bulge drifted eastward soon after that, and the magnetic record shows the recovery from the negative bay at that time.

Figure III-44 (b) shows another example of the poleward expanding bulge and the associated magnetic change observed at Scott Base. Just before this substorm, the aurora was beyond the field of view of Scott Base. The first sign of the substorm was seen there at 0454 UT: the bright auroras advanced rapidly poleward (toward Scott Base) from the direction of the midnight part of the auroral oval and reached the zenith at about 0512 UT. The all-sky camera records from Byrd (which was located in the early morning sector of the auroral oval at that time) indicated



**Fig. III-44a. Examples of the all-sky photographs of the expanding auroral bulge and associated magnetic records. Mould Bay, Canada, Nov. 5, 1965. (Photographs in negative).**





**Fig. III-44b. Examples of the all-sky photographs of the expanding auroral bulge and associated magnetic records. Scott Base, Antarctica, July 5, 1957.**

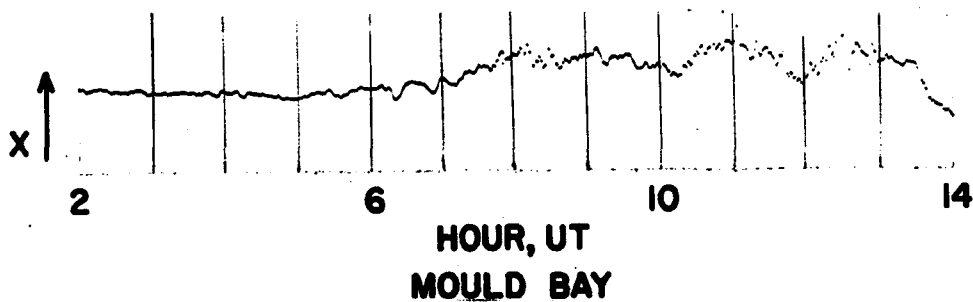
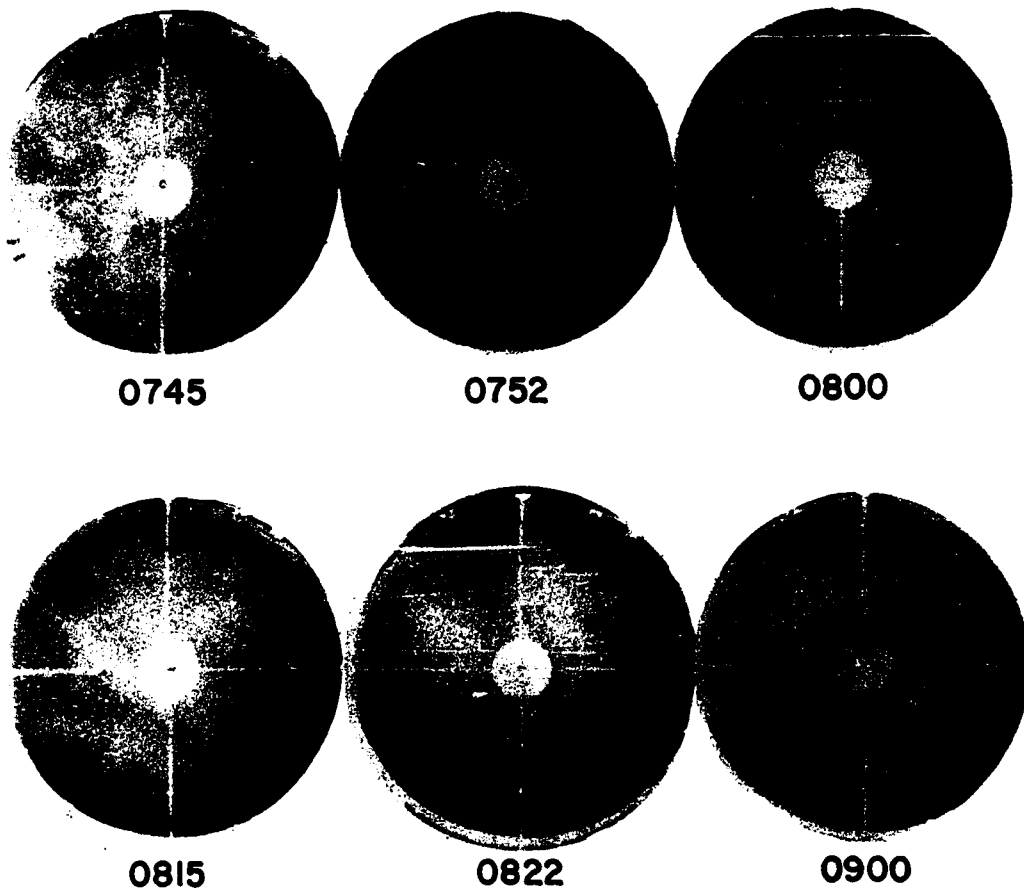
the onset of the substorm at about 0430 UT. The Scott Base Y component magnetic record (which corresponds approximately to the H component) shows a gradual positive increase change from about 0430 UT, which was followed by a sharp negative change at about 0544 UT; this positive change attained its maximum at about 0515 UT. Then the bulge began to shrink toward the midnight part of the oval.

Figure III-44 (c) shows an example of auroras in the southern part of the sky at Mould Bay; the auroral bulge did not reach the zenith there. The simultaneous Mould Bay magnetic record indicates only a gradual positive change, without any negative bay.

In general, the bulge starts to contract soon after it attains the highest latitude, and this is the beginning of the recovery phase of the auroral substorm (Akasofu, 1964). Therefore, the polar electrojet remains in the vicinity of Mould Bay for only a short period, compared with the lifetime of the substorm. As soon as the current retreats equatorward, Mould Bay is placed on the poleward side of the bulge again (this in the region of the eastward return current). The same explanation may also be applied to some of the so-called 'cusped bay' extensively studied by Knapp (1961). Therefore, the combined dynamical morphology of both the auroral and magnetic substorm can reasonably explain such a complicated feature of magnetic variations at very high latitudes. The situation is a little more complicated at College, depending on the location of the oval with respect to College during the recovery phase.

Magnetic records taken at a similar latitude, such as at Godhavn (dp lat 79.9°N) also show a similar indentation. It may be noted that Lassen (1961) reported instances of bright auroras approaching from the

1 DEC 1965



**Fig. III-44c. Examples of the all-sky photographs of the expanding auroral bulge and associated magnetic records. Mould Bay, Canada, Dec. 1, 1965. (Photographs in negative.)**

southern horizon toward the zenith at Godhavn, indicating that the bulge does reach sometimes as high as  $80^\circ$ . Since the Mould Bay station was not in operation during the IGY, we have examined the occurrence frequency of negative bays in the evening hours (between 2000 and 0600 UT) at Godhavn for the first three months of the years 1958 and 1964. It was found that the number of bays was 2.7 times more in 1964 than in 1958. This confirms Lassen's study (1958) and is also in agreement with the fact that the auroral oval contracts poleward during quiet periods of the sun (cf. Stringer, Belon and Akasofu, 1965).

The above results suggest that essentially the same process occurs frequently both well inside the polar cap and along the evening sector of the auroral zone. Since there is little doubt about the fact that the positive change in the polar cap is caused by the eastward return current, the positive change along the auroral zone in the evening hours is also likely to be caused by an eastward return current from the polar (westward) jet. That is, an intense westward current flows along the auroral oval and its return current flows on both the poleward and equatorward sides of it.

The oval current system thus accounts for the results obtained by two different approaches, namely the DS analysis and the spiral analysis. Previously it seemed that the results obtained by the two approaches were mutually exclusive; instead they reveal different aspects of the pattern of the polar electrojet. What hindered us in understanding the whole feature was due to the fact that the auroral oval is eccentric with respect to the dipole pole and that too much emphasis had been placed on the auroral zone which is now found to be the locus of the midnight part of the auroral oval.

### (c) Auroral Substorms Near the Dipole Pole\*

For the present work the all-sky camera data from Alert, (dp lat  $85.9^\circ$ ), Thule (dp lat  $88^\circ$ ), Vostok (dp lat  $90^\circ$ ) and Resolute Bay (dp lat  $84.2^\circ$ ) taken during and subsequent to the IGY were examined. Particular attention was paid to the association of the auroral observed at these stations with the disturbance magnetic field, also to what has been called the polar substorm (DP), the sharp bay events occurring at the auroral zone simultaneously with the auroral substorm. The occurrence of such events was monitored by means of records from four magnetic observatories approximately equally spaced around the auroral zone. The stations employed were College (Alaska), Dixon (USSR), Leirvogur (Iceland) and Churchill (Canada)\*, the data from each station being used during the interval when the station was between about midnight and 6 AM local geomagnetic time. (\* The conjugacy of the polar substorm will be discussed in the following section.)

The most common auroral events recorded by the cameras in the polar cap were in the form of sun-aligned arcs reported by earlier workers. However, there was another class of events in which no systematic orientation of the arcs was discernible. The aurora in these cases consisted of active arcs that moved over the zenith mostly from the sector of the horizon lying in the midnight direction. Such events were associated with polar magnetic substorms, indicating that these were again instances of the poleward expansion. What is remarkable about these events is that they occur even at the geomagnetic pole.

Figure III-45 displays a sequence of all-sky camera frames from Vostok along with the magnetogram from Leirvogur, Iceland which was at

\*This work was done jointly with Dr. R. N. DeWitt.

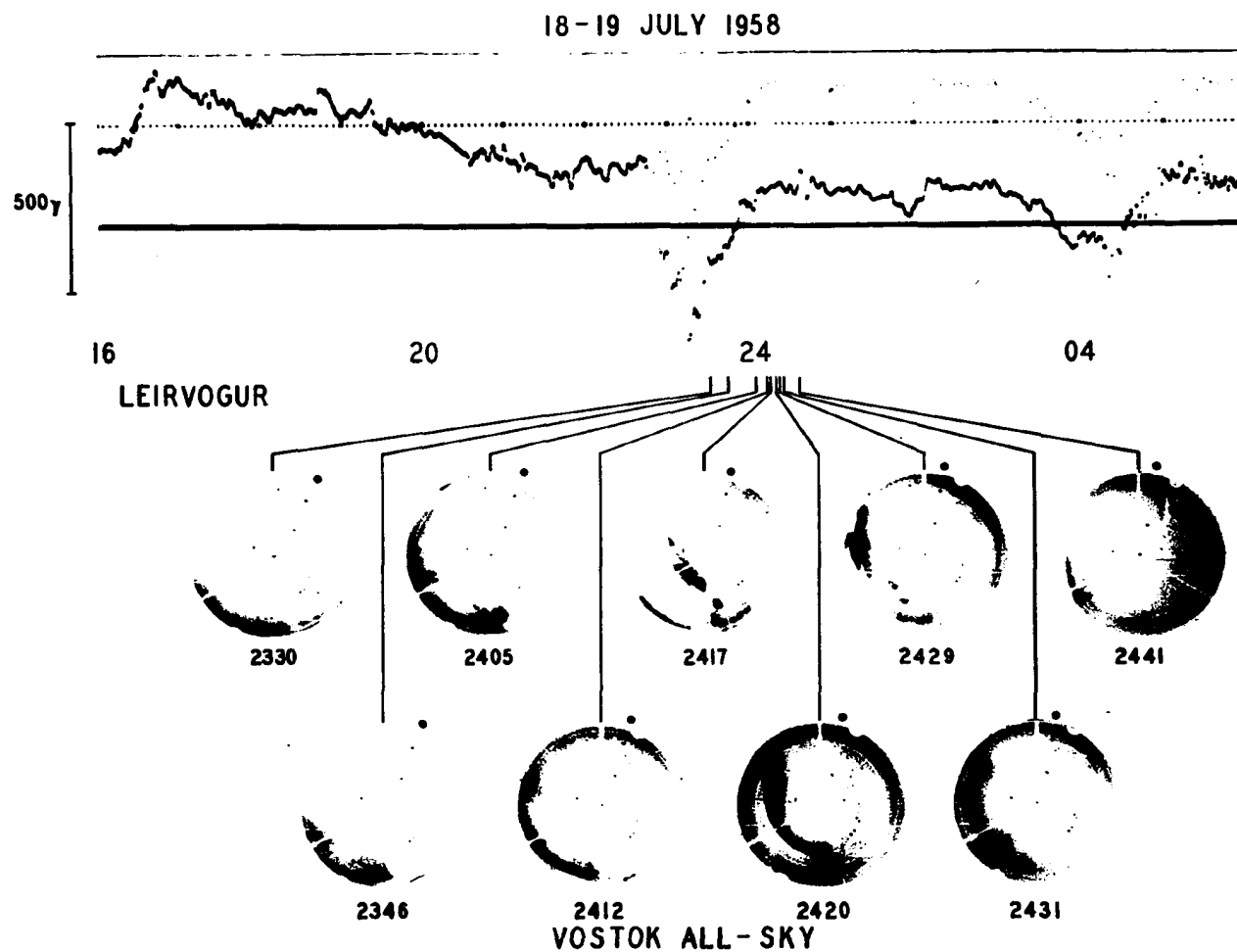


**Fig. III-45.** Poleward expansion of the aurora from the midnight sector of the auroral oval (photographs in negative). In this case the expansion reaches the south geomagnetic pole. The direction of the sun is marked by a dot next to the photographs.

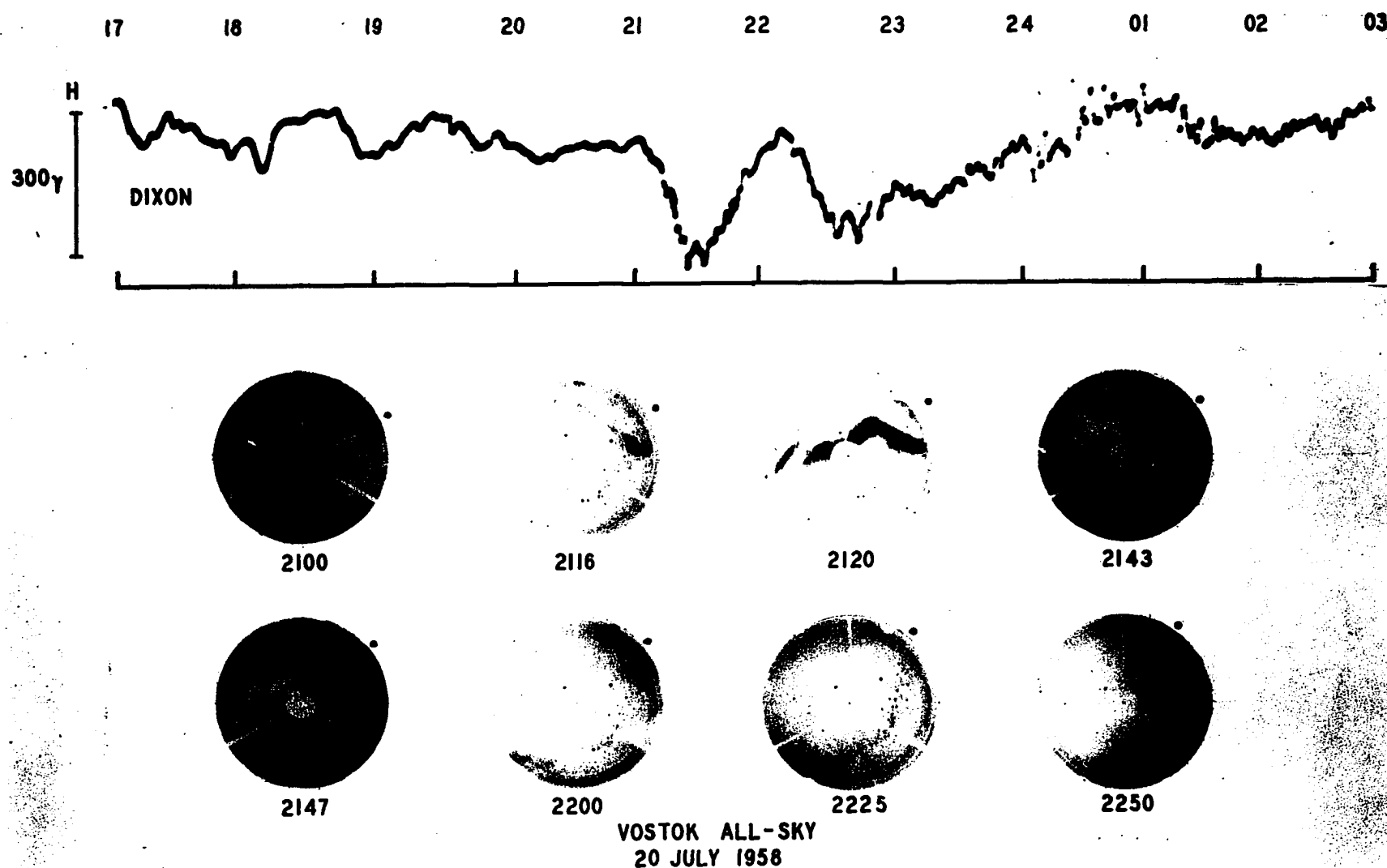


Fig. III-46. Poleward expansion to the south geomagnetic pole of the aurorally active region at the dawn sector of the auroral oval. (Photographs in negative). The direction of the sun is marked by a dot next to the photographs.

that time in the geomagnetic midnight sector of the auroral zone. This example is typical of the cases in which the auroral substorm expansion reached the pole. In Figure III-46 is shown another example, this time with the aurora moving from the dawn sector of the auroral oval. Such events as those shown in Figure III-45 and Figure III-46 are infrequent; some idea of the proportion of the auroral expansions that extend so far may be gained from Figure III-47 where, for nine consecutive days, the magnetograms from auroral zone observatories in the post-midnight quadrant of the auroral zone are displayed, along with indications of the occurrence of aurora over Vostok. Of approximately thirty magnetic substorms that occurred during intervals when the all-sky camera was operating, only three were associated with poleward expansions of the aurora that extended to the sky over Vostok. It may further be seen from Figure III-47 that it does not seem to be simply a matter of the intensity of the substorm which determines the poleward extent of the auroral expansion. There are several instances of magnetic substorms with amplitudes exceeding 500  $\gamma$  for which there was no corresponding auroral effect seen at Vostok, while the 200  $\gamma$  bay of 2130 July 20 did produce a poleward expansion reaching the pole.

### 3. Conjugacy of the Polar Substorm

#### 1) Introduction

Magnetic disturbances at magnetically conjugate areas have been studied extensively by Nagata and Kokubun (1960), Wescott (1961), Wescott and Mather (1965a, 1965b, 1965c, 1965d) and many others (cf. Wescott (1966)). Wescott and Mather (1965a) studied the conjugacy of geomagnetic bays in



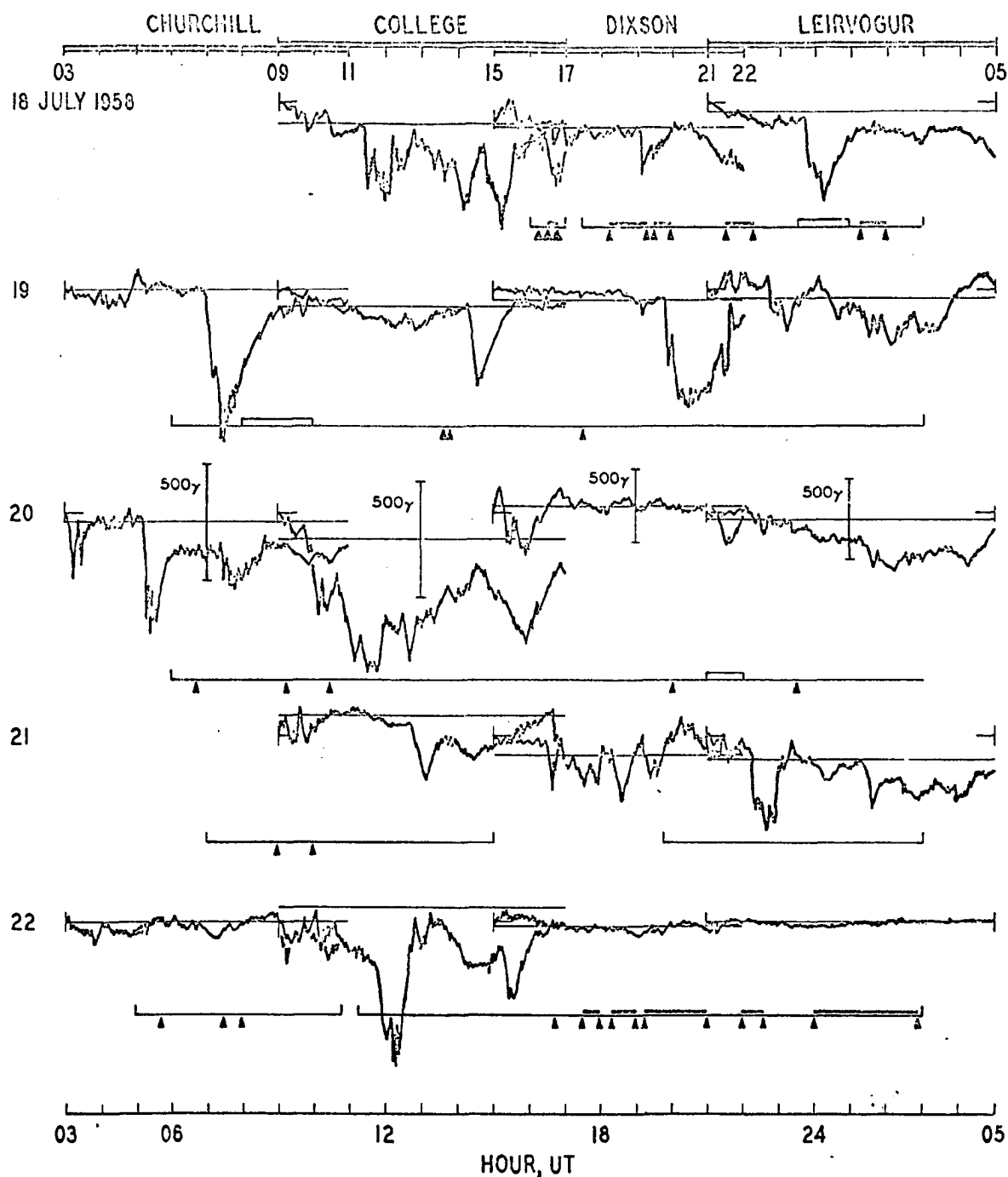


Fig. III-47. Magnetic records from the post midnight quadrant of the auroral zone for nine consecutive days. Times when the Vostok all-sky camera was operating are marked by a line below the magnetograms. The occurrence of sun-aligned arcs (S.A.) is marked by solid bars and triangles, and of substorm associated auroras (S.S.), by open bars.

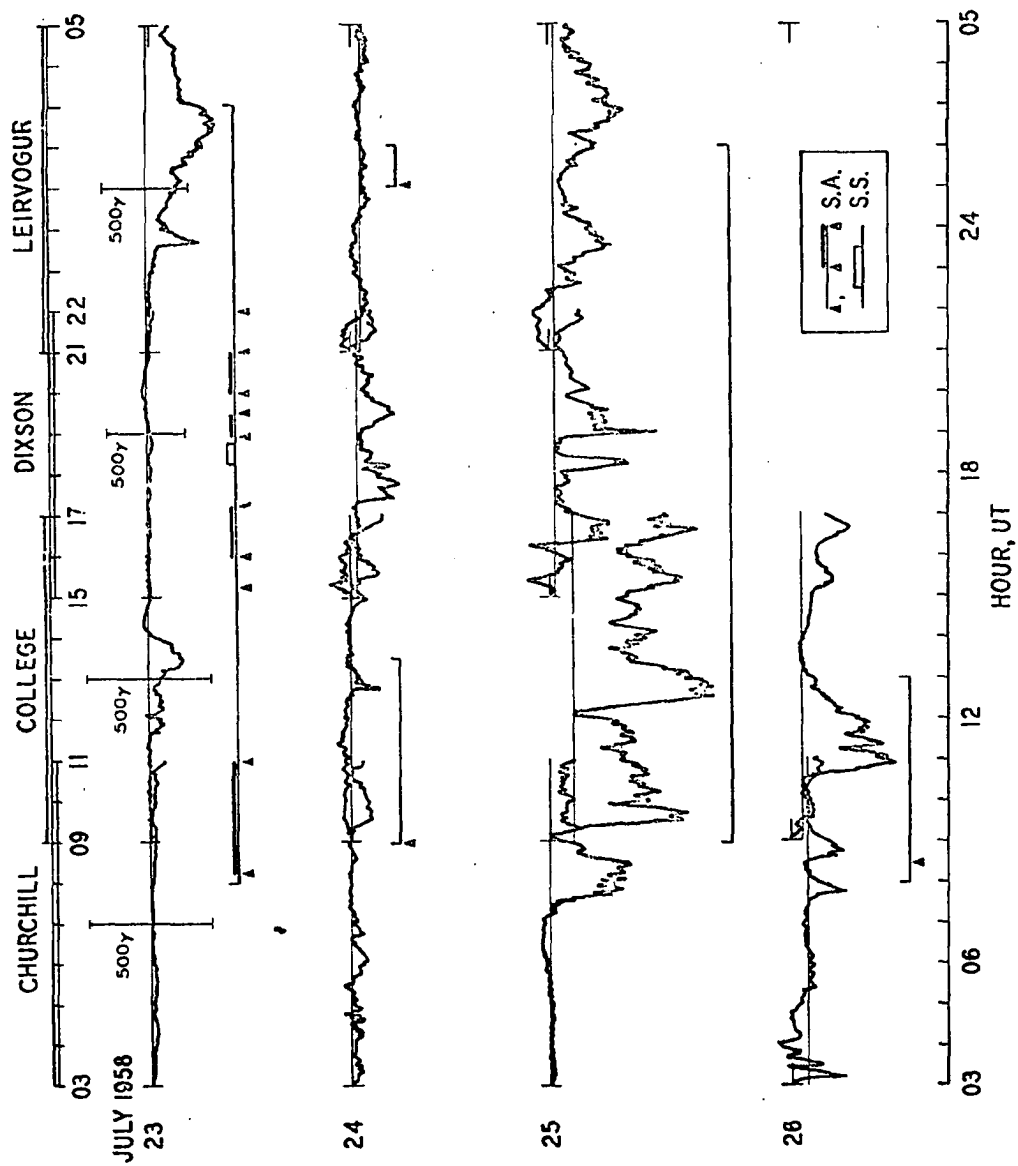


Fig. III-47 (Continued).

the auroral zone on four IGY days during the northern winter. They also studied the conjugacy of the daily and seasonal change of magnetic disturbance fields in the auroral zone on twenty-nine days. They found that the correlation between conjugate points was less for positive bays than for negative bays and that the relative amplitude of positive bays to negative bays exhibited a clear seasonal variation. Wescott and Mather (1965a) suggested that the nature of the positive bays be further investigated. Recently the concept of polar substorms, both magnetic and auroral, has been introduced, and the current system to explain polar magnetic disturbances has been revised (see Section 2). One purpose of this section is to investigate the degree of conjugacy of polar magnetic substorms based on this new current system. IGY/C data from two pairs of conjugate stations, College-Macquarie and Reykjavik-Syowa, were used for this study; see Table III-2. The calculated area conjugate to Macquarie Island should include Kotzebue; however, Wescott (1966) showed that for the auroral zone magnetic variations the conjugate areas are elongated along iso-L lines. Thus, since the quality of the magnetograms from College, which is about 700 km east of Kotzebue, is superior to those of Kotzebue, College magnetograms were used.

For the first pair of conjugate stations (College and Macquarie Island) magnetograms of January and June, 1958 and for the second pair of stations (Reykjavik-Syowa), magnetograms of June and December, 1959 were used. The horizontal component records were scaled by a semi-automatic OSCAR machine and were then plotted for comparison to the same force and time scales. The magnitude of each bay, both positive and negative, was then determined by choosing the base level, inferred from the trace in

TABLE III-2  
Stations Used in this Study

Station	Geographic		Dipole		L
	Latitude	Longitude	Latitude	Longitude	
College	64.85°	-147.83°	64.6°	256.5°	5.43
Macquarie	-54.30	158.60	-61.1	243.1	5.25
Reykjavik	64.18	-21.70	70.2	71.0	6.27
Syowa Base	-69.03	39.60	-69.7	77.7	6.16
Shepherd Bay	68.75	-93.75	78.3	(312)	29.31
Scott Base	-77.85	166.75	-79.0	294.4	34.27
Mould Bay	76.20	-119.40	79.1	256.4	37.32

the afternoon and late morning hours. For the "associated bays", which occurred at the conjugate stations with the same sign, the magnitudes were compared by determining the ratio  $R = S/W$ , where  $S$  is the peak magnitude of the bay at the summer hemisphere station (as at Macquarie Island in January and College in June) and  $W$  that at the winter hemisphere station (as at Syowa in June and Reykjavik in December). To investigate the nature and the daily variation of the conjugacy of the bays, as well as to compare the conjugacies between the two pairs of stations, the ratio  $R$  was plotted separately according to the sign of the bays and the season for each pair of stations.

The second purpose of this section is to examine the magnetic conjugacy for two conjugate stations well inside the polar cap. Wescott and Mather (1965d) have already shown that at the high latitude Shepherd Bay-Scott Base pair (see Table III-2) the conjugacy breaks down. We show that the breakdown is associated with a marked seasonal dependence of the occurrence of positive and negative bays.

## 2) Auroral Zone Conjugate Pairs

### (i) Conjugacy for the College-Macquarie Pair

#### a) Northern Winter-January 1958

In the conjugate areas the general shapes of bay-type records are very similar; but the positive bays are larger in the local summer, i.e. in the sunlit hemisphere. The magnitudes of negative bays are approximately the same in both hemispheres. Figures III-48, January 1, 1958, illustrates a typical case (00 UT = 14 LT at College; 11 LT at Macquarie). Between 00 to 04 UT, both College and Macquarie recorded small positive

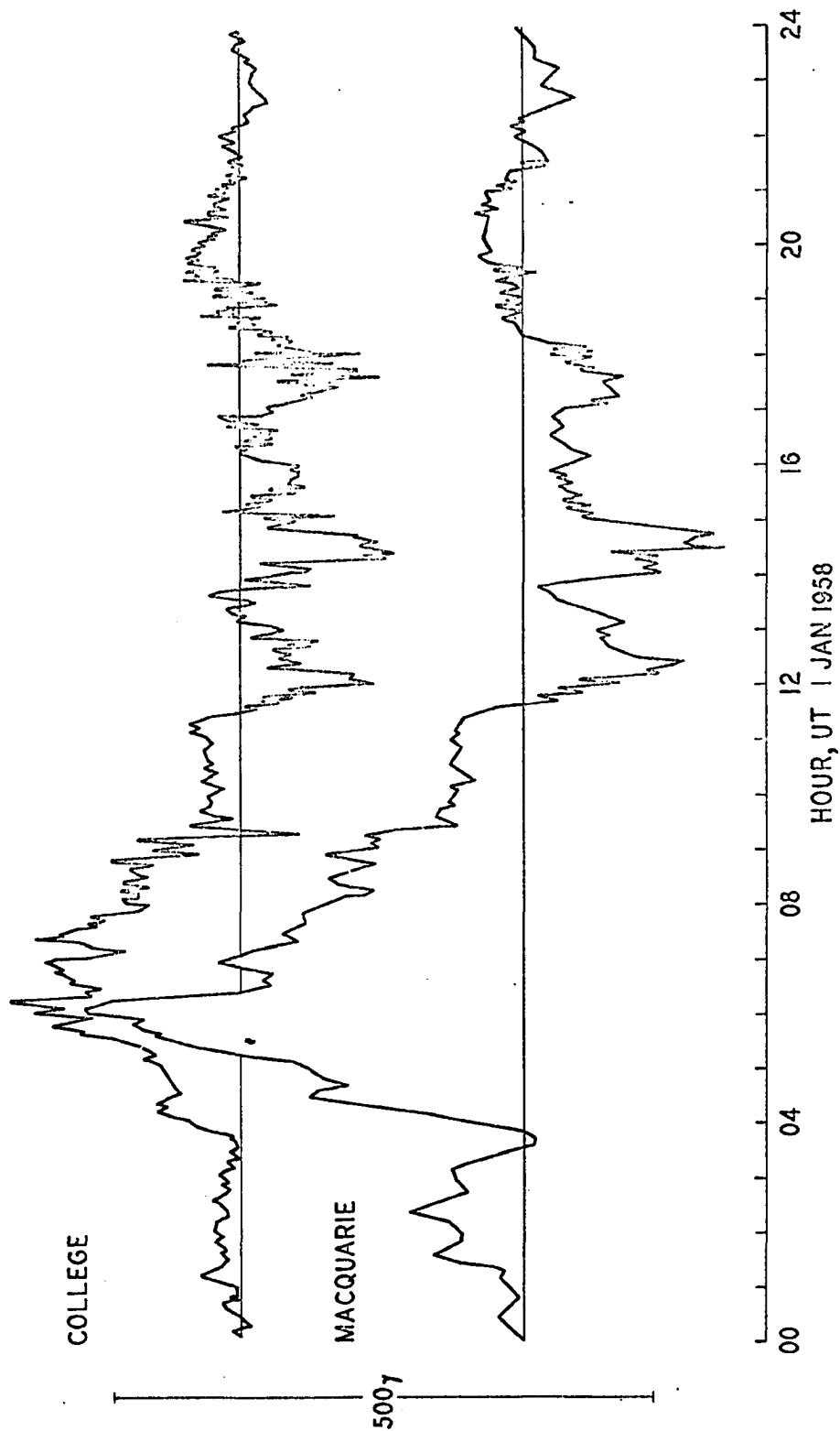


Fig. III-48. Typical example of magnetic records (the horizontal component) from the near conjugate pair stations College and Macquarie.

disturbances, but the magnitude was much greater at Macquarie Island. At 0400 UT a polar magnetic substorm became intense; it reached its maximum at about 0600 UT, subsiding at about 1000 UT at both stations. The gross form of the positive disturbance was similar at the two stations, but the magnitude was much greater at the sunlit station. After 1100 UT at least three negative bays occurred at 1200 UT, 1430 UT and 1700 UT. They were very similar in both form and magnitude.

January 1953 provided a total of 36 positive and 47 negative "associated" bays; the ratio for Macquarie/College was plotted as a function of universal time. This is shown in Figure III-49 (a). The data points of Figure III-49 (a) are rather scattered, ranging from  $R = 1$  to  $R = 5$ ; the average (about  $R = 2$ ) indicates that in the northern winter a positive bay at Macquarie Island has about twice the magnitude of one at College. There is some slight indication that  $R$  diminishes as time progresses from early afternoon to midnight; LM denotes local midnight at College. This tendency can be seen more clearly in the next conjugate pair. There was, however, one exception which occurred on January 29. On this day the positive bay at College was larger than that at Macquarie (Fig. III-50). The positive bays started at 0330 UT at both stations and reached their maxima (520  $\gamma$  at College and 370  $\gamma$  at Macquarie Island), simultaneously at 0515 UT.

For the negative bays, the  $R$  values are less than or close to unity; thus, in general, negative bays at Macquarie are less intense in the northern winter than at College; this can be explained by the greater proximity of College than of Macquarie to the center line of the auroral zone. In Figure III-49 (a), one interesting feature is the converging of the data points toward  $R = 1$  as the morning progresses.

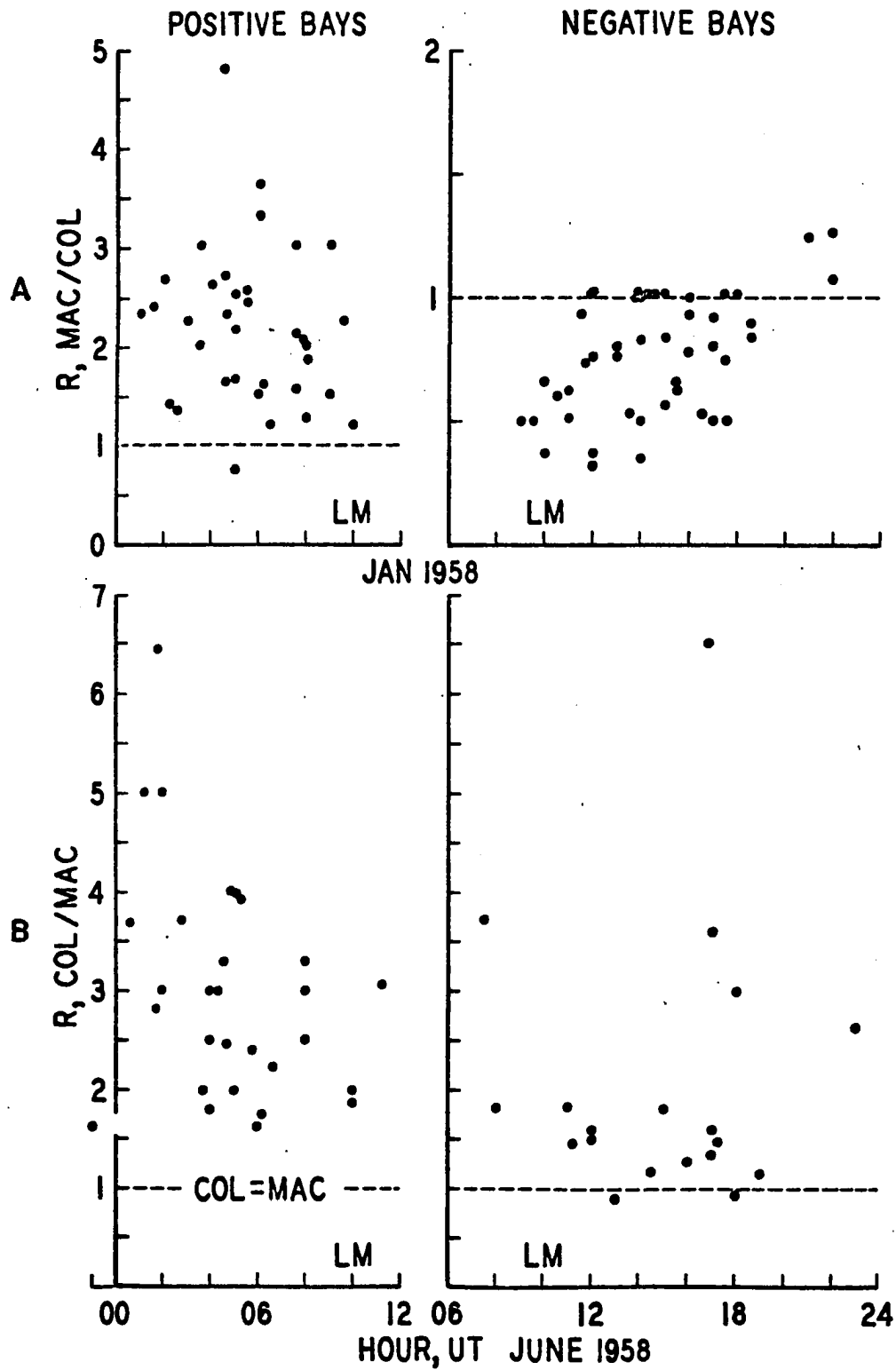


Fig. III-49. Relative magnitude ratio (R) for the associated bays for the College-Macquarie pair:

- a) Northern Winter, January 1958
- b) Northern Summer, June 1958.



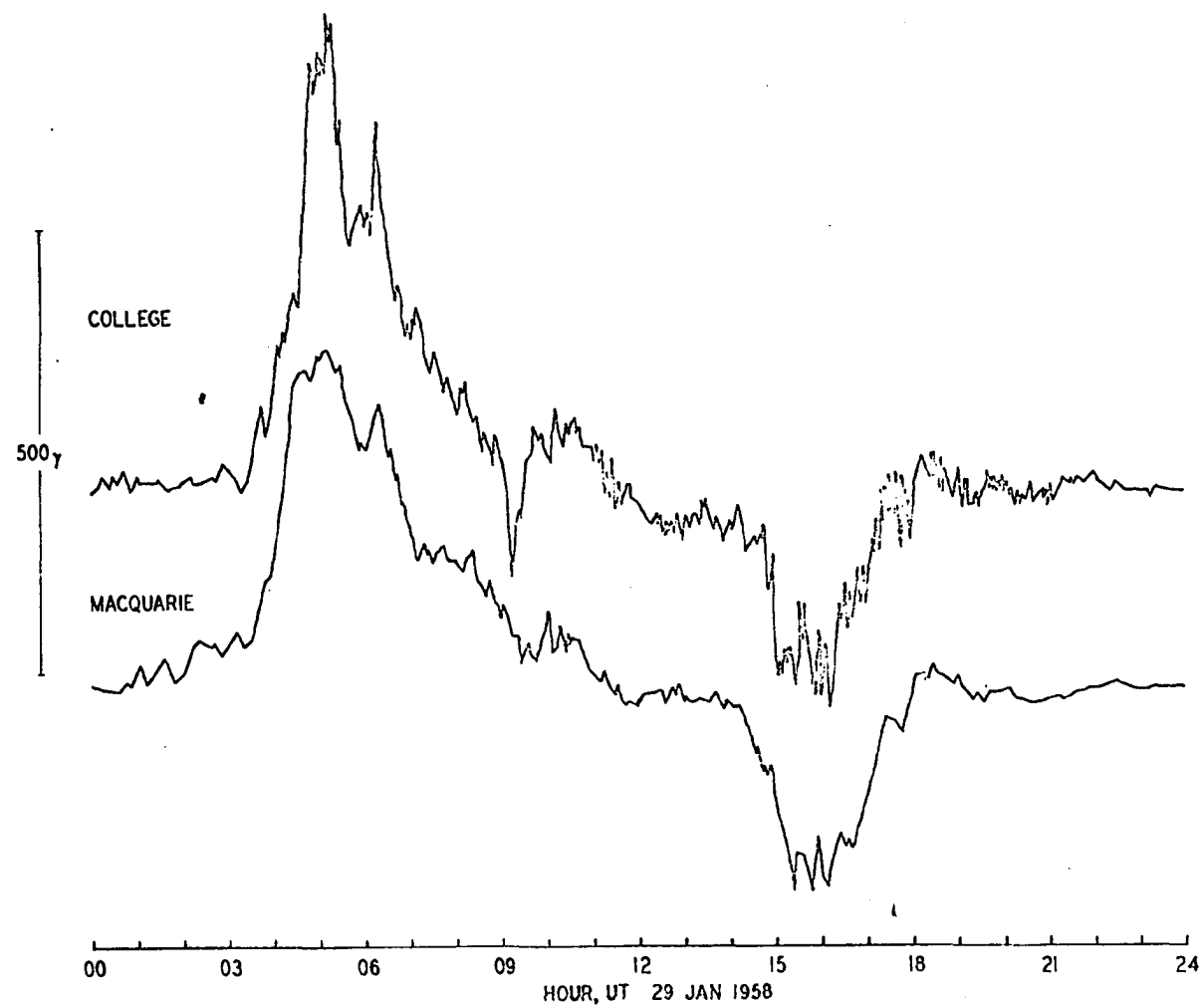


Fig. III-50. Exceptional case to show that the positive bay at College was larger than that at Macquarie (January 29, 1958).

b) Northern Summer - June 1958

To determine whether the relative magnitude of arctic and antarctic disturbances changes seasonally, a similar study for the northern summer was made; thirty-one positive and nineteen negative bays were used. Figure III-49 (b), for June 1958, is analogous to Figure III-49 (a), except that  $R$  is the ratio for College/Macquarie, i.e. as before, summer/winter. It shows that positive bays in the sunlit hemisphere, namely at College, are larger than those at Macquarie Island in the opposite hemisphere. The same is true for almost all negative bays. For the positive bays the ratio lies between  $R = 1.5$  and  $6.5$ , with an average of about  $R = 3$ , and there is a clear tendency for  $R$  to diminish from early afternoon to midnight. For negative bays,  $R$  lies between  $R = 6.5$  and  $R = 1$ , with an average of approximately  $R = 1.5$ .

(ii) Conjugacy for the Reykjavik-Syowa Pair

a) Northern Winter; December 1959

A similar study, confirming the above conclusions, was made for a different pair of conjugate stations, Reykjavik-Syowa; results analogous to those of Figure III-49 are plotted in Figure III-51 for 27 positive and 30 negative "associated" bays. Positive bays at the summer hemispheric station always exceed those at the winter hemispheric station; the average ratio  $R$  is 2; with only one exception, the ratio is between  $R = 1$  and 3. For negative bays, most of the points fall close to  $R = 1$ , With only three exceptions. On the average, the negative bay at the summer hemispheric station (Syowa) is about 1.25 larger than at the winter hemispheric station (Reykjavik) see Figure III-51 (b).

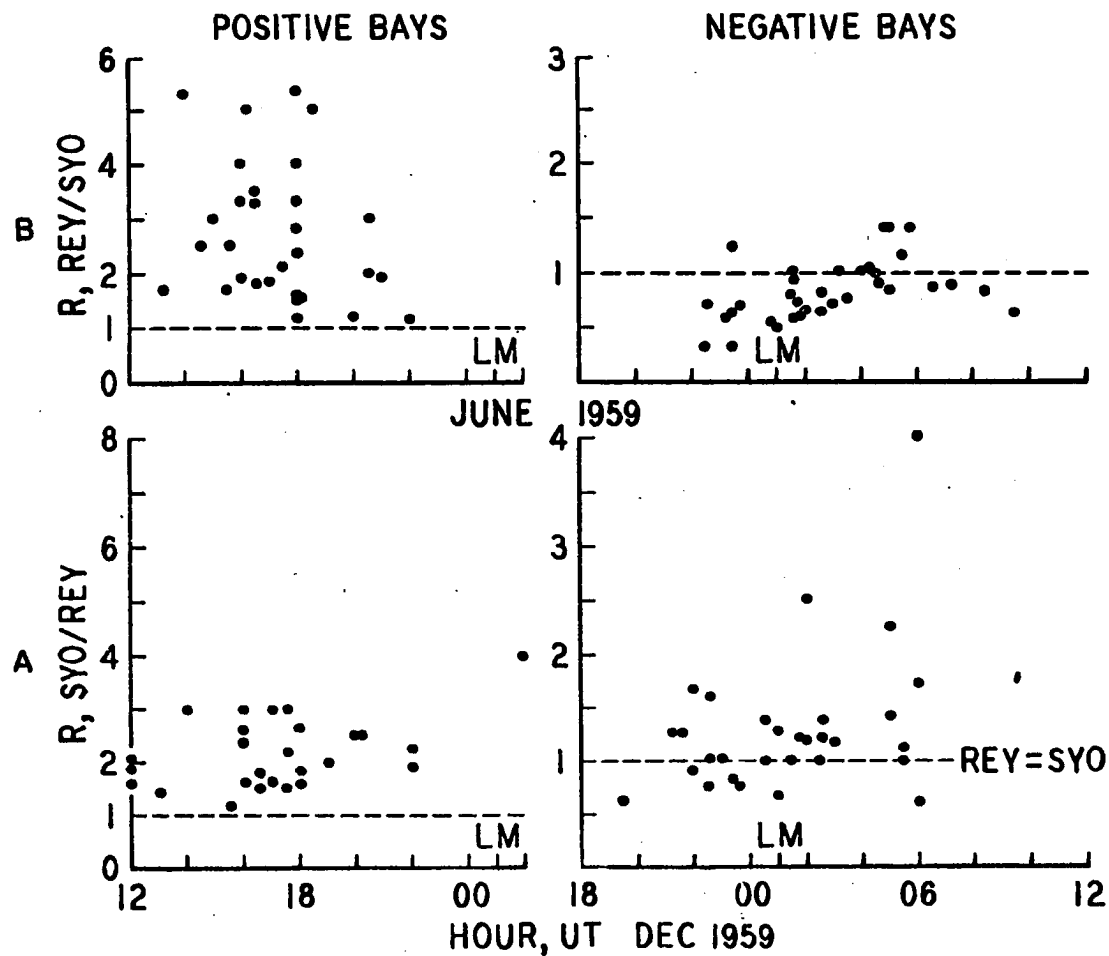


Fig. III-51. Relative magnitude ratio (R) for associated bays for the Reykjavik-Syowa pair:

- a) Northern Winter, December 1959
- b) Northern Summer, June 1959

b) Northern Summer - June 1959

Figure III-51 (b) is analogous to Figure III-49 (b), all 29 positive associated bays are larger at the summer hemispheric station (Reykjavik) than at the winter hemispheric station (Syowa);  $R$  varies from 1 to 5.5, with an average of about 3 (higher than that in the northern winter). The ratio for the 35 negative associated bays lies between  $R = 1.5$  and  $R = 0.33$ , rather close to  $R = 1$ . On the average the amplitude of negative bays at the summer hemispheric station (Reykjavik) was about 0.8 as large as that at the winter hemispheric station (Syowa).

iii) Discussion

Stagg (1935) was the first to note that the afternoon maximum of magnetic disturbances is larger in summer months than in winter months; see also Hope (1961). The present study confirms this by using the data from two pairs of conjugate stations. Since positive bays are more intense at a summer polar station than at the conjugate, a local winter station, and since the difference decreases from afternoon to midnight, one can infer that ionization by solar radiation largely determines the magnitude of positive bays. This suggests that the ionization due to auroral particles, if any, is not more than  $10^5/\text{cm}^3$  in the E region, since  $f_oE$  is not more than 3 Mc/s. This may be compared with the number density of at least  $10^5 - 10^7/\text{cm}^3$  in active auroras associated with negative bays (Ulwick, Phister, Haycock and Baker, 1965).

There is additional evidence to support the above conclusion. Positive bays at College are found to be much less associated with significant cosmic noise absorption than negative bays. Figures III-52 (a) and (b), show that cosmic noise absorption differs significantly for positive and

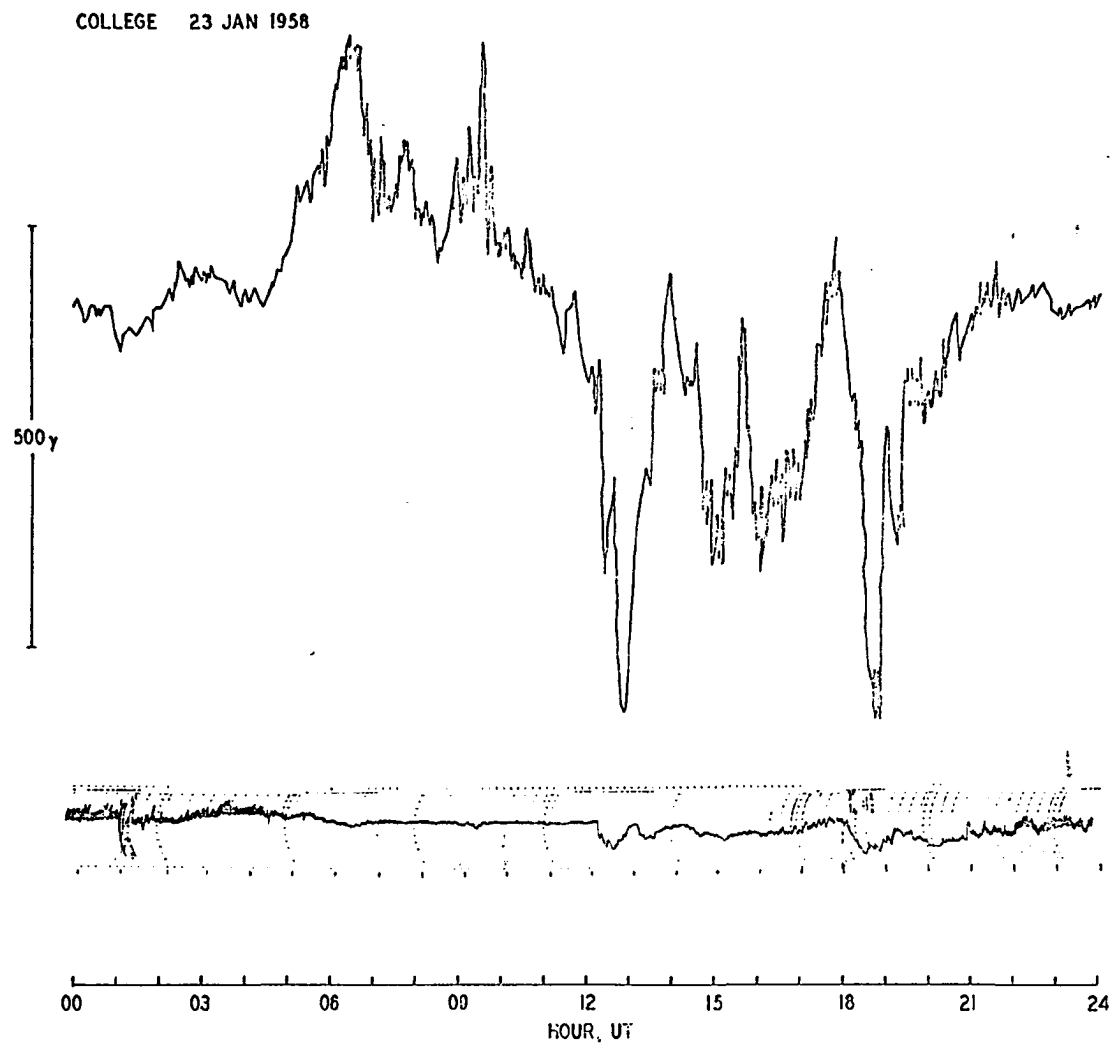


Fig. III-52a. Simultaneous H component and riometer records from College; January 23, 1958.

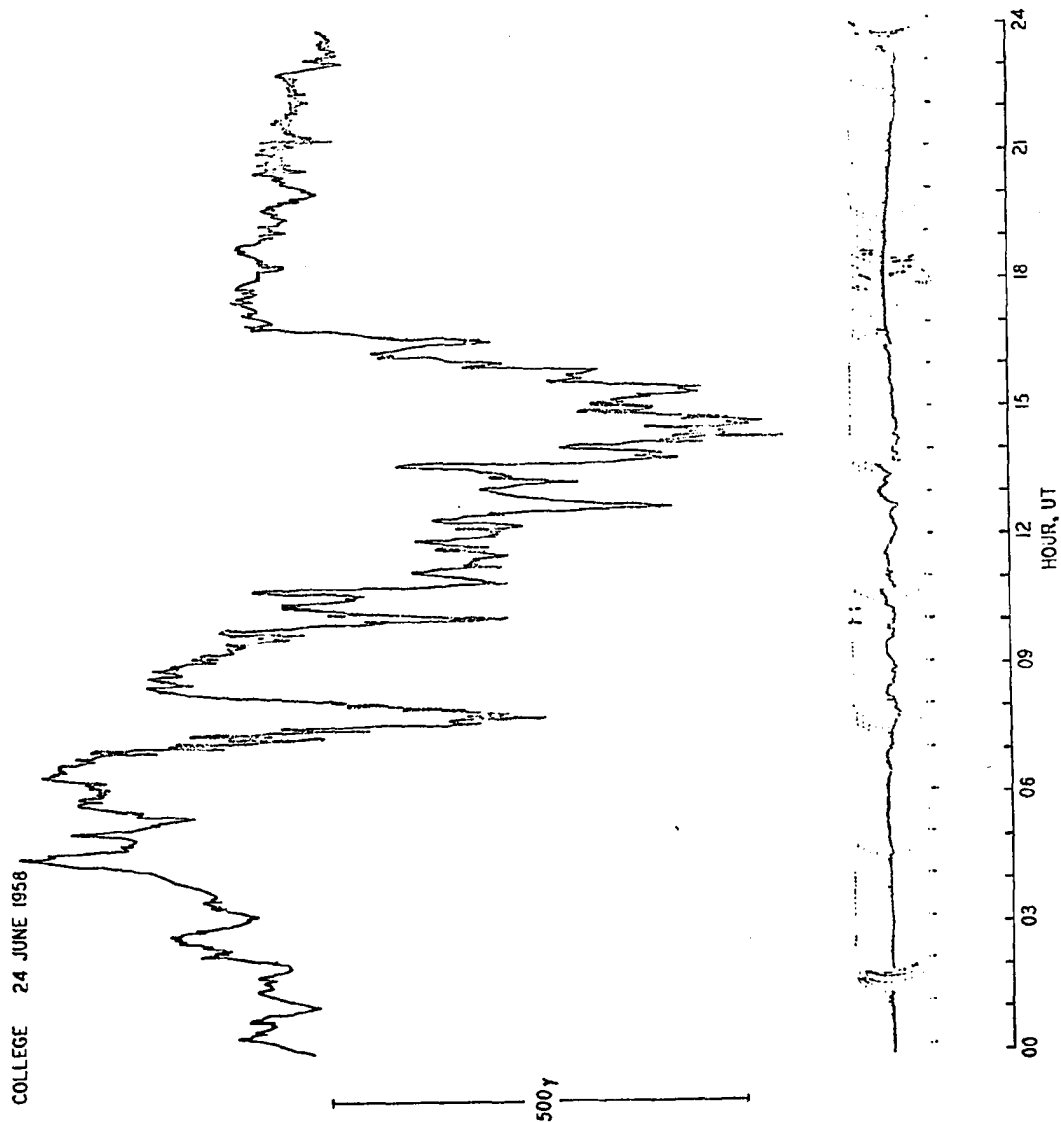


Fig. III-52b. Simultaneous H component and riometer records from College;

negative bays of similar magnitude, although a part of the difference must undoubtedly be due to change in the energy spectrum of auroral electrons. These are indications of important differences between the nature of the eastward current (which causes a positive bay) and the westward current (which causes a negative bay). We conclude that the polar electrojets are associated with intense particle influx and its return current on the equatorial side is much influenced by solar radiation.

### 3) Polar Cap Conjugate Pairs

Wescott and Mather (1965d) have demonstrated that in some cases there is a breakdown of conjugacy; they gave examples in which negative bays at Shepherd Bay (Canada) were associated with positive bays at Scott Base (Antarctica) during night hours (Fig. III-53). A further examination of the records from the two stations in December and January shows the same tendency. Based on a limited amount of data, it appears also that in May and June positive bays at Shepherd Bay were associated with negative bays at Scott Base.

It is not difficult to confirm this by using even single stations. This is because the occurrence of both positive and negative bays shows a remarkable seasonal variation at about  $\text{dp lat } 75^\circ - 80^\circ$ , where in local summer months only a few negative bays occur. Figure III-54 shows the occurrence frequencies of well-defined positive bays and negative bays at Mould Bay, Canada ( $\text{dp lat } 89.1^\circ$ ) during a period of 24 months (September 1963-August 1964; September, December 1964; January 1965-August 1965; October, November, 1965) and at Godhavn, Greenland ( $\text{dp lat } 79.9^\circ$ ) for a two year period.

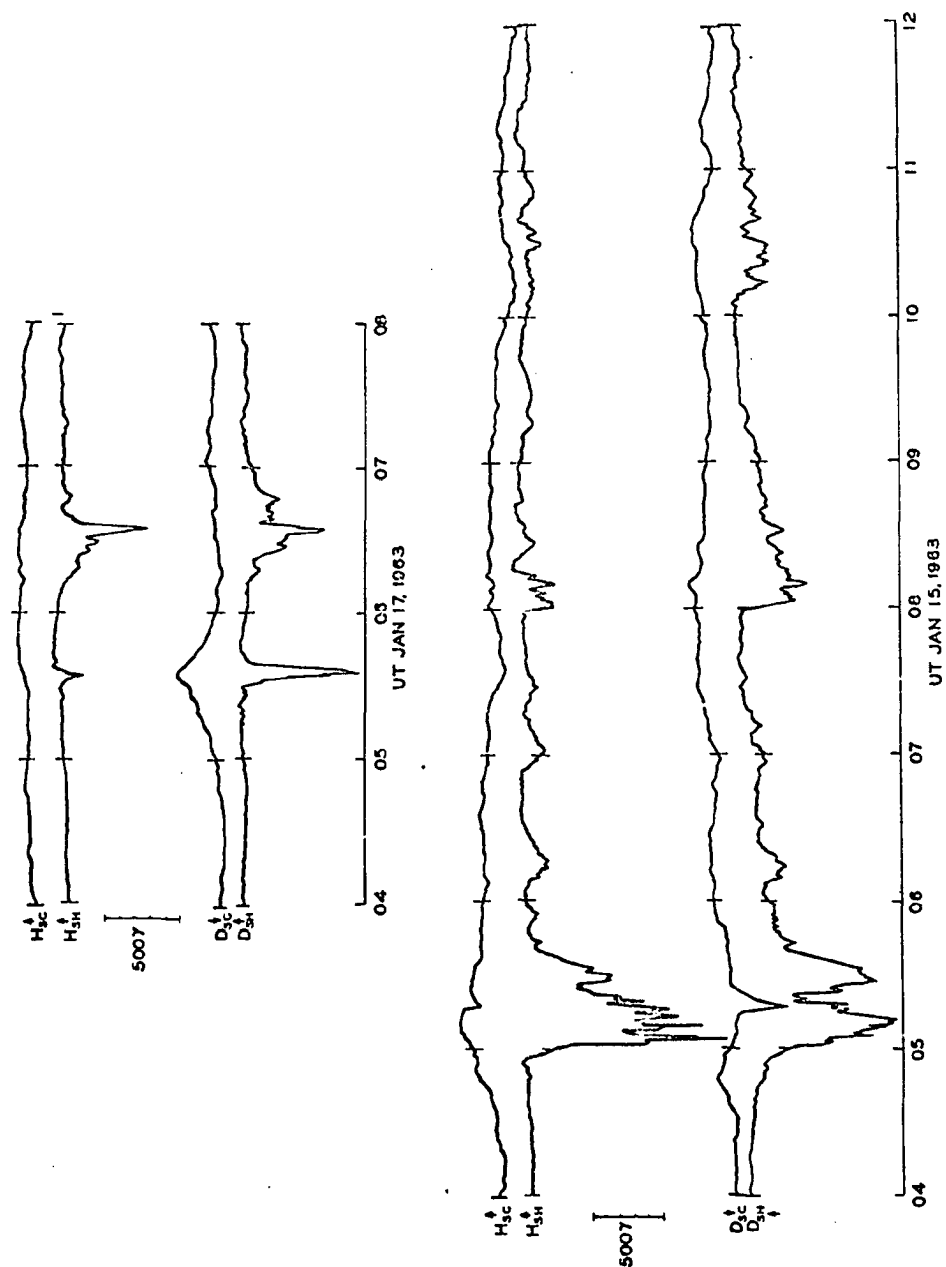


Fig. III-53. Examples of non-associated bays from the Shepherd Bay-Scott Base pair (after Wescott and Mather 1965).



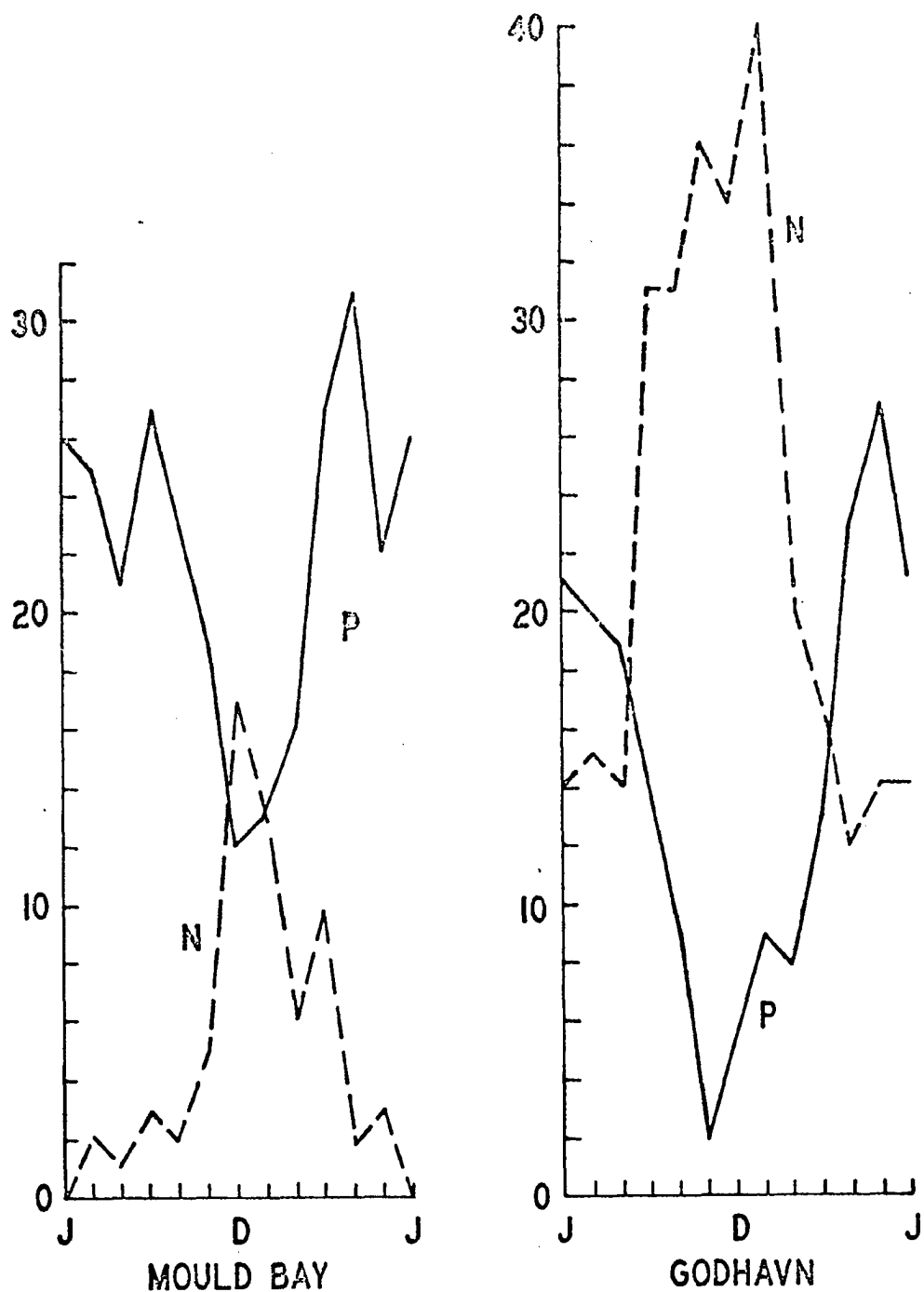


Fig. III-54. The seasonal variation of the occurrence frequency of well-defined positive and negative bays at Mould Bay and Godhavn.

At such a high latitude stations, at night, positive bays are more common than negative bays. This is because the return current from the polar electrojet across the polar cap has an eastward component; see, for example, Silsbee and Vestine (1942). In the last section it was shown that intense negative bays do occur at night even at such a high latitude station as Mould Bay and Godhavn.

Thus, positive bays at Shepherd Bay are "associated" with negative bays at Scott Base in June and July. Therefore, the break-down is not complete.\* (\* It was thought that the calculated conjugacy means little for a high latitude (dp lat  $75^{\circ}$  to  $80^{\circ}$ ) pair). A further examination of this phenomenon has been hindered by the lack of conjugate stations at dp lat  $80^{\circ}$ . Therefore, we have examined the Murchison Bay - Mirny pair ( $L = 19.55^{\circ}$ ) for the entire IGY period. Figure III-55 and Figure III-56 show the result.

In northern winter months (Fig. III-55), negative bays at Murchison Bay tend to be much greater than that at Mirny. In some cases negative bays at Mirny are not very clear or are entirely absent.

On the other hand, in northern summer months (Fig. III-56), negative bays at Mirny are much greater than those at Murchison Bay.

We have found that negative bays are observed only when the poleward expanding bulge (during the auroral substorm) comes very close to the station. Positive bays are recorded when the bulge is seen far to the south of the station.

Thus we can conclude that negative bays are observed only when an intense precipitation of auroral electrons occurs near stations well inside the polar cap (in the midnight sector). If this conclusion is correct and if auroral electrons originate in the same region of the magnetosphere,

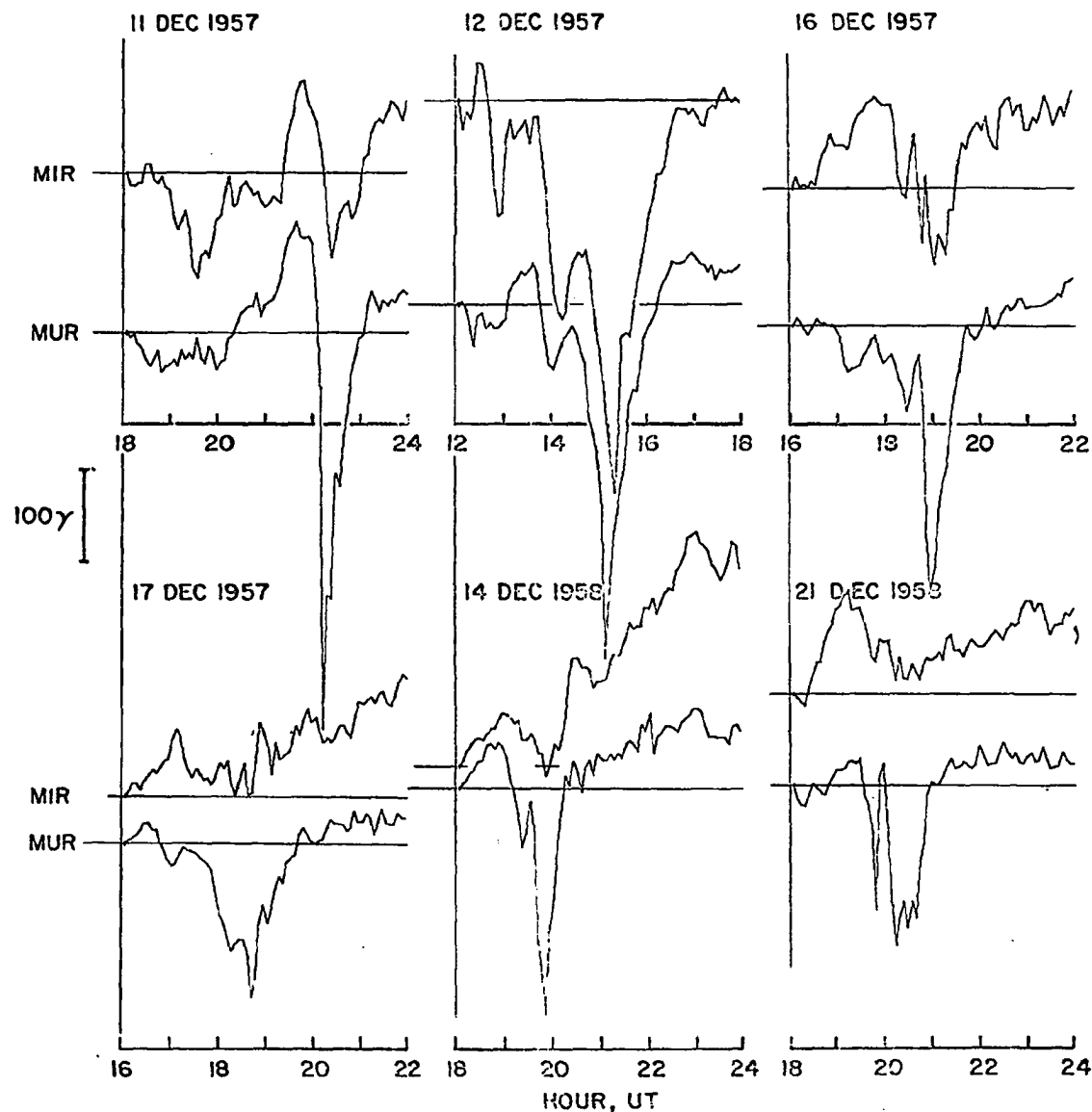


Fig. III-55. The simultaneous magnetic records of H component from a pair of high latitude conjugate stations (Murchison Bay and Mirny) in northern winter.

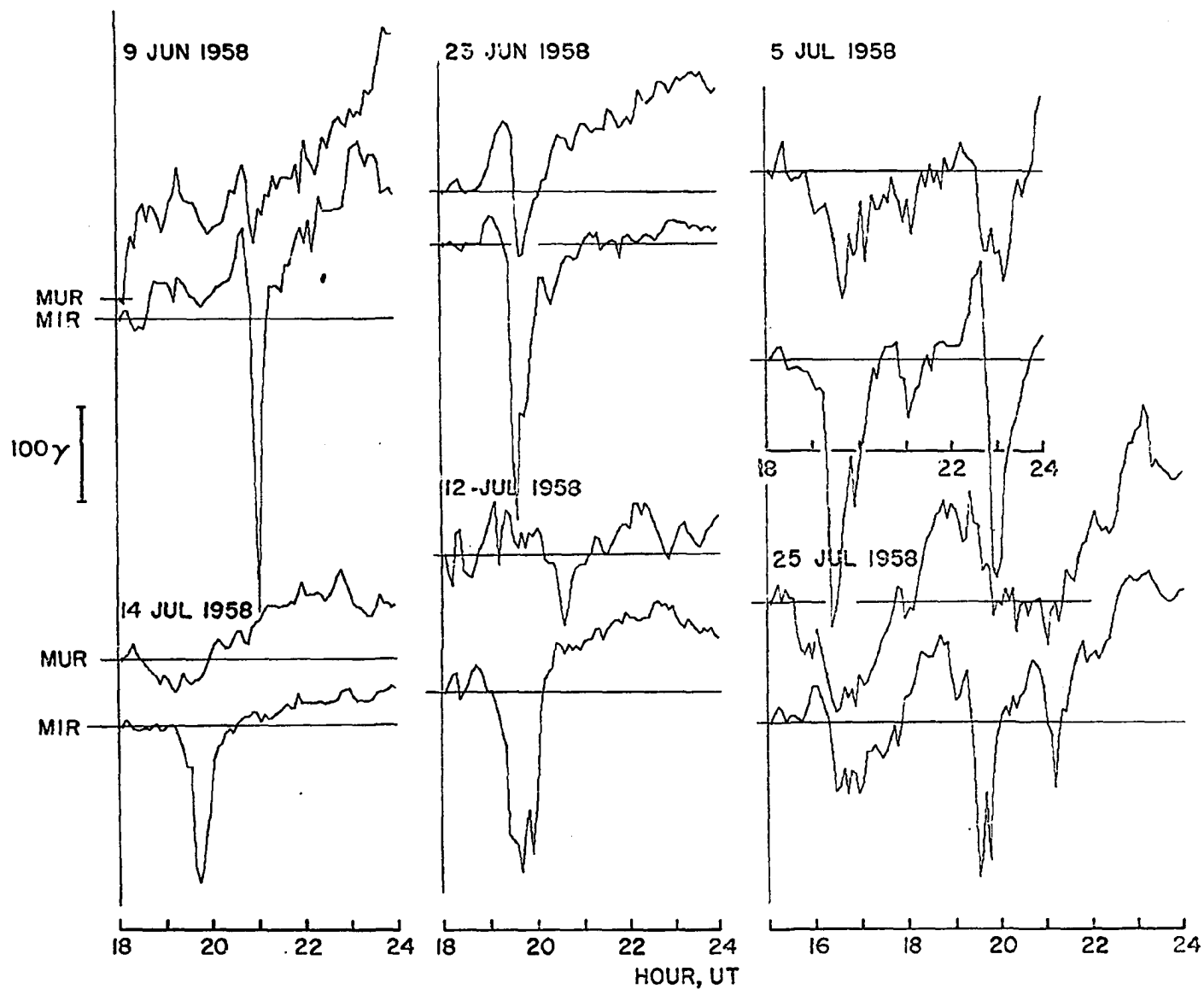


Fig. III-56. The simultaneous magnetic records of H component from a pair of high latitude conjugate stations (Murchison Bay and Mirny) in northern summer.

there appears to be a remarkable asymmetry of the precipitation (with respect to the geomagnetic equator) in solstice months. This could be due either to a greater displacement (toward the dark side) of the auroral oval in the summer polar cap than in the winter polar cap or to a greater poleward extension of the polar jet in the winter polar cap. In either case, in the winter polar cap, both the electrojet and the precipitation of auroral particles approach the dipole pole more closely than in the summer polar cap. The breakdown of conjugacy is thus likely to be partly due to an asymmetric distortion of the geomagnetic field in the magnetosphere, rather than to an inadequacy of the spherical harmonic representation of the main field; if the latter were of major importance for the breakdown, we would not expect the above seasonal difference.

The northern summer configuration of the magnetosphere is schematically shown in Figure III-57; the minimum angle between the dipole axis and the solar wind velocity vector is about  $56^\circ$ . If auroral particles come from the same region in or near the magnetospheric tail during a polar magnetic and auroral substorm, the field lines would be distorted in such a way that point A in the northern hemisphere would be connected to point B which is appreciably higher than its "normal" conjugate point marked by B'; both the points A and B indicate the simultaneous location of the advancing front of the auroral bulge. During northern winter months the precipitation of auroral particles occurs in higher latitudes in the northern hemisphere than in the southern hemisphere.

The morphology presented in this chapter can be very briefly summarized as follows:

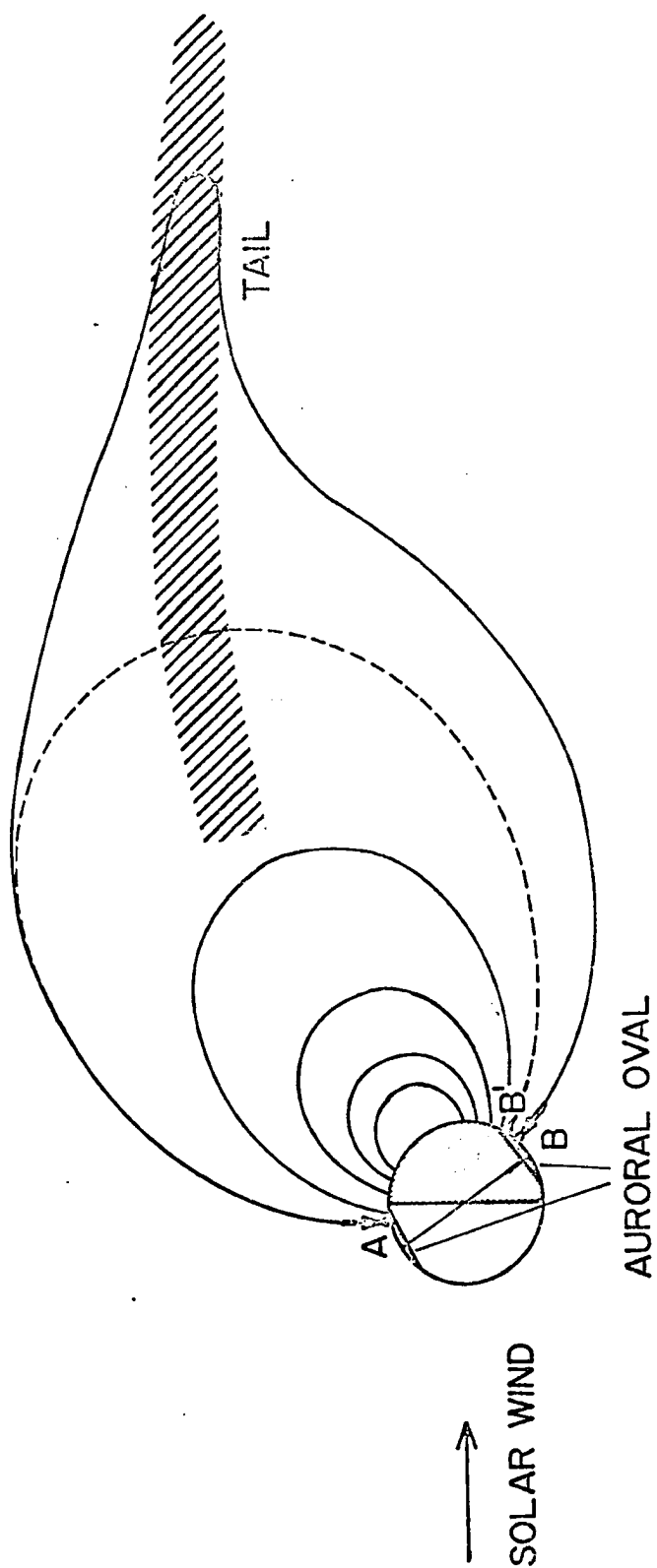


Fig. III-57. The schematical configuration of geomagnetic field lines in the magnetosphere for the northern summer.

1. Along the auroral oval both the auroral substorm and the polar magnetic substorm occur together and can be considered as one high latitude geophysical phenomenon, namely the polar substorms. In the morning sector, a negative bay with irregular fluctuations is associated with eastward moving patches. In the midnight sector an intense negative bay is associated with a poleward and equatorward expansive motion of auroral bulges. In the late evening sector an intense negative bay preceded by a small positive bay is associated with an intense westward surge. The positive bay is usually observed in the early evening sector approximately along  $dp$  lat  $65^\circ$  when the surge is seen in the northern sky from the station. According to observations at stations over the polar cap, negative bays are observed only when an intense precipitation of auroral electrons occurs near the station.

2. The effect of polar substorms is principally confined to the region in and near the auroral oval; but disturbances which appear to be associated with the polar substorm are observed over the polar cap and in middle latitudes.

3. The polar substorm occurs simultaneously in both hemispheres. However, there is a seasonal variation in their conjugacy. The positive bay is more intense at a summer hemispheric station than at its conjugate winter hemispheric station; but the negative bay is about the same at both hemispheric stations. According to observations at stations over the polar cap, the breakdown of conjugacy is likely to be due to an asymmetric distortion of the geomagnetic field in the magnetosphere.

## CHAPTER IV

### Low Latitude Negative Bays and the Polar Substorm

#### 1. Introduction

As discussed in Chapter III, at any auroral zone station, geomagnetic disturbances are characterized by positive changes of the horizontal component (H) in the afternoon and evening hours and by negative changes in the midnight and early morning hours. They have been called 'positive bays' and 'negative bays' respectively. They are referred to as AP bays and AN bays; 'A' signifies the auroral zone.

On the other hand, in middle and low latitudes, simultaneous changes of the H component often occur but with the opposite signs, namely a negative change in the afternoon and evening hours and a positive change in the midnight and early morning hours. They are denoted by LN and LP, respectively; 'L' stands for the low latitude. It has long been believed that there is a cause-effect relationship in these changes. To be more specific, it has been considered that an eastward electrojet, flowing along the auroral zone in the afternoon sector and causing AP bays there, completes a part of its circuit in the middle and low latitudes by creating a westward return current which produces LN bays. On the other hand, a westward electrojet, flowing along the auroral zone in the midnight and early morning hours and causing AN bays there, completes a part of its circuit by creating an eastward return current which produces LP bays. Akasofu



and Chapman (1964) first cast some doubt on this interpretation. Their study was based on the fact that polar magnetic substorms occurring at about the maximum epoch of the main phase of geomagnetic storms are associated with only a LP change over most of the middle and low latitude belt; according to the DS current system a pair of bays must always appear, namely LP and LN bays.

According to the revised polar electrojet current system discussed in Chapter III, Section 2, the eastward return current is spread in the middle and low latitude region between the northern and southern auroral ovals. Therefore, the revised electrojet model does not allow for LN bays caused by the return current. This view appears to be in contradiction with the observed fact that AP bays are often associated with LN bays. The purpose of this Chapter is to find the nature of LN bays.

Before going into details, it may be instructive to examine a few typical examples of AP, AN, LN and LP bays in actual magnetic records. Figure IV-1 shows simultaneous magnetic records from College (dp lat  $64.7^{\circ}\text{N}$ ) and Honolulu (dp lat  $21.0^{\circ}\text{N}$ ). In Figure IV-1 (a), an AP bay at about 0300 UT at College is associated with an LN bay at Honolulu, and an intense AN bay at about 0900 UT at College is associated with an LP bay at Honolulu. In Figure IV-1 (b), a similar relation is also seen.

It is well known that AN bays are, in general, more intense than AP bays and that their onset is more sharply defined (Chapman and Bartels (1940)). This is well illustrated in Figure IV-1. On the other hand, LN and LP bays have similar magnitudes, and in fact in many cases LN bays are only slightly greater than LP bays (Fukushima, 1953). This is illustrated in the diagram constructed by Fukushima and Ono (1952), which is reproduced

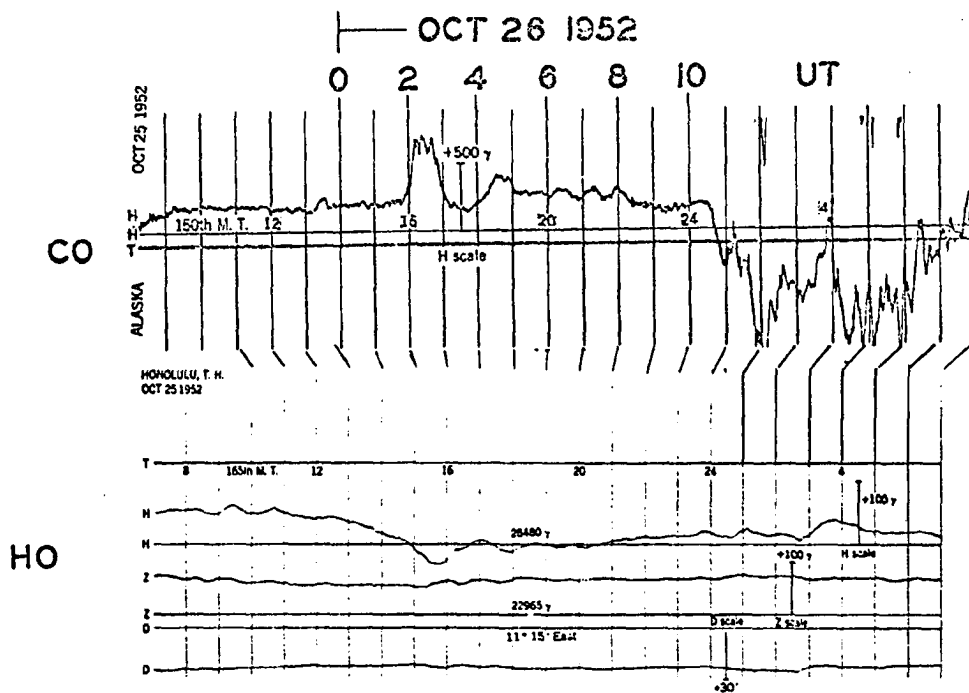
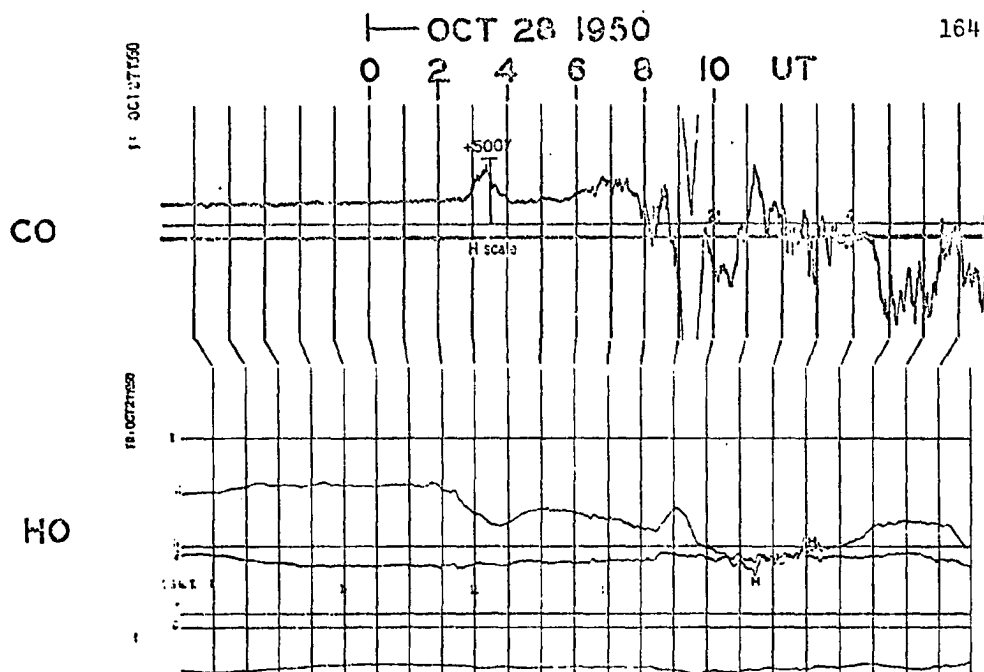


Fig. IV-1. The simultaneous magnetic records from College (dp lat  $64.7^{\circ}\text{N}$ ) and Honolulu (dp lat  $21.0^{\circ}\text{N}$ ).

here as Figure IV-2. In Figure IV-2, the time variation of the mean horizontal disturbance vectors during bays is shown for different local time hours. The magnitude of LN bays at 15-18 LT is greater than that of LP bays at 0-3 LT.

## 2. Low Latitude Negative Bays

In this section, the results of an extensive analysis of simultaneous magnetic records at seven magnetic stations in the Europe-Africa sector are shown. Figure IV-3 shows the location of stations used in the analysis. Kiruna (dp lat  $65.3^{\circ}\text{N}$ ) is located in the auroral zone, and the rest are distributed in the middle and low latitude belt. The records used were taken during the whole IGY period (18 months).

In this study, the major features of simultaneous geomagnetic changes associated with polar magnetic substorms are classified into four types, from the simplest type to the very complicated type. Each type is quite common throughout the period examined.

### (i) DR-Type

When Kiruna magnetic records show a weak and well-defined AP bay, the simultaneous magnetic changes at the rest of the stations is simply a well defined LN bay. Figure IV-4 (a) shows such an example. The quiet day level of the X component at Kiruna is approximately at the level shown between 1100 and 1200 UT. There is then a gradual build-up of positive changes from about 1230 UT with the peak at about 1800 UT, although there are minor irregular changes superposed on it. First of all, it is quite clear that a well defined negative change (LN) occurred at Lovo and in lower latitudes when a rather sudden enhancement of AP appeared at Kiruna between 1600 and 2000 UT. The peak value of the AP bay was  $300\gamma$  at Kiruna. The intensity of LN bays was about  $50\gamma$  at Wingst and the lower latitude stations and was about  $30\gamma$  at Lovo. It should be noted, however, that there

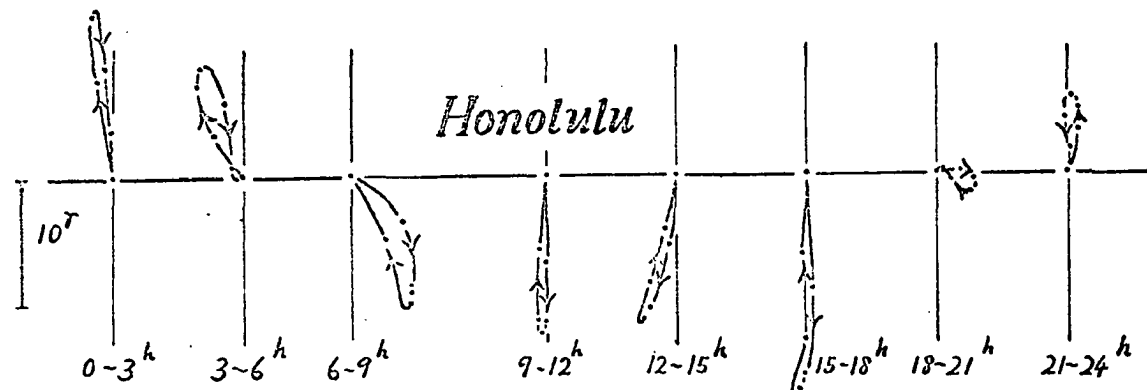


Fig. 12. Vector-diagrams of the mean horizontal disturbing force of geomagnetic bays observed at Honolulu. (after N. Fukushima and H. Ōno)

Fig. IV-2. Vector-diagrams of the mean horizontal disturbing force of geomagnetic bays observed at Honolulu. (After N. Fukushima and H. Ōno).

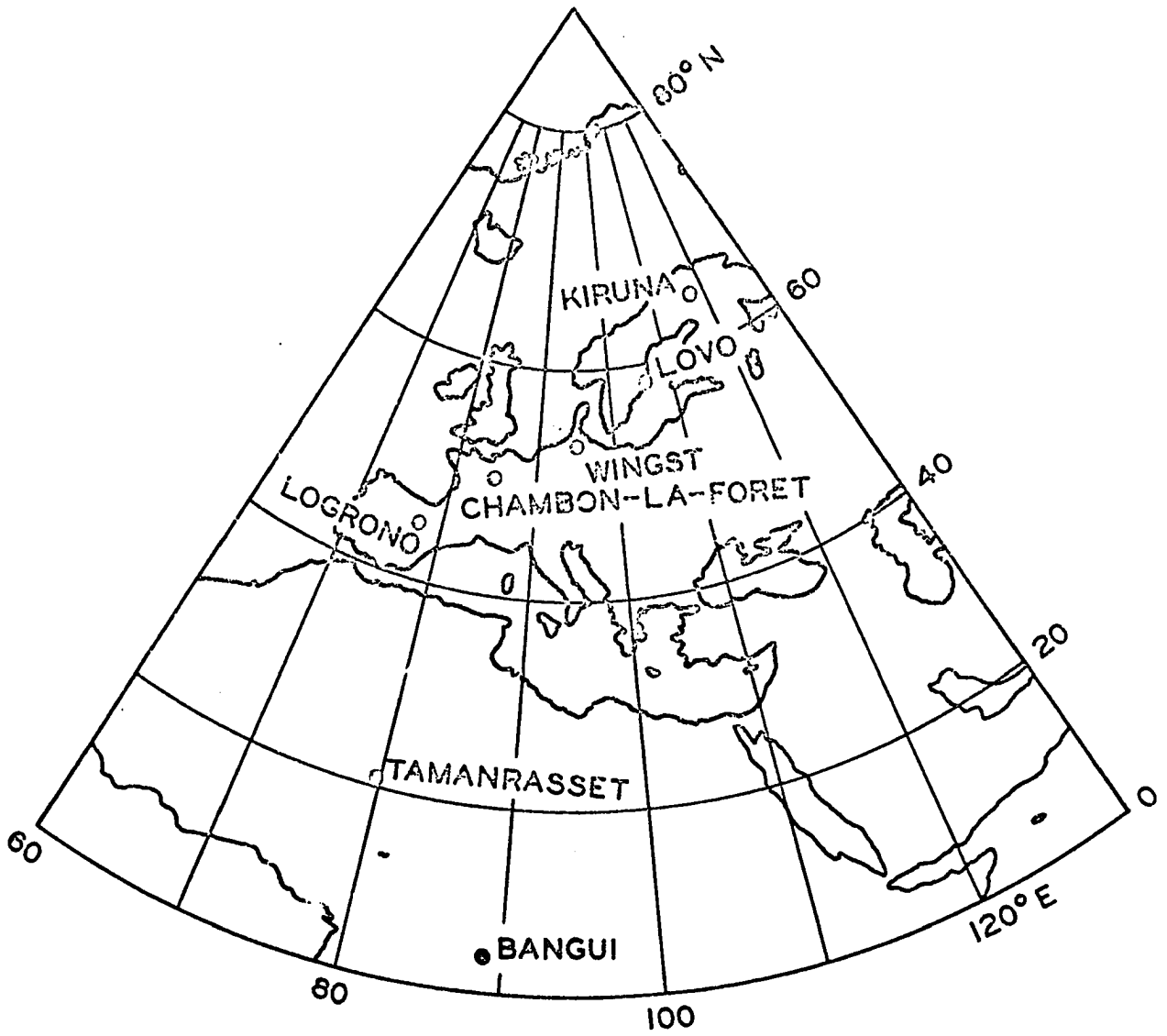


Fig. IV-3. The N-S chain stations in the Europe-Africa sector whose records are used in this paper.

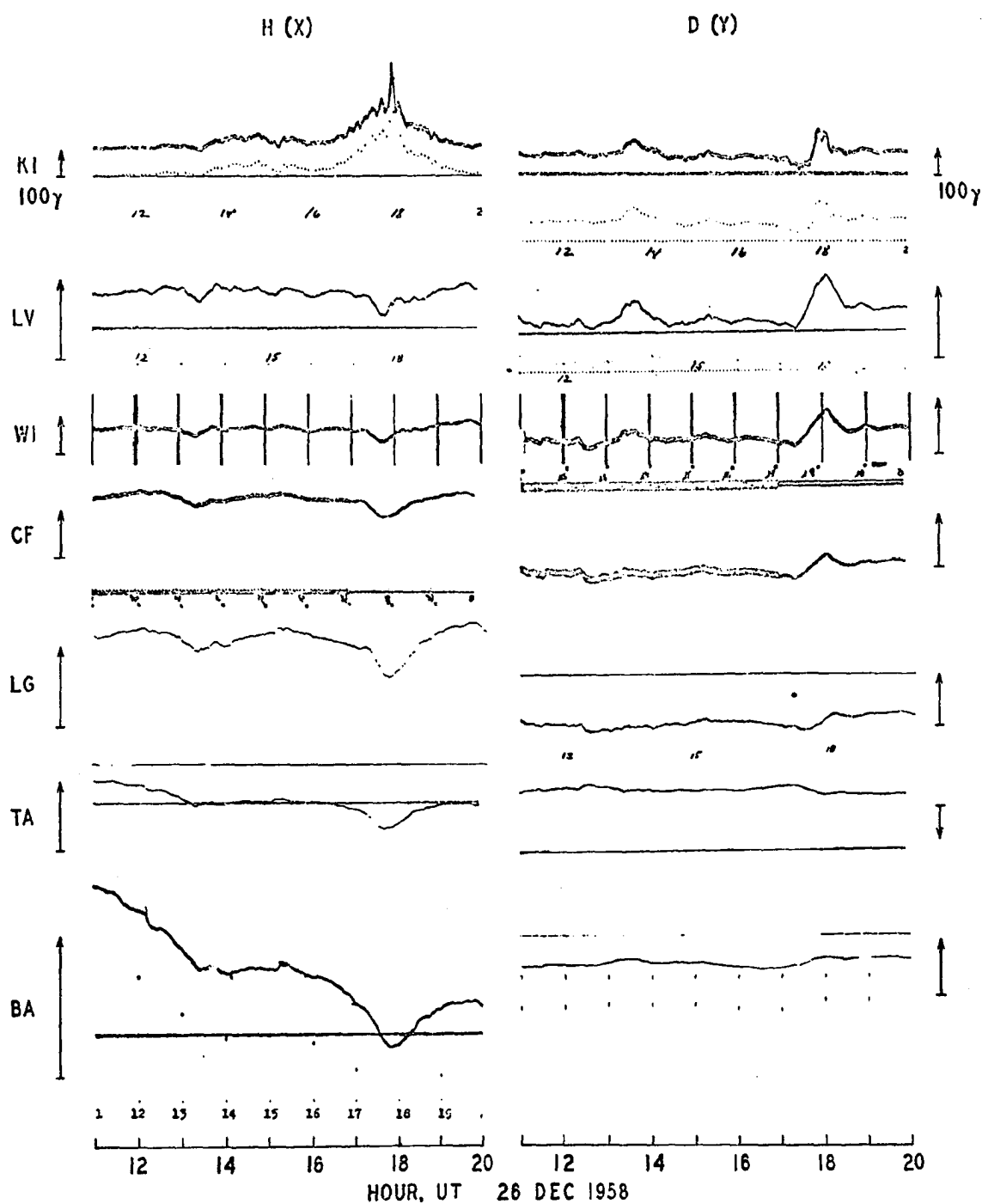


Fig. IV-4a. The DR type: an example of geomagnetic changes in middle and low latitudes when the corresponding AP bay in the auroral zone is weak, (Dec. 26, 1958).

is no corresponding part in the LN bays for the impulsive enhancement of the of the AP bay at Kiruna at 1750 UT, so that it could be of very local origin; therefore the magnitude of the AP can safely be taken to be of order 200  $\gamma$ .

The Y component at Kiruna and the D component variation at all stations are remarkably similar, with its major change being positive (eastward), although the magnitude decreases rapidly toward lower latitude stations.

Let us suppose that all these changes were caused by ionospheric currents. Assuming that the eastward current causing the positive bay is flowing in a band as wide as  $10^\circ$  (between  $60^\circ$  and  $70^\circ$  dp lat), the total current would be of order  $2.2 \times 10^5$  amperes ( $+ \Delta H \sim 200 \gamma$ ). On the other hand, if the LN bays were caused by an ionospheric current, the current flowing between  $0^\circ$  and  $60^\circ$  dp lat would be as large as  $3.3 \times 10^5$  amperes. The example shows that even if the total eastward current completes its circuit below dp lat  $60^\circ$ , it cannot supply enough current to produce the observed negative change. Furthermore, it is difficult to believe that the return current intensity is fairly uniform over a wide range of latitude and even a little greater in lower latitudes. Akasofu (1966) has recently shown that a typical ratio of LP bays at Honolulu to AN bays at College is of order 0.035. Note that the ratio of LP bays at Tamanrasset to the AP bay at Kiruna is as large as 0.25. Thus, LN can not be produced by the return current.

Akasofu and Chapman (1963) showed that the storm-time radiation belt (namely, the so-called 'ring current') grows simultaneously with an enhanced activity of the polar magnetic substorm. Obviously, this relation can be observed best during the growing phase of the main phase of a geomagnetic storm. However, there is no reason to believe that the simultaneous growth cannot occur during individual polar magnetic substorms, if they are intense

enough. In fact, the Dst values obtained by Sugiura (1963) shows a well defined negative change corresponding to all LN bays discussed in this section.

Figure IV-4 (b) shows a slightly more complicated example. There are two successive AP bays at Kiruna. However, the general features are essentially the same as those in Figure IV-4 (a). There are two LN bays, corresponding to the two AP bays; the intensity of the two AP bays is of order 200  $\gamma$ , and that of the LN bays is of order 50  $\gamma$ . The major Y or D change is positive at all stations, but the magnitude decreases rapidly equatorward. Both LN bays were associated with an enhanced Dst decrease obtained by Sugiura (1963).

#### (ii) DR Type

When AP bays at Kiruna are intense, positive changes are seen as far south as Chambon-la-Forêt (Fig. IV-5, (a)). However, the magnitude of the positive change decreases rapidly toward lower latitudes. The corresponding negative change (LN) is clearly seen only at Tamanrasset and Bangui; it becomes intense at about 1300 UT, about 10 minutes after a rather sudden enhancement of the AP bay at Kiruna. In such a case, the Y or D component at all the stations tends to be slightly negative (westward), but its magnitude is much less than those discussed in (i), in spite of the fact that the X component at Kiruna is much greater than that in (i).

It is reasonable to infer in this case that the eastward current which caused the AP bay at Kiruna, spread as low as 50° latitude or even lower and partly masked the growth of the ring current field there. Figure IV-5 (b) shows essentially the same features as those in Fig. IV-5 (a); for a further discussion of Figure IV-5 (b) see (iii).



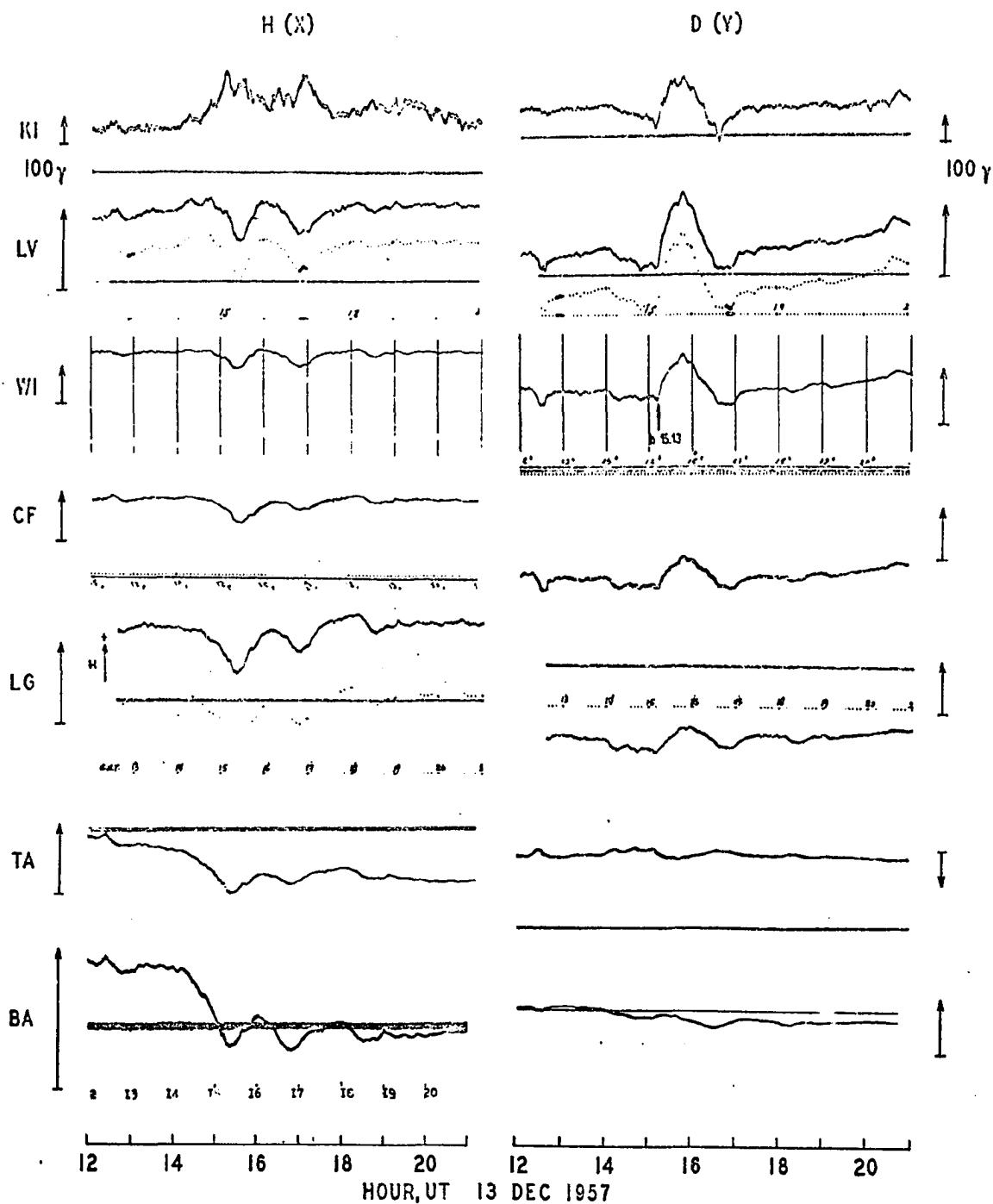


Fig. IV-4b. The DR type: an example of geomagnetic changes in middle and low latitudes when the corresponding AP bay in the auroral zone is weak, (Dec. 13, 1957).

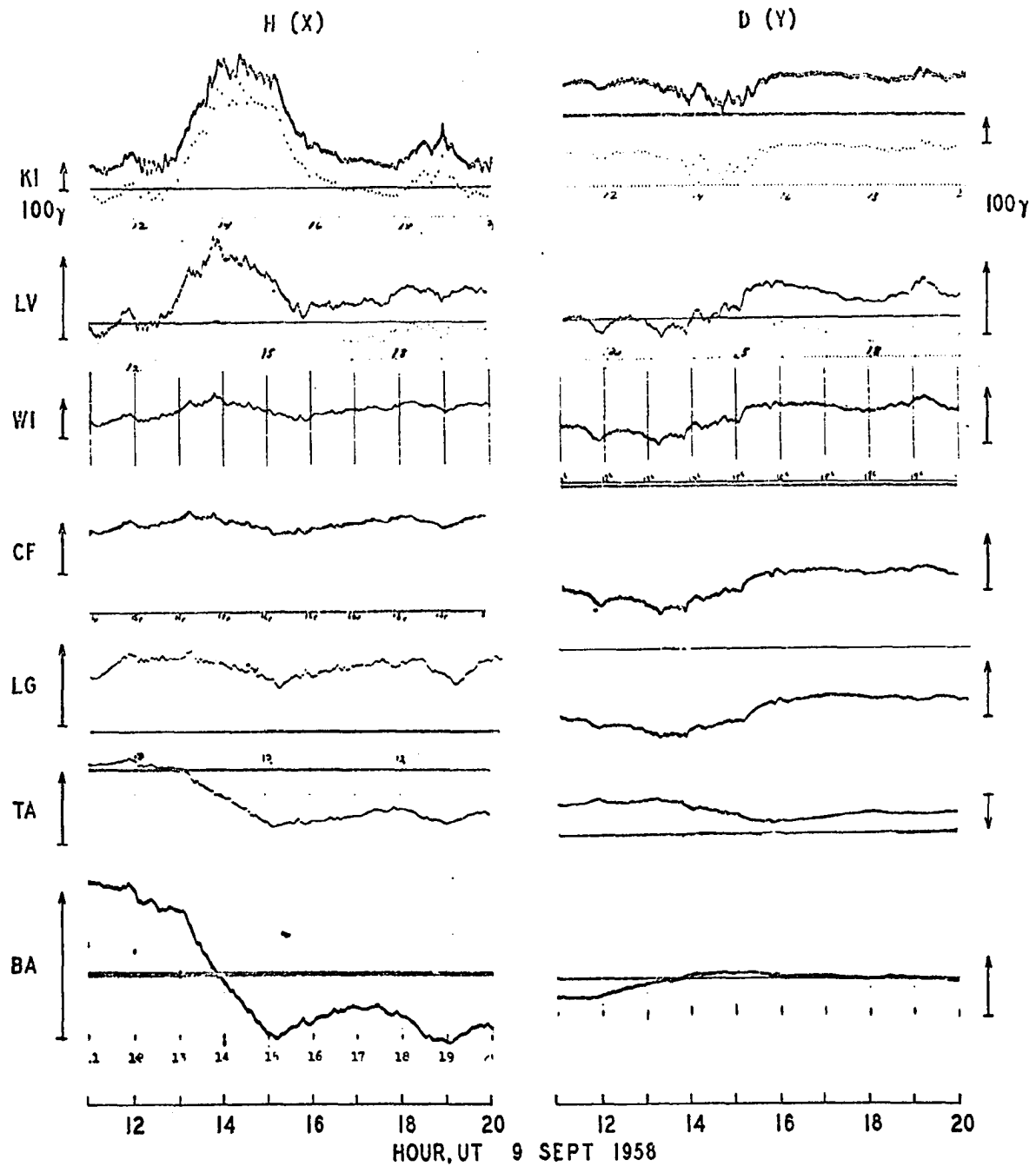


Fig. IV-5a. The DP type: an example of geomagnetic changes in middle and low latitudes when the corresponding AP bay in the auroral zone is intense, (Sept. 9, 1958).

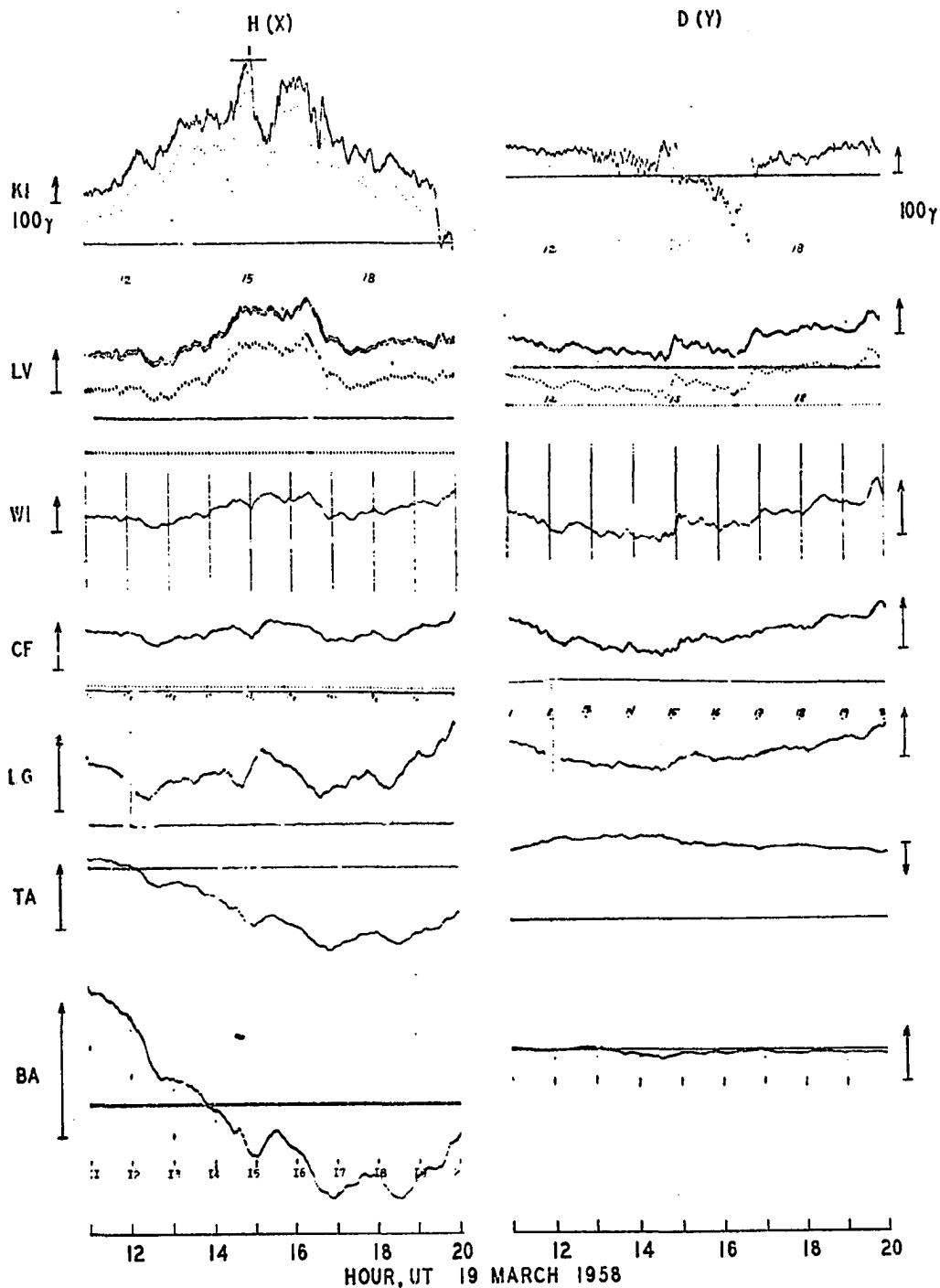


Fig. IV-5b. The DP type: an example of geomagnetic changes in middle and low latitudes when the corresponding AP bay in the auroral zone is intense, (Mar. 19, 1958).

## (iii) DR ~ DP Type

When AP bays at Kiruna are intense, another type of change occurs at the rest of the stations. In Figure IV-6, an AP bay at Kiruna began at about 1350 UT and became quite intense between 1515 and 1700 UT. The corresponding change at Lovo was first a negative change and then positive during the period of the intense AP bay at Kiruna and then became a negative change again which subsided at about the time the AP bay ceased at Kiruna. Similar changes were seen at all stations. However, the positive change became less and less obvious toward lower latitudes and the negative change more and more conspicuous.

This type of change can be considered as a combination of the changes discussed in (i) and (ii). The growth of the ring current, which is quite obvious at low latitude stations, was partly obscured by the intensification of the spreading eastward current. A close examination of Figure IV-5 (b) shows essentially the same features. That is, there is a definite indication of the growth of a LN bay at about 1215 UT, but it was partly masked by an intense positive change. The growth of the LN appeared to be disrupted there, particularly at about 1515 UT when the AP became suddenly intense.

It is reasonable to suppose that what we observe here is a combination of two fields, namely the ring current field (DR) and the field (DP) of spreading eastward current from high latitudes,

$$D = DR + DP$$

Here, the DR field is always negative and tends to increase toward the equator, but the DP field is positive south of the auroral oval and its

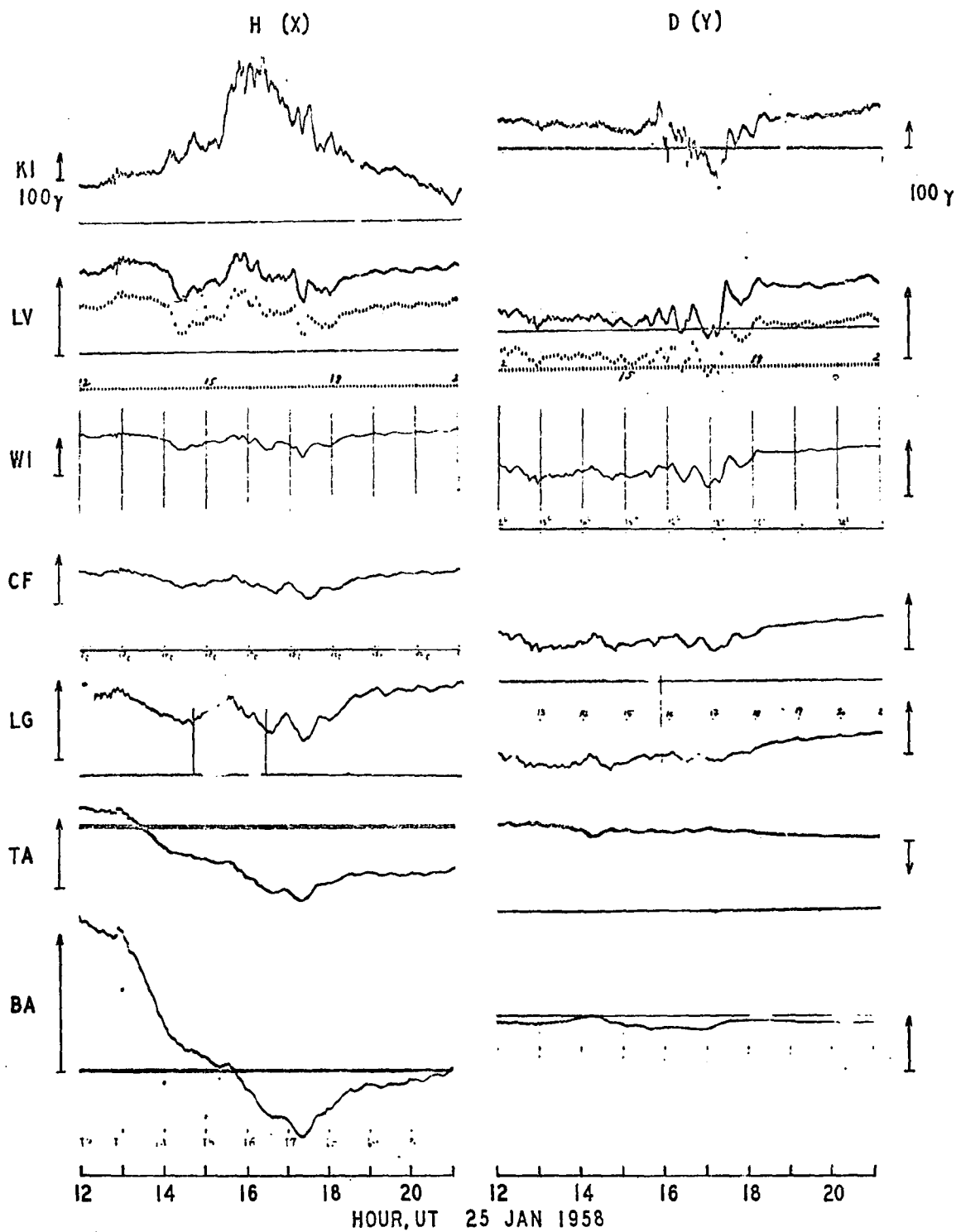


Fig. IV-6. The (DR~DR) type: an example of geomagnetic changes when both the DR and DP fields grow strongly.

intensity decreases rapidly toward lower latitudes. In the evening sector, below dp lat  $20^\circ$ ,  $|DR| > |DP|$ , so that LN bays are seen in most cases. Between dp lat  $20^\circ$  and  $60^\circ$ , either of the two fields can be greater than the other, so that geomagnetic changes will be neither a simple positive nor a negative one. Therefore, the variety of geomagnetic field changes in middle latitudes are caused by different combinations of the two different fields of different relative intensities. Only when AP bays are weak,  $|DR| > |DP|$  at all latitudes below  $60^\circ$  dp lat, so that relatively simple LN bays are observed there.

Such an interpretation can also explain an apparent large difference in the ratios of  $LN/AP = 0.1$  to  $0.3$  and  $LP/AN = 0.035$ . The large ratio of  $LN/AP$  is most likely due to the fact that we have taken the ratio  $DR/AP$  and considered that it was  $LN$  (return current)/ $AP$ . Taking the magnitude of the positive change during the large LN in Figure IV-6 to be of order  $20 \text{ Y}$  at Tamanrasset, the ratio of this positive change to the AP bay is given by  $20 \text{ Y} / 500 \text{ Y} = 0.04$  which is quite reasonable. The above statement is demonstrated more clearly in Figure IV-7. At Kiruna, there was a very sharp impulsive enhancement of an AP bay at about 1500 UT superposed on a gradual positive build-up. At Lovo, a similar but less intense positive change is superposed on the growing negative change. The sharp change at Kiruna is probably caused by an intense westward traveling auroral surge to the poleward side of Kiruna as discussed in Chapter III, section 2; in fact, at Murchinson Bay (dp lat  $75^\circ\text{N}$ ), the DP current was much more intense than that at Kiruna. Unfortunately, because the stations were not in the same meridian line, there is a progressive delay of the occurrence of the corresponding positive change from Kiruna to Logrono

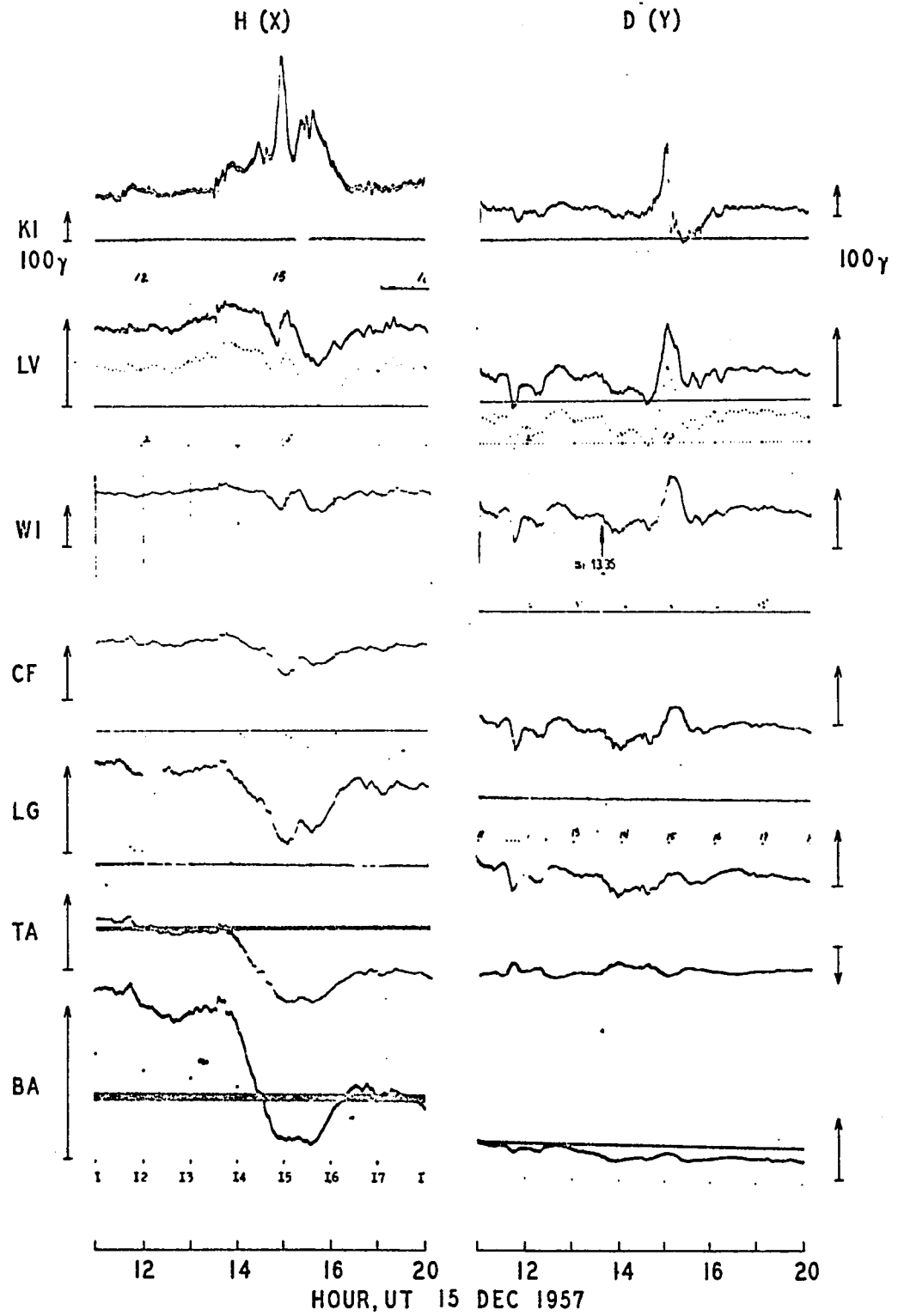


Fig. IV-7. The (DR ~ DP) type: an example of geomagnetic changes when both the DR and DP fields grow strongly.

(see also Fig. IV-3). In spite of this complication, however, it can easily be seen that the positive changes decreased rapidly toward the equator. On the other hand, the negative change becomes more obvious in lower latitudes. The Y or D component change also supports such a conclusion.

(iv) DP + DR Type

Figure IV-8 shows another interesting example which occurs quite commonly. At Kiruna, there was a gradual enhancement of positive changes at 1200 UT, which became suddenly intense at about 1615 UT. The corresponding Lovo magnetic record shows the enhanced positive change at about the same time. At 1705 UT, a 'bite' occurred on the positive change. In lower latitude stations, a similar tendency is seen at all the stations. However, the first positive change decreases its magnitude toward the equator, but the negative change becomes more and more obvious in lower latitudes. It appears that the DR field began to grow rapidly a little after the onset of the polar magnetic substorm in this particular case.

This is a good example illustrating how difficult it is to infer the nature of disturbances from a single station (like Lovo), without having a N-S chain of stations.

We also chose twenty other cases for a detailed study by examining magnetic records from elsewhere (such as College, Tixie Bay and Kakioka), as well as the stations in Figure IV-3, all of which were associated with AN bays and LP bays. Therefore, the AP bays used above are a part of the field of polar substorms and there is nothing unusual about them. We have also examined the Dst values obtained by Sugiura (1963) for all the events and confirmed that all of them were associated with an enhancement of the storm-time radiation belt of order 5 to 10  $\gamma$ .



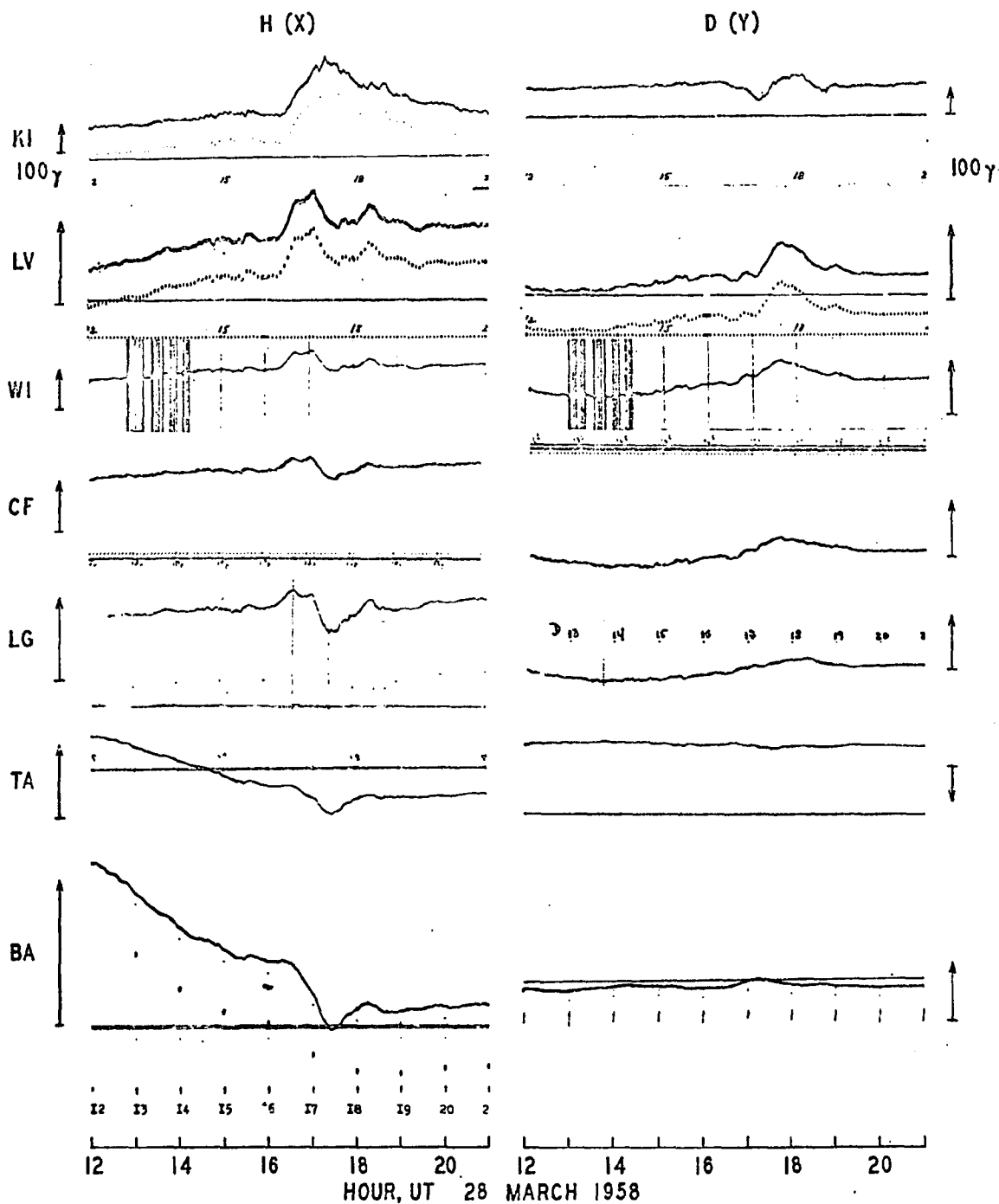


Fig. IV-8. The (DP + DR) type: an example of geomagnetic changes when the growth of the DP field appears to precede that of the DR field.

### 3. A World-wide Magnetic Disturbance During a Simple Intense Polar Substorm

A world-wide magnetic disturbance can be divided into two classifications, magnetic storms and polar substorms based on the geographic location of the disturbance. Both these disturbances, namely the low latitude magnetic storm and high latitude polar substorm have been studied in detail in Chapters II and III, respectively. In the last section, the simultaneous growths of the polar electrojet and ring current were discussed based on the data from several stations in the Europe-Africa sector. A detailed study, with good time and spatial accuracy over the entire northern hemisphere, of a simple polar substorm is needed for better understanding of the nature of polar substorms and the growth of the ring current related to the substorm. Despite many past studies of polar magnetic substorms, two major problems remain. The first problem is to obtain the accurate change distribution of the magnetic disturbance vectors over the entire earth during the life time of the substorm. There has been much discussion as to the flow pattern of the polar electrojet which causes polar magnetic substorms. It is likely that the polar electrojet flows along the auroral oval as suggested in Chapter IV, but the nature of the eastward current (positive bays) in the afternoon sector of the auroral zone is a matter of discussion. The second problem is to infer (not to determine) a three dimensional current system in the magnetosphere, rather than the two dimensional equivalent current system, from the distribution of the disturbance vectors.

The ideal polar substorm for this purpose must be a well isolated and intense one. A substorm occurring when Europe (which has a dense

distribution of magnetic observatories) is in the early evening sector is particularly suitable for this study. During the IGY/C period, polar substorms were intense and frequent, thus it is almost impossible to find a well isolated simple substorm. In the period of IQSY, the polar substorms were not frequent, however they were generally not intense enough to produce an observable world-wide effect. After scanning all the available magnetograms, it was found that very few substorms met all criteria and the best of these was chosen for a detailed study. Figure IV-9 shows the AE index from December 11 to December 30, 1964 (Davis and Wong). During this period it is seen that December 16, 1964 approaches the ideal case.

Magnetograms of a total of 73 stations were used (Table IV-1); 72 of them on the dipole northern hemisphere and one on the dipole southern hemisphere. Since the operation of a key station inside the auroral zone, Murchison Bay, was discontinued after the IGC, the data from its conjugate station in the southern hemisphere (Mirny) was used. The conjugacy of the polar substorm was discussed in Chapter III, Section 2-3 in which the conjugacy between Murchison Bay and Mirny was specifically studied and in which it was shown that a conjugacy of negative bays exists between the two stations. Thus it is reasonable to substitute the data from Mirny for that of Murchison Bay. Both H (or X) and D (or Y) components of these magnetograms were scaled, by using a semi-automatic OSCAR machine, at five minute intervals between 1000 and 1700 UT, December 16, 1964.

For the convenience of discussion, 73 stations were grouped according to their latitudes as well as to the similarity of magnetic disturbances observed at each station. Figure IV-10 illustrated the disturbances in the midnight and early morning sectors along the auroral zone. There were

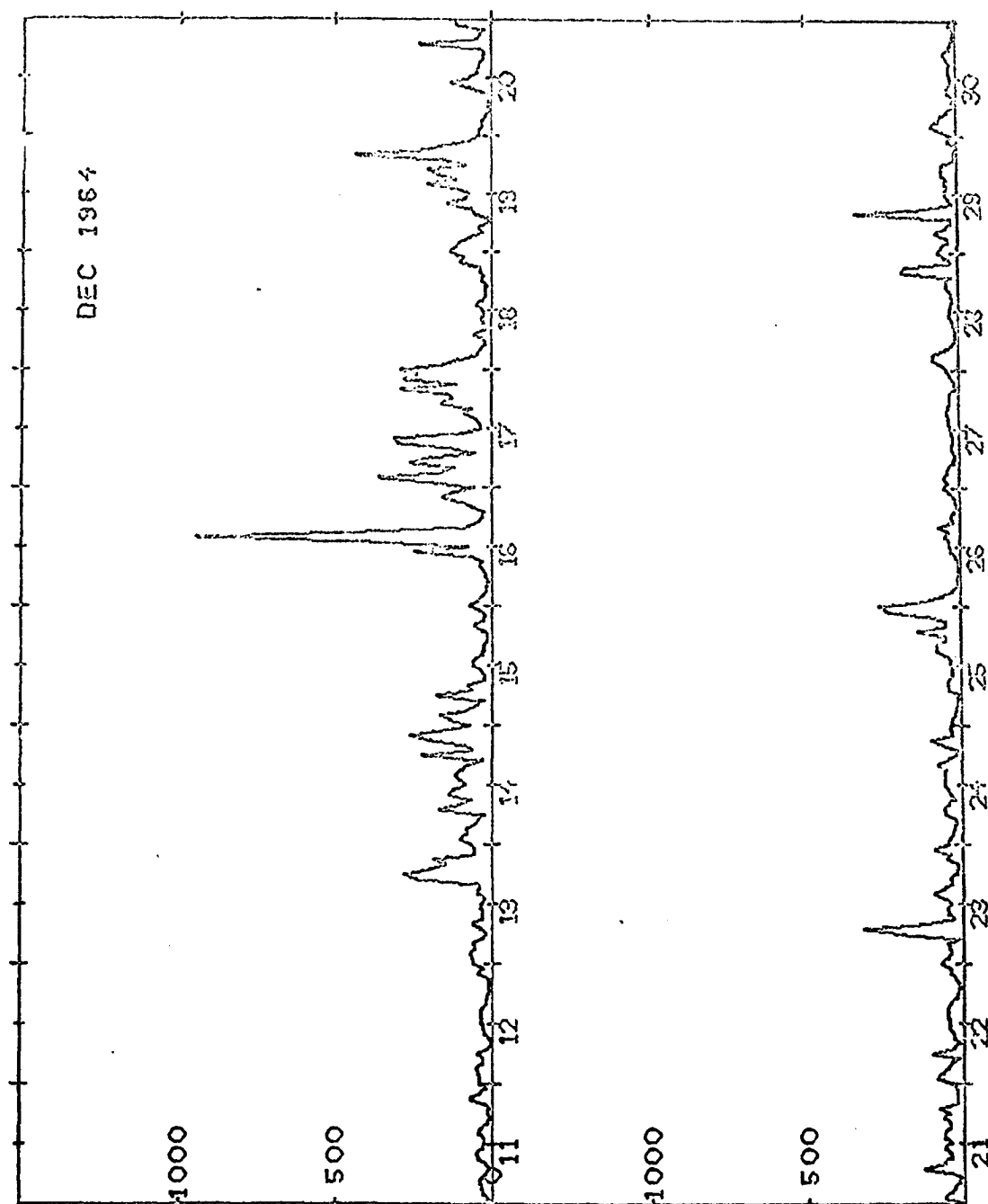


Fig. IV-9. Hourly values of AE index from Dec 11 to Dec 30, 1964 (after Davis and Wong, 1967).

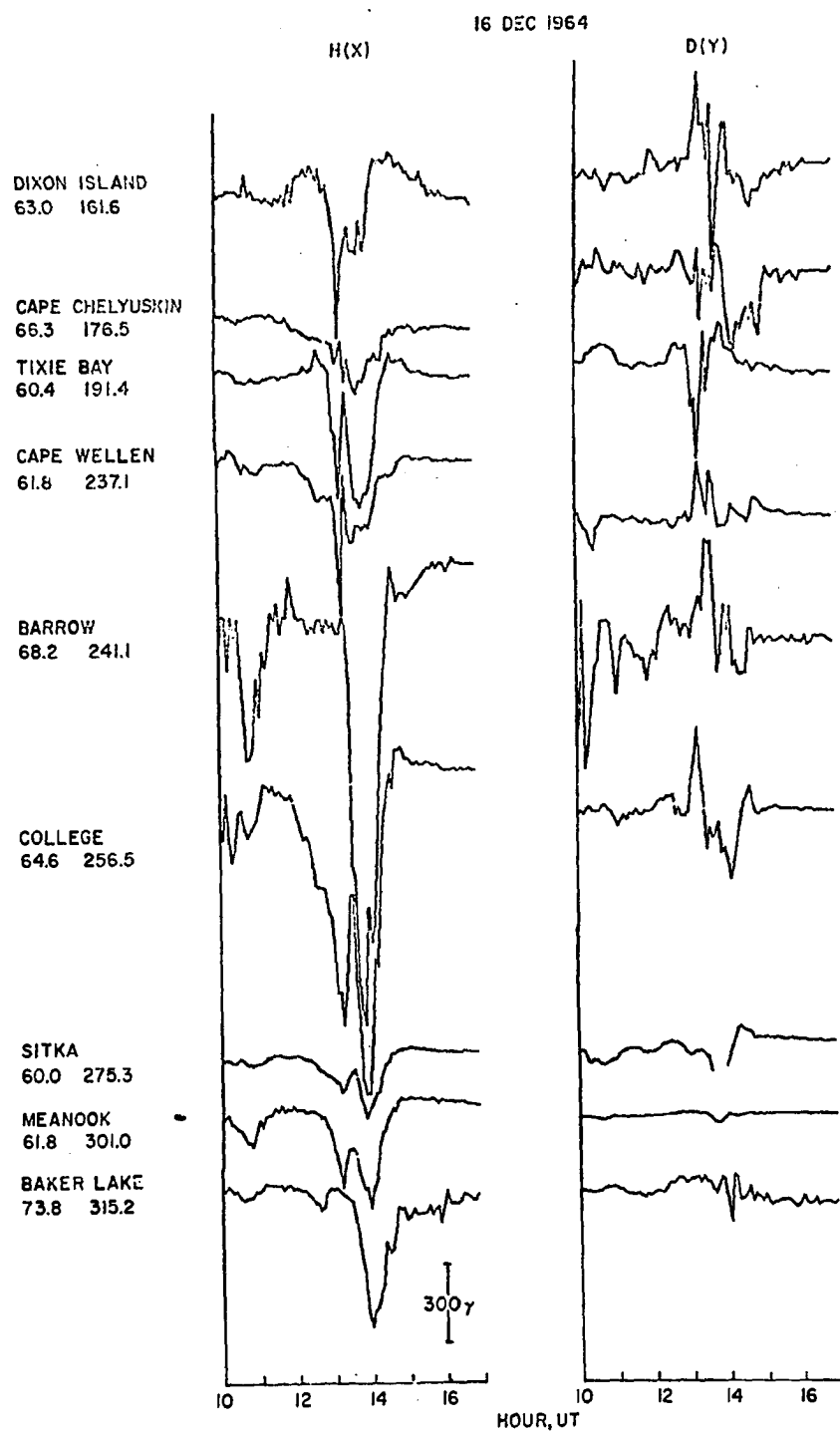


Fig. IV-10. Variations of the magnetic field (both H and D components) between 1000 UT and 1700 UT, Dec 16, 1964 at stations above  $+60^\circ$  in the midnight and morning sector.

**TABLE IV-1**
**Magnetic Observatories used in the Study**

Number	Station	Geomagnetic	
		Latitude	Longitude
1	Addis Ababa	5.4°	109.2°
2	Agincourt	55.1	347.0
3	Alert	85.9	168.2
4	Almeria	40.6	75.3
5	Ashkhabad	30.5	133.1
6	Baker Lake	73.8	315.2
7	Bangui	4.8	88.5
8	Barrow	68.5	241.1
9	Boulder	49.0	316.5
10	Cape Chelyuskin	66.3	176.5
11	Cape Wellen	61.2	237.1
12	Chambon-La-Foret	50.5	84.4
13	College	64.6	256.5
14	Cuba	34.1	345.3
15	Dallas	43.0	327.7
16	Dixon Island	63.0	161.6
17	Dourbes	52.0	87.7
18	Fredricksburg	49.6	349.8
19	Fuquene	16.9	355.1
20	Furstenfeldbruck	48.8	93.3
21	Godhavn	79.9	32.5
22	Guam	4.0	212.9
23	Hartland	54.6	79.0
24	Heiss Island	71.3	156.1
25	Hel	53.4	103.7
26	Honolulu	21.1	266.5
27	Irkutsk	40.7	174.8
28	Julianehaab	70.8	35.5
29	Kakioka	26.0	206.0
30	Kanoya	20.5	198.1
31	Kazan	49.3	130.4
32	Kiruna	65.3	115.6
33	Kodaikanal	0.6	147.1
34	Leirvogur	70.2	71.0
35	Leningrad	56.2	117.3
36	Logrono	46.1	77.2
37	Lovo	58.1	105.8

of a Simple Polar Substorm

Geographic		Declination	
Latitude	Longitude		
9° 02' N	38° 46' E	-1 °	
43 47 N	79 16 W	-8	
82 30 N	62 30 W	-78	
36 51 N	2 28 W	-7	35 '
37 57 N	58 06 E	4	17
64 20 N	96 02 W	5	
4 26 N	18 34 E	-5	
71 18 N	156 45 W	26	
40 08 N	105 14 W	13	30
77 43 N	104 17 E	25	10
66 10 N	169 50 W	14	
48 01 N	2 16 E	-6	
64 52 N	147 50 W	28	30
22 58 N	82 09 W	0	
32 59 N	96 45 W	10	
73 33 N	80 34 E	30	
50 06 N	4 36 E	-5	11
38 12 N	77 22 W	6	43
5 28 N	73 44 W	1	
48 10 N	11 17 E	-2	
69 14 N	53 31 W	-51	50
13 35 N	144 52 E	2	
51 00 N	4 29 W	-9	30
80 37 N	58 03 E	25	
54 36 N	18 49 E	1	
21 19 N	158 00 W	10	30
52 10 N	104 27 E	-2	30
60 43 N	46 02 W	-38	
36 14 N	140 11 E	-6	
31 25 N	130 53 E	-5	
55 50 N	48 51 E	10	30
67 50 N	20 25 E	2	
10 14 N	77 28 E	-3	30
64 11 N	21 42 W	-25	
59 57 N	30 42 E	7	
42 27 N	2 30 W	-7	
59 21 N	17 50 E	0	

TABLE IV-1 (Cont'd)

## Magnetic Observatories used in the Study of a Simple Polar Substorm

Number	Station	Geomagnetic		Geographic		Declination
		Latitude	Longitude	Latitude	Longitude	
38	Lvov	48.0°	105.9°	49° 54' N	23° 45' E	2° 30'
39	M'Bour	21.3	55.0	14 24 N	16 58 W	-15 30
40	Meanook	61.8	301.0	54 37 N	113 20 W	24
41	Memambetsu	34.0	208.4	43 54 N	144 12 E	- 8 10
42	Minsk	51.5	110.4	54 06 N	26 31 E	4 30
43	Murchison Bay (Mirny)	75.2 (-77.0)	137.5 (146.8)	80 03 N (66 33 S)	18 15 E (93 01 E)	2 2
44	Missalat	26.9	105.9	29 31 N	30 54 E	1 30
45	Moscow	50.9	120.5	55 29 N	37 19 E	7 50
46	Mould Bay	79.1	256.4	76 12 N	119 24 W	70
47	Muntinlupa	3.0	189.7	14 22 N	121 01 E	1
48	Murmansk	63.5	125.8	68 15 N	33 05 E	12 30
49	Niemegk	52.2	96.6	52 04 N	12 41 E	-2
50	Nurmijarvi	57.9	112.6	60 31 N	24 39 E	4
51	Odessa	43.7	111.1	46 47 N	30 53 E	2
52	Paramaribo	17.0	14.3	5 49 N	55 13 W	-12
53	Rude Skov	55.9	98.5	55 51 N	12 27 E	- 2
54	San Fernando	41.0	71.3	36 28 N	6 12 W	- 8 11
55	San Juan	29.6	3.1	18 07 N	66 09 W	- 8
56	Sitka	60.0	275.3	57 04 N	135 20 W	29
57	Stonyhurst	56.9	82.7	53 51 N	2 28 W	350 10
58	Sukkertoppen	76.1	28.7	65 25 N	52 54 W	313 10
59	Tashkent	32.3	144.0	41 20 N	69 37 E	5
60	Tbilisi	36.7	122.1	42 05 N	44 42 E	5 10
61	Tenerife	35.0	58.6	28 29 N	16 17 W	-13
62	Thule	89.0	358.0	77 29 N	69 10 W	-81 40
63	Tixie Bay	60.4	191.4	71 35 N	129 00 E	-10
64	Toledo	43.9	74.7	39 53 N	4 03 W	- 8
65	Tortosa	43.9	79.7	40 49 N	0 30 E	- 6
66	Tromso	67.1	116.1	69 40 N	18 57 E	2
67	Tucson	40.4	312.2	32 15 N	110 50 W	13 30
68	Valentia	56.6	73.5	51 56 N	10 15 W	-13
69	Victoria	54.2	293.0	48 31 N	123 25 W	24
70	Vladivostock	32.8	198.1	43 41 N	132 10 E	- 9 20
71	Witteveen	54.1	91.2	52 49 N	6 40 E	- 3 30
72	Yakutsk	51.0	193.8	62 01 N	129 43 E	-14
73	Zaria	13.6	79.1	11 09 N	7 39 E	- 7



two substorms during this period. The first one occurred between 1000 and 1100 UT and was a very small one, in fact only stations close to the mid-night meridian, namely Barrow, College and Meanook observed substantial disturbances. The second one which occurred after 1200 UT was a very intense one with a magnitude of more than 1500  $\gamma$  at Barrow. From the hourly AE index, these two substorms can be clearly identified (Fig. IV-11). Generally, only during a magnetic storm can a polar substorm with more than 1000  $\gamma$  be observed. Thus, this intense substorm of more than 1500  $\gamma$  can be considered an unusual case. The onset of this substorm was when the negative bay was observed at College and the positive bay at Dixon Island at about 1200 UT, or even earlier. The record from College suggests that this particular polar substorm had a double structure. The polar electrojet appeared to grow at about 1200 UT near College, but not at Barrow. The Bar-I all-sky camera station recorded a sudden brightening of auroras very near the southern horizon between 1239 and 1245 UT. Thus, the growth of the jet appeared to occur along  $dp$  lat  $65^\circ$  in Alaska. At about 1320 UT, the polar electrojet began to diminish, but about 10 minutes later (about 1330 UT) it increased suddenly all along the auroral oval. The Bar-I all-sky films showed a violent explosive poleward motion of auroras, which began at 1327 UT near the southern horizon. The magnitude of the substorm increased to the unusual magnitude of more than 1500  $\gamma$  at Barrow in the early morning sector and about 1200  $\gamma$  at Heiss Island in the late afternoon sector (Fig. IV-12). Simultaneously, negative bays were observed at Barrow ( $dp$  lat  $68.2^\circ$ ) and College ( $dp$  lat  $64.6^\circ$ ) (Alaska) in the early morning sector, Heiss Island ( $dp$  lat  $71.3^\circ$ ) (Russian Arctic Ocean) and Murchison Bay ( $dp$  lat  $75.2^\circ$ ) (Spitsbergen) (based on its

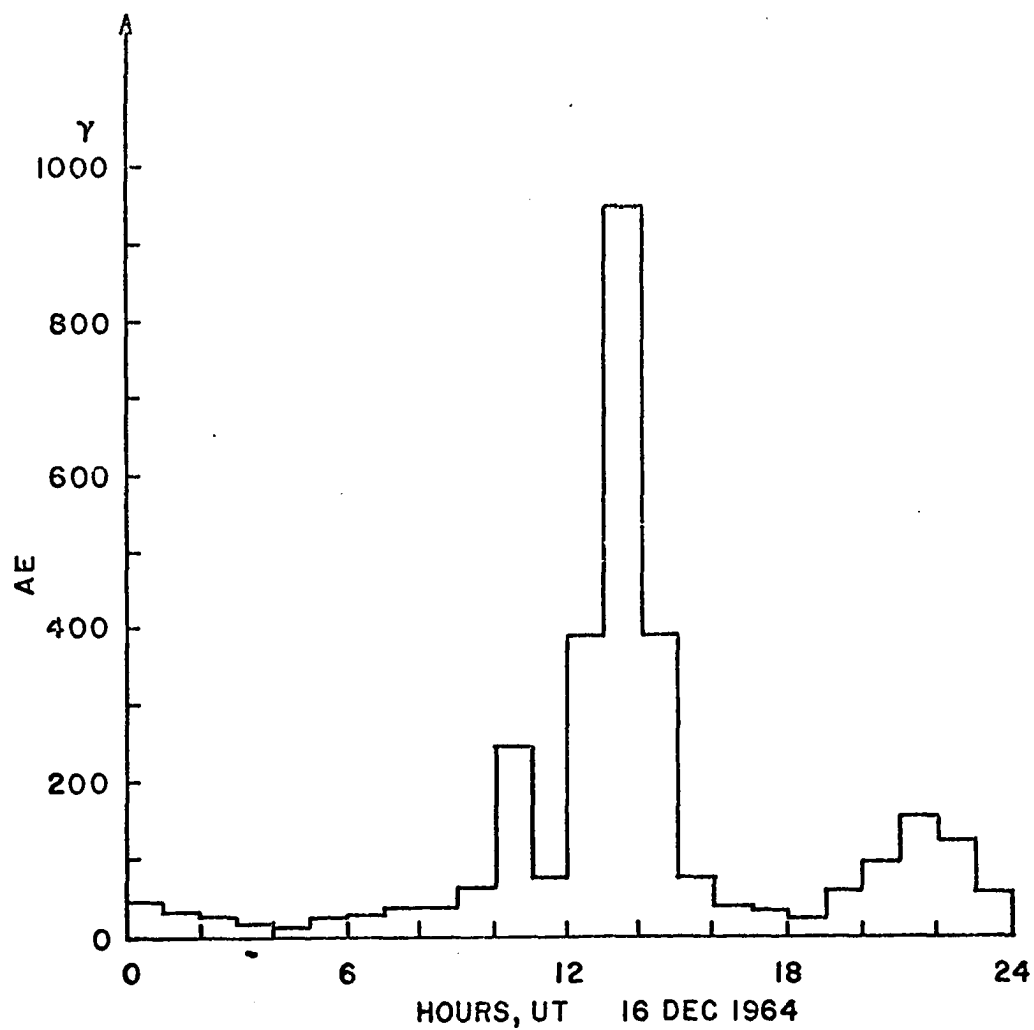


Fig. IV-11. Hourly AE index for December 16, 1964.

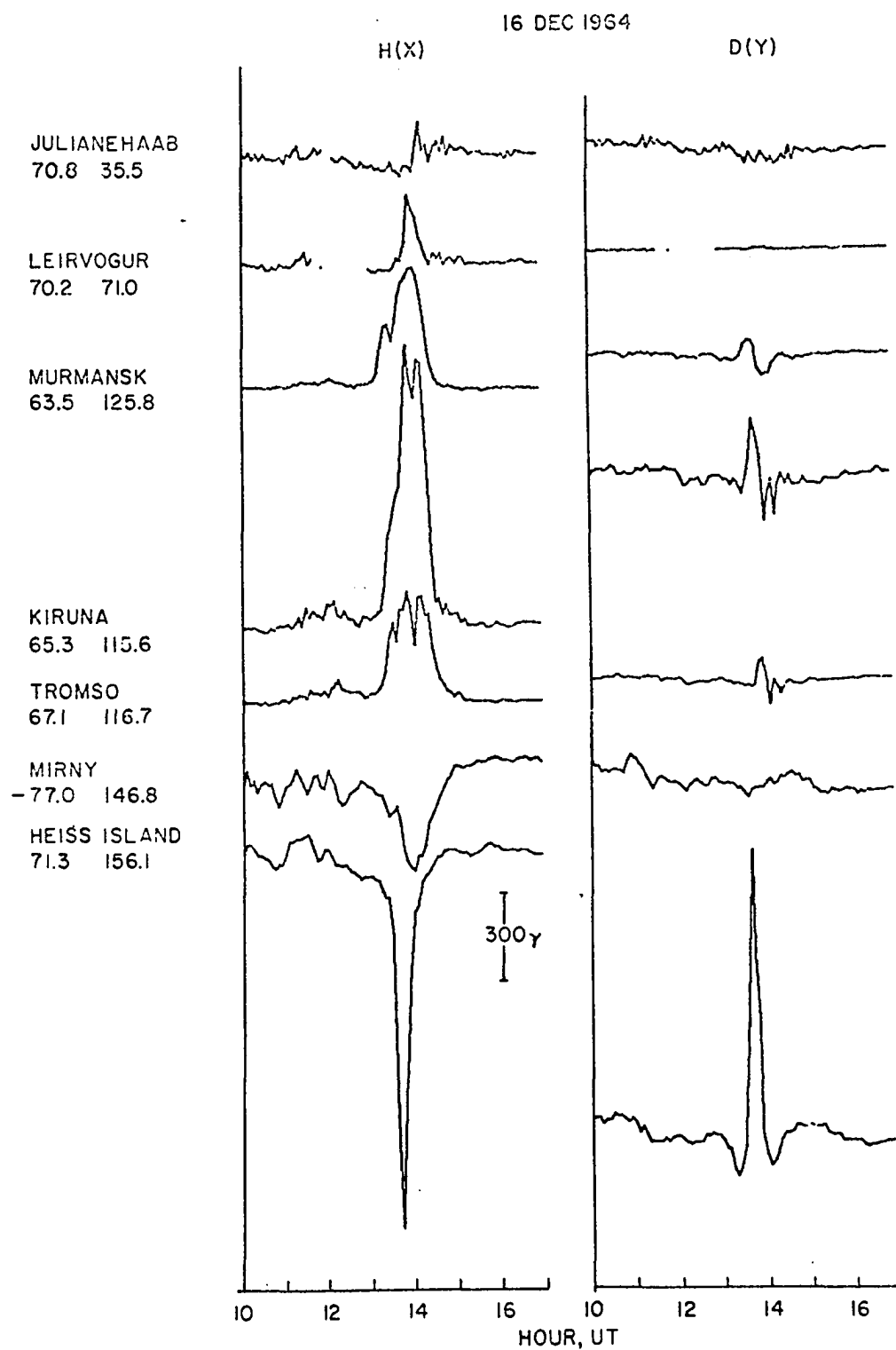


Fig. IV-12. Magnetic disturbance recorded above  $+60^\circ$  in the afternoon and noon sectors between 1000 UT and 1700 UT, Dec 16, 1964.

conjugate data at Mirny) in the afternoon sector, Godhavn (dp lat  $79.9^\circ$ ) (Greenland) in the noon sector and Baker Lake (dp lat  $73.8^\circ$ ) (Canada) in the morning sector (Figs. IV-10, IV-12 and IV-13). Figure IV-14 shows the location of stations higher than dp lat  $60^\circ$  used in this analysis together with the auroral oval at 1400 UT.

Near or along the "auroral zone" which is on the equatorward side of this oval band in the afternoon sector (in the sunlit hemisphere) the intense positive bays were observed at Murmansk (dp long  $125.8^\circ$ ), Tromsø (dp long  $116.7^\circ$ ), Kiruna (dp long  $115.6^\circ$ ), Leirvogur (dp long  $71.0^\circ$ ) and even Julianehaab (dp long  $35.5^\circ$ ) which was in the midday sector (see Figs. IV-12 and IV-14); the magnitude of the positive bay decreased toward the noon sector. This magnetic disturbance was also recorded at the three polar cap stations during this substorm (Fig. IV-13). Thus, for this intense but simple polar substorm the magnetic disturbances which occurred higher than dp lat  $60^\circ$  agree with the revised polar electrojet and also the morphology of the polar substorm discussed in Chapter III, section 2. The stations between dp lat  $60^\circ$  and the geomagnetic equator are divided into four groups according to their dipole longitudes. Figure IV-15 illustrates the low latitude disturbances between dp long  $100^\circ$  and dp long  $160^\circ$  which is in the afternoon sector at 1400 UT. The most distinct feature is the onset of a negative change over all latitudes after 1300 UT. Another important feature is the small positive change of the H component superposed on the negative change in a higher latitude station. The shape of the negative bay changes gradually from a square-well type to a sharp minimum type with decreasing latitude. For the D(or Y) component, the increase of the disturbance is almost identical in all the stations, but

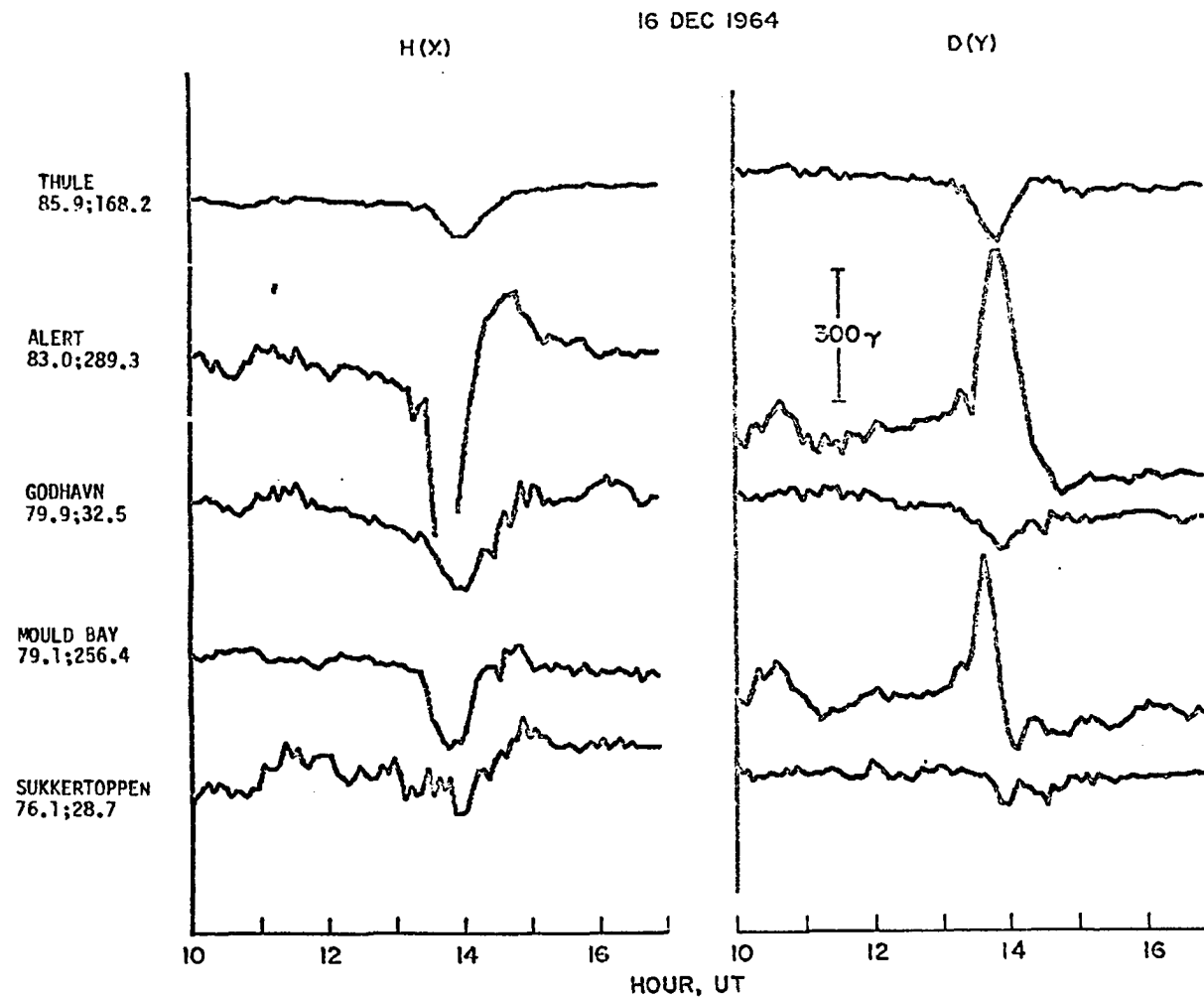


Fig. IV-13. Magnetic disturbances recorded in the polar cap between 1000 UT and 1700 UT, December 16, 1964.

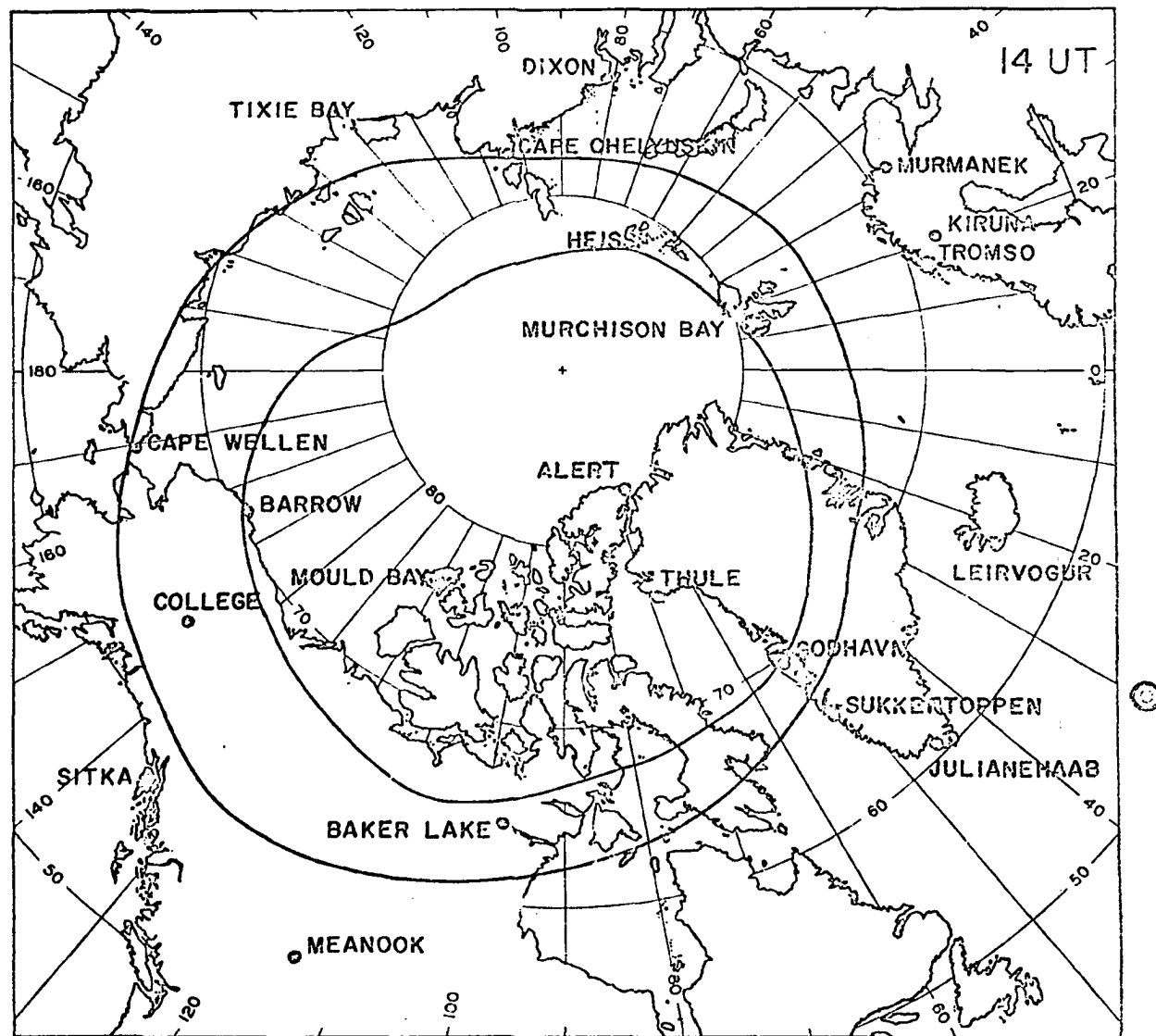


Fig. IV-14. Locations of magnetic stations above  $+60^\circ$  used in this analysis together with the location of auroral oval at 1400 UT.

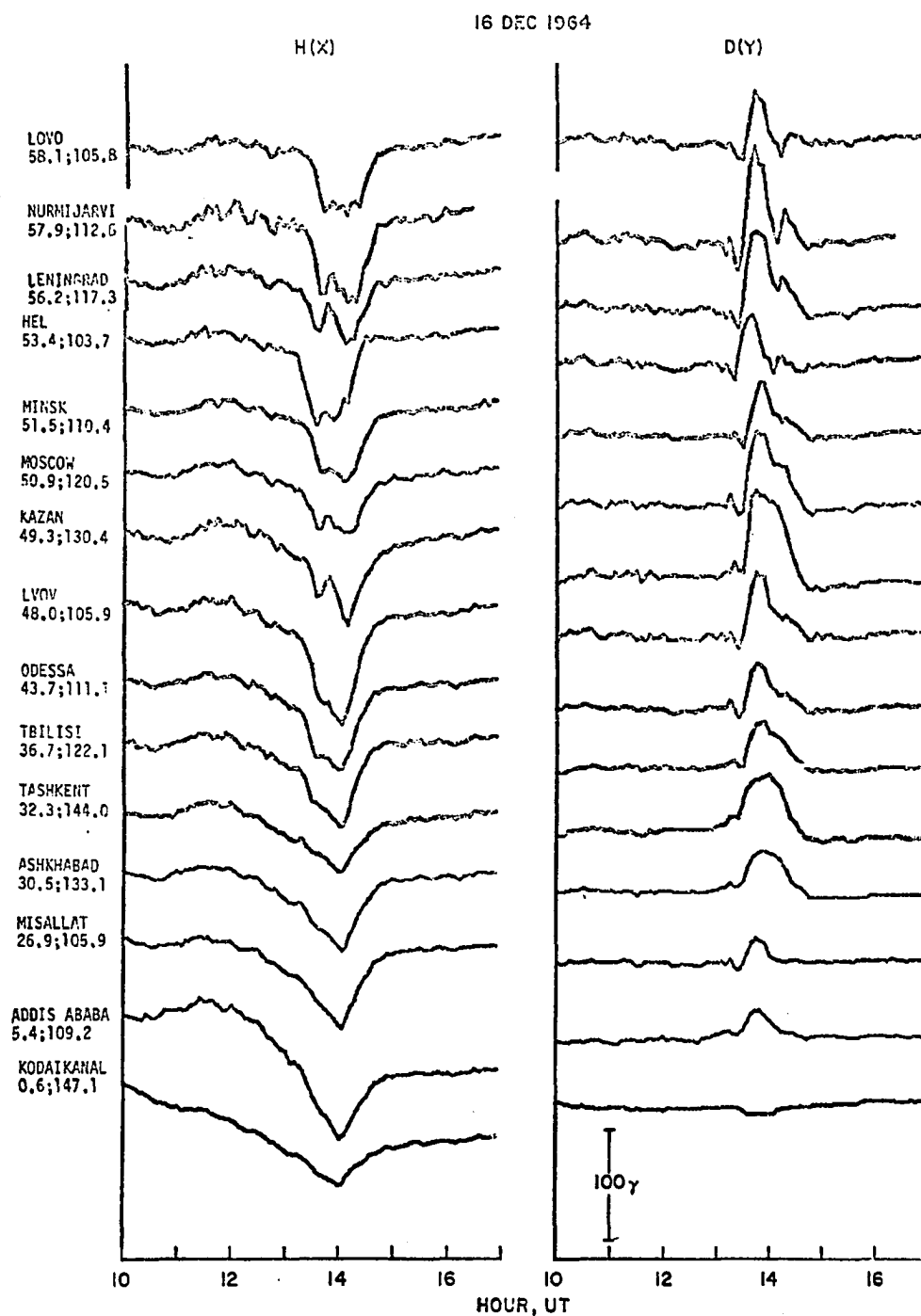


Fig. IV-15. Magnetic disturbances recorded below  $+60^\circ$  in the afternoon sector (at 1400 UT) between 1000 UT and 1700 UT, Dec 16, 1964.

its magnitude decreases from high to low latitudes. Figure IV-16 illustrates the disturbances during this substorm in the noon and early afternoon sector (at 1400 UT) between dp long  $30^\circ$  and dp long  $100^\circ$ . For H (or X) component, both the shape and magnitude of about 75 Y are similar in the whole sector; while for D (or Y) component, disturbances are rather small. Figure IV-17 shows that in the late morning sector at 1400 UT (between dp long  $280^\circ$  and dp long  $30^\circ$ ) the negative change of the H (or X) component is rather small, but that of the D (or Y) is very large, especially at Boulder (dp lat  $49.0^\circ$ ). Also the systematic change of D (or Y) with the latitude seen in other sectors is not seen in this late morning sector. Figure IV-18 shows the disturbance in the midnight and early morning sector. For the H component, the positive bays are seen in all the stations below dp lat  $35^\circ$  with similar structures at about 1300 UT. But the smooth decrease of H before the positive bay and the smooth increase of H after the positive bay can be seen in all stations. The two stations, namely Yakutsk (dp lat  $51.0^\circ$ ) and Irkutsk (dp lat  $40.7^\circ$ ), recorded negative bays with some positive changes which are typical of the 'transition type' studied in detail by Rostoker (1966). The D (or Y) component shows a very systematic positive change with decreasing magnitude toward lower latitudes in this sector, except for Honolulu which was very close to the late morning sector.

The low and middle latitude magnetic disturbance during this intense substorm can be summarized as follows. The low latitude negative bay which is attributed to the increase of the ring current is observed rather uniformly and systematically in the entire afternoon sector. The low latitude positive bay which is attributed to the return current of the polar



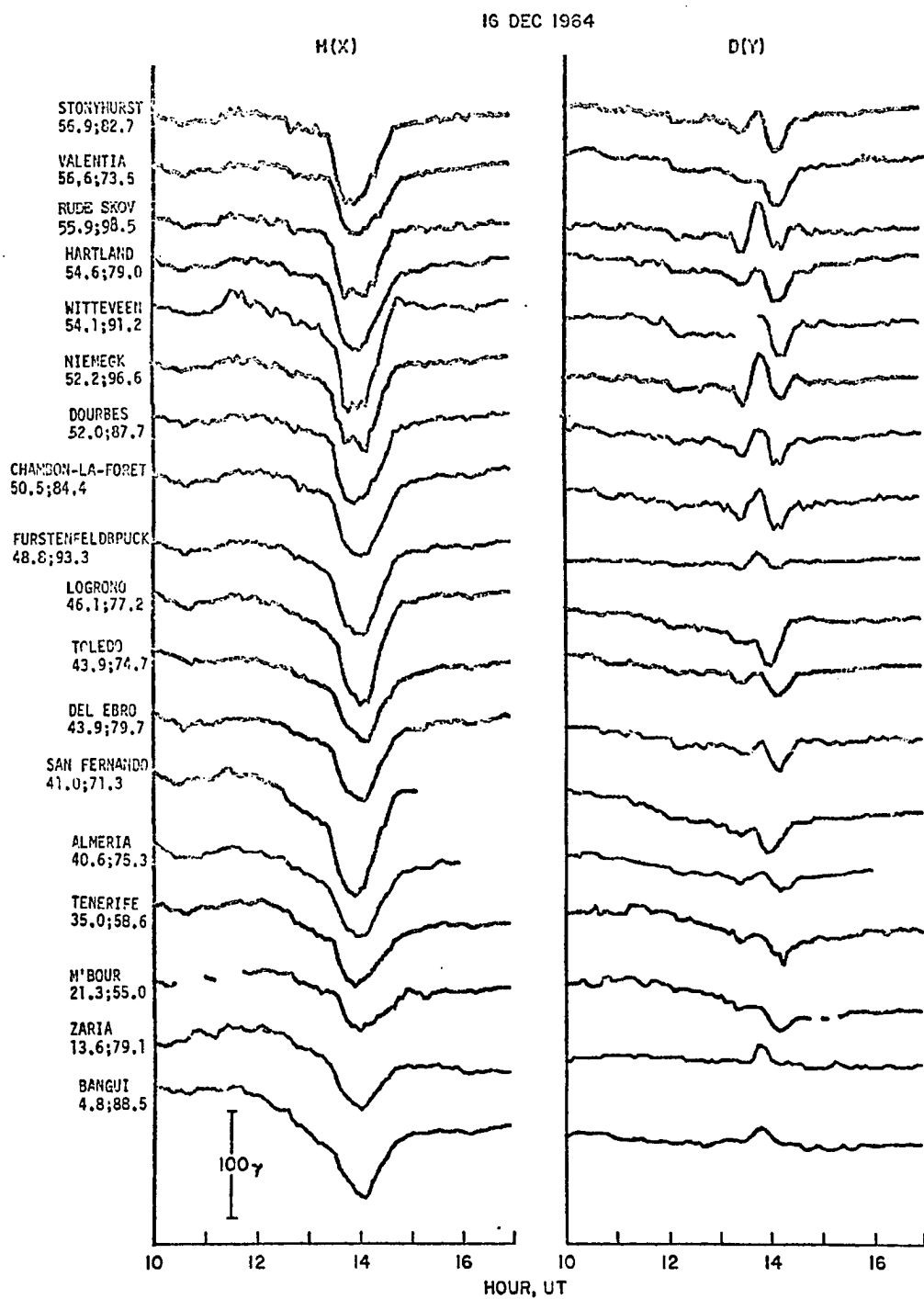


Fig. IV-16. Magnetic disturbances recorded below  $+60^\circ$  in the noon and early afternoon sectors (at 1400 UT) between 1000 UT and 1700 UT, Dec 16, 1964.

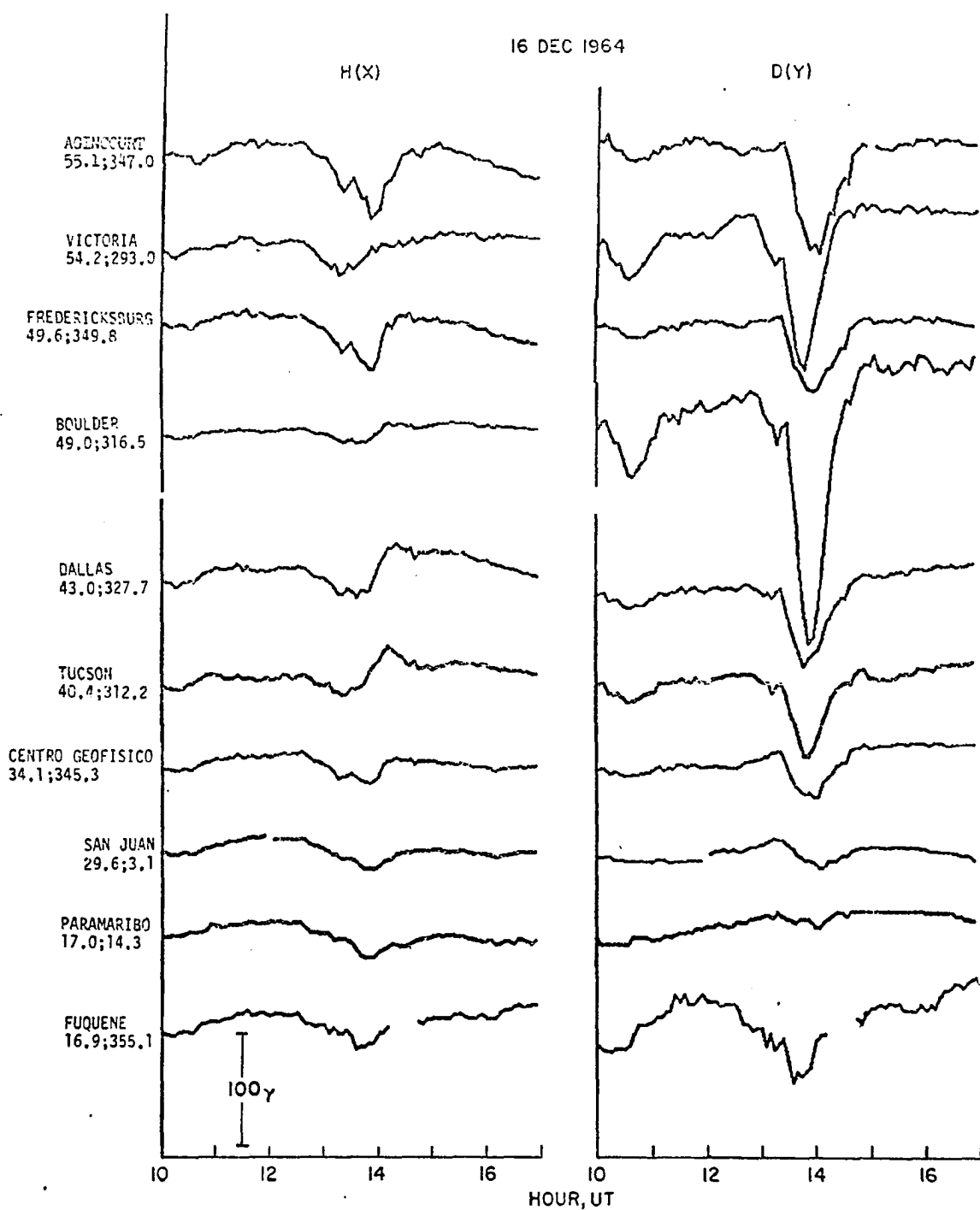


Fig. IV-17. Magnetic disturbances recorded below +60° in the morning sector (at 1400 UT) between 1000 UT and 1700 UT, Dec 16, 1964.

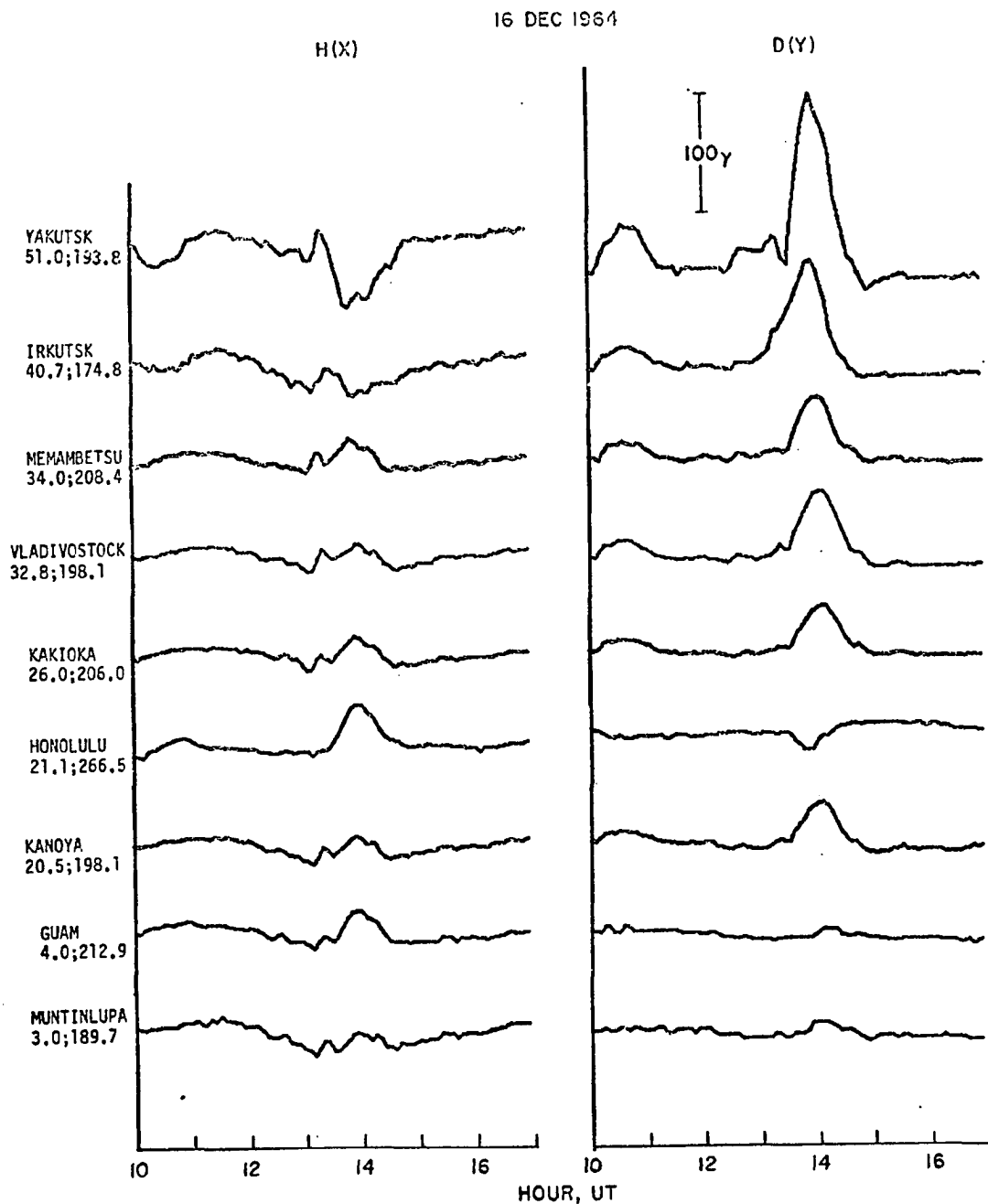


Fig. IV-18. Magnetic disturbances recorded below  $+60^\circ$  in the midnight sectors (at 1400 UT) between 1000 UT and 1700 UT, Dec 16, 1964.

electrojet from high latitudes is observed very systematically in the mid-night sector. In the late morning sector, the disturbances are rather complicated and can be explained by the superposed effect of both the ring current and the return current of the polar electrojet; but the effect of the polar electrojet is dominant in the change of D (or Y) component.

In order to examine the simultaneous magnetic disturbance vector at all stations, magnetic disturbances of H and D or of X and Y geographically oriented components were transformed into that of the X' and Y' geomagnetic components. Equations of transformation are

$$\begin{aligned} X' &= X \cos \alpha - Y \sin \alpha \\ Y' &= X \sin \alpha + Y \cos \alpha \\ \text{or} \quad X' &= H \cos \beta - D \sin \beta \\ Y' &= H \sin \beta + D \cos \beta \\ \text{where} \quad \beta &= \alpha + d \end{aligned}$$

'd' is the declination angle of the station and  $\alpha$  is determined from the following equations

$$\sin \alpha = \frac{\sin (\frac{\pi}{2} - \phi_0)}{\sin (\frac{\pi}{2} - \phi)} \sin (\Lambda - 180^\circ)$$

$$\text{or } \cos \alpha = \sin (\Lambda - 180^\circ) \sin (\lambda_0 - \lambda) \cos (\frac{\pi}{2} - \phi_0) - \cos (\Lambda - 180^\circ) \cos (\lambda_0 - \lambda).$$

The notations of these equations are listed as follows:

- $\phi$  = geographic latitude, positive north.
- $\lambda$  = geographic longitude, positive eastward.
- $\Lambda$  = dipole longitude positive eastward from the meridian plane containing the boreal and geographical poles.
- $\phi_0, \lambda_0$  = geographic coordinates of the dipole poles of a centered dipole  
( $\phi_0 = 78.6^\circ\text{N}$ ,  $\lambda_0 = 289.9^\circ\text{E}$ ).

The baseline which was chosen for each component at any station is the line connecting 1130 and 1630 UT abscissas with ordinates as the mean values of the 1100 to 1200 UT and 1600 to 1700 UT respectively. Part of the Sq variation at middle and low latitudes can be corrected by this baseline. Then, the instantaneous horizontal geomagnetic variations of all stations were plotted on polar plots. The above mentioned calculation and plotting were performed by an IBM 360 computer. The program for the transformation of the geomagnetic variations in the X and Y directions or H and D directions to the dipole directions is in Appendix I and that for the polar plot is in Appendix II.

Figure IV-19 shows the location of 73 stations on the polar plots (the data from Mirny with a factor of 2.35 was used for that of Murchison Bay). Since the magnetic disturbance is very intense in high latitudes; the magnitude scale for stations higher than  $dp\ lat\ 60^\circ$  is 1000  $\gamma$ /inch, and that for stations below  $60^\circ$ , is 200  $\gamma$ /inch; the inch scale is also shown in Figure IV-19. The polar plots of the horizontal magnetic disturbance vectors at 5 minute intervals between 1200 UT and 1535 UT are shown in Figure IV-20.

The development of the world-wide magnetic disturbance during this period can be divided into four stages. Between 1200 and 1235 UT only a few stations, mainly in the midnight sector along the auroral oval, showed some magnetic disturbance of very low intensity (the noon meridian is approximately along  $dp\ long\ 60^\circ$ ). In the lower latitude, the magnetic disturbance is practically nil except at a few stations near the noon meridian; this could be due to the effect of Sq which can not be completely eliminated near the noon meridian by the above chosen baseline. Between 1230 and 1330 UT, the negative bay at College (station No. 13) became

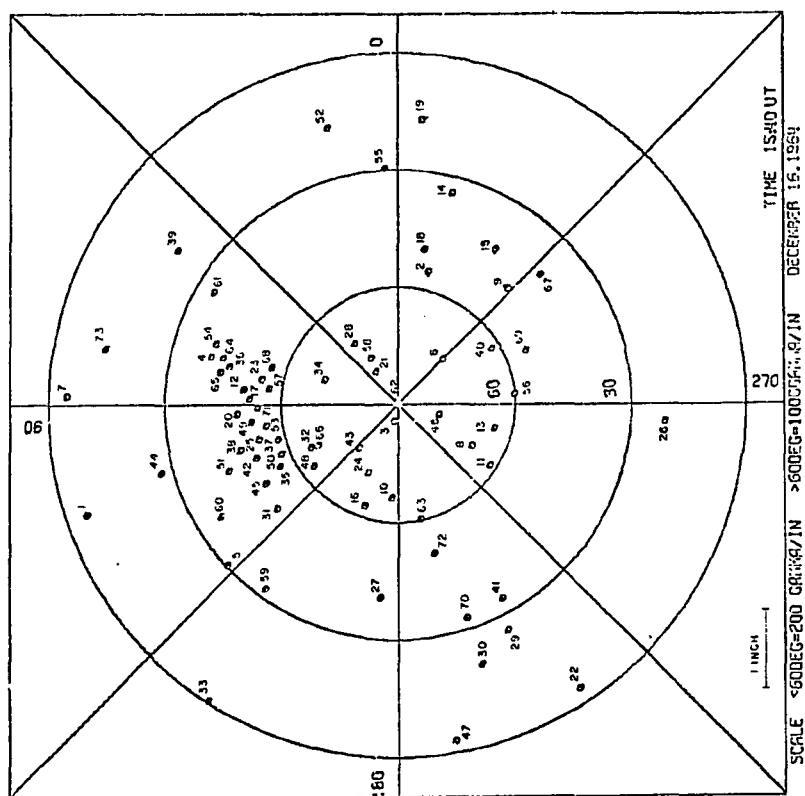


Fig. IV-19. The location of 73 stations used in the study of a simple polar substorm on the polar plot. The code number of these stations can be found in Table IV-1.

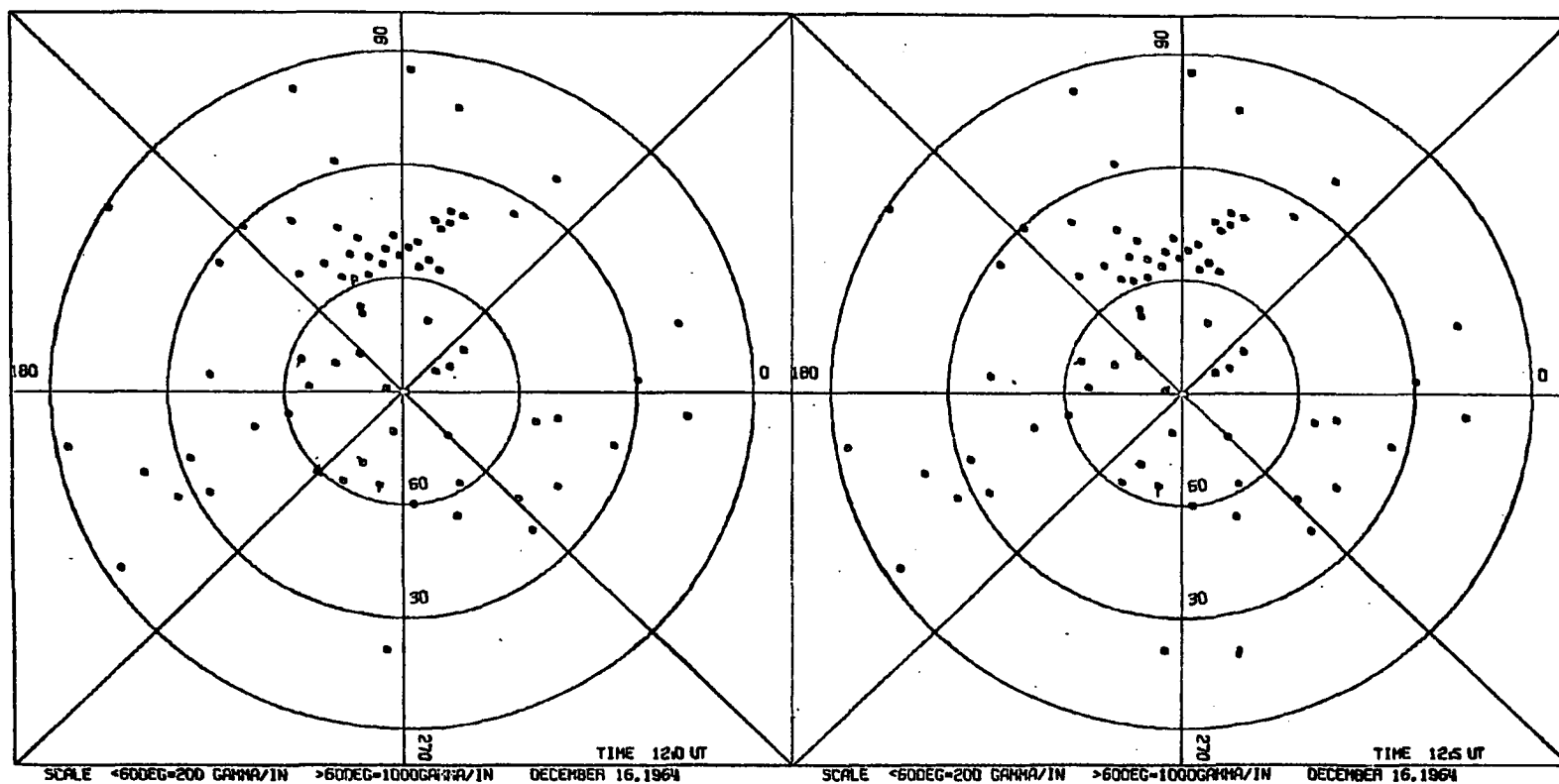


Fig. IV-20a to v. Polar plots of the magnetic disturbance vectors during a simple polar substorm of Dec 16, 1964. The length of the disturbance vector is reduced five times for stations higher than  $\text{dp lat } 60^\circ$ . The interval between each plot is 5 minutes, with the first one at 1200 UT and the last one at 1535 UT.

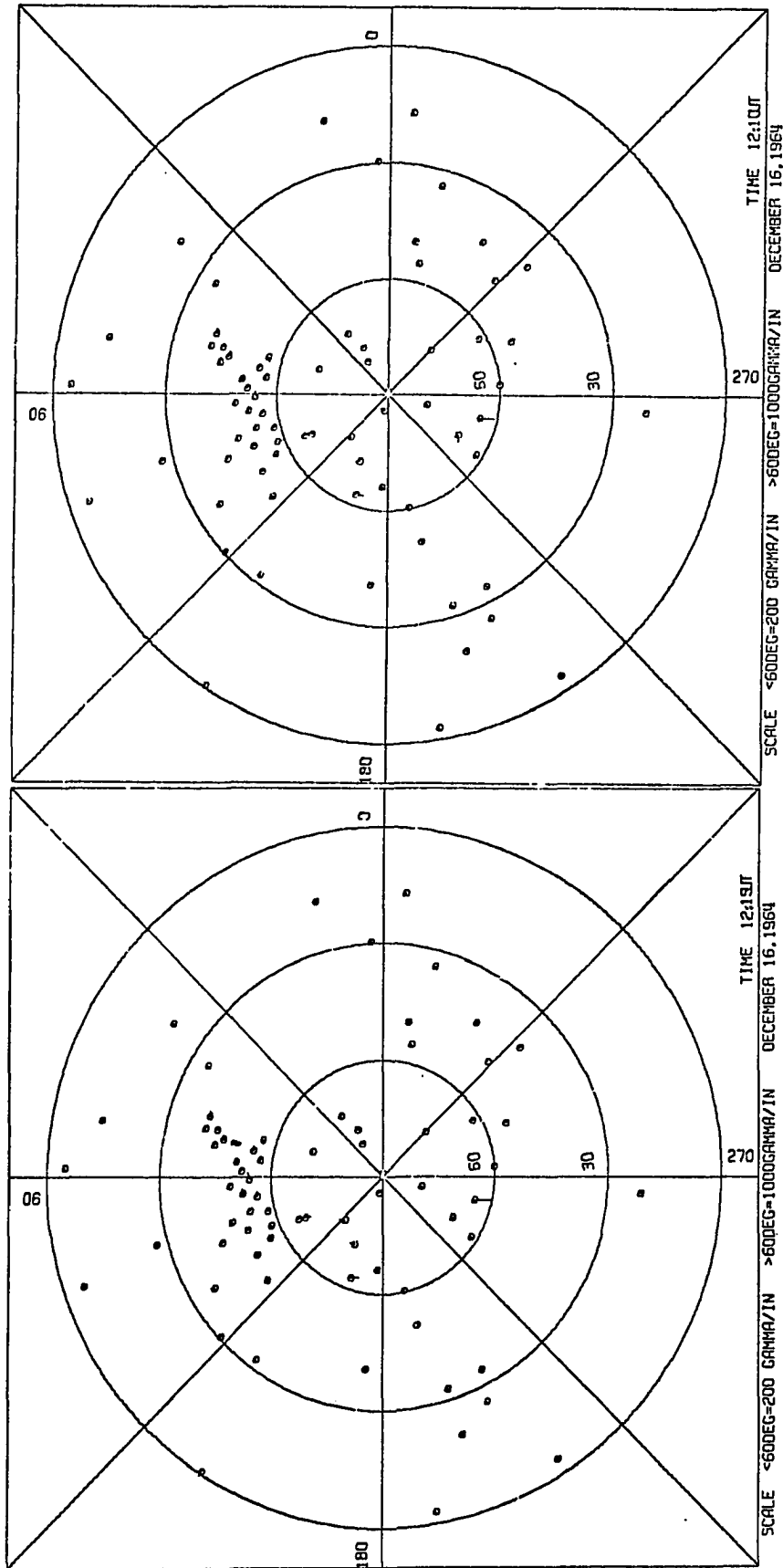


Fig. IV-20b



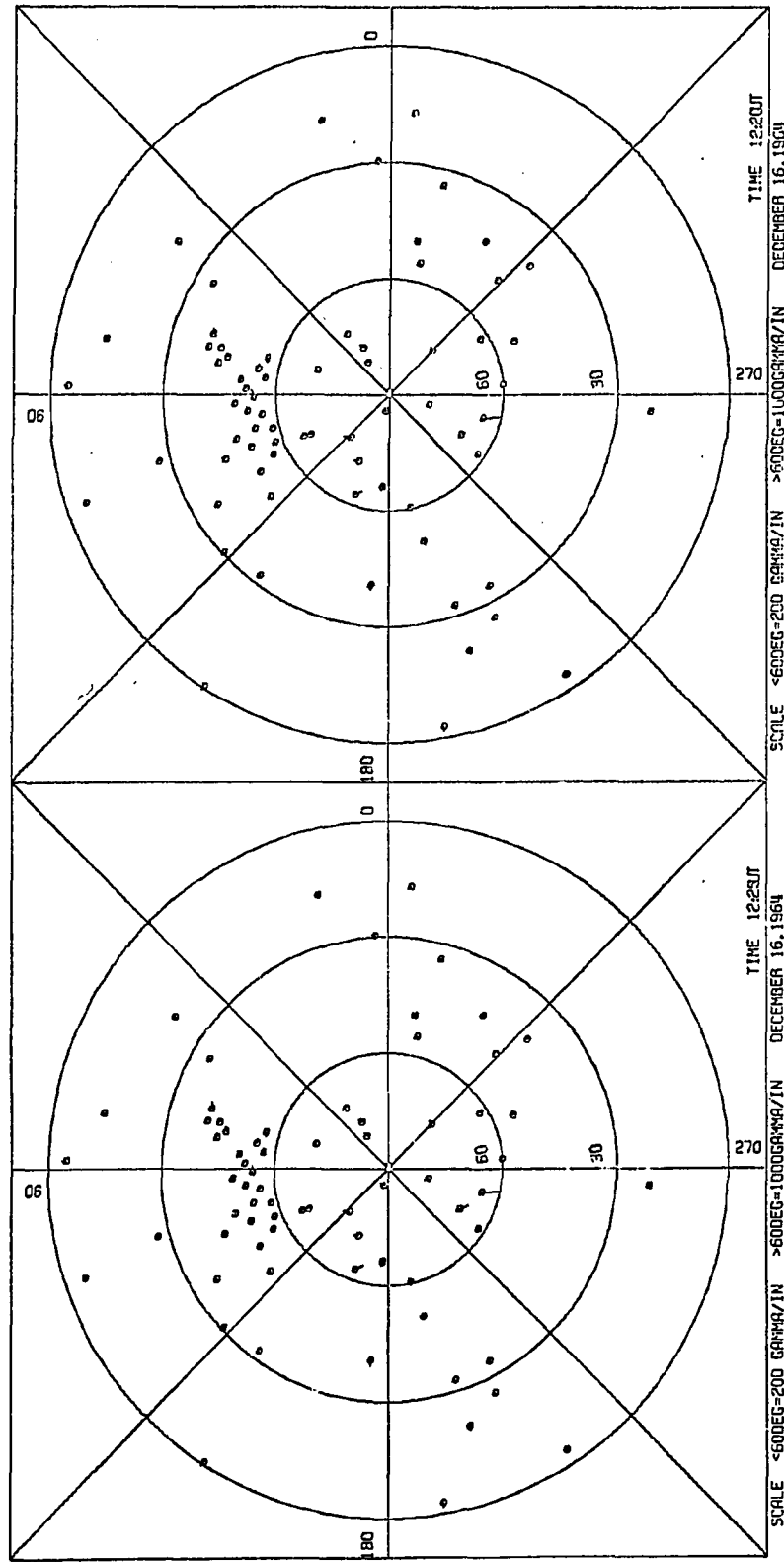


Fig. IV-20c

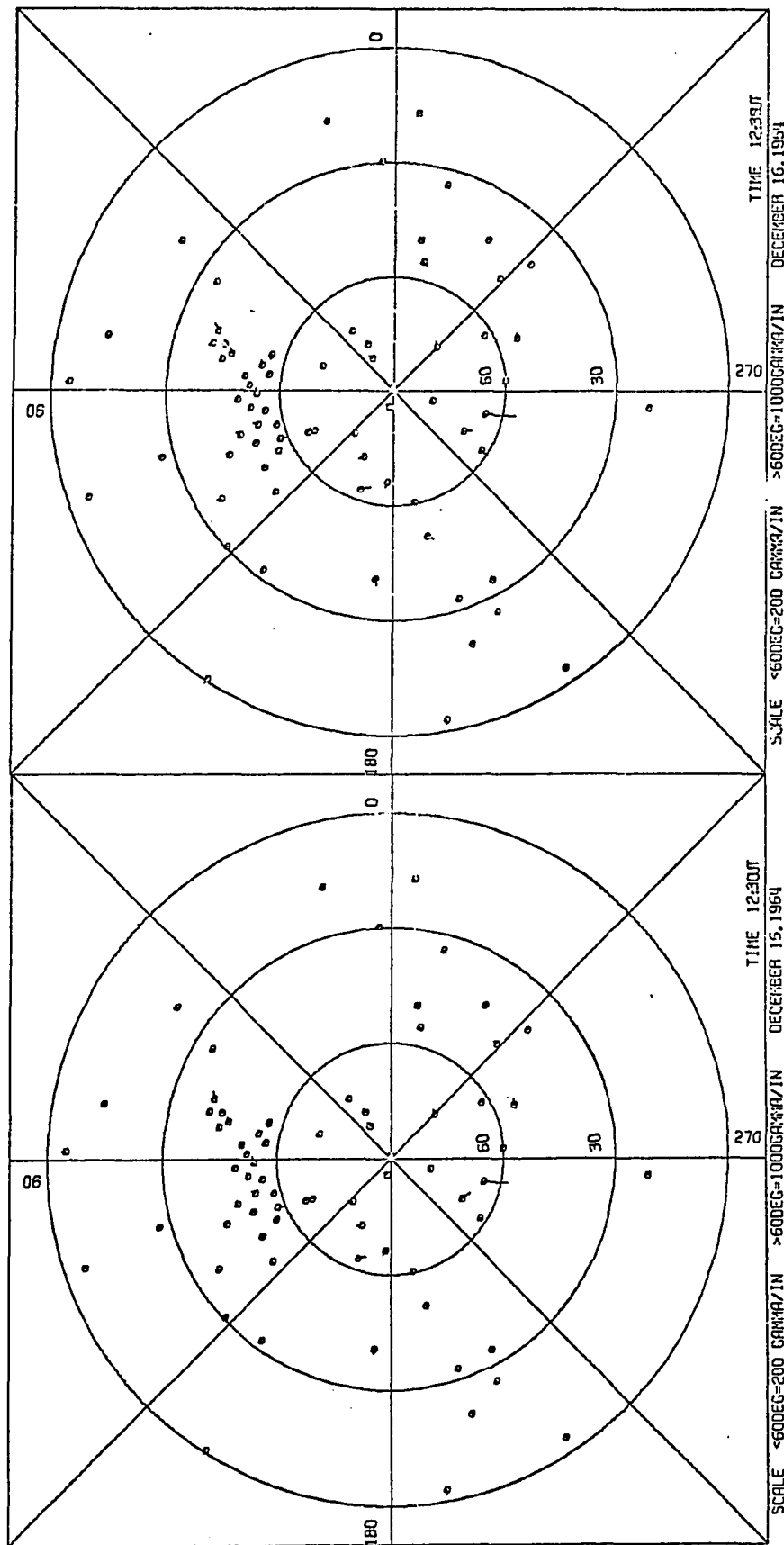


Fig. IV-20d

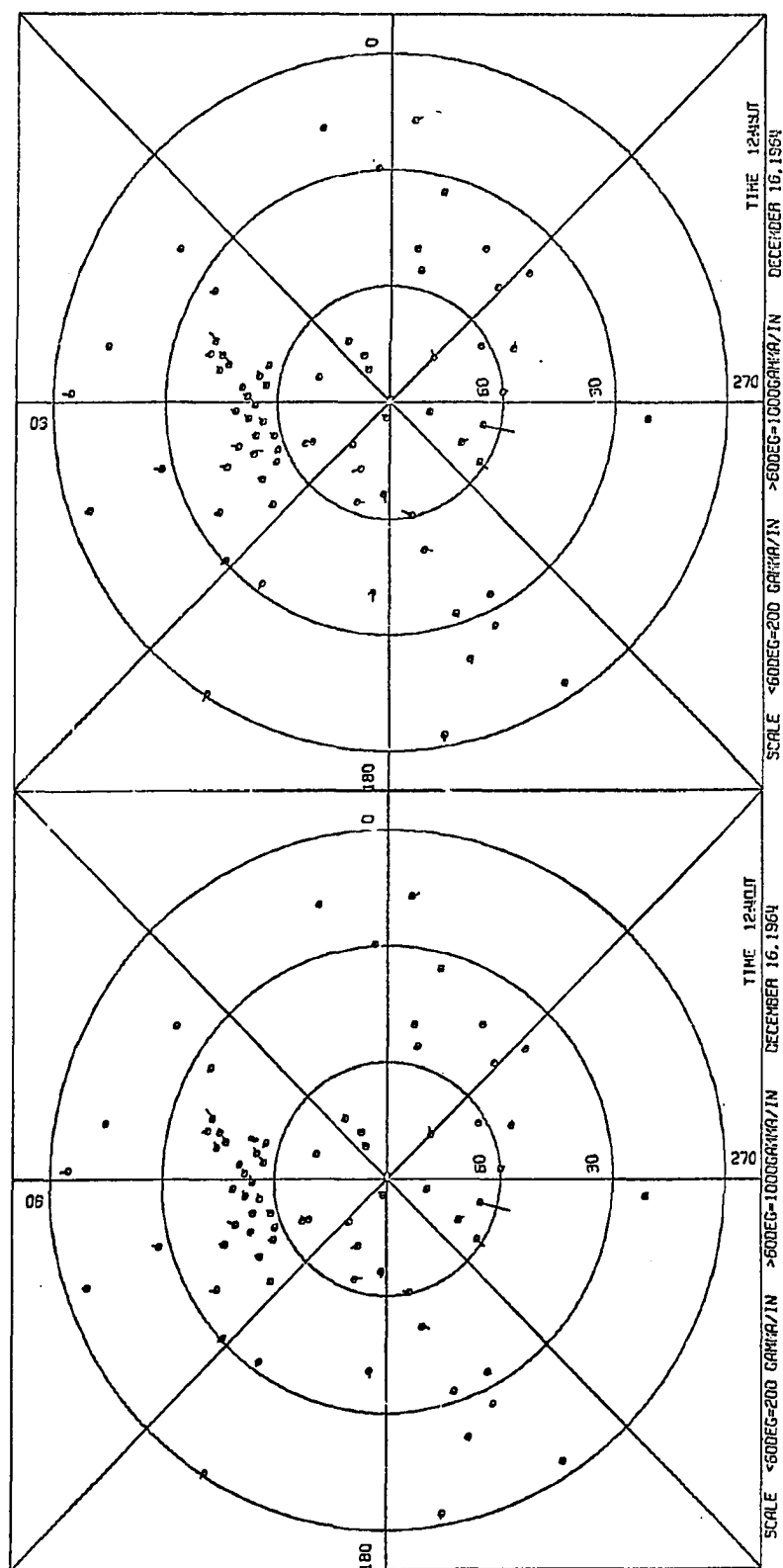


Fig. IV-20e

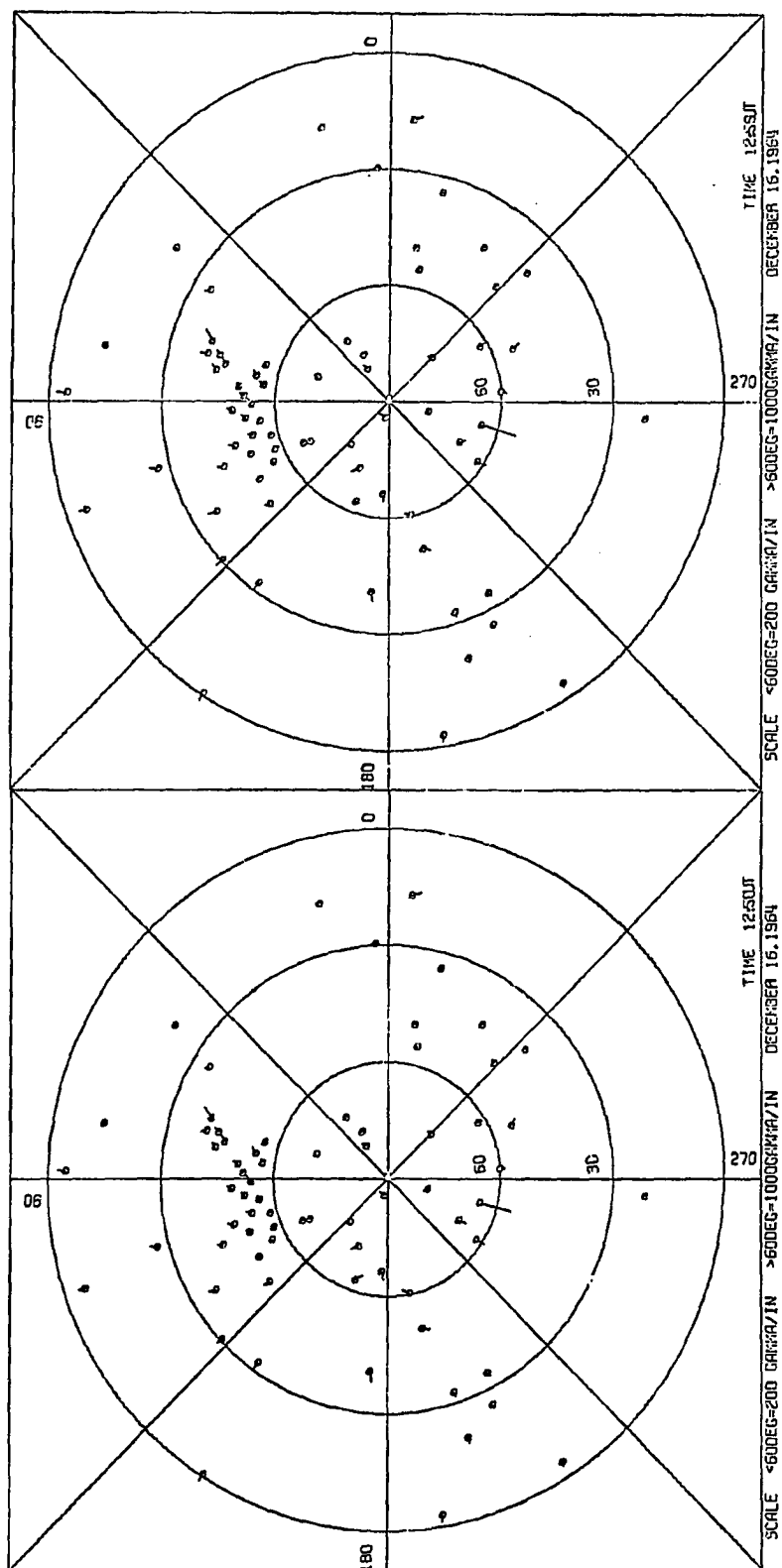


Fig. IV-20f

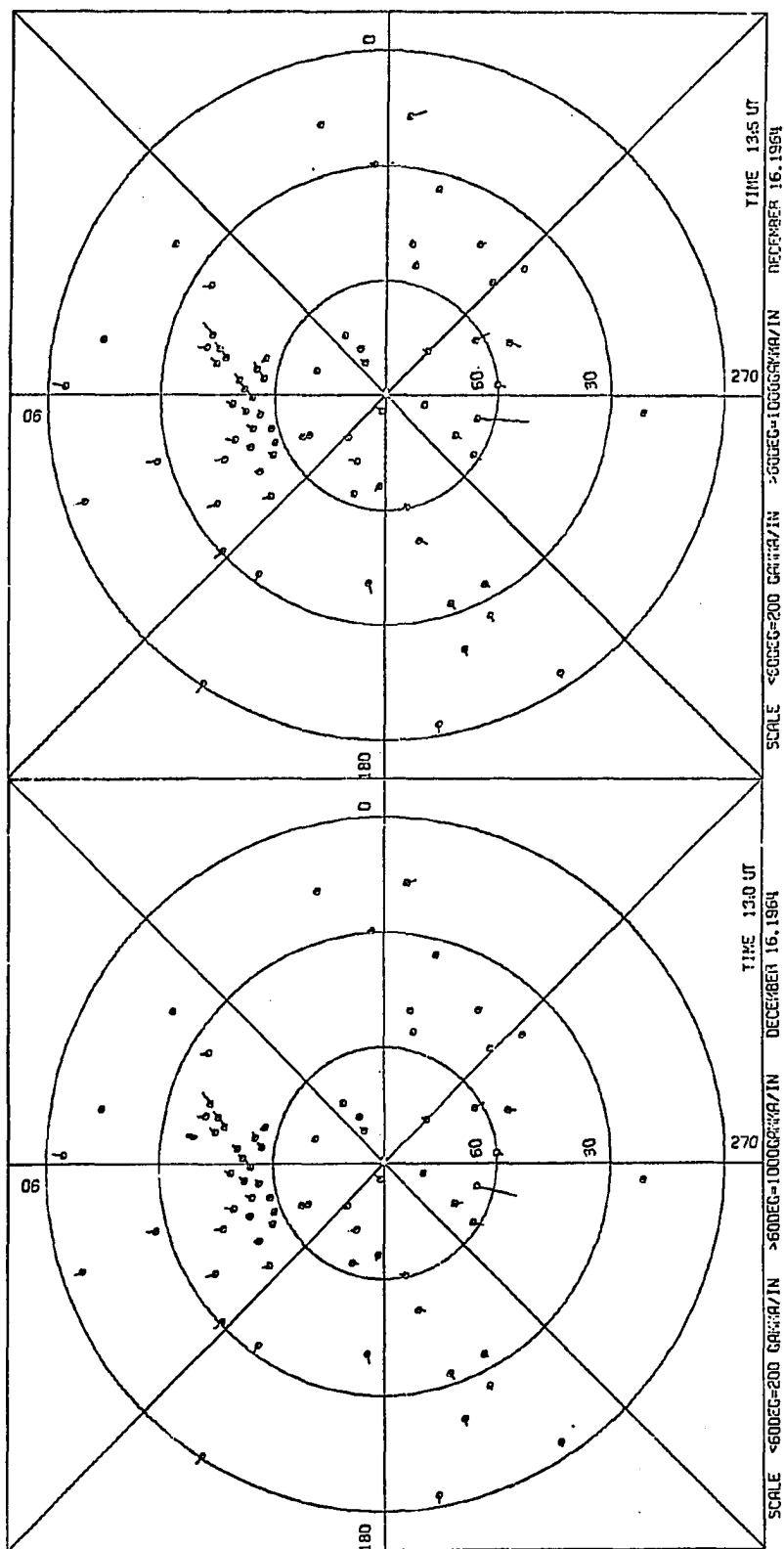


Fig. IV-20g

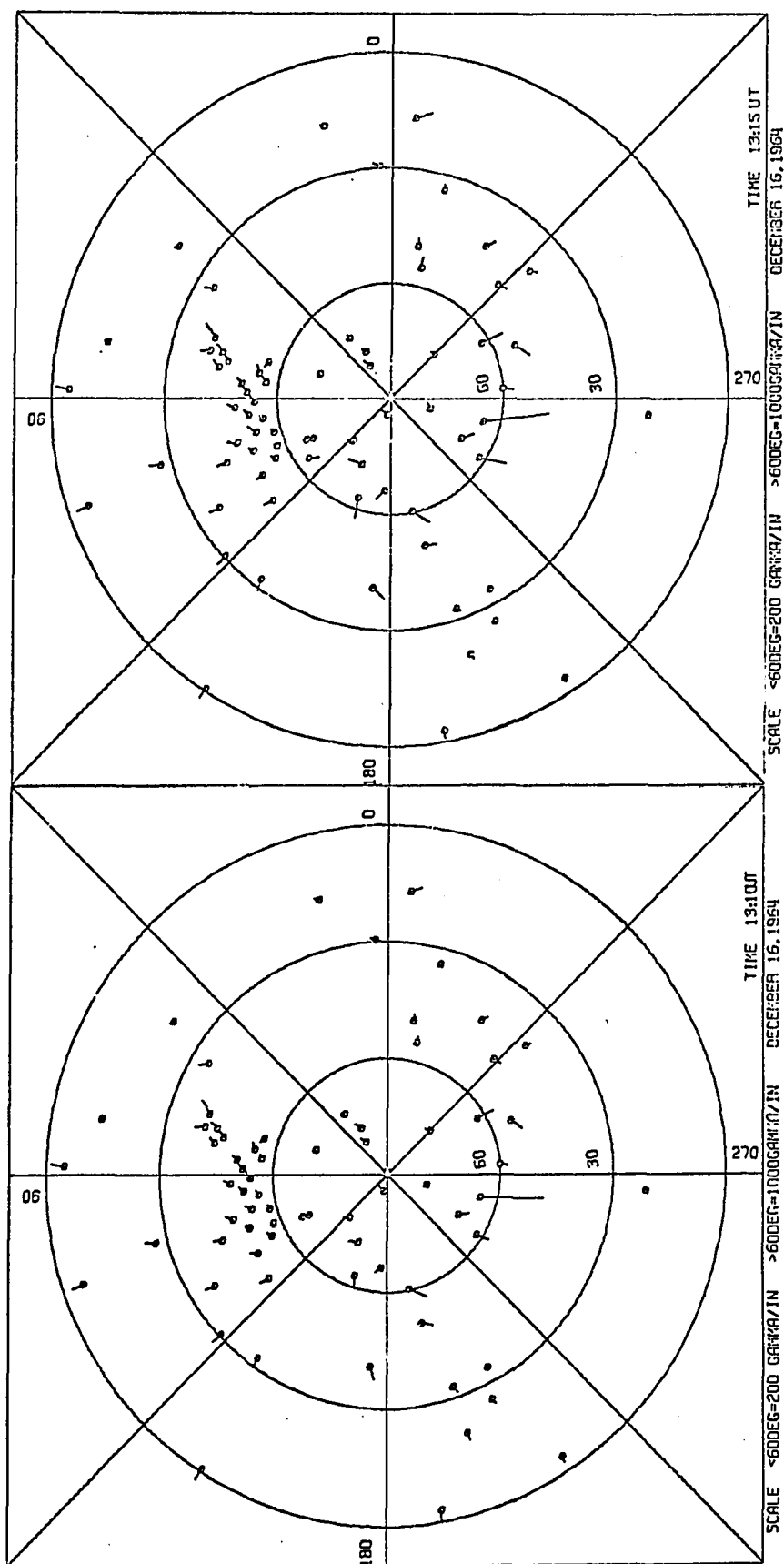


Fig. IV-20h

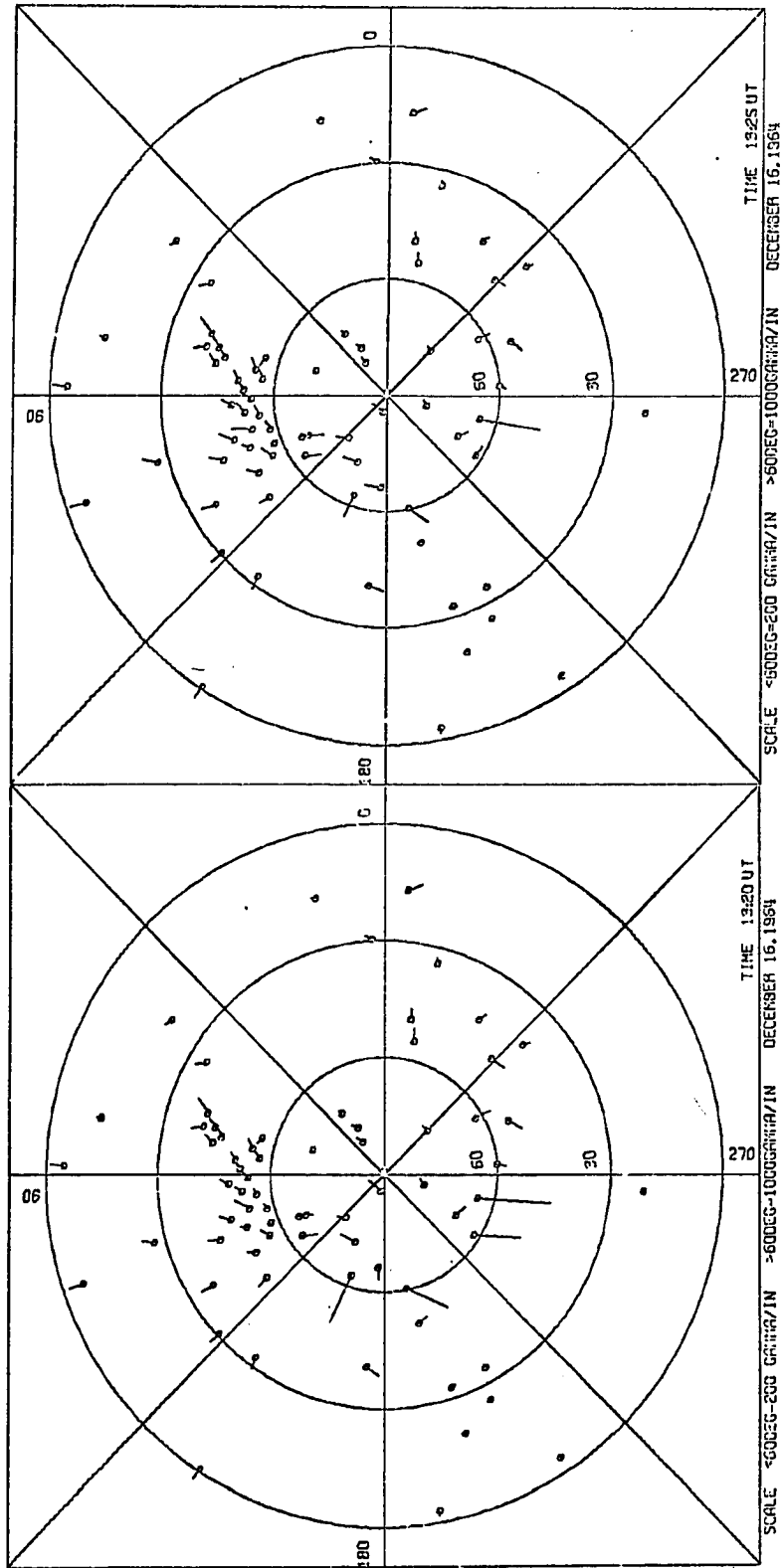


Fig. IV-201

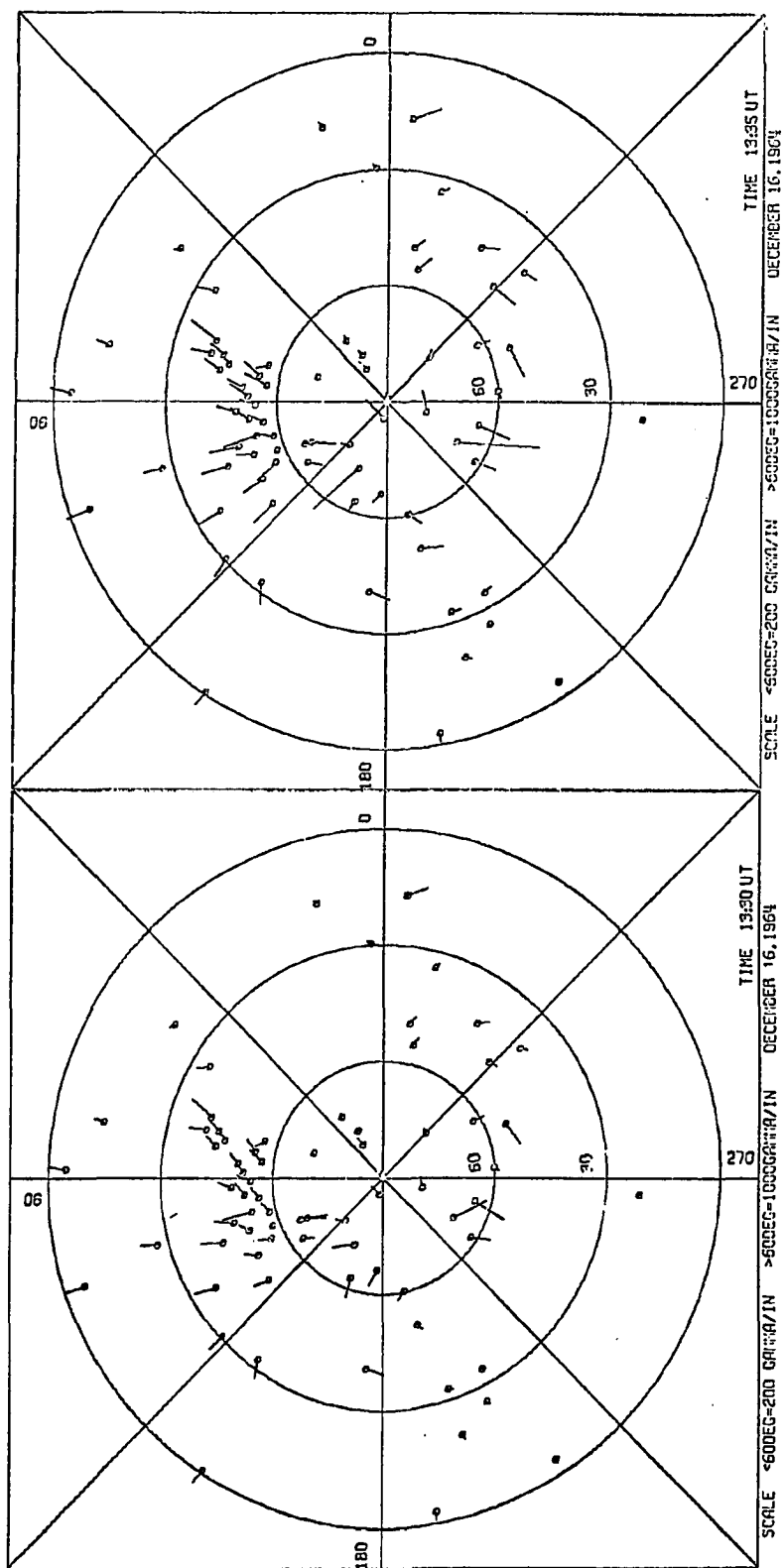


Fig. IV-20j



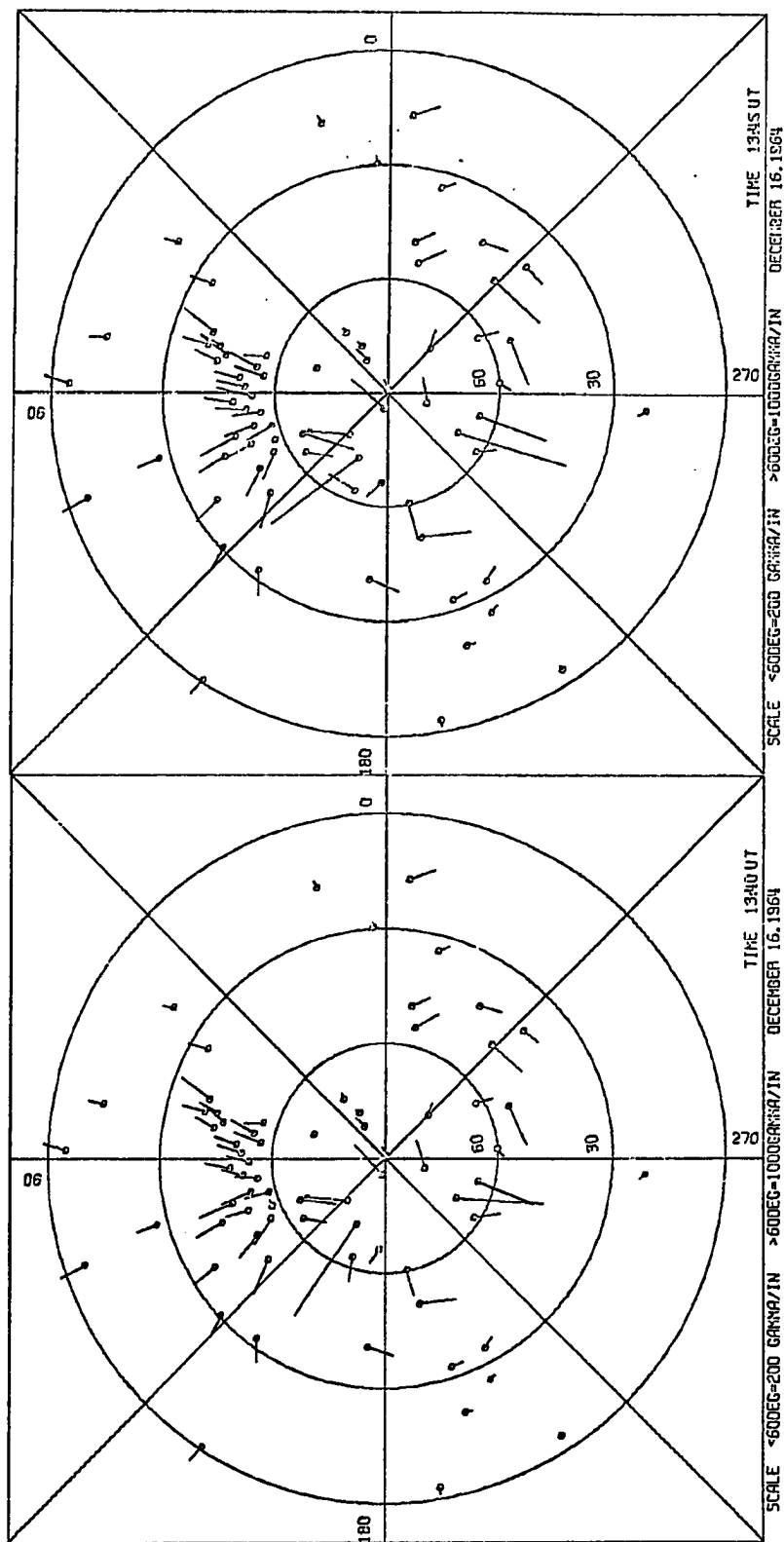


Fig. IV-20k

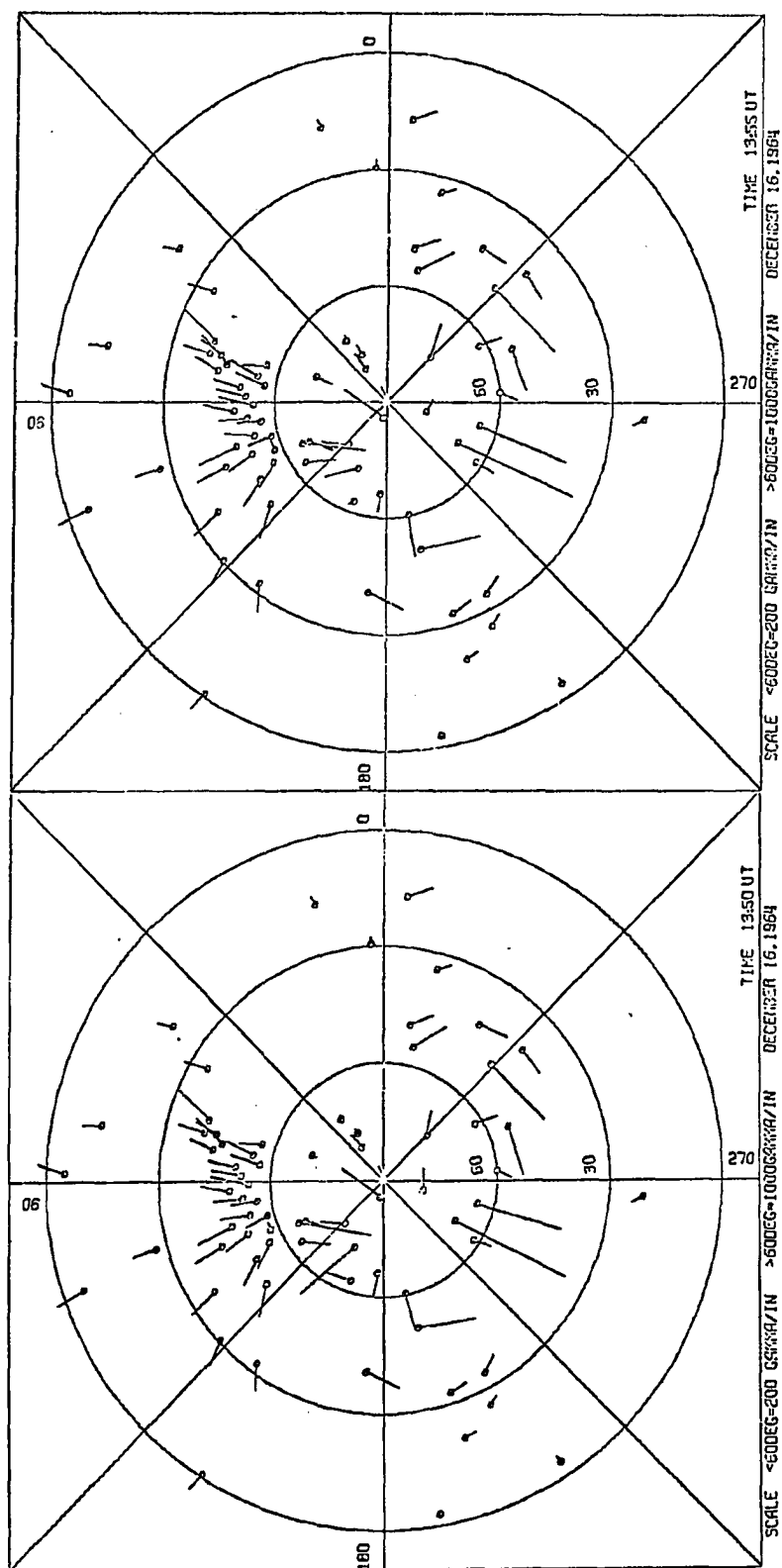


Fig. IV-202

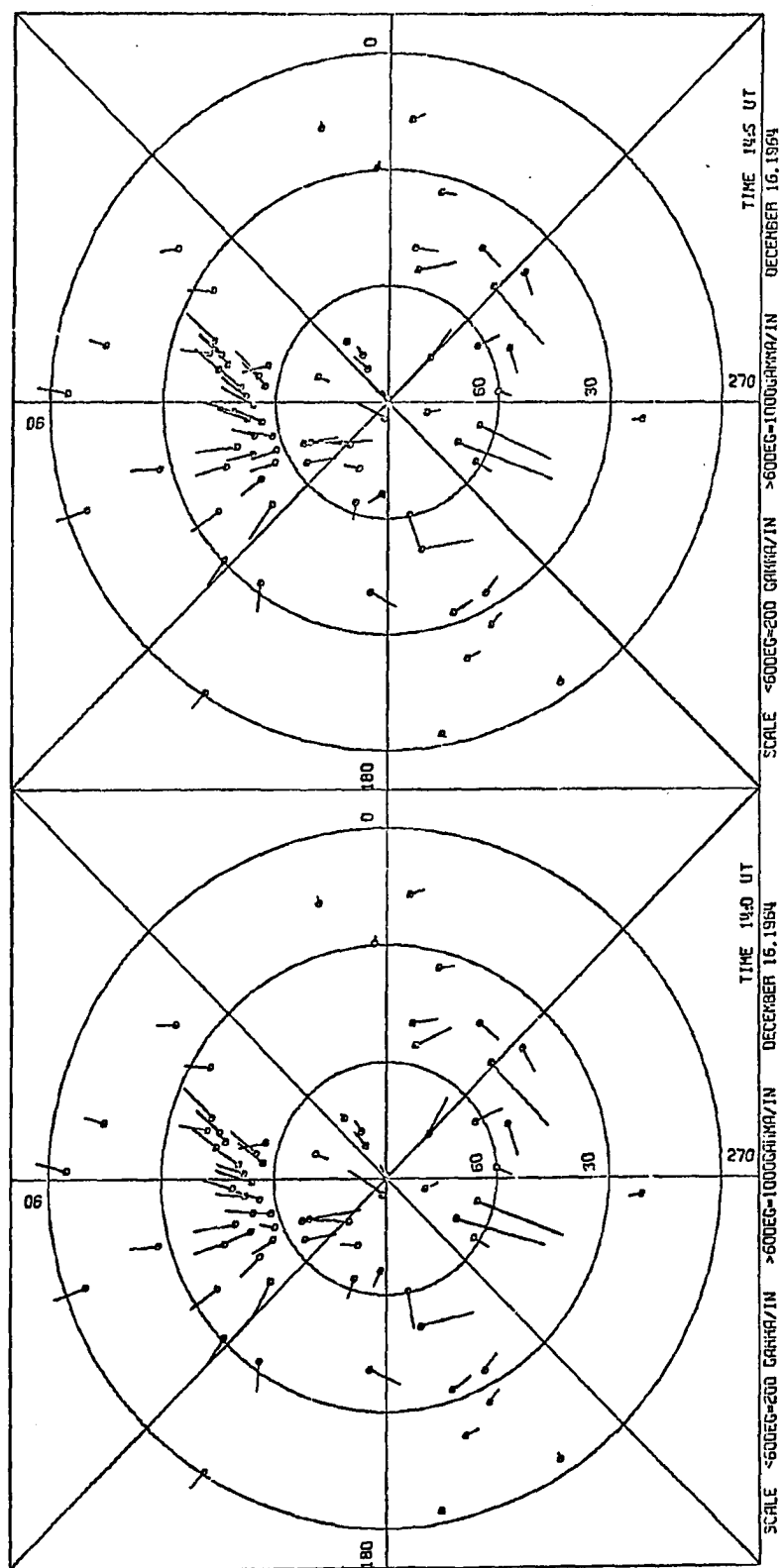


Fig. IV-20m

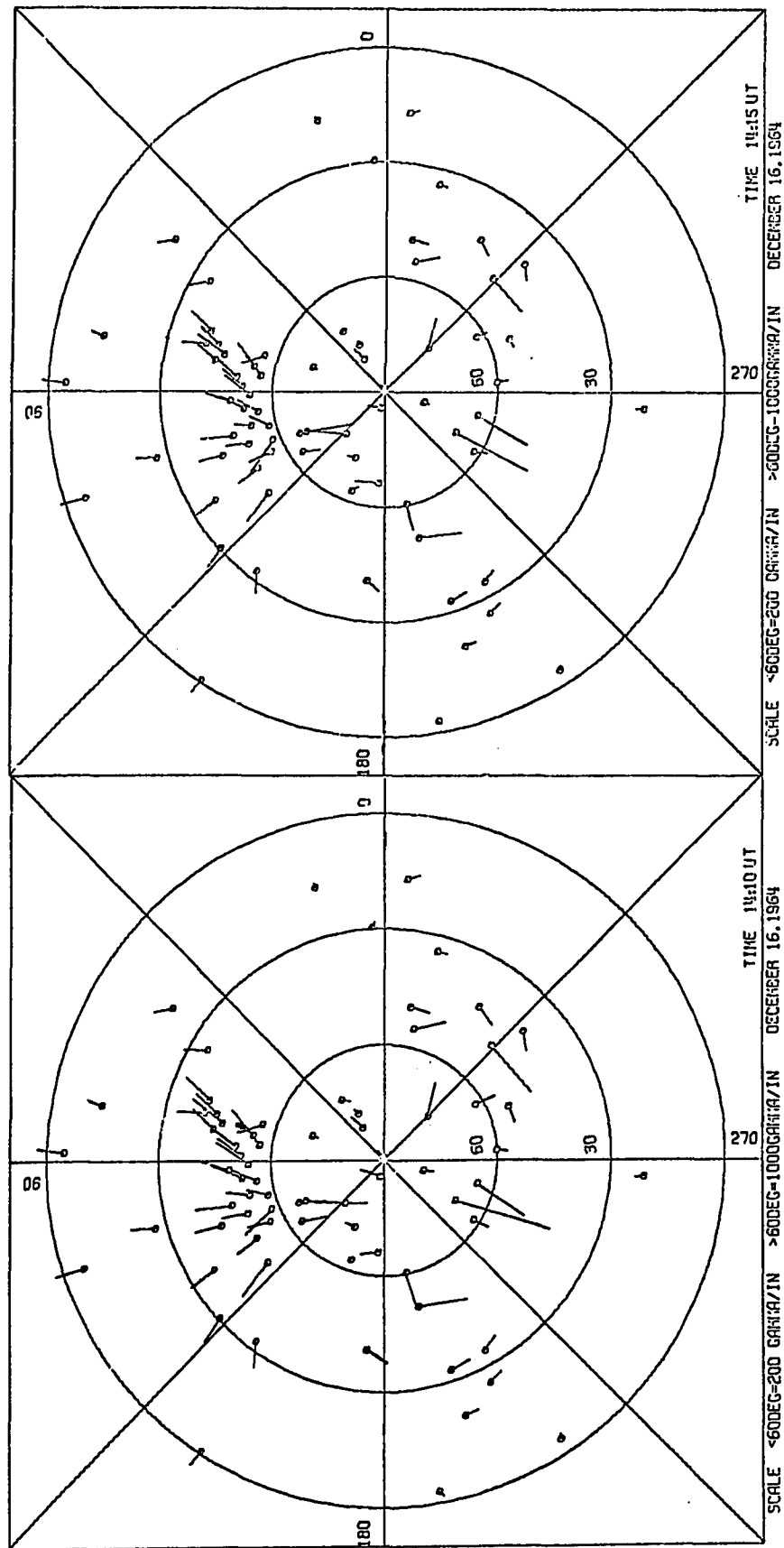


Fig. IV-20n

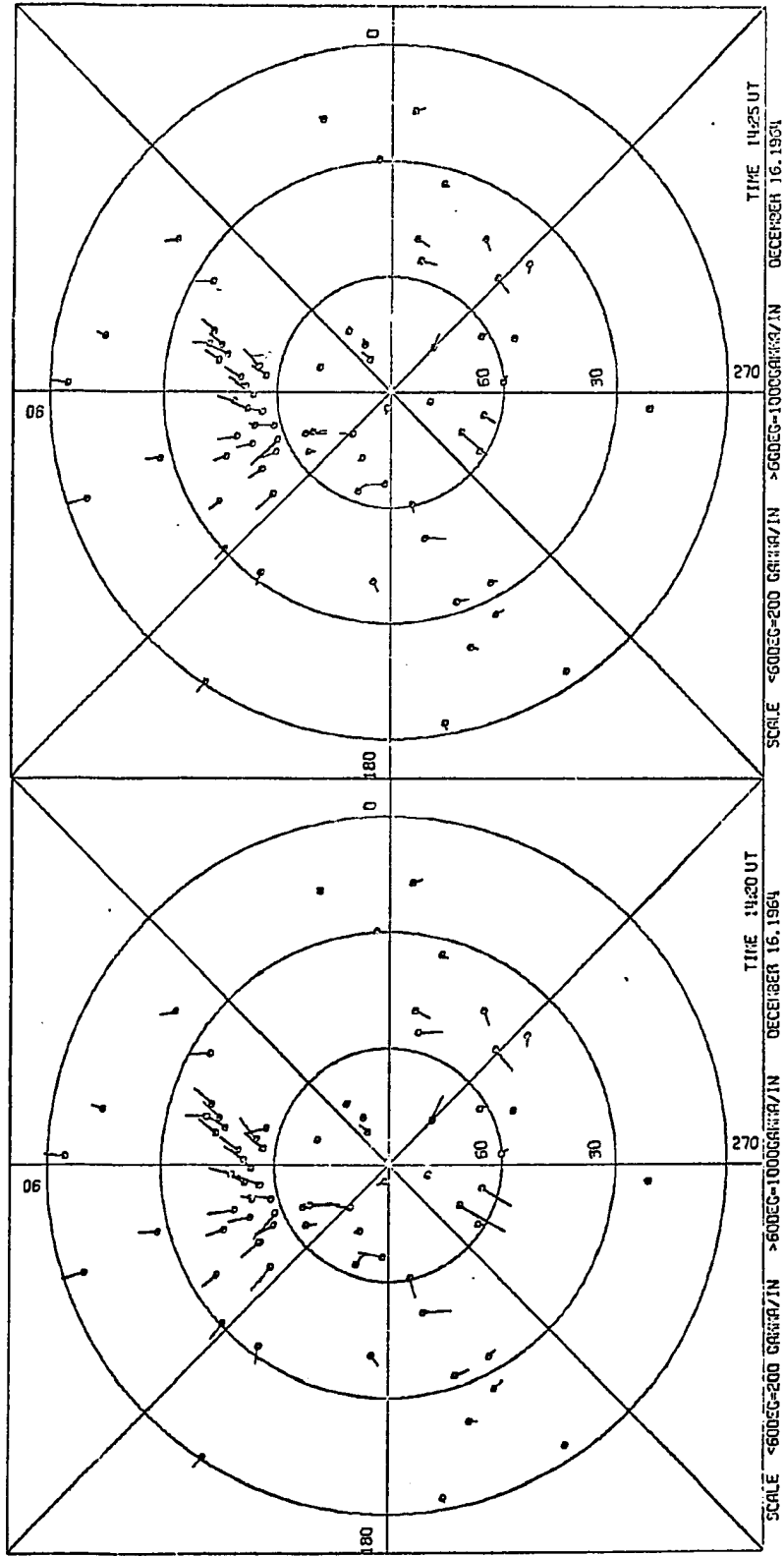


Fig. IV-20c

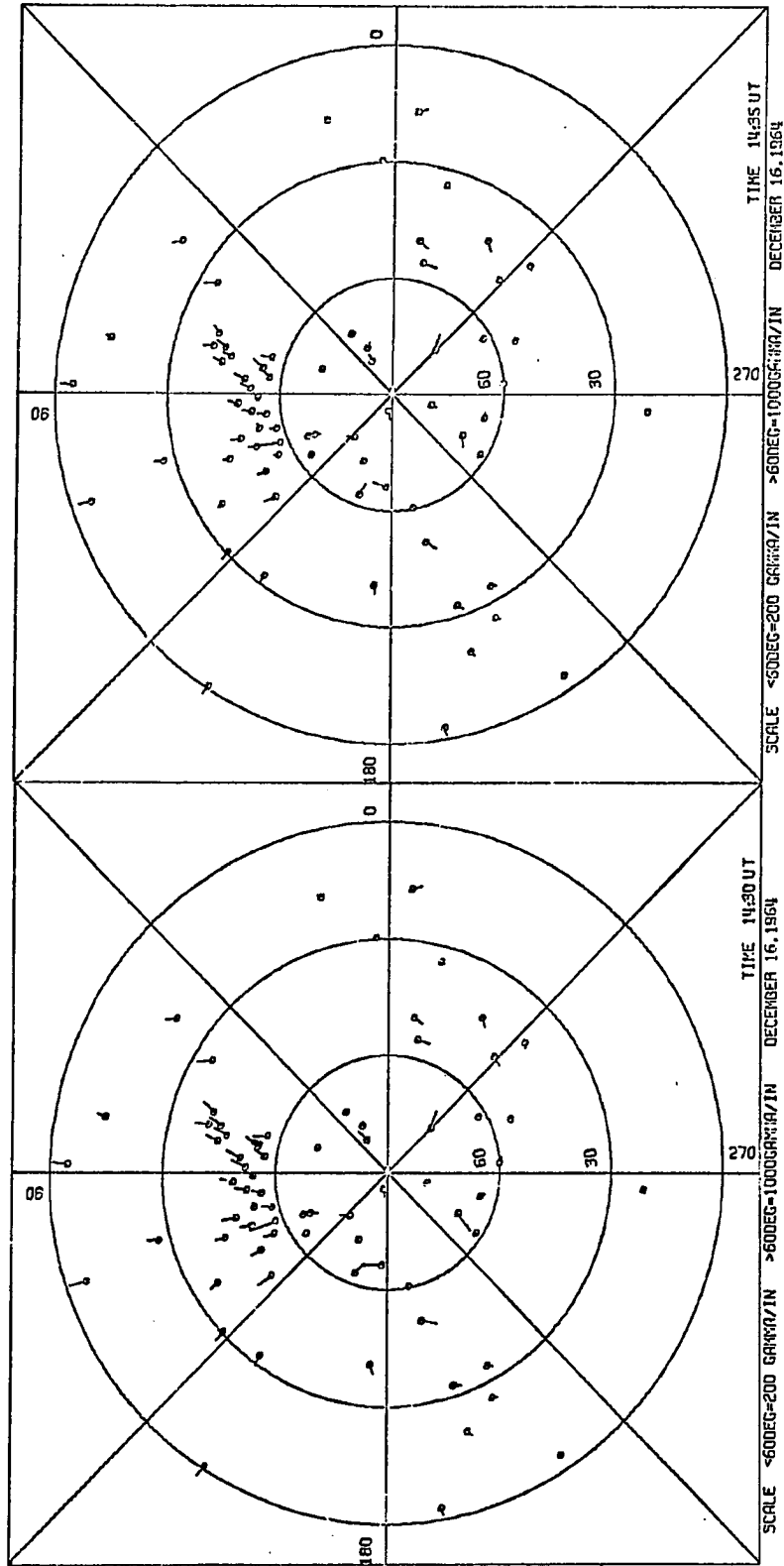


Fig. IV-20p

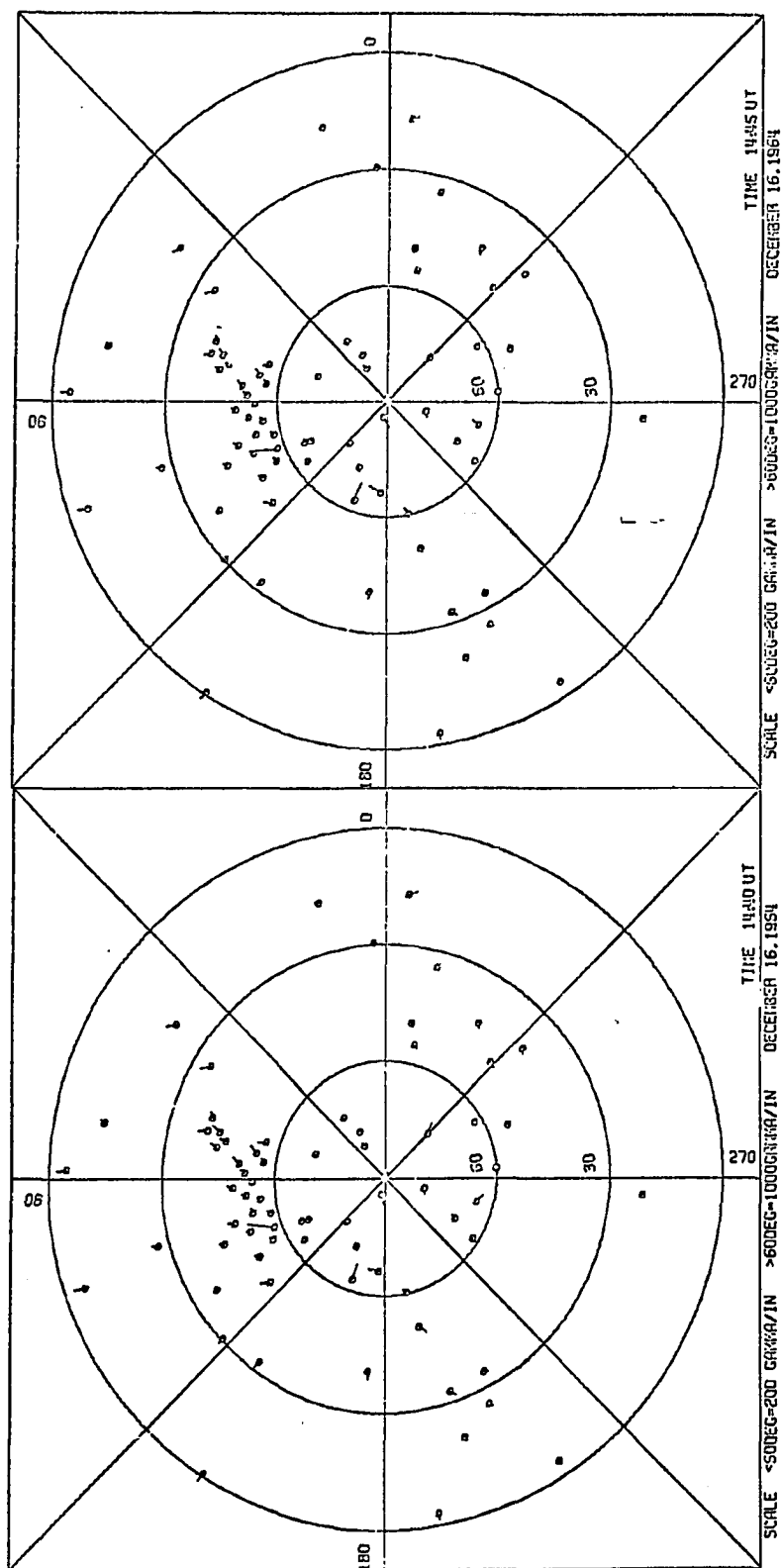


Fig. IV-20g

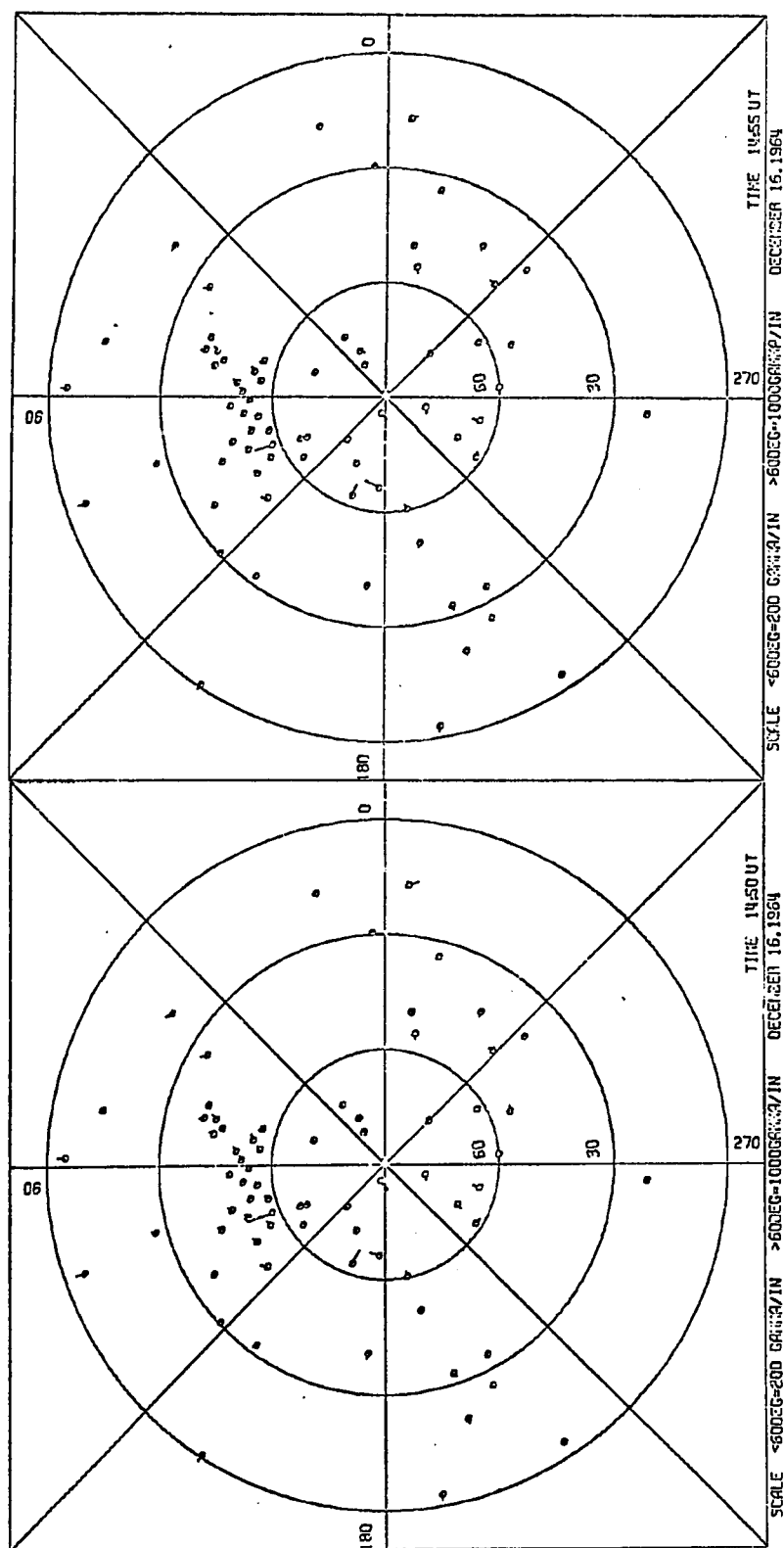


Fig. IV-20r



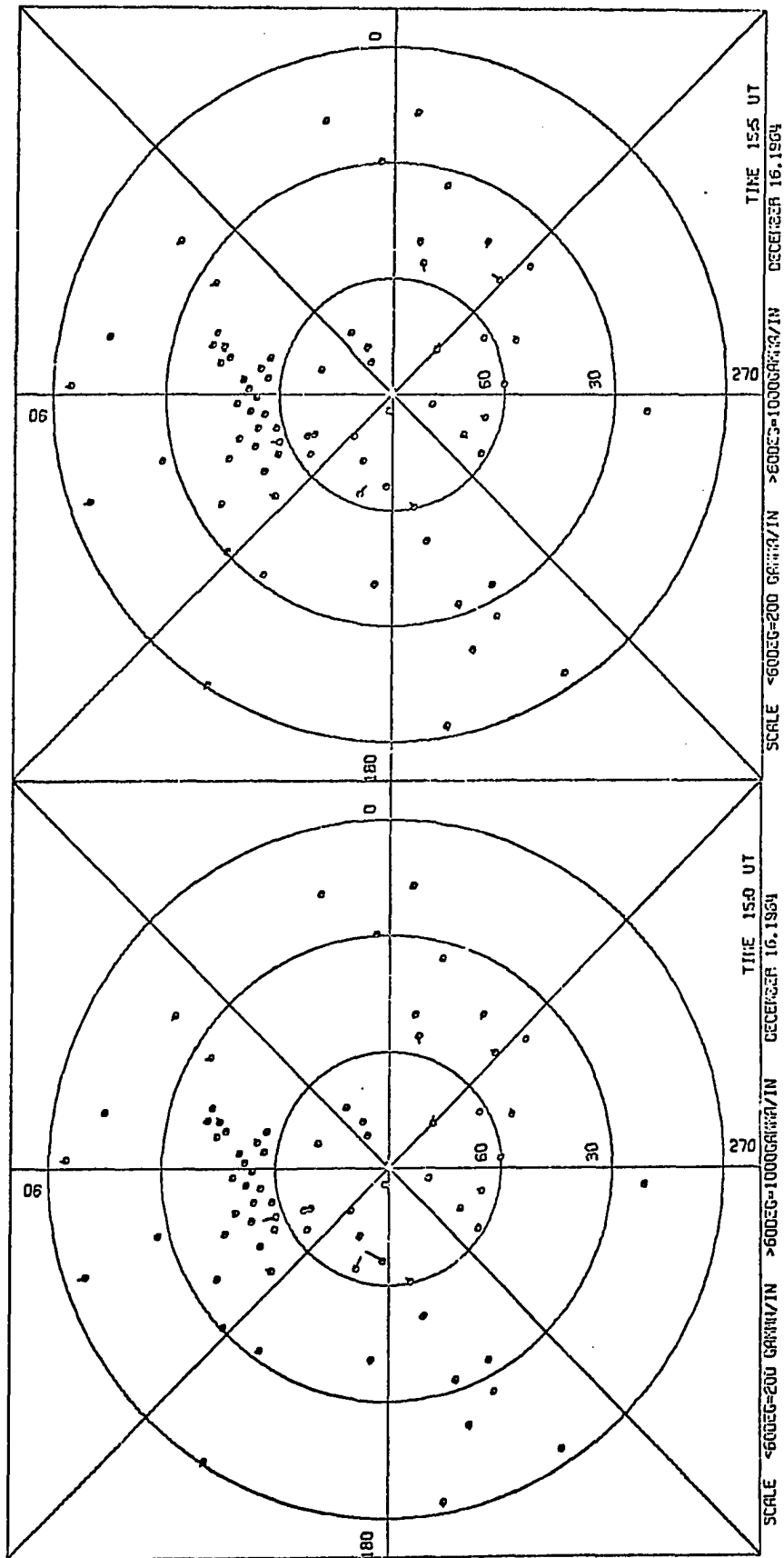


Fig. IV-20s

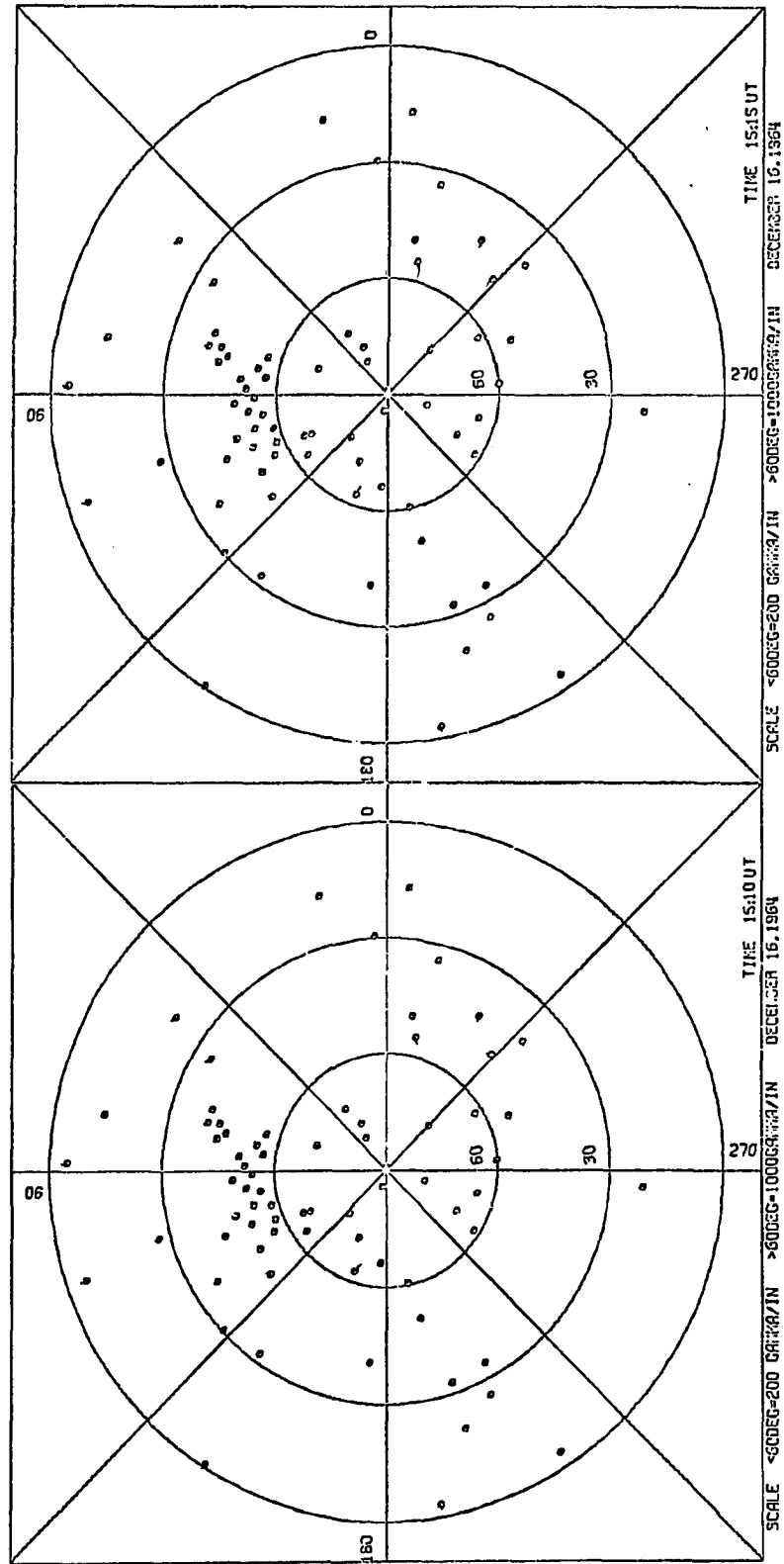


Fig. IV-20t

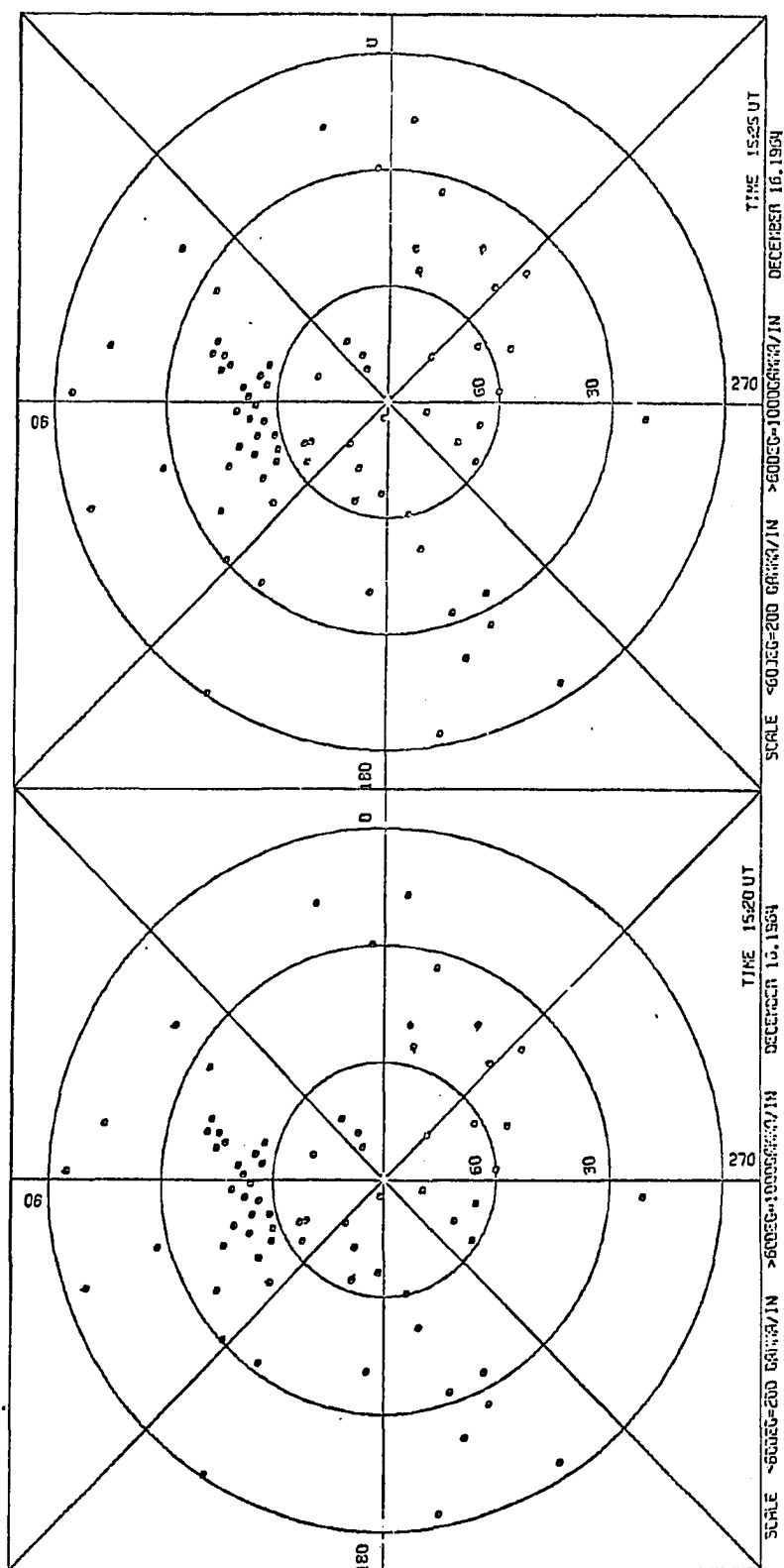


Fig. IV-20u

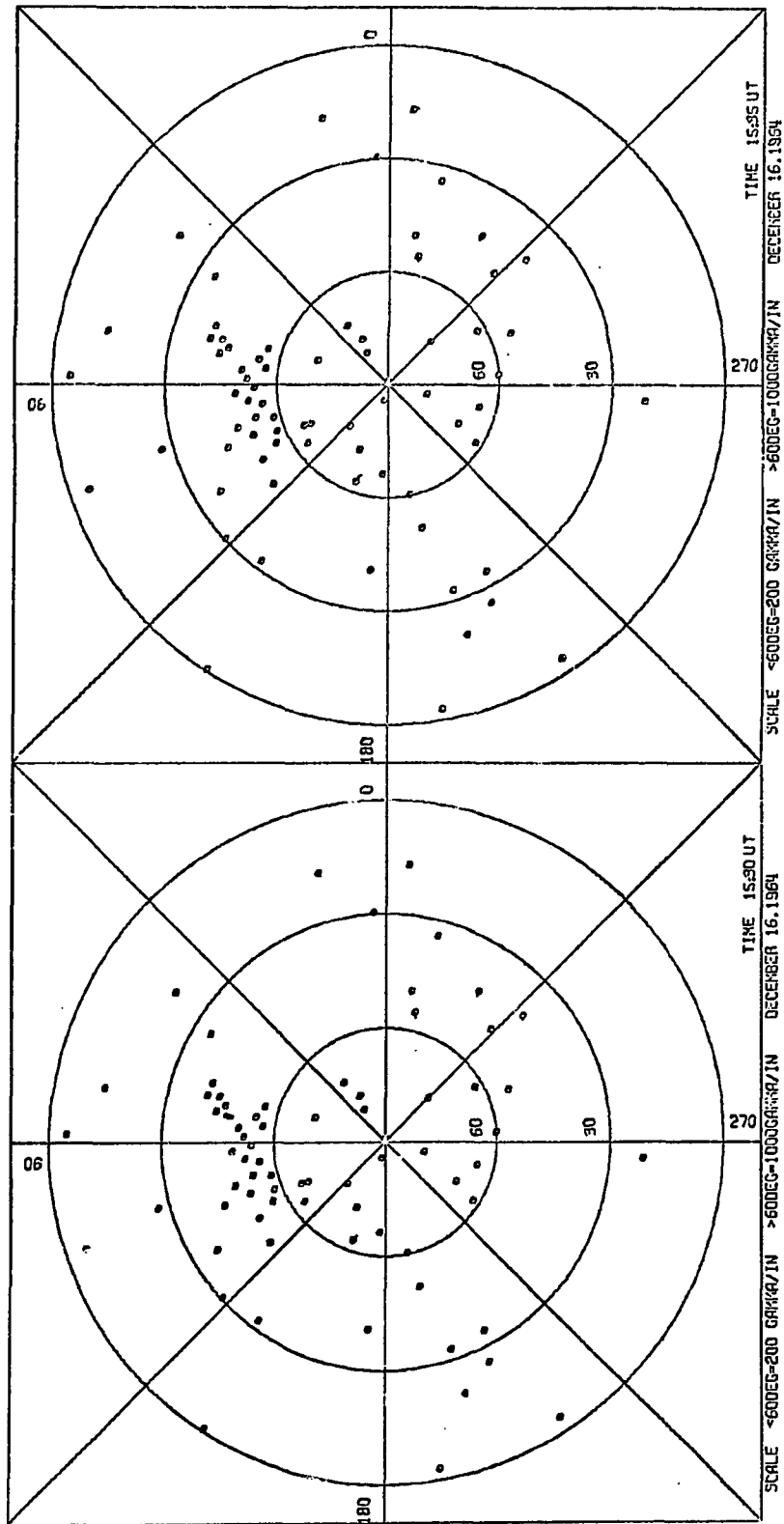


Fig. IV-20v

intense, and at lower latitudes especially in the afternoon meridian, also gradually increased in intensity. The main activity started at about 1335 UT when very intense negative bays of more than 1000  $\gamma$  were recorded at Barrow (station No. 8) and Heiss Island (station No. 24); the magnitude of the disturbance vector in lower latitudes was also suddenly increased. The activity in both high and low latitudes subsided at about 1420 UT, and at 1505 UT almost no trace of disturbances were seen.

During the entire disturbed period, the direction of the magnetic disturbance vector at each station, particularly those in the middle and low latitudes, did not show any drastic change. Below  $60^\circ$  latitude there was a very systematic distribution of the direction of the disturbance vectors. In the noon and afternoon sectors, all magnetic disturbance vectors were directed equatorward. In the evening sector, the direction of disturbance vectors gradually changed from equatorward to eastward from early evening meridian to late evening meridian. In the morning sector, the direction of disturbance vectors gradually changed from equatorward, near the noon meridian, to westward, near the midnight meridian. The distribution of the disturbance vectors higher than  $60^\circ$  is rather complicated, but agrees in general with that of the revised polar electrojet.

It is quite clear from the examples shown in this chapter that the relationship between the auroral zone positive bay and the low latitude negative bay is rather simple only when AP bays are weak, but becomes obscure and more complex for intense bays.

It is shown that most of the complexity of middle and low latitude changes associated with AP bays can be reasonably explained by a combination of two fields, the field of the eastward current over a wide range

of latitude (at least from the center line of the auroral zone to the equator) and the field of the storm-time radiation belt which appears to develop at about the same time. This complexity is caused by the combination of these two fields with different relative intensities.

A further complexity involved in this phenomenon is due to the fact that the field (DR) of the storm-time belt is a function of longitude and is thus quite asymmetric with respect to the dipole axis; it is most intense in the evening sector (Akasofu and Chapman, 1964). This was recently confirmed by satellite observations (Cahill, 1966). This, together with the fact that the eastward current is most intense in the evening sector along the auroral zone, can easily mislead one to suppose that there is a pair of bays (LP and LN) caused by the return current from a pair of electrojets.

The present study shows that the major part of LN bays in low latitudes is not caused by the return current from the polar electrojet and that the eastward current causing AP bays spreads to the equator. It also shows a close relationship between the storm-time radiation belt and the polar electrojet and thus also the auroral substorm; this relationship was originally suggested by Akasofu and Chapman (1961) for intense geomagnetic storms. It appears, however, that such a close relationship exists even for the growth of individual polar electrojets. We have realized that the auroral substorm and the polar magnetic substorm are only different manifestations of the same phenomenon which takes place deep in the magnetosphere (cf. Akasofu, 1966). The present study also strongly suggests that the formation of the storm-time radiation belt is another aspect of the same phenomenon.

It has recently been demonstrated by Cummings and Coleman (1967) that magnetic variations at Honolulu and at the geocentric distance of 6.6 earth radii (ATS-1) in the same sector are strikingly similar. The 'negative bays' at Honolulu are associated with very similar negative changes at 6.6 radii. We believe that this is direct proof of our conclusion in this chapter, since it is most likely that the ATS-1 satellite recorded effects of the ring current at that distance, and since the hypothetical westward return current cannot give rise to such a change there. Frank (1967) has also shown that protons of energy of order  $1 \sim 10$  kev appear in the evening sector of the trapping region.

## CHAPTER V

### AURORAL ACTIVITY OVER THE POLAR CAP ASSOCIATED WITH MAGNETIC DISTURBANCES

Auroras in very high latitudes can be classified into two types, namely the oval auroras and the polar cap auroras. The former appears within the narrow oval band called the auroral oval (see Chapter III, section 2). The latter appears during the magnetically quiet conditions within the oval and their alignment is approximately parallel to the sun-earth line. (Mawson, 1925 p. 181, Davis, 1960, 1962; Denholm, 1962). Because of the eccentricity of the auroral oval, stations between about  $\text{dp lat } 68^\circ$  and  $\text{dp lat } 76^\circ$  will be under the auroral oval for a portion of each day, while stations poleward of about  $\text{dp lat } 76^\circ$  will not be under the oval throughout the day.

#### 1. Daytime Auroras

Auroras which occupy the dayside of the auroral oval are called the daytime auroras; the term "dayside" refers to the period between 06 AM and 06 PM dipole (geomagnetic) local time.

In the northern hemisphere, both Pyramida and the Ice Floe T-3 were suitably located to study midday auroras; these are located geographically high enough (so that the 24 hour darkness is secured), but geomagnetically low enough (so that the midday part of the oval can be seen). In Figure V-1, photographs of daytime auroras (in negative) taken from Pyramida are shown; the upper three were taken at about magnetic midday (09 UT) and the lower three were taken at about local midday (11 UT). The daytime auroras are mostly rayed arcs; Feldstein (1966) suggested that they are isolated rays



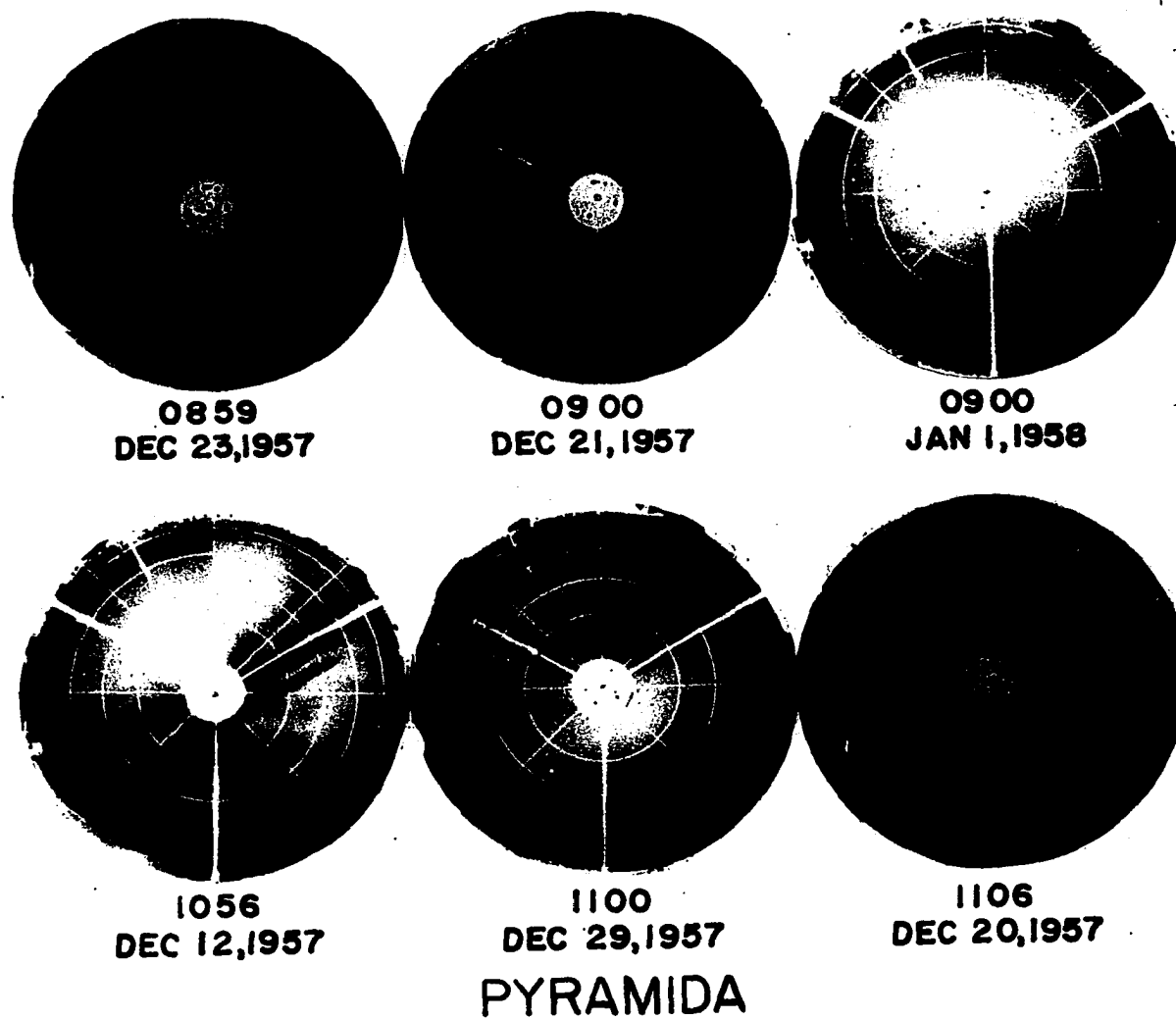


Fig. V-1. Example (in negative) of the midday auroras observed at Pyramida; the upper three photographs were taken at about the magnetic midday and the lower three at about the local midday.

(see in his Fig. 6). However, there were many days during the IGY when the orientation of the rayed arcs could be definitely measured (see below and also Fig. V-3). Therefore, it seems to be more appropriate to treat them as rayed arcs.

In the upper three, an arc is seen in the northern sky of Pyramida on December 23, and about the zenith on December 21, and in the southern sky on January 1. The first one (December 23, 1957) corresponds to a quiet condition ( $K_p = 1_+ 1_+ 1_0 1_+ \quad 1_0 1_- 1_-$ ), the second to a moderately active condition ( $K_p = 3_- 5_- 4_0 2_+ \quad 2_0 2_0 2_0 2_0$ ) and the third to a very disturbed condition ( $K_p = 6_0 6_+ 5_+ 4_0 \quad 3_+ 4_- 5_+ 4_0$ ). The Dst curves (Sugiura, 1963) during the above three periods are shown in Figure V-2. It can be seen clearly that the location of the aurora shifts toward lower latitudes as magnetic activity increases. This suggests an expansion of the oval in the day sector (Feldstein, 1966; Zumuda et al, 1966). Akasofu and Chapman (1964) showed that the expansion of the oval in the nightside depends on the intensity of the storm-time radiation belt. Although we do not have enough data to confirm this point for the dayside of the oval, Figure V-2 suggests the same tendency. In the lower three, the second one (December 29, 1957) was a quiet day and the first and third days were moderately active days ( $K_p = 4_+ 4_+ 4_0 5_- \quad 3_+ 4_0 4_+ 4_0$ ) and ( $K_p = 4_- 5_- 3_0 3_0 \quad 3_0 3_- 3_+ 4_-$ ), respectively.

Stringer (1966) showed that the daytime aurora also appeared over the T-3 station (practically every possible day), with a very high occurrence frequency higher even than that of the midnight aurora during the quietest period of the IQSY.

The midday aurora tends to align along the east-west direction. Figure V-3 shows the orientation measured for all the available data obtained

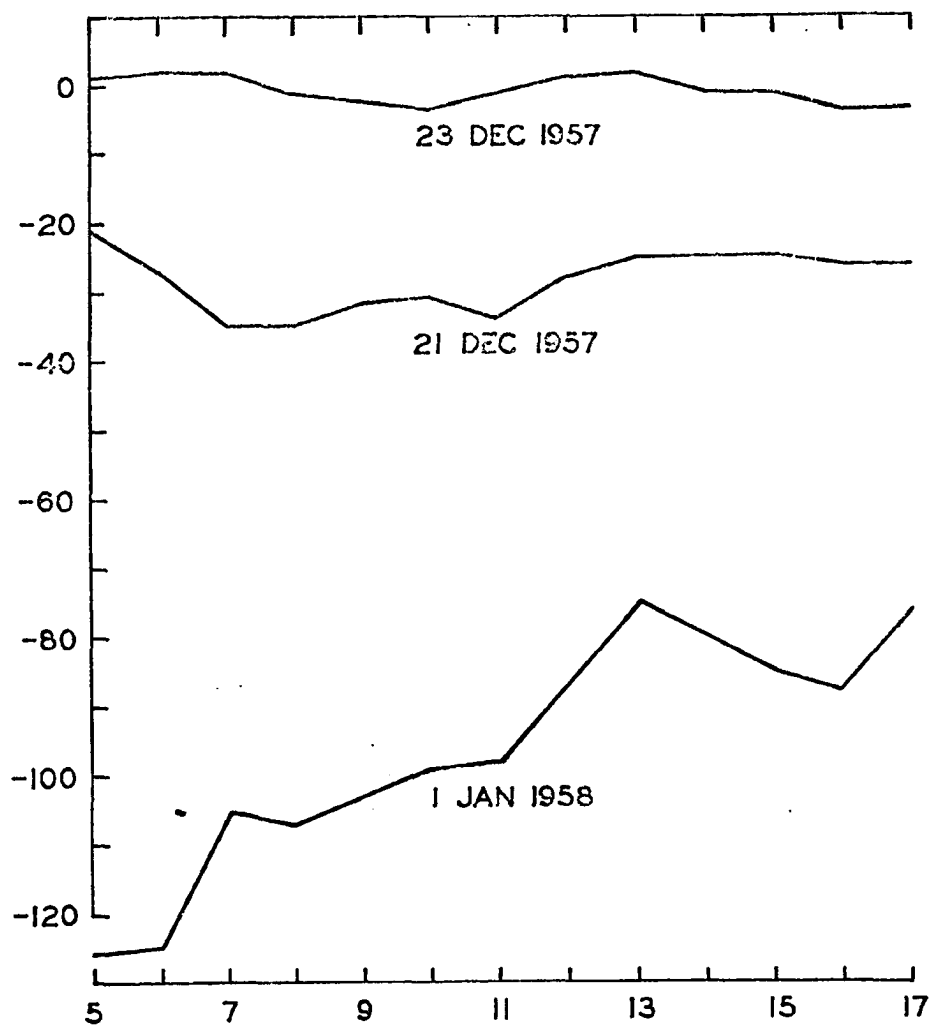


Fig. V-2. The Dst curves for three days in Figure V-1.

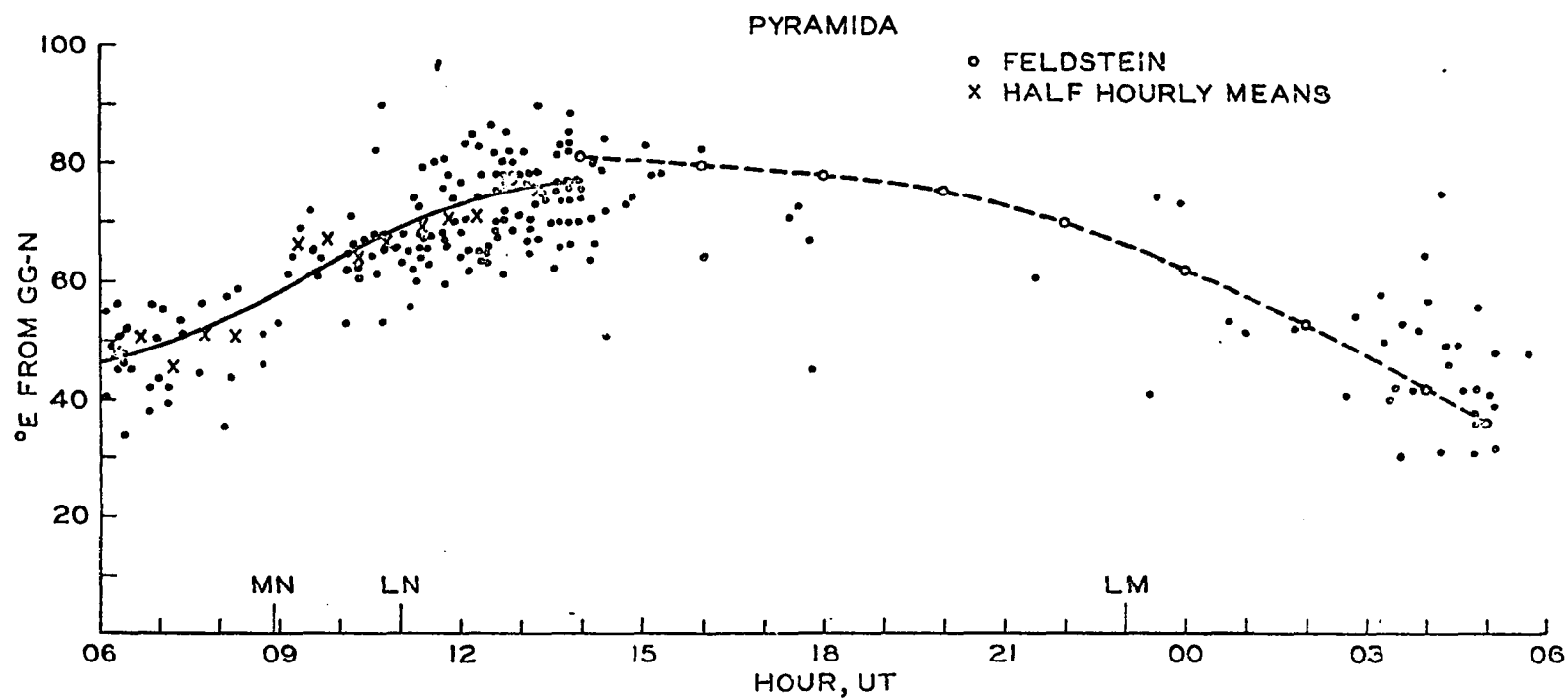


Fig. V-3. The orientation of auroral arcs observed at Pyramida; MN, LN, LM refer to the magnetic noon, the local noon and midnight, respectively.

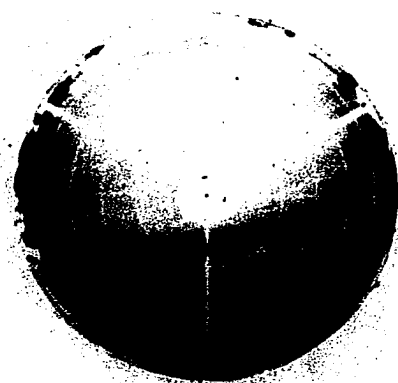
during the IGY at Pyramida. Stringer (1966) showed the same tendency by using records taken from the T-3 station. The aurora may be single or multiple (Fig. V-4).

The midday aurora appears to show a slow poleward motion. For example, observing it at Pyramida, an arc seems to develop often in the middle southern sky and then moves slowly toward the zenith. However, the first fact could well be due to the aspect sensitivity of midday auroras; that is, they become visible only when their zenith angle becomes less than a certain critical value.

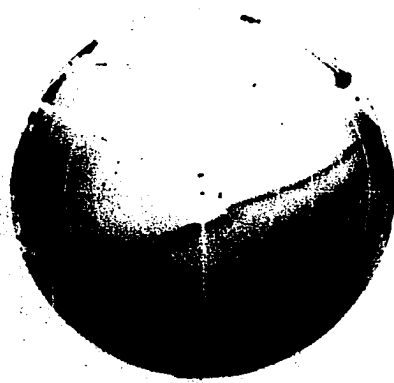
During high geomagnetic activity, a violent eastward motion of the auroras occurs in the midday sector of the oval. Since the eastward motion is the most common feature of the aurora during the auroral substorm in the morning sector of the auroral oval, it is natural to infer that the eastward motion of the daytime auroras is an extension from the early morning sector. This suggests that midday auroras are affected by the auroral substorm activity which originates in the midnight sector of the oval.

## 2. Polar Cap Auroras

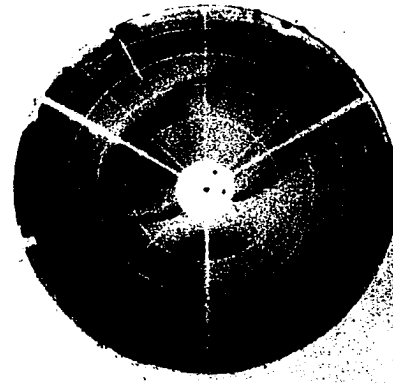
The occurrence of sun-aligned arcs in the auroral cap for nine consecutive days is shown in Figure V-5, permitting a somewhat more detailed demonstration of the tendency of these auroras to occur during magnetically quiet times than was provided by the study of Davis (1963), where the occurrence of aurora in the polar cap was correlated with the 3 hour  $K_p$  index. In particular, Figure V-5 shows that sun-aligned arcs, symbolized by solid bars and triangles, sometimes occur during intervals of several hours between polar magnetic substorms. Also, the tendency of the sun-aligned



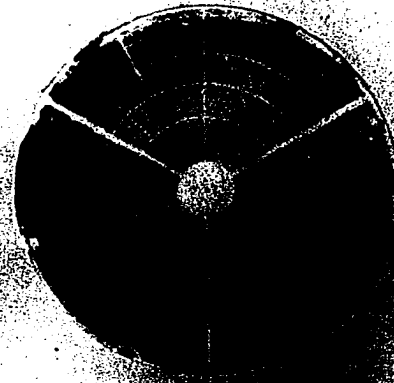
**1159**  
**Dec 20**



**1257**  
**Dec 20**



**1310**  
**Nov 30**



**1100**  
**Dec 12**

### **PYRAMIDA**

**Fig. V-4. Examples (in negative) of the midday auroras; except the first one (Dec 20, 1959), they are multiple.**

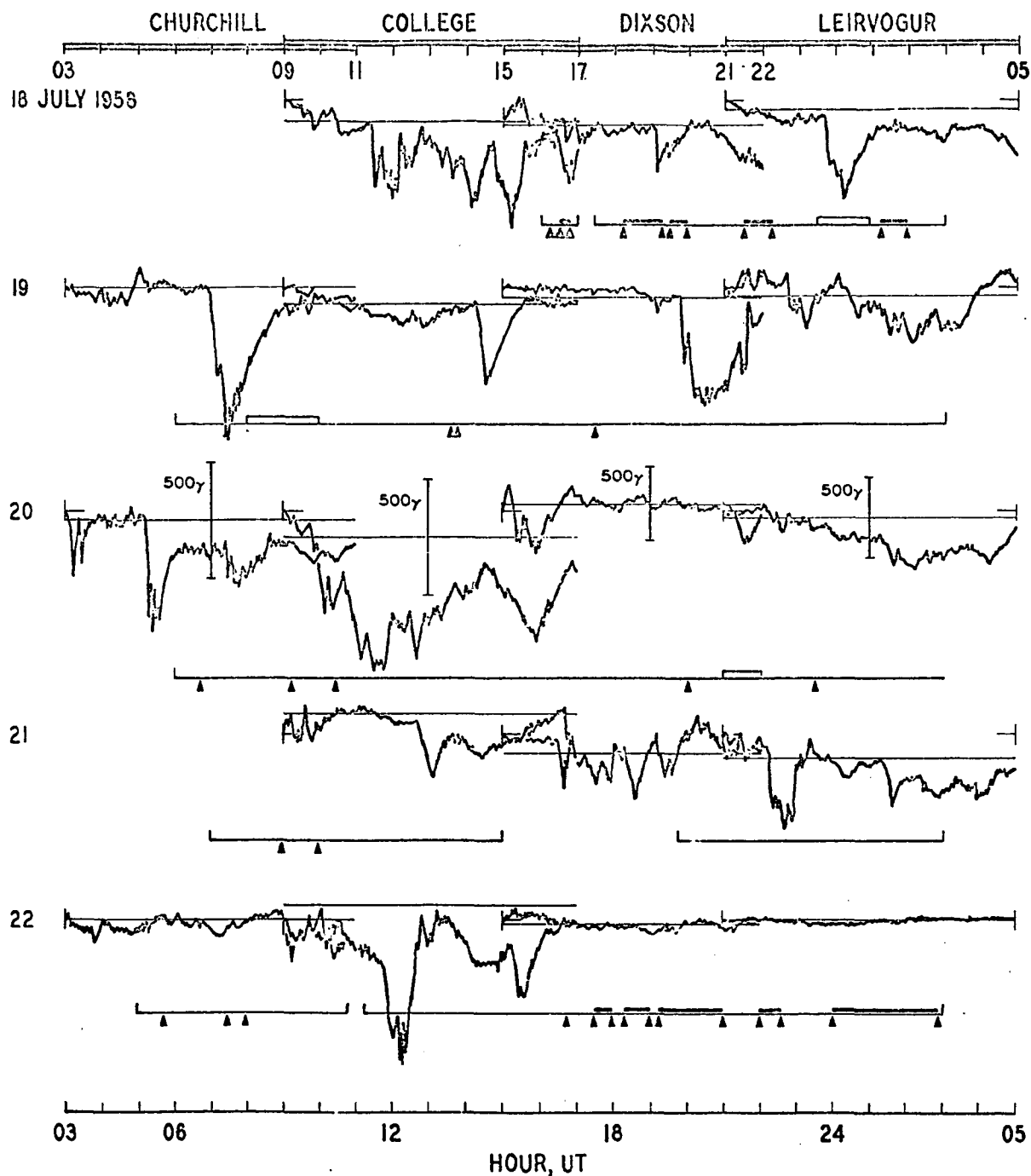


Fig. V-5. Magnetic records from the post midnight quadrant of the auroral zone for nine consecutive days. Times when the Vostok all-sky camera was operating are marked by a line below the magnetograms. The occurrence of sun-aligned arcs (S.A.) is marked by solid bars and triangles, and of substorm associated auroras (S.S.), by open bars.

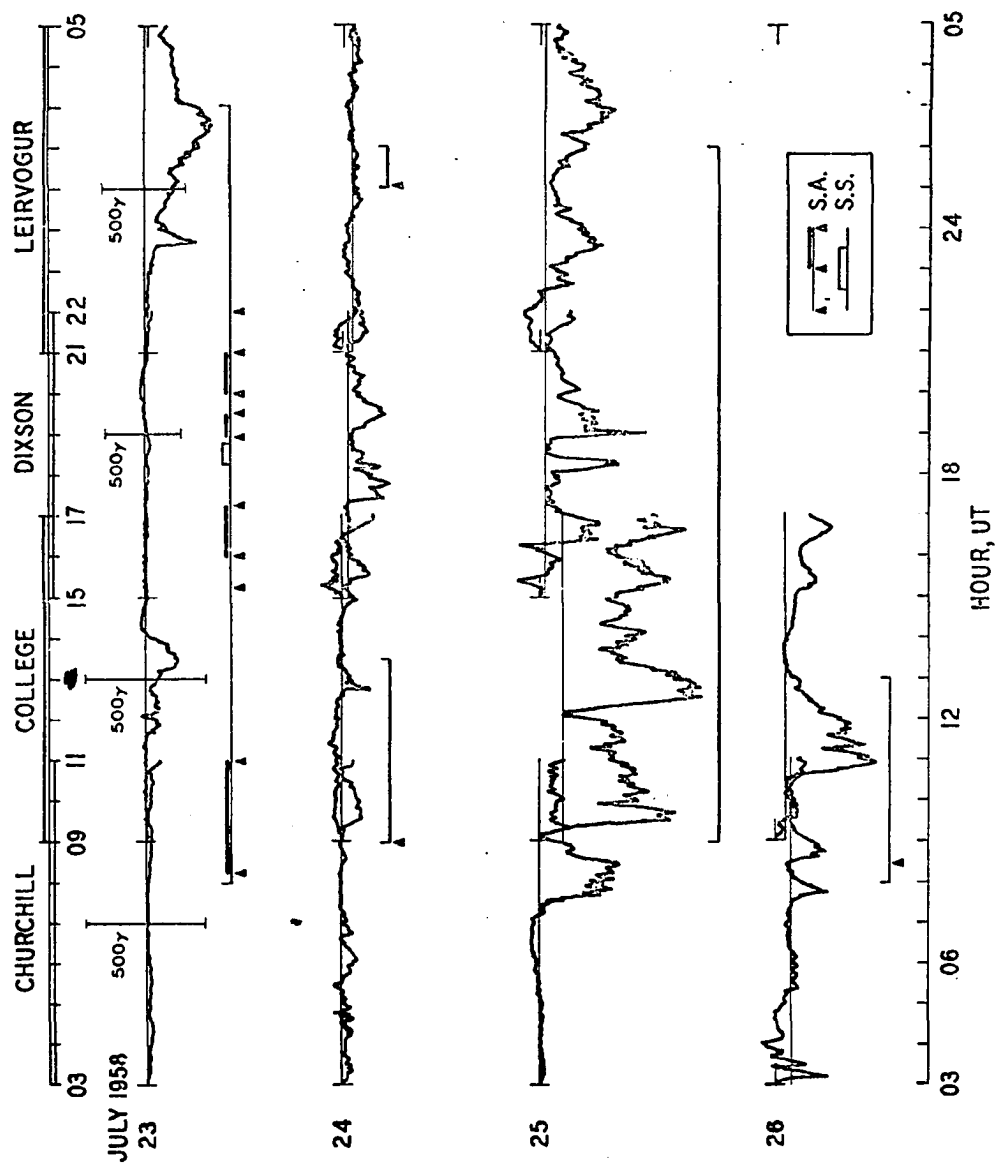


Fig. V-5. (Continuation.)



aurora to avoid times when even weak magnetic substorms are occurring is well demonstrated during the period July 22 and 23. During this interval nearly continuous all-sky camera records were taken at Vostok, and these indicate the almost continuous presence of sun-aligned arcs. However, during the period of moderately strong polar magnetic substorms from 0900 to 1700 UT on July 22 and of weak substorms from 1130 to 1430 UT on July 23, and following 2300 UT on July 23, there was a complete absence of sun-aligned auroras. This behavior is typical of the rather extensive sample examined in the course of this study, as might be expected in view of the results of Davis' (1963) statistical study.

A question of considerable interest is how the sun-aligned arcs in the polar cap are related to those of the auroral oval. We find several instances when both kinds of auroras occur simultaneously. However, when polar cap auroras were bright the oval auroras were faint, and vice versa. For this reason, it was not possible to determine their direct geometrical relationship. In particular, no answer can be given to the question regarding possible connections of the sun-aligned arcs to the auroral oval arcs in the night side; the answer to such questions awaits a more painstaking analysis and perhaps more sensitive observations of the aurora at the auroral oval.

### 3. Auroral Activity Near the Dipole Pole and Storm Sudden Commencement\*

#### 1) Sudden commencements followed by polar magnetic substorms

Feldstein (1960) reported the appearance of auroras over Vostok at the south geomagnetic pole following the sudden commencements of three successive geomagnetic storms which occurred in July 1959. The present study has disclosed a number of additional examples which permit elaboration upon

\*This work was done jointly with Dr. R. N. DeWitt.

this earlier work. In the three examples cited by Feldstein, as well as in one of the new examples presented here, (the sudden commencement storm of July 8, 1958) polar cap auroras took the form of bands of fragmentary forms showing pronounced drifts. There was no tendency for these auroras to align themselves along the sun-earth direction. In appearance the forms were not unlike those of the polar cap auroras observed in association with polar magnetic substorms that were discussed in Chapter III, section 2-2. Indeed, the feature of the concurrent magnetic activity which distinguishes these four events, which will be denoted as Group I (Fig. V-6), from the remaining examples is the abrupt occurrence of a strong polar magnetic substorm simultaneously with each of the sudden commencements. In three of the Group I examples, the growth of the polar magnetic substorm was quite sharp, and auroras appeared immediately. In the remaining example of Group I, that of July 15, 1959, the polar magnetic substorm grew more slowly, taking nearly an hour to reach a peak value exceeding 1000 gammas, as observed at Byrd Station in the Antarctic, so that the aurora in this instance did not appear until about thirty-seven minutes after the sudden commencement.

However, it is not entirely clear that the polar cap auroras observed in the above four examples can be considered to be simply cases of auroral substorms in which the poleward expansion reached the geomagnetic pole. In only one case, that of the slowly growing bay that occurred on July 15, 1959, could the auroral region be observed to move from the horizon nearest the midnight sector of the auroral oval. In two other examples, July 8, 1958, and July 17, 1959, auroras appeared in place overhead, while in the remaining case, that of July 11, 1959 (see Fig. V-7) the auroral forms moved overhead from the horizon nearest the midday sector of the auroral oval.

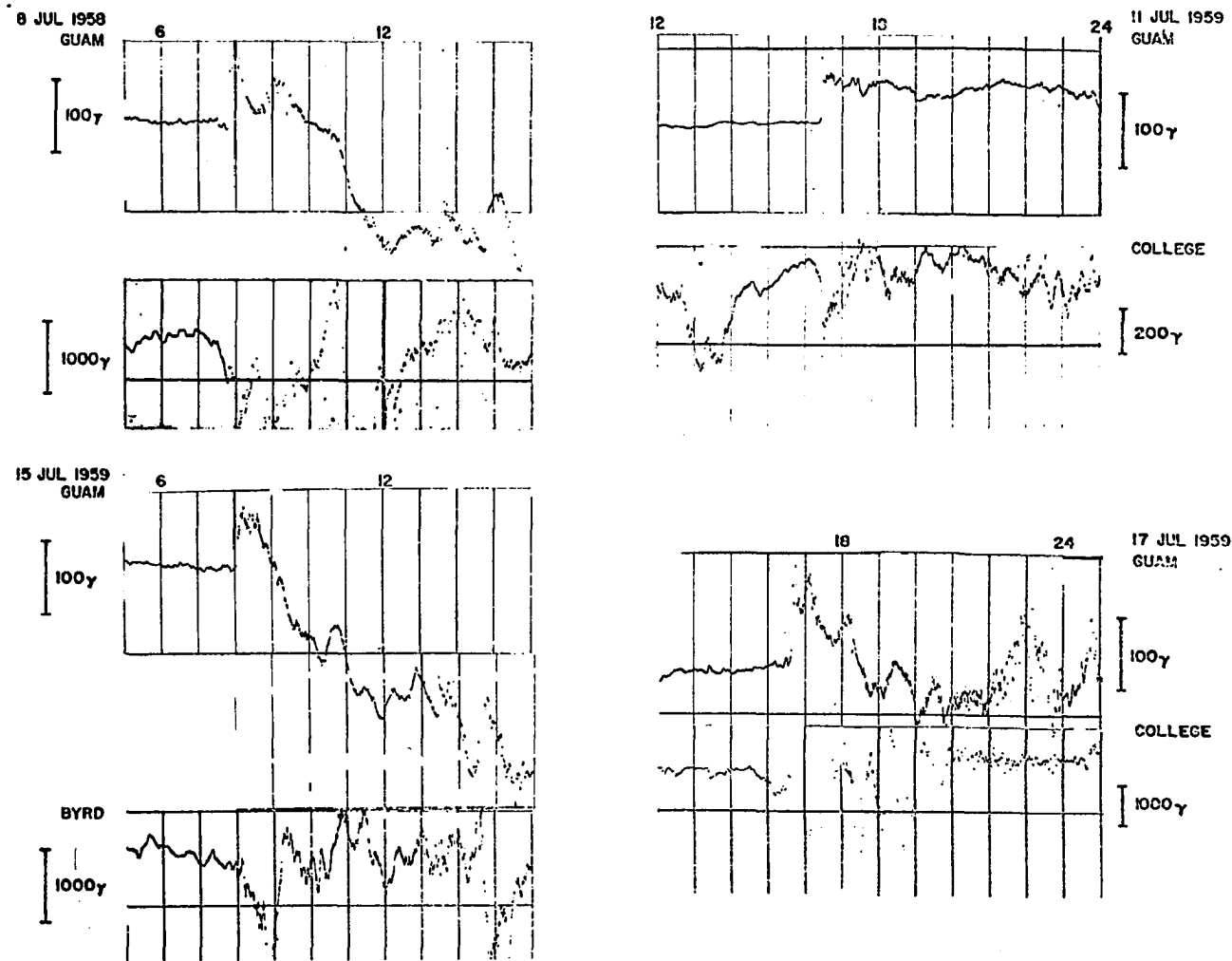


Fig. V-6. Sudden commencement magnetic storms accompanied by bright substorm type auroras (Group I). The times at which sun-aligned arcs appeared are marked by triangles, and the intervals during which substorm type auroras appeared are marked by black bars. Magnetic midnight at the auroral zone stations whose magnetograms were shown is indicated by an upward pointing arrow.

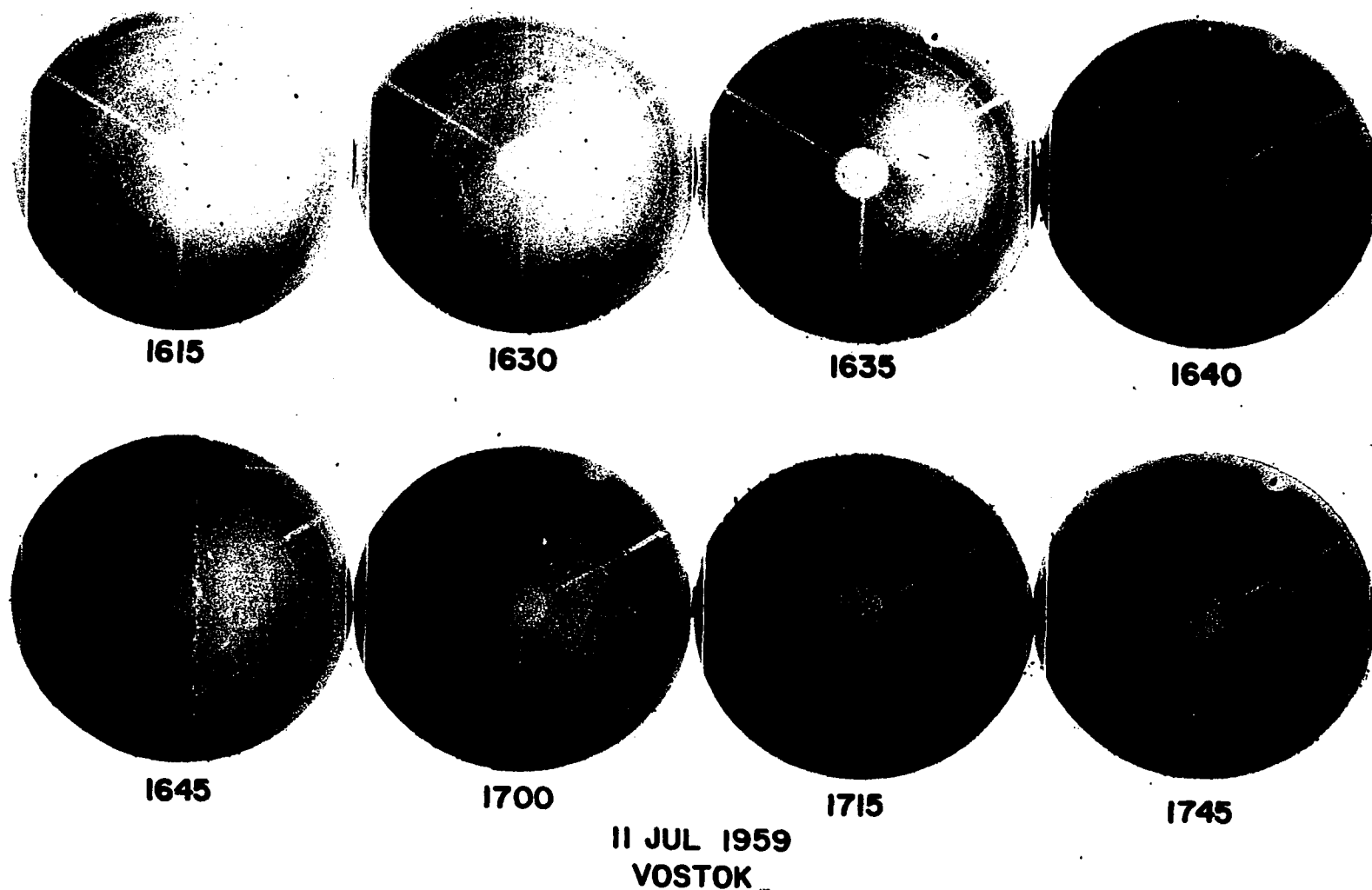


Fig. V-7. All-sky camera pictures (in negative) taken at Vostok following the ssc at about 1630 UT, July 11, 1959. Cinematic projection of the data indicates that the motion of the auroral forms was in the direction away from the sunward horizon. (The sunward direction is marked by a dot next to the photographs.)

Another feature of these four examples is that in each case the sudden impulse occurred at a time when a weak polar magnetic substorm was already in progress. In three of the examples the H component at a post-midnight auroral zone observatory showed a departure of a few hundred gammas below its undisturbed level, while in the fourth case, that of July 11, 1959, the H component was about sixty gammas below its undisturbed value and was decreasing rapidly when the sudden commencement occurred (see Fig. V-6). It will subsequently be noted that another group of examples occurred at times when no magnetic substorm was in progress, and that those events evolved in a somewhat different manner.

## 2) Sudden Impulses Followed by Quiet Periods

In six of the remaining examples, Group II, (Fig. V-8), auroras in the form of sun-aligned arcs appeared in the polar cap following a sudden impulse (si) or sudden commencement (ssc). The magnetic activity associated with each of these events can be characterized by a period of half an hour or more following the si or ssc during which no polar magnetic substorm could be detected at the auroral zone; it was during this quiet period that the sun-aligned arcs appeared. In contrast with the events of Group I, magnetic activity at the time of the sudden impulse was absent except in the case of the July 5, 1957 event. In this exception the ssc was preceded by a period of about five hours of rather strong magnetic activity which reached a peak about an hour prior to the ssc, and then underwent a rather rapid recovery, the H component at Kiruna having returned to quite near its normal value at the time of the ssc. Thus, even in this case it might be concluded that the conditions necessary to produce a polar magnetic substorm no longer prevailed at the time the ssc occurred.

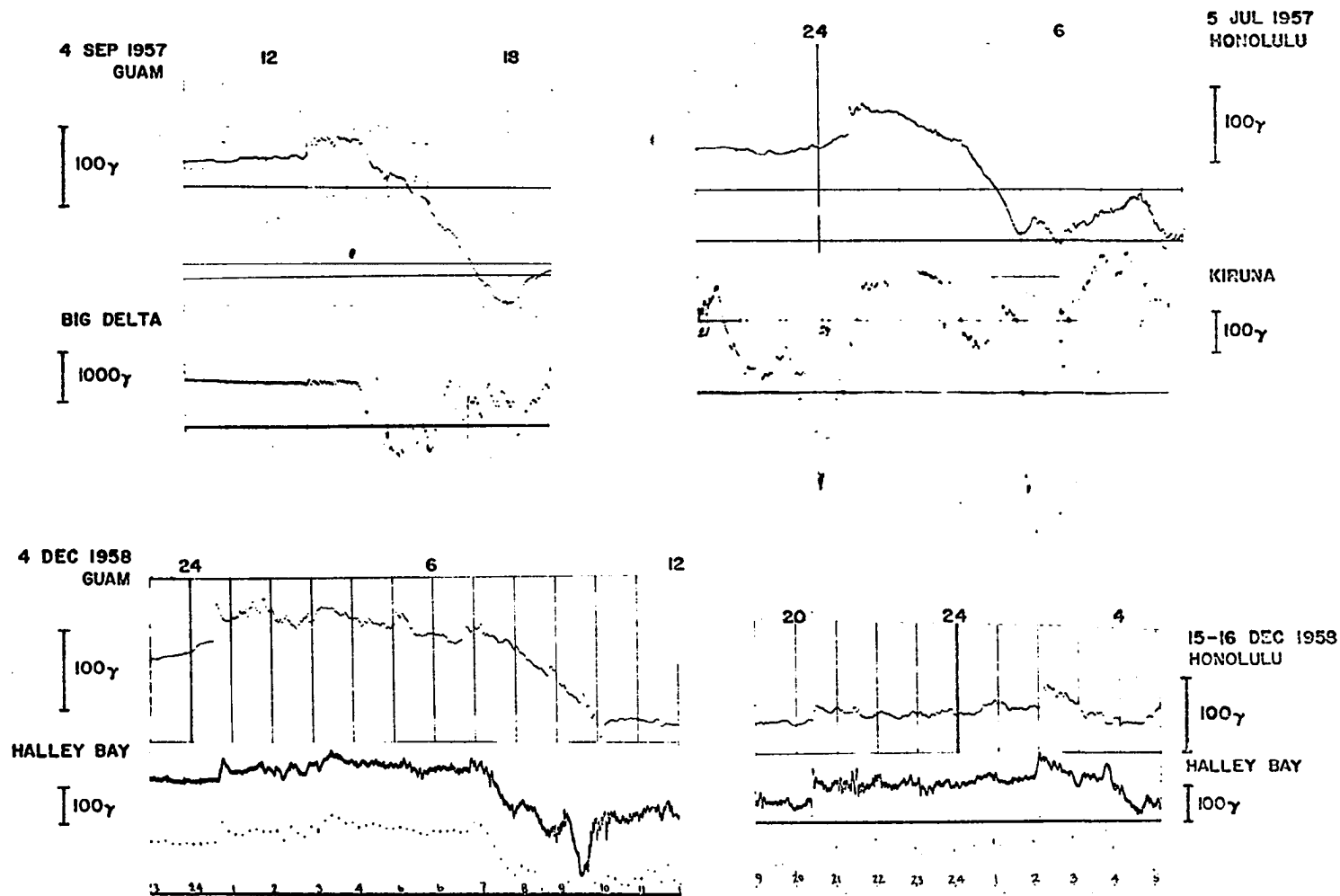


Fig. V-8. Sudden commencements and sudden impulses accompanied by sun-aligned auroras (Group II). In this figure both triangles and black bars indicate times at which sun-aligned arcs appeared. The upward pointing arrow indicates magnetic midnight at the auroral zone station.

Although a few of the events of Group II seem to indicate that the brightness and occurrence of the sun-aligned arcs is affected by the sudden commencement, the evidence is not consistent. Auroras visible at Scott Base brightened at the time of the ssc on September 4, 1957 but on the other hand a sun-aligned arc visible at Alert became dimmer at 0200 UT, December 16, 1958 when the ssc occurred. On December 15, 1958 no sun-aligned arcs appeared for some hours preceding the ssc of December 15, 1958 but did occur about thirty-five minutes after. The December 4, 1958 events give no indication of a sudden commencement effect, sun-aligned arcs being visible in the polar cap prior to the sudden impulse as well as after. On July 5, 1957 sun-aligned arcs appeared immediately at Scott Base at the time of the sudden commencement. No such arcs had been visible prior to the ssc but the ending of the polar magnetic substorm that preceded this particular ssc could be considered to have set the stage for the occurrence of the sun-aligned arcs regardless of the occurrence of the sudden impulse.

In summary the examples in Group II constitute a class of sudden commencements that, in contrast to the events of Group I, did not give rise to an immediate polar magnetic substorm. The polar cap auroras that occurred following the Group II sudden commencements took the form of sun-aligned arcs, the kind of auroras that would be expected in association with the magnetically quiet condition that prevailed at these times.

### 3) Unclassified Example

One other event (Fig. V-9) does not fit into either Group I or Group II. On June 28, 1958 a sudden commencement occurred at 0713 UT. Evidence of a weak polar magnetic substorm appears in the magnetograms of Byrd Station and College, but no auroras appeared over Scott Base or Vostok until 0900 UT,

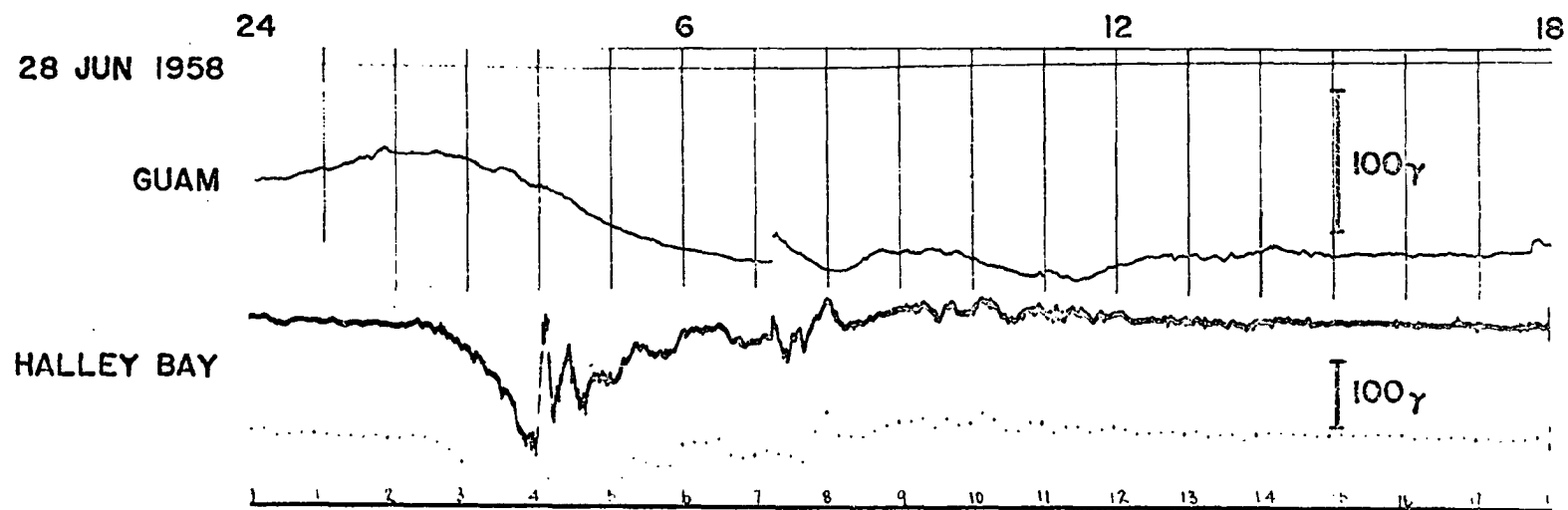


Fig. V-9. Sudden commencement immediately followed by a polar magnetic substorm, but not immediately accompanied by substorm type aurora. The black bar indicates an interval during which diffuse patches could be seen at Scott Base and Vostok in the Antarctic. The upward pointing arrow marks magnetic midnight at the auroral zone station.



when auroras appeared and persisted until 1000 UT. The auroras were in the form of diffuse patches. At this time, Byrd Station was experiencing a 200 to 300 gamma negative displacement in the H magnetic component, which is suggestive of a weak polar magnetic substorm.

The present study supports the idea that there are two classes of aurora that occur over the polar cap. One of these, consisting of auroral arcs oriented in the sun-earth direction, occurs during times of geomagnetic quiet. These arcs usually disappear at or before the onset of a polar magnetic substorm. The second class, associated with polar magnetic substorms, consists of auroras which show no preferred orientation, and which most often move into the polar cap region from the midnight sector of the auroral oval. These auroras may be identified as extreme cases of poleward expansion of the aurorally active region that has been discussed by Akasofu (1964) as part of the auroral substorm.

The discovery of several examples of polar cap auroras at the time of magnetic sudden commencements or sudden impulses permits the identification of a class of events of different character than those reported earlier by Feldstein (1960). While the events reported by Feldstein, as well as one of the new events reported here, are characterized by the occurrence of a polar magnetic substorm and the appearance of randomly aligned and contorted auroral forms immediately after the sudden commencement, the six new examples belonging to Group II are characterized by magnetic quiet and the occurrence of sun-aligned auroral arcs for a half hour or more following the sudden commencements.

It was noted that the evolution of the magnetic and auroral activity into a Group I or Group II type event appears to be related to the presence

or absence respectively of magnetic substorm activity at the time of the ssc. One possible interpretation of this is that the behavior of the auroral and magnetic activity of the Group I events represents an enhancing effect of the ssc upon already present activity, while the events of Group II are cases in which the magnetosphere was in a stable or "quiet time" state which the ssc by itself was unable to overcome. Such an interpretation would be consistent with a magnetospheric model of the kind suggested by Dungey (1961). In this model at a time when the interplanetary magnetic field has a southward component, the magnetosphere will be in an active state in which the field lines emanating from the vicinity of the poles are interconnected with the interplanetary field. At other times when the component of the interplanetary field perpendicular to the ecliptic is directed northward, there will be no interconnection of the terrestrial with the interplanetary field leaving the magnetosphere relatively immune to the effects of the ssc shock wave. Observational support for such a theory has been increasing in the past few years (e.g. Fairfield and Cahill, 1966, Zelver, et al., 1967). There are undoubtedly other theories that would be equally consistent with this interpretation of the observations; indeed any that call upon a parameter of the interplanetary medium in addition to the momentum of the solar wind to be influential in the production of the polar magnetic substorm would suffice.

On the other hand a reader, inclined to favor the concept of an interplanetary medium with a single parameter effective in producing terrestrial magnetic effects, may upon careful examination of the examples find some comfort in noting that the sudden commencements in the examples of Group I are consistently of greater magnitude (50 to 100 gammas) than those of the

Group II examples (less than 50 gammas), roughly speaking the former being about twice as great as the latter. However, the distinct difference in the development of the activity between the two groups of examples is clearly more than a simple matter of degree. This suggests that a one parameter theory must at least be complicated to the extent of engendering a threshold level that the sudden commencement must exceed in order to produce an event of the Group I type.

## CHAPTER VI

## CONCLUSION AND DISCUSSION

1. The Important Morphological Features of Magnetic Storms and Polar Substorms

The magnetic storm is a world-wide disturbance of the earth's magnetic field and is associated with many other geophysical phenomena, especially in the polar regions. In reality, the magnetic disturbance is an almost permanent feature of the geomagnetic field, but usually when severe manifestations of disturbance, namely the magnetic storm and polar magnetic substorm are absent, it is still called magnetically quiet.

The magnetic storms vary considerably in their time development. The main features of the magnetic storms are 1) a sudden change in the H component level (ssc), 2) an initial positive change of the magnetic field (initial phase), 3) a depression of the geomagnetic field in the low latitude (main phase), 4) polar magnetic substorms and 5) auroral substorms.

The sudden onset of magnetic storms is one of the most striking features of geomagnetic disturbances. This step-function-like change has been attributed to a sudden impact of solar plasma flow on the geomagnetic field. Recent progress in space physics has indicated that this sudden increase is caused by an interplanetary shock wave generated by solar plasma ejected during solar flares. The duration of this step-function-like change, namely the initial phase, can vary from several hours to fractions of one hour. The so-called "gradually commencing storm" (Sg storm) does not have the initial phase. During the initial phase, magnetic activity increases considerably over the polar cap, particularly at about  $\text{dp lat } 80^\circ$  in the sunlit noon sector. In low latitudes, some irregular changes superpose on the

step-function-like change, indicating the irregular change of the plasma pressure. Along the auroral zone, the polar substorm can occur during this period. The magnetic storm of April 17-18, 1965 showed an example of the occurrence of a polar substorm during the initial phase. Therefore there is no substantial energy introduction into the magnetosphere to produce the ring current belt and the polar substorm by an enhancement of the solar plasma flow.

Following the initial phase, a large world-wide decrease of the horizontal component occurs in low latitudes, namely the main phase decrease. The main phase develops rapidly first in the evening sector and then in the afternoon sector. Because of this non-uniform development of the main phase a remarkable asymmetry of the main phase decrease grows. After the maximum epoch of the main phase, the decrease begins to decay and the above mentioned asymmetry disappears during this recovery phase. Near the auroral zone, the magnetic storm is characterized by frequent occurrences of intense polar substorms in the growing stage of the main phase. However, the polar substorms are not as obvious during the initial phase or recovery phase of the magnetic storm. In the storm of April 17-18, 1965, which can be considered as a typical example, a small polar magnetic substorm of about 300  $\gamma$  occurred during the initial phase, but the major activity of polar magnetic substorms began at about the beginning of the main phase decrease, between 0100 and 0200 UT, April 18 and subsided at the beginning of the recovery phase of the storm. From the simultaneous solar wind measurement, it is found that the onset of the polar magnetic substorm is not directly related to any change of the interplanetary solar wind speed, number density or temperature. This fact, suggests that the onset of the polar magnetic substorm may be an internal process of the magnetosphere.

The growth and decay of the polar magnetic substorm is closely related to that of the auroral substorm. In fact they are different manifestations of the same substorm. The onset of the polar magnetic substorm is always accompanied by the onset of the auroral substorm. Since the auroral substorm can be observed by the all-sky camera, the simultaneous study of the auroral substorm and polar magnetic substorm can improve our understanding of these two polar geophysical phenomena.

It has recently been recognized that the distribution of the aurora at a particular instant may greatly differ from the location of the auroral zone. The instantaneous auroral belt, in which overhead auroras are seen, has an oval shape on the average and its center is appreciably displaced from the center of the auroral zone, namely the dipole pole, toward the darkside along the midnight meridian. Such an instantaneous belt is called the auroral oval.

The auroral oval changes its location greatly, depending on solar conditions. When the sun is extremely quiet, the oval tends to be circular. A slight increase in the solar activity causes an elongation of the oval toward the dark hemisphere. During intense geomagnetic storms the oval descends toward the equator, as far as  $\text{dp lat } 50^\circ$ . The average location of the oval in the midnight sector is about  $\text{dp lat } 67^\circ$ , namely the auroral zone.

In addition to such a change, the auroral system centered in the midnight sector of the auroral oval repeatedly undergoes an expansion and subsequent contraction. This phenomenon is called the auroral substorm. The substorm has two characteristic phases, an expansive phase and a recovery phase, and its lifetime is of order 1 to 3 hours.

The auroral substorm originates in the midnight sector of the auroral oval where quiet arcs exist. The first indication of the substorm is a sudden brightening of one of the quiet arcs followed by a rapid poleward motion. This produces a 'bulge' around the midnight sector. The bulge produces a large-scale fold at its western edge, which moves rapidly westward; the fold is called the westward traveling surge which is a common feature in the evening sector of the oval. In the morning sector, auroras break-up into patches or become folded during the substorm and drift eastward as a whole.

The auroral substorm reaches its maximum stage at the end of the expansive phase when the northernmost active band attains its highest latitude, and then the recovery phase begins. The active bands which moved into the polar cap begin to return toward their original location. During this period, the westward surge is traveling farther to the west along the oval in the evening sector, and in the morning sector the patches continue to drift eastward. At the end of the substorm, the condition before the onset of the substorm is restored.

In the region swept by bright poleward advancing bands, a sharp negative change in the horizontal component of the geomagnetic field is observed; such a negative change is called the negative bay. The expansion of the bulge during the expansive phase of the auroral substorm indicates the expansion of the region in which a negative bay is observed. Since the westward surge may be considered to be the western leading edge of the bulge, the region of the negative bay is advancing with the surge. It is also found that the greater part of the polar electrojet is concentrated in the edge of the auroral bulge where the aurora is very bright. The auroral substorm and

polar magnetic substorm are only different aspects of a specific disturbance, namely the polar substorm.

Another important feature of the polar substorm is that it occurs simultaneously in both hemispheres. However, there is a seasonal variation in their conjugacy. Since the negative bays are observed only when an intense precipitation of auroral electrons, shown as the increase of the cosmic radio noise absorption recorded by riometer, occurs near the observatory, there appears to be a remarkable asymmetry of the precipitation with respect to the geomagnetic equator in solstice months. This could be due either to a greater displacement toward the dark side of the auroral oval in the summer polar cap than in the winter polar cap or due to a greater poleward extension of the polar electrojet in the winter polar cap. In any case, in the winter polar cap, both the electrojet and the precipitation of auroral particles approach the dipole pole more closely than in the summer polar cap. We also learned that positive bays are more intense at a summer polar station than at the conjugate winter station. This suggests that ionization by solar radiation largely determines the magnitude of the positive bay rather than the ionization due to the precipitation of auroral particles. Therefore, there are important differences between the nature of the positive bay and that of the negative bay.

The important morphological features of polar substorms and magnetic storms may be summarized as follows:

- 1) The main phase decrease is the main feature of magnetic storms in low latitudes. The duration and intensity of the main phase decrease has no obvious relation to the initial phase.



- 2) During the growing stage of the main phase, there is an asymmetry of the magnitude of the main phase decrease (DR) due to its non-uniform development. The development occurs earlier and is more intense in the afternoon and evening sectors than in any other sector.
- 3) The polar substorm becomes more intense and frequent during the growing stage of the main phase; and the onset of the polar substorm is not directly related to the change of solar wind pressure.
- 4) During a polar substorm, which occurs simultaneously in both hemispheres, auroras have an expanding motion resulting in a westward surge, poleward motion and eastward moving patches, in the evening sector, midnight sector and morning sector, respectively. The negative bay is observed within the region of the bulge and also along the auroral oval.
- 5) During simple polar substorms which are not related to any magnetic storm, low latitude negative bays are observed in the afternoon and evening sectors. This low latitude negative bay is due to the growth of the ring current in the magnetosphere.

## 2. Energy Requirement for the Magnetic Storm and the Polar Substorm

The energy budget in a model magnetic storm was discussed in detail by Akasofu (1964) and is outlined in the following:

Assuming the auroral particles are 5 keV electrons with flux of about  $10^{10}$  electrons/cm<sup>2</sup> sec and the total cross-sectional area exposed to incoming auroral particles is also assumed to be of order  $10^{15}$  cm<sup>2</sup>, for the moderate polar substorm the energy injection rate is about  $10^{17}$  ergs/sec. For a typical substorm with lifetime of about one hour the total energy input is of order  $10^{20}$  ergs.

The main phase decrease is attributed to the growth of the ring current in the inner magnetosphere and is produced by the increase of the number, as

well as the energy, of ring current particles. The increment of total kinetic energy of ring current particles for a 100 Y Dst, which corresponds to the main phase of the moderate magnetic storm, is of order  $3 \times 10^{22}$  ergs; and the estimated energy injection rate for a moderate magnetic storm is of order  $8 \times 10^{17}$  ergs/sec. Therefore, it is obvious that the appearance of polar substorms and magnetic storms requires tremendous amounts of energy. During the magnetic storm the increment of the energy is about  $10^{22} - 10^{23}$  ergs at a rate of  $10^{18} - 10^{19}$  erg/sec.

Where is the energy source, and if the energy source is extraterrestrial, how is it brought into the magnetosphere? The energy for the earth's rotation (about  $10^{37}$  ergs) would be quite sufficient to produce all geomagnetic storms and polar substorms. Assuming 100 magnetic storms occur every year, the energy of the earth's rotation can supply the energy of magnetic storms for  $10^{12}$  years, but at present no theory has been proposed to convert this energy into that of magnetic storms.

Since the earth's rotation is a permanent phenomenon and the magnetic storm and the polar substorm are sporadic phenomena, this possibility may be excluded. The outer part of the dipole field (about  $8 \times 10^{24}$  ergs) and the radiation belts (about  $10^{22}$  ergs), also cannot be the required energy source; thus the energy source must be solar-terrestrial.

A close relation of magnetic storms and polar substorms with solar activity is well known and the solar wind energy flow over the whole magnetosphere (about  $10^{20}$  ergs/sec) is quite sufficient to produce these two geophysical phenomena. Therefore, it is likely that the sun is the ultimate source of magnetic storms and polar substorms, but the problem is, that based on present knowledge, the solar wind parameters which have been measured so

far (density, velocity, energy and magnetic field) do not vary so much as the intensity and the types of magnetic storms and polar substorms.

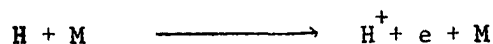
### 3. Magnetic Storm and Polar Substorm Theories

#### A. Energy Injection Models

At present, there has been a number of suggestions to introduce energy into the magnetosphere from the solar wind.

- 1) Direct entry of neutral particles model (Akasofu and McIlwain 1963, Akasofu, 1964)

If the solar plasma clouds contain an appreciable amount of neutral hydrogen atoms, they can penetrate directly and deeply into the magnetosphere without any interaction with the earth's magnetic field. Thus the solar wind energy can be introduced into the magnetosphere and is stored in the ring current belt through the reactions, such as



where M denotes a terrestrial atom or molecule. As a consequence of this direct entry of neutral particles into the magnetosphere, the injection can only take place on dawn and dusk sectors (Swift, 1968). In this model, the secondary process is necessary to give rise to the polar substorm and other auroral zone geophysical phenomena. The required flux of hydrogen atoms of about 10 kev, for introducing enough energy into the magnetosphere during the magnetic storm, is of order  $10^9$  number/cm<sup>2</sup> sec. The observed asymmetric development of the ring current also can be produced by this model (Akasofu and Chapman 1964).

This model has been seriously criticized by Brandt and Hunten (1966) and Cloutier (1966) based on the argument that the required high proportion of neutral hydrogen atoms contained in the solar plasma flow is

extremely unlikely. The percentage of the neutral particles in the solar wind has not been measured due to technical difficulties; but Swift (1968) suggested a possible way to examine this neutral hydrogen mechanism by measuring amplitudes of fluctuation of the electric field on geomagnetic field lines passing through the earth's terminator. At present, this model is still one of the favorable possibilities because of the sufficient energy input, the asymmetrical development of the ring current and the requirement of the secondary process to generate the polar substorms. The appearance of peak densities of ring current particles in the afternoon and evening sectors has been observed, but the corresponding peak in the morning sector has not been observed.

## 2). Neutral point model (Mayaud, 1953)

In the dayside of the magnetosphere, there are two neutral points (one in each hemisphere) which separate field lines crossing the equator along the noon meridian from the crossing along the midnight meridian. At these points, the magnitude of the field is zero and the boundary of the magnetosphere is tangential to the direction of the solar wind (Mead, 1964). Therefore, at these two points, the magnetosphere is open to solar wind particles; the particles can "leak" into the magnetosphere and bring the energy into the dayside of the magnetosphere, then they are brought to the nightside, where the polar substorm originates, by a drift or corotation with the earth.

It is doubtful that the required energy injection rate ( $\sim 10^{19}$  ergs/sec) for a magnetic storm, or even for a polar substorm, can be sufficiently supplied by this "leaking-in" process through two neutral points; also, the process to inject energy into the inner magnetosphere has not been explained.

3) Viscous-like interaction model (Axford and Hines 1961, and Piddington 1964).

There are two basic processes involved in this model:

- (a) Electric polarization fields set up at the magnetospheric boundary to transfer part of the solar wind energy or momentum into the magnetosphere.
- (b) Internal electric fields of the magnetosphere give rise to various auroral phenomena. Axford and Hines (1961) suggested that there must be a positive space charge near the dawn boundary of the magnetosphere (A) and a negative space charge near the dusk boundary (B) (see Fig.VI-1 (a), (b)), based on the hydromagnetic approximation

$$\underline{E} + \underline{V} \times \underline{B} = 0$$

where the electric field  $\underline{E}$ , in quasi-stationary conditions, can be derived from a potential:

$$\underline{E} = - \nabla \phi$$

so that  $\underline{V} \times \underline{B} = \nabla \phi$

Thus,  $\underline{V}$  and  $\underline{B}$  both lie in equipotential surfaces. We may think of some pattern of motion imposed on the ionization at some level and we may represent that motion by a pattern of flow lines. These flow lines must then be equipotential lines, and the equipotential surfaces, must be derivable simply by mapping along the geomagnetic field lines in each direction. Thus, they project these space charges onto the polar cap. This internal electric field will drive a current system in the polar regions.

The convective motion of the magnetosphere is a very important concept for understanding the "quiet" magnetospheric phenomenon. At present no detailed theoretical result of this model is available, and some of the results are based on some observations which are considered to be inconclusive. The existence of the viscosity between the solar wind and the

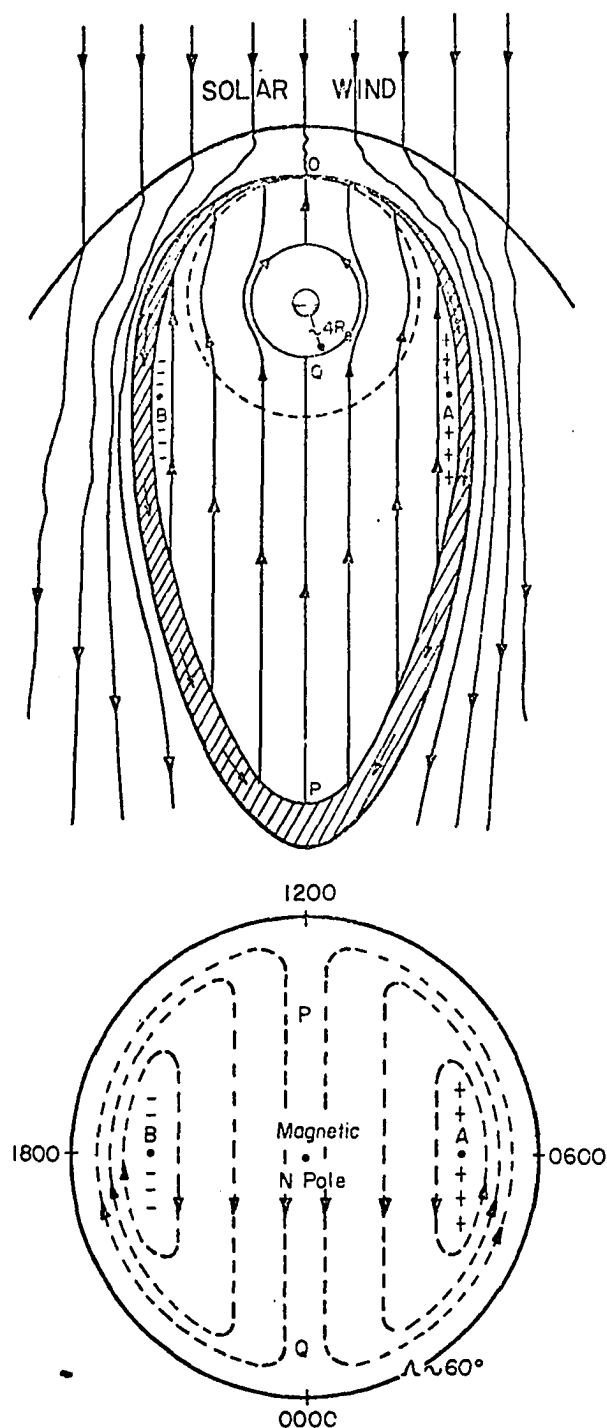


Fig. VI-1a. A sketch of the Equatorial section of the earth's magnetosphere looking from above the North Pole. Streamlines of the solar wind are shown on the exterior, and the internal streamlines refer to the circulation which it is proposed is set up by viscous interaction between the solar wind and the surface of the magnetosphere. The internal streamlines are also equipotentials of an associated electric field which may be regarded as being due to accumulations of positive and negative charges as indicated at A and B.  
 b. A sketch of the circulation at ionospheric levels in the North Polar Cap corresponding to the internal circulation in the magnetosphere shown in (a). (Axford, 1964).

magnetospheric boundary, which is the foundation of this model, has not been observed yet.

- 4) Open polar region model (Dungey 1961, 1963, 1965, and Levy, Petschek and Sisco, 1964).

Dungey (1961) assumed that a southward directed interplanetary magnetic field exists at times of magnetic disturbance. The interaction between a southward oriented interplanetary field and the earth's magnetic field plays an important role. The interaction results in an X-type neutral point at the apex and rear of the magnetosphere and the high-latitude field lines extend into the interplanetary medium. The combined effect of the solar wind and the plasma flow in the vicinity of the X-type neutral point causes a convective motion of the field lines. Dungey inferred that the projection of the convection pattern onto the ionosphere has a resemblance to the SD variation.

Observational support for such a model has been increasing in the past few years. Fairfield and Cahill (1966) found a good correlation between the southward directed interplanetary magnetic field just outside the magnetospheric boundary and the occurrence of polar substorms. The observation of geomagnetic micropulsations and Mariner 2 interplanetary magnetic field and plasma velocity measurements, (Zelwer, et.al. (1967)), also support this model. Auroral activity over the polar cap during the storm sudden commencement discussed in Chapter V also supports the open polar region magnetospheric model.

Based on the ability of transferring the solar wind energy into the magnetosphere to provide sufficient energy for magnetic storms and polar

substorms, the neutral particle model and the open polar region model are considered to be two favorable models.

#### B. Polar substorm theories

After Birkeland's study (1908, 1913), the mechanism to produce the auroral display and polar magnetic disturbance became an interesting topic to many geophysicists. There are numerous publications on this topic, but according to the approach in finding the mechanism, they can be classified into three groups, namely SD (or DS) current system approach, auroral morphology approach and plasma instability approach. These theories have been reviewed in two recent review papers (Cole 1966 and Akasofu 1966), thus the detail of each theory will not be mentioned.

##### 1) SD (or DS) current system approach

Practically, all early tries belong to this group, in which their main concern is to produce the SD (or DS) current system, and the auroral morphology was not considered. This group includes the following theories:

- a) Discharge from an extraterrestrial source (Birkeland, 1908, 1913; Alfven 1950, 1955; Karlson 1962, 1963 and Block 1966)
- b) Diamagnetism (Maris and Hulburt 1929)
- c) Charge separation (Martyn 1951, Show 1959, Chamberlain, Kern and Vestine 1960, Chamberlain 1961, Kern 1962, Kern and Vestine 1961, Fejer 1961, 1963, 1964, 1965)
- d) Dynamo action (Rikitake 1947, Fukushima and Oguti, 1953, Obayashi and Jacobs 1957, Cole 1960, 1962 and Swift 1963)
- e) Steady state solar-wind-generated electric fields or convective motion (Piddington 1960, 1962 a,b, 1963, 1966; Cole 1961, Axford and Hines 1961 and Hines 1964)
- f) Neutral point discharge (Dungey 1957, 1961).



Since the SD current system has not proven a correct one to represent magnetic disturbance during a polar substorm, these theories can be considered as early conjectures.

## 2) Auroral morphology approach

Based on some of the auroral morphological features, Akasofu and Chapman (1962) and Akasofu, Chapman and Kendall (1967) proposed the neutral line discharge theory and Krassovsky (1968) proposed the electric polarization of ionosphere-magnetosphere theory.

## 3) Plasma instability approach

Since the auroral oval is the intersecting line between the outer boundary of the trapping region and the ionosphere and is also the nature reference frame of the polar substorm, the polar substorm must be a manifestation of interactions between the magnetospheric plasma near the outer boundary of the trapping region and the neutral atmosphere. Therefore the polar substorm is most likely to be due to plasma instability.

Two kinds of plasma instability have been proposed. One is the neutral sheet instability by Petschek (1964), Coppi, Laval and Pellat (1965) and Piddington (1966). The other is the interchange instability of the ring current by Swift (1967).

Based on the neutral sheet instability calculation of Coppi, Laval and Pellat (1966), the neutral sheet instability mechanism was extensively discussed in two recent papers by Axford (1967a,b). In this model, auroral and polar magnetic substorms are directly caused by the sudden reconnection of magnetic field lines in the tail of the magnetosphere. The solar wind energy is transferred into the magnetosphere by viscous-like interaction (convection) causing the inflation of the inner magnetosphere at first

mainly on the nightside, but later, more or less uniformly over other areas; therefore it should be more inflated on the nightside than on the dayside. Axford claims: "As a consequence of this process, the polar substorm should occur most intensely during the transition from the initial to the main phase; that this is the case on the average has been demonstrated very clearly by Sugiura and Chapman (1960)",

There are some inconsistencies between this model and the observational results. First, DS magnetic variation obtained by Sugiura and Chapman does not represent the magnetic variation of the polar substorm, it primarily represents the asymmetric component of the ring current. Thus, the result of Sugiura and Chapman (1960) that the maximum DS magnetic variations during a storm coincides roughly with the maximum of  $|d(Dst)/dt|$  and precedes the maximum of  $|Dst|$  may be just a simple consequence of the fact that the asymmetry of the ring current is more severe in the development phase of the magnetic storm as shown in Chapter II. Secondly, that polar substorms are most intense during the transition from the initial to the main phase, does not uniquely point to Axford's mechanism. It is reasonable to assume that based on the interchange instability model in the growing stage of the main phase, the ring current is very unstable, thus the polar substorm should occur more frequently and be more intense in the transition from initial phase to main phase.

The procedure of generating polar substorms and magnetic storms in my 'opinion', can be described as follows: The solar energy is more or less continuously supplied into the magnetosphere and stored there. The secondary process, namely a plasma instability, releases some of the energy

into the ionosphere and produces the polar substorm. From a study of a simple polar substorm, the increase of the ring current energy in the afternoon sector is observed during the polar substorm. In the midnight sector, the positive bay is observed both in low latitude on the earth's surface and also at about 6.6 earth radii away from the center of the earth (Coleman and Cummings 1968). Figure VI-2, shows the simultaneous H components at Honolulu and ATS-I satellite. The positive bay recorded by ATS-I can be inferred as the decrease of the ring current energy. Thus, during the polar substorm, the ring current energy is increased in the afternoon sector but decreased in the midnight sector. It could be due to the redistribution of ring current particles during the polar substorm. The decrease of the ring current energy in the midnight sector during the polar substorm contradicts the consequence of Axford's neutral sheet instability mechanism, and agrees with that of Swift's mechanism. The redistribution of ring current particles was not shown in Swift's calculation, but it may be considered as a natural consequence of the instability of the ring current boundary. If this is a proper explanation, then Swift's interchange instability of the ring current might be a favorable mechanism to give rise to the polar substorm.

When the sun becomes active, the energy injection rate increases and the ring current energy increases also. Frank (1967) showed that during the main phase of the magnetic storm, the ring current boundary becomes sharper. The ring current also should become unstable during the growing stage of the main phase. As a consequence of this sharp boundary and unstable condition, the growth rate of the interchange instability increases, therefore the polar substorms occur more frequently and are more intense in the developing phase of the main phase decrease.

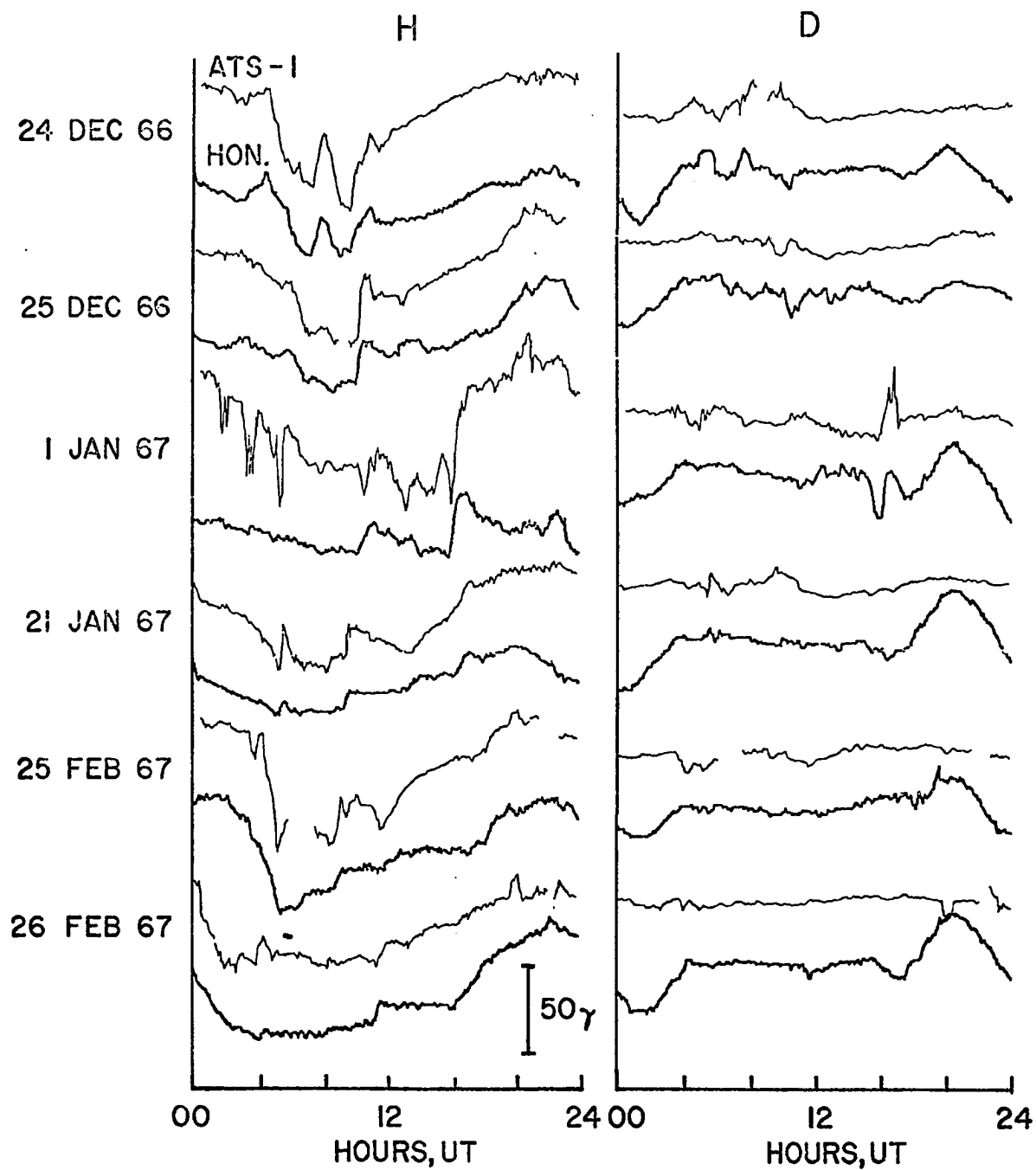


Fig. VI-2. The simultaneous H components at Honolulu and ATS-I Satellite.

### C. Ionospheric Model Current

The magnetic disturbance during the polar substorm is attributed to the ionospheric electric current. The theoretical calculation of the ionospheric current has been discussed by many workers. It has already been shown that during the polar substorm the asymmetry of the ring current is also observed; thus asymmetric injection of the ring current could be associated with the polar magnetic substorm, namely the auroral electrojet. The asymmetric injection of ring current particles and its consequences were first studied by Fejer (1961) and recently extended by Swift (1967, 1968) and the comparison between the polar magnetic substorm and the ionospheric currents calculated by Swift is discussed in the following paragraph.

During the polar substorm the main features of magnetic disturbance are that the intense negative bay corresponding to the westward ionospheric current is observed along the auroral oval and that the positive bay corresponding to the eastward ionospheric current appears equatorward of the oval with less intensity. When the ionospheric conductivity is assumed to be uniform, the feature of westward currents on the poleward side of the eastward currents is shown in the calculated currents, but the eastward current is stronger than the westward current. When the improvement of adding a high conductive ring representing the auroral oval on the uniformly conducting ionosphere is made, the model current in the nightside, assuming that the  $0^\circ$  meridian is the direction of the sun, is surprisingly consistent with that of the auroral electrojet. In the dayside, an intense eastward current is flowing along the high conductive ring and no intense westward current is obtained; these results do not agree with the observed magnetic disturbances in the early afternoon and late morning

sectors. In the observation, an intense westward current should co-exist with the intense eastward current and it is not seen in the model current. Inside the polar cap, the direction of the calculated model current is mainly toward the sun which is also consistent with the observation. The direction of the equivalent ionospheric current during polar substorms in the middle and low latitudes is southeast in the evening sector and northeast in the morning sector. The calculated ionospheric current in the low latitude is not consistent with the observation, but if the whole model current in the low latitude is rotated  $90^\circ$  counterclockwise, then it will be consistent with our observation. The major discrepancy between the model current and the observation is the intense eastward current in the dayside of the high conducting auroral ring. This discrepancy could be due to lack of day-night asymmetry in the auroral ring and also in the background conductivity as suggested by Swift (1968). Besides the consistency of the ionospheric current in the midnight sector along the auroral region, the other consequence of this asymmetric development of the ring current, namely an enhanced asymmetry of the ring current produced by the rapid depopulation in the midnight sector, also has been observed and discussed previously.

The most interesting feature of this model calculation is that the asymmetric ring current can develop significant electric fields by charge transfer between the outer boundary of the ring current and ionosphere and also can drive an electrojet resembling the polar electrojet. Thus, it is very reasonable to believe that the interchange instability of the ring current can be one of the possible mechanisms to produce polar substorms. The only question that could be raised about the validity of the

above model current is that all of these calculations were based on the small asymmetry of the ring current, but during an intense magnetic storm the ring current asymmetry does not necessarily remain small, for detail see Chapter II, therefore the consideration for large asymmetry of the ring current may be needed.

#### 4. The Relationship between the Polar Substorm and the Growth of the Ring Current.

A possible relation between polar substorm activity and the growth of the ring current has been discussed by a number of workers. The most important reason for this study is that it has been suggested that clues to the causes of the polar substorm and the ring current may be found by studying their relationship to each other. The mechanism of generating a polar substorm has been the subject of intensive study during the last few years. If the growth of the ring current occurs before major substorm activity, there is a possibility that the energy for the substorm may be stored in the ring current, and the mechanism for a polar substorm could be related to the growth of the ring current. On the other hand, if the onset of the development of polar substorms precedes that of the ring current, then the energy for the ring current could be introduced into the trapping region from the tail region when the merging of the tail fields causes polar substorms, as suggested by Axford (1967a,b). Therefore, it is worthwhile to study carefully the growth of both phenomena and examine the above possibilities.

Akasofu and Yoshida (1966) approached this question empirically by using a number of geomagnetic storms without the sudden commencement. The growth of the ring current can thus be determined more accurately with

little or no contamination of the DCF field. They found that the onset of the development of the ring current precedes that of the polar substorm. Cole (1966) questioned their results. Later, Davis and Parthasarathy (1967) found by using the hourly AE index defined by Davis and Sugiura (1966) and hourly Dst values (Sugiura 1965), that major DP substorms (polar substorms) precede the development of the ring current.

The development of polar substorms and the ring current during magnetic storms can be discussed on the basis of examples in Chapter II. It is known that the polar substorm is more intense and frequent during the growing stage of the main phase decrease of the magnetic storm. The question is then "when do these intense polar substorms develop?". Figure VI-3 shows the maximum decrease of the H component approximately along the  $dp$  lat  $25^\circ$  circle, together with the envelope of the negative change of H component in the high latitude at 5 minute intervals for the April 17-18, 1965 magnetic storm. One moderate polar substorm occurred during the 11 hour long initial phase of the storm, but the major intense polar substorm started at about the onset of the main phase and reached its peak activity during the growing stage of the main phase decrease. Since there is no sharp onset of the main phase decrease, and since the development of the main phase is not uniform in all sectors, the exact onset time can not be determined within the accuracy of 10 or even 30 minutes. If the flow of the solar plasma is assumed to be continuous during magnetic storms, then the surface current on the magnetospheric boundary, namely the DCF part, is constant. Unless facts contrary to this assumption are found, it is proper to state that the onset of the main phase decrease may be defined as the time of the first sign of decrease



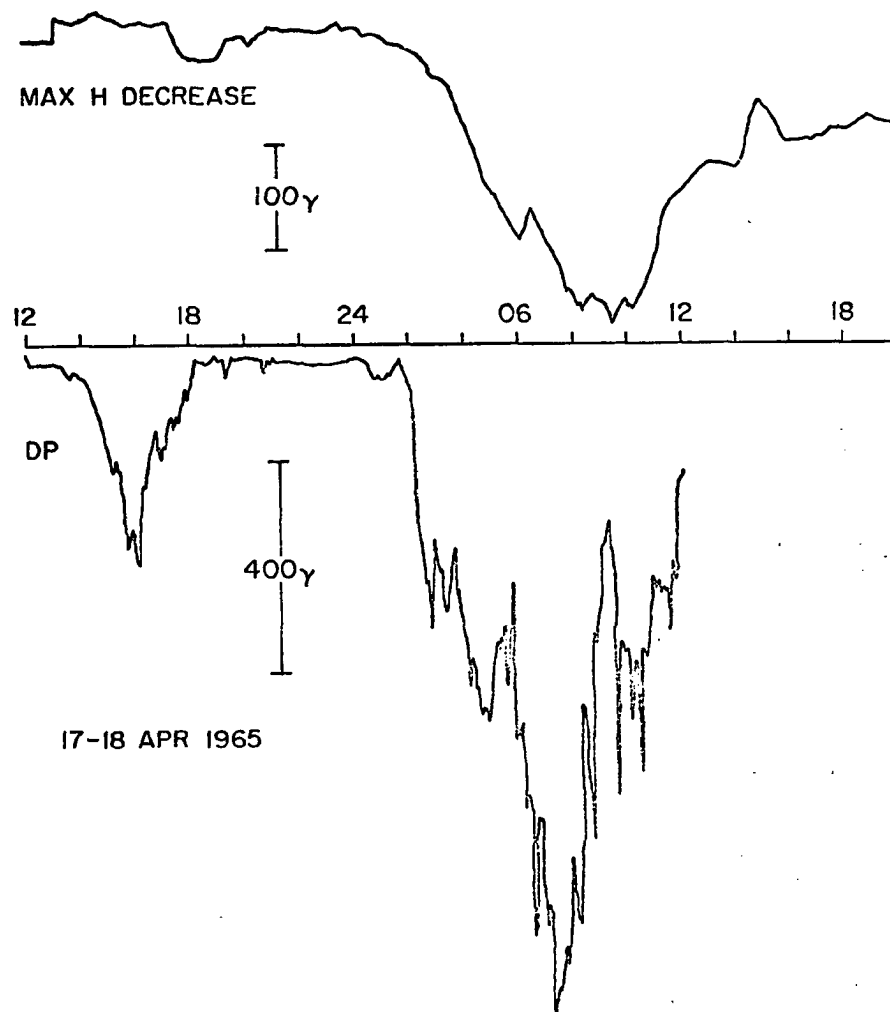


Fig. VI-3. The maximum decrease of H along the dp lat 25° circle and the envelope of the negative change of H in the high latitude for April 17-18, 1965 magnetic storm.

from the level of the initial phase. Figure VI-4 shows the development of the magnetic storm of Sept. 13, 1957 by using five almost evenly distributed stations along  $\text{dp lat } 25^\circ$  together with the hourly AE index (Davis, Echols and Wong, 1968). Again, the major polar substorm activity started at about the onset of the main phase and reached its peak during the developing state of the main phase. A similar result, namely that the peak of the polar substorm activity (or AE) preceded the maximum stage of the main phase, is also shown in the paper by Davis and Parthasarathy (1967). However, the fact that the AE peak precedes the Dst peak by a few hours does not necessarily imply that the onset of the development of the polar substorm precedes that of the ring current. This is because the lifetime of the polar substorm is much shorter than that of the ring current, so that even if the onsets for both phenomena are simultaneous, the peak times can differ greatly. It is known that the developing phase of the polar substorm is about 30 minutes, which means from the onset to the peak activity of the polar substorm takes about 30 minutes, and the growing phase of the ring current during a magnetic storm is about 10 hours; therefore if onsets of both phenomena occur simultaneously, then the peak activity of the substorm will lead that of the ring current, namely the maximum main phase decrease, by more than 9 hours. In reality, many polar substorms can occur during the growing phase of the ring current; combining all these substorm activities, the substorm peak activity can occur any time from 30 minutes after the onset of the main phase decrease to about the peak of the main phase decrease. The relation between the polar substorms and the main phase decrease shown in Figure VI-4 is consistent with the above conclusion.

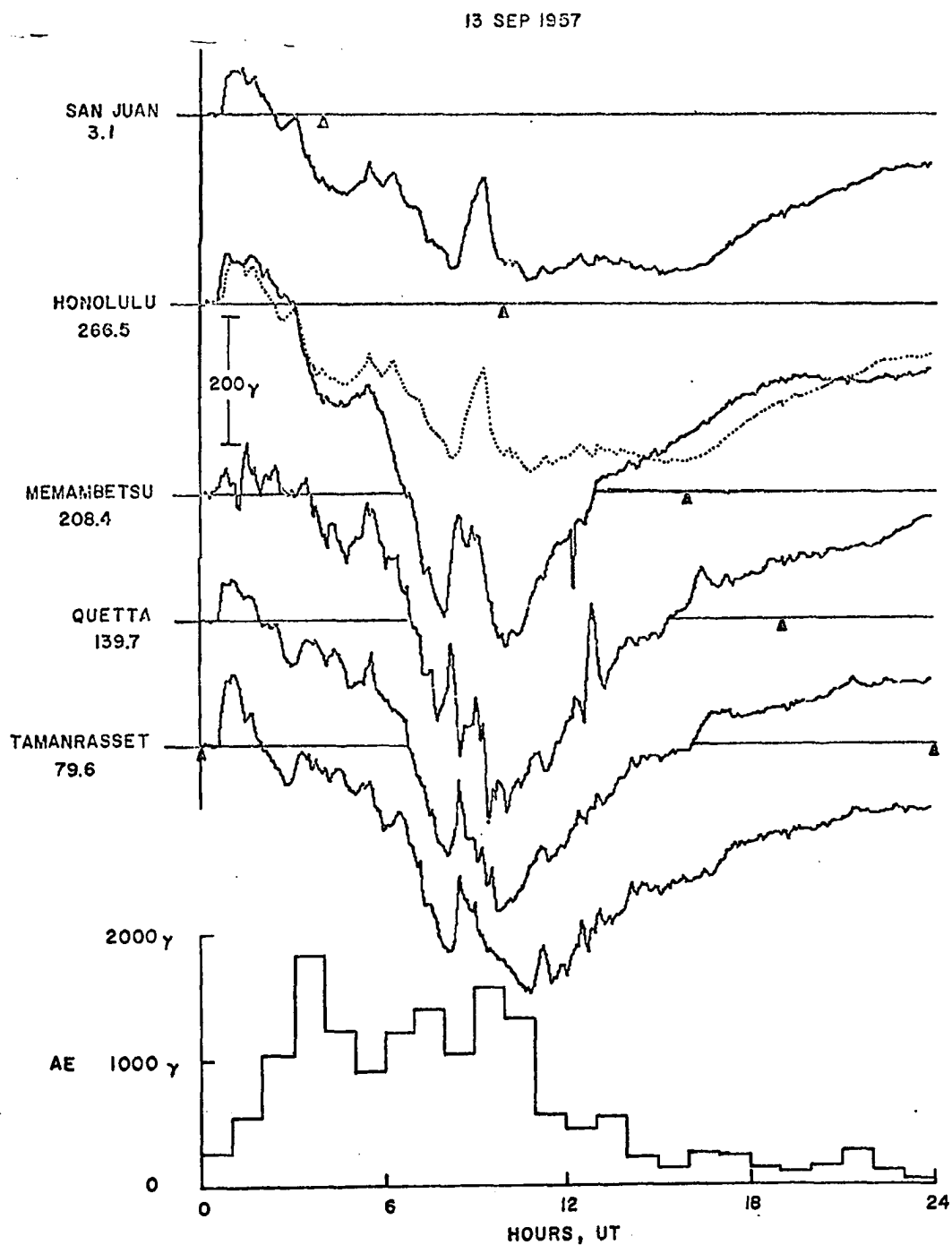


Fig. VI-4. Changes of H component in the middle latitude for different sectors; together with the hourly AE index (Davis, Echols and Wong, 1968), for September 13, 1957 magnetic storm.

The above examples show that the onset of the intense polar substorm activity approximately coincides with that of the main phase decrease, but that the peak activity of the polar substorm does not necessarily coincide with that of the main phase decrease and their times can be appreciably different.

In Chapter IV, it was demonstrated that each auroral zone positive bay was closely related with each low latitude negative bay and this one to one correspondence was about simultaneous within the accuracy of our study; the growth of the low latitude negative bay is gradual, but since these examples were chosen during magnetically quiet periods, the time accuracy of the onset of the bay is within 10 minutes. Since the auroral zone positive bay in the evening sector is a part of the polar substorm and the low latitude negative bay in the evening sector is attributed to the asymmetric ring current, it is believed that the polar substorm and the ring current are growing "almost" simultaneously. In fact, Cummings and Coleman (1968) and Figure VI-2 show that magnetic variations, at Honolulu and at geocentric distance of 6.6 radii (ATS-1), in the same sector are strikingly similar. This is direct proof of the above statement. Davis and Parthasarathy (1967) demonstrated that small DR (ring current) events follow after DP (polar substorm) substorms perhaps by as long as 15 hours. Their parameters, AE and Dst, are based on hourly values, so that they are not necessarily suitable in the examination of this particularly important point. A finer time-scale AE index seems to be needed. Further, the concept of Dst index is based on the assumption that by averaging the main phase values obtained from stations along a constant  $d\phi$  latitude circle we can eliminate the return current effect. The DS component

in low latitudes had been thought to be the return current effects, but it is now found to be mostly the asymmetric component of the ring current. Therefore, the Dst index is not necessarily the best index to indicate the intensity of the ring current. This is particularly the case in our study and it is indeed not very suitable in solving one of our crucial problems such as the cause-effect relationship between polar substorms and the growth of the ring current.

Since it is a rather difficult problem to find the definite solution, the following precautions should be taken in future studies.

- 1) When the duration of the initial phase is very short, the hourly mean values are not accurate enough to determine the difference between the onset of the main phase and that of the polar substorm.
- 2) It is necessary to distinguish between the onset of the development and the maximum epoch of each phenomenon.
- 3) It is necessary to reexamine whether or not the difference of the peak times for both phenomena indicates the cause-effect relation, as Axford suggested.
- 4) A comment on the AE index: The present AE index is evaluated on the basis of data obtained from northern hemispheric stations. In the summer months, the positive bay is largely enhanced by the increase of ionospheric conductivity due to solar radiation (for detail see Chapter III, Section 3). This seasonal variation of the positive bay can be very clearly seen in Figure IV-5 which is the hourly value of H component at College from 1957 to 1965. The AE index is the combination of the AU, which is the envelope resulting from the maximum positive H deviations along the auroral zone, and AL which is the envelope of the

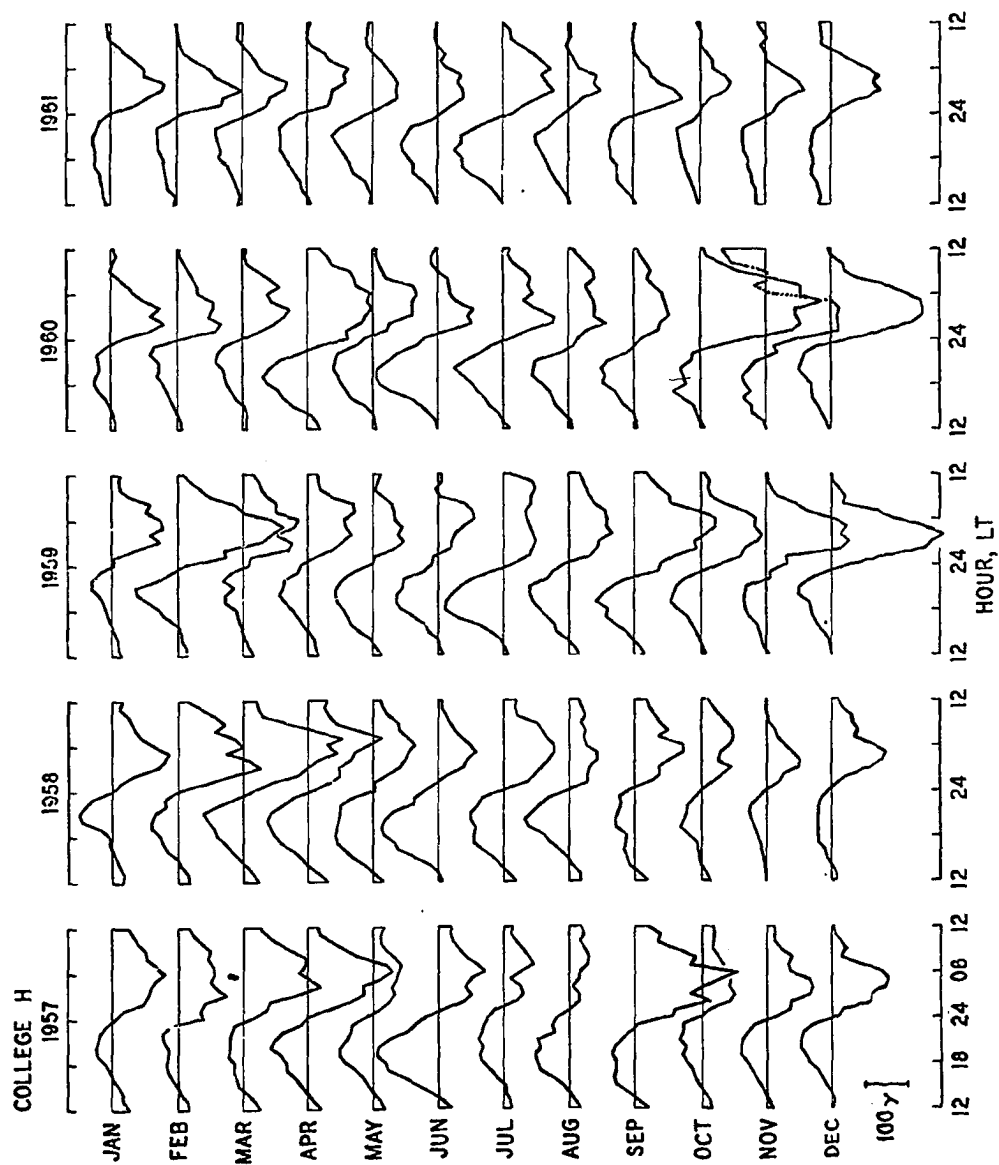


Fig. VI-5. The hourly value of H component at College from 1957 to 1965.

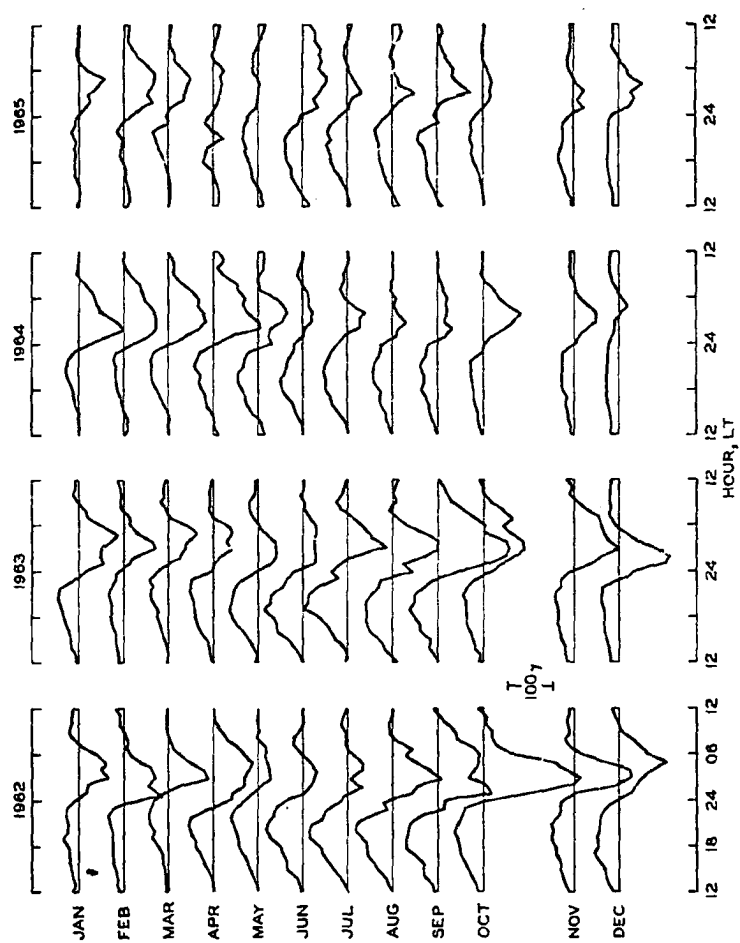


Fig. VI-5. (Continuation).

maximum negative H deviations along the auroral zone. If only the northern auroral zone stations are used to produce AE, then the seasonal variation of the positive bay will show up in AE. More explicitly, AE is larger in the northern summer than in the northern winter, and this seasonal variation is not due to the increase of polar substorm activity but due to the increase of conductivity in the northern winter. Therefore, the same number of stations should be taken from both hemispheres to eliminate this seasonal variation of the positive changes of the H component.

- 5) As already discussed in Chapter V, the ssc can enhance the already present polar substorm activities which also could be misinterpreted as the development of the polar substorm preceding that of the main phase.

The onset of the development of the intense polar substorm and the growth of the ring current can not be very accurately defined at present, but it is believed that they occur "about" simultaneously with the accuracy of our study, and it is very unlikely that the polar substorm activity preceding the main phase of the storm by 10 hours is related to the development of the ring current based on this study. In a detailed comparison, a fine time scale is required and the asymmetry has to be considered as the major feature of the ring current during its growing stage.

##### 5. Eastward Current in the Afternoon Sector of the Auroral Zone

Magnetic disturbances recorded along the auroral zone are very systematic. Positive bays, an increase in the H (horizontal) component of magnetic force, occur in the evening hours. A sharp negative change occurs in the midnight sector and is called a negative bay. A broad negative



change in H occurs in early morning hours. Since disturbances of the geomagnetic field may be expressed by means of equivalent electric current systems (in the ionosphere), the conventional SD (or DS) type current system, has been used to represent the equivalent current system of polar magnetic substorms (geomagnetic bays). The magnetic disturbances due to this SD type current system fit the average features of the magnetic disturbances recorded at any single station along the auroral zone. But in the past few years, by using the IGY/C and IQSY simultaneous data all over the world, it is found that the fields of the polar magnetic substorm do not fit the magnetic disturbance represented by the SD current system. Even the average features of polar magnetic substorms are different from the magnetic disturbance field of this conventional SD type current system.

- 1) The conventional SD current system does not represent the observed polar magnetic disturbance fields (Chapter III, Section 2-1).

According to the SD current system (Figs. II-1, and III-5), there are two primary electrojets along the auroral zone. There is an eastward electrojet in the evening sector and a westward electrojet in the midnight and morning sectors. The magnitude of the westward electrojet is usually larger than that of the eastward electrojet. The return current of these two primary electrojets spreads both poleward and equatorward of the auroral zone. Therefore, in the evening sector, the station located poleward of the auroral zone (point B in Fig. VI-6a) should observe a negative bay; the station along the auroral zone (point A in Fig. VI-6) should observe a positive bay with a larger magnitude. The station located equatorward of the auroral zone (point C in Fig. VI-6) should observe a negative bay. From the analysis in Chapter III, Section 2-1(a) and (b),

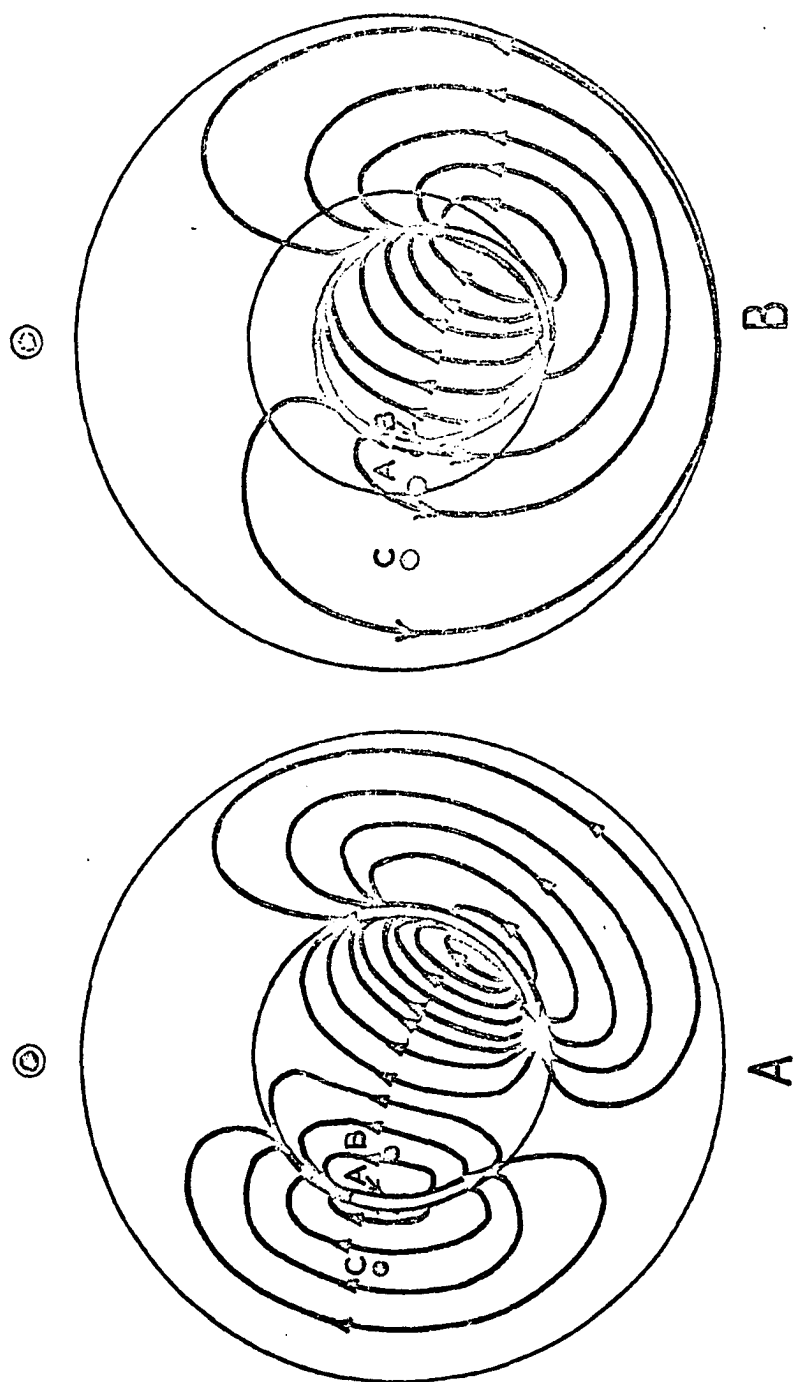


Fig. VI-6. A. Earlier model current system (schematic) for polar magnetic substorms.

B. New model current systems (schematic) for polar magnetic substorms.

it is shown that the results obtained by analyzing the simultaneous observation along a north-south chain station across the auroral zone are not consistent with what is expected from the SD type current system. A more intense negative bay is observed poleward of the auroral zone (at point B), and a positive bay, rather than the expected negative bay, is observed a little equatorward of the auroral zone (at point C) in the evening sector. This is not in agreement with what the SD current system indicates and is also shown in the statistical study of the high latitude magnetic disturbance as shown in Chapter IV, Section 2 (c). Therefore, the results from the high latitude magnetic disturbance study, by using both the individual case method and the statistical method indicate that the SD current system cannot accurately represent the equivalent current system for magnetic disturbances during polar substorms.

From the statistical study of the polar magnetic disturbance (see Fig. III-15), negative bays are observed not only in the dark hemisphere of the polar region but also in the dayside of the polar region between  $dp$  lat  $70^\circ$  to  $80^\circ$ . Negative bays are observed along the auroral oval. Since, the ionospheric conductivity is higher in the region where auroras exist, it is reasonable to assume that during a polar magnetic substorm, the westward electrojet, which produces a negative bay, can flow along the auroral oval. The observation of simultaneous magnetic disturbances over the polar region (see Fig. IV-16, Fig. IV-19 and also Chapter III, Section 3) is consistent with this suggestion. The magnitude of this westward electrojet decreases toward the noon meridian and this decrease can be attributed to the spreading of the current over the polar cap and toward lower latitudes (Fig. VI-6b).

- 2) The nature of the eastward current in the evening sector is different from that of the westward electrojet (Chapter III, Section 3).

Positive bays along the auroral zone in the evening sector are very intense and in some cases, they can be as large as 1000Y as in Figure IV-12. Therefore, some workers believe that such a positive bay is produced by a primary electrojet flowing eastward, even though they agree that the polar westward electrojet flows along the oval. Thus, whether such a positive bay is due to the return current or an independent primary electrojet has been a matter of argument.

Polar substorms occur simultaneously in the conjugate areas. The study of the conjugacy of positive and negative bays (for details see Chapter III, Section 3), shows that positive bays are more intense at a summer hemispheric station than at the conjugate winter hemispheric station, but the magnitude of negative bays is approximately the same at both conjugate stations. It is also shown that positive bays are much less associated with significant cosmic noise absorption recorded by riometer than negative bays (see Fig. III-52). This implies that ionization by solar radiation largely determines the magnitude of positive bays and it is not directly associated with intense auroral particle influx. However, negative bays, which are produced by the westward polar electrojet, are associated with intense auroral particle precipitation. Therefore, it is very obvious that the nature of positive bays produced by the eastward current is different from that of negative bays produced by the westward polar electrojet which is believed to be the primary current during a polar substorm.

- 3) The positive bay in the evening sector is probably due to the return current of an intense westward electrojet (Chapter III, Section 2-2)

On the basis of the simultaneous study of polar magnetic substorms and auroral substorms, the following morphological feature of negative bays and positive bays in the evening sector should be noted.

When positive bays are observed at a typical auroral zone station, westward traveling auroral surges are observed in the northern sky of the observatory, and negative bays are observed when the westward surge is overhead. It is known that the westward auroral surge propagating westward along the auroral oval is one of the most important types of auroral activity during the polar substorm. Since the auroral zone is the locus of the midnight part of the auroral oval, the majority of the oval lies inside the auroral zone. In the evening sector, say at 2000 local time, the oval is located, on the average, between  $\text{dp lat } 68^\circ$  and  $73^\circ$ . The oval is located at about 400 km or even farther to the north at typical auroral zone stations such as College and Kiruna. It is almost impossible to observe the major auroral activity from such a station. In other words, when a positive bay is observed at an auroral zone station, a negative bay produced by the westward polar electrojet is observed to the north of the auroral zone. This strongly suggests that the positive bay in the evening sector along the auroral zone is not produced by the primary electrojet similar to the westward polar electrojet along the auroral oval.

- 4) Other supporting evidence to support the new current system

By studying magnetic disturbances at subauroral stations, Rostoker (1966) showed that the magnetic change of the D component showed a drop in occurrence frequency around local midnight relative to the number of

events before and after and also that the occurrence of the midlatitude transition bay agreed with the new current system.

Scrase (1967) studied polar magnetic substorms by using the record at Lerwick and two neighboring temporary stations to determine the associated ionospheric current system. He found that on the average the polar substorm can be explained by a current system in which the primary current is a polar electrojet flowing westward. This intense westward electrojet causes the negative bays of polar substorms while the positive bays are due to the weaker eastward return flow. This result also supports the new polar electrojet system.

#### 5) Arguments against the new current system

This newly suggested polar electrojet was criticized by Heppner (1967). The points which he questioned are the following:

(a) Direct spatial association between the occurrence of aurora and the eastward current.

As mentioned in 3), positive bays are associated with auroral activity, the westward traveling surge. Unfortunately, this activity is not clearly observable at College, since the distance between the surge and the station is at least 500 kms. Heppner could not see the center of the auroral activity, he could see only minor activity which occurred near the southern fringe of the surge and associated it only with the positive bay (the curtain-like diffuse aurora, rather than the auroral surge).

(b) The low latitude negative bay as an indication of the return current from the eastward electrojet along the auroral zone.

This problem was explicitly discussed in Chapter IV. It was shown that these negative bays cannot be due to the return current of the eastward electrojet. In fact negative bays in middle and low latitudes in the evening sector are due to the asymmetric growth of the ring current.

(c) The existence of an intense westward current beyond the auroral zone in the evening sector.

Heppner questioned the existence of an intense westward electrojet beyond the auroral zone. The existence of this intense westward electrojet is discussed in Chapter III, Section 2. Feldstein's (1966) results also showed the existence of an intense westward current beyond the auroral zone.

Foppl et. al. (1968) measured the electric field at Kiruna by the barium ion cloud method. One of the five experiments showed a northwestward current slightly to the west of the region where the westward electrojet is flowing. This result does not fit the new polar electrojet system. However, since the magnetic disturbances during the experiment were very weak, they stated that this result could not be conclusive evidence.

## 6) Conclusion

Based on these studies, it is suggested that the westward current which flows between dipole latitudes  $70^\circ$  and  $80^\circ$  in the evening and afternoon sectors is an extension of the westward polar electrojet flowing along the auroral oval in the midnight sector. This westward current produces an eastward return current and thus is observed as a positive bay in the auroral zone and also in middle latitudes in the same sector.

Unless definite reasons are found that the westward electrojet cannot leak toward lower latitudes, the observational evidence strongly suggests that a significant part of the positive bay is produced by the return flow

of the intense westward electrojet along the auroral oval. This problem still needs further investigation by using the closely spaced north-south magnetometer chain network or the electric field measurement. However, one cannot completely ignore the occasional occurrence of an eastward electrojet as for example in the case found by Akasofu and Chapman (1960).



```

// JOB ASA-PO 448 R. PORTER JAN,68 POLAR PLOTS FOR 7HR SPECIAL
* GEOPHYSICAL INSTITUTE COURIER SERVICE
// OPTION LINK
// EXEC FORTRAN
C
C
C      X' AND Y' TAPE IS STORED IN SLOT NO 267 (G1011026)
C      CONTROL HEADER CARD FORMAT
C      COL 1 (IPC) PLOT CONTROL. 1 FOR POLAR PLOT, 2 FOR EQUATORIAL PLOT
C      COL 2-3 (NS) NUMBER OF STATIONS (NOT TO EXCEED 80)
C      COL 4-6 (NA) 'TIME' OF FIRST PLOT 1=1200,2=1205,...,48=1555.
C      COL 7-9 (NB) 'TIME' OF LAST PLOT
C      COL 10-12 (NC) 'TIME' INTERVAL 1=EVERY 5MIN, 2=EVERY 10 MIN ETC.
C      COL 13 (ITC1) CONTROLS WRITING OF DATA TAPE ON DRIVE 180
C      O=NO TAPE WRITTEN 1=WRITES TAPE WITH ALL DATA CALCULATED
C      COL 14 (ITC2) CONTROLS READING OF A DATA TAPE INSTEAD OF CARDS
C      O=READS AND CALCULATES FROM CARDS, 1=READS AND USES TAPE DATA
C
C      ALSO SEE PREHEADER,HEADER AND DATA CARD FORMATS
C
C
C
C      DIMENSION XP(80,48),YP(80,48),CR(2,48),      GPLAT(80),GMLONG(80)
C      DIMENSION SL(4),R(84)
C
C
C      READ CONTROL HEADER
C      READ(1,100)IPC,NS,NA,NB,NC,ITC1,ITC2
100 FORMAT(I1,I2,3I3,2I1)
C      IF ITC2 IS 1 DATA WILL COME FROM A TAPE
C      IF(ITC2-1)2,500,2
C      DATA COMES FROM CARDS-SO READ THEM AND CALIBRATE
2 DO 3 N=1,NS
C      LABEL PAGE FOR STATION LIST
C      WRITE(3,200)
200 FORMAT('1','NO. GEOM.LAT. GEOM.LONG GECG.LAT.      GEOG.LONG. DECL
1IN. STATION NAME')
C      READ(1,101)GPLAT(N),GMLONG(N),GGLAD,GGLAM,GGLAS,GGLOD,GGLOM,GGLOS,
1DECD,DECM,(SL(K),K=1,4)
101 FORMAT(2F10.3,F4.0,2F2.0,2X,F4.0,2F2.0,2X,F4.0,F2.0,17X,4A4)
C      WRITE(3,201)N,GMLAT(N),GMLONG(N),GGLAD,GGLAM,GGLAS,GGLOD,GGLOM,
1GGLOS,DECD,DECM,(SL(K),K=1,4)
201 FORMAT(' ',I3,2F10.3,F5.0,2F4.0,F5.0,2F4.0,F5.0,F4.0,2X,4A4)
C      PRE-HEADER IS NOW READ AND LISTED
C
C      READ AND CALIBRATE 1ST COMPONENT- READ ITS HEADER
C      DO 10 M=1,2
C      READ(1,102)OSCCTS,GAMMAS,ICHECK,(SL(K),K=1,4)
102 FORMAT(16X,F8.0,F8.0,18X,I1,12X,4A4)
C      IF(ICHECK-9)99,4,99
99 WRITE(3,202)(SL(K),K=1,4)
202 FORMAT('1','STATION ',4A4,' CARDS OUT OF SEQ. PROCESSING STOPPED')
C      STOP

```

```

      4 C=GAMMAS/OSCCIS
      DO 5 L=1,7
      L1=((L-1)*12)+1
      L2=L1+11
      READ(1,103)(R(K),K=L1,L2),ICOMP
103  FORMAT(12F4.0,2X,11)
      5 CONTINUE
C
C   CALIBRATE ALL READINGS
      DO 6 L=1,84
      6 R(L)=R(L)*C
C
C   FIND 11-12 AVERAGE
      TOT=0.0
      DO 7 L=13,24
      7 TOT=TOT+R(L)
      AV1=TOT/12.
C
C   FIND AVERAGE FOR 16 TO 17
      TOT=0.0
      DO 8 L=73,84
      8 TOT=TOT+R(L)
      AV2=TOT/12.
      AVC=AV2-AV1
C
C   SUBTRACT OUT MOVING BASE LINE AND STORE IN CALIBRATED READING (CR)
      DO 9 L=1,48
      Z=L
      LR=L+24
      9 CR(M,L)=R(LR)-((((6.+Z)/60.)*AVD)+AV1)
10  CONTINUE
C
C   LIST CALIBRATED VALUES FOR CHECKING
      WRITE(3,204)
204  FORMAT('0','H OR X CALIBRATED VALUES')
      DO 97 L=1,4
      L1=((L-1)*12)+1
      L2=L1+11
      WRITE(3,205)(CR(1,K),K=L1,L2)
205  FORMAT(' ',12F10.2)
      97 CONTINUE
      WRITE(3,206)
206  FORMAT('0','D OR Y CALIBRATED VALUES')
      DO 98 L=1,4
      L1=((L-1)*12)+1
      L2=L1+11
      WRITE(3,205)(CR(2,K),K=L1,L2)
      98 CONTINUE
C
C   CONVERT READINGS TO XPRIME (XP) AND YPRIME(YP).
C   IF ICOMP IS 2 THEN CONVERT FROM HAND D. IF ICOMP IS 4 CONVERT
C   FROM X AND Y.
C
C   FIRST FIND ALPHA

```

```

C
C FIND ANGLE ALPHA
C FIND RADIANS FOR ALL ANGLES
C RGMLA=GEOMAGNETIC LATITUDE IN RADIANS
C RGMLG=GEOMAGNETIC LONGITUDE IN RADIANS
C RGGLA=GEOGRAPHIC LATITUDE IN RADIANS
C RGGLG=GEOGRAPHIC LONGITUDE IN RADIANS
C RDEC=DECLINATION IN RADIANS
C RPLAT=LATITUDE OF POLE IN RADIANS
C RPLONG=LONGITUDE OF POLE IN RADIANS
C
C NOTE ON ABOVE. EASTWARD (AND NORTH) ARE ALWAYS CONSIDERED PLUS.
C
C 90 DEG IS PI/2 RADIANS (1.57079)
C 180 DEG IS PI RADIANS (3.14159)
C 360 DEG IS 2*PI RADIANS (6.28318)
C
C RGMLA=GMLAT(N)*.01745329
C RGMLG=GMLONG(N)*.01745329
C RGGLA=(ABS(GGLAD*.01745329))+(GGLAM*.000290888)+(GGLAS*.000004848)
C IF(GGLAD)11,12,12
11 RGGLA=6.28318-RGGLA
12 RGGLG=(ABS(GGLGD*.01745329))+(GGLGM*.000290888)+(GGLGS*.000004848)
C IF(GGLGD)13,14,14
13 RGGLG=6.28318-RGGLG
14 RDEC=(ABS(DECD*.01745329))+(DECM*.000290888)
C IF(DECD)15,16,16
15 RDEC=6.28318-RDEC
16 RPLAT=78.6*.01745329
C RPLONG=289.9*.01745329
C
C PROGRAMMED MODIFIED FOR C.MENG'S EQUATIONS AND METHOD OF JAN 24,68
C
C Q1 IS PI/2-PHIZERO PHIZERO IS GEOGRAPHIC LAT.OF POLE(78.6)
C Q2 IS PI/2-PHI PHI IS GEOGRAPHIC LAT OF STATION (RGGLA)
C Q3 IS LAMBDZERO-LAMBDA LAMBDZERO IS GEOGRAPHIC LONG.POLE(289.9)
C Q4 IS CAPLAMBDA-180 CAPLAMBDA IS GEOMAG. LONG OF STAT(RGMLG)
C Q1=1.57079-RPLAT
C Q2=1.57079-RGGLA
C Q3=RPLONG-RGGLG
C Q4=RGMLG-3.14159
C
C FIND THE SIN(ALPHA) AND COS(ALPHA) FROM CHING'S 1/24/68 EQUATIONS
C SINA=(SIN(Q1)/SIN(Q2))*SIN(Q4)
C COSA=(SIN(Q4)*SIN(Q3)*COS(Q1))-(COS(Q4)*COS(Q3))
C Z=SINA/COSA
C ALPHA=ATAN(Z)
C ALPHAD=ALPHA*57.295779
C SQ=(SINA*SINA)+(COSA*COSA)
C WRITE(3,208)SINA,COSA,ALPHA,ALPHAD,SQ
208 FORMAT('O','SINA=',F10.6,5X,'COSA=',F10.6,5X,'ALPHA(RADIANS)=' ,F10
1.5,5X,'ALPHA( DEG)=' ,F10.3,5X,'SINA**2+COSA**2=' ,F10.6)
C WRITE(3,220)

```

```

220 FORMAT(' ', 'NOTE ALPHA MAY BE IN WRONG QUADRANT. IT IS PRINTED FOR
REFERENCE ONLY')
C
C   CONVERT TO XPRIME AND YPRIME
IF(ICOMP-2)18,17,18
17 WRITE(3,221)
221 FORMAT('0', 'THIS IS AN H-D STATION. NEW SINA AND COSA ARE FOUND BY
SUBTRACTING DECLINATION (USING ANGLE DIFFERENCE RELATIONS)')
SINAA=SINA
SINA=(SINA*COS(RDEC))-(COSA*SIN(RDEC))
COSA=(COSA*COS(RDEC))+(SINAA*SIN(RDEC))
Z=SINA/COSA
ALPHA=ATAN(Z)
ALPHAD=ALPHA*57.295779
SQ=(SINA*SINA)+(COSA*COSA)
WRITE(3,222)SINA,COSA,ALPHA,ALPHAD,SQ
222 FORMAT('0', 'SINA=',F10.6,5X,'COSA=',F10.6,5X,'ALPHA(R)=',F10.5,5X,
1'ALPHA(DEG)=',F10.3,5X,'SINA**2+COSA**2=',F10.6)
18 DO 19 L=1,48
XP(N,L)=(CR(1,L)*COSA)+(CR(2,L)*SINA)
YP(N,L)=(CR(2,L)*COSA)-(CR(1,L)*SINA)
19 CONTINUE
C
C   LIST XP AND YP VALUES FOR CHECKING
WRITE(3,210)
210 FORMAT('0', 'XPRIME VALUES')
DO 95 L=1,4
L1=((L-1)*12)+1
L2=L1+11
WRITE(3,205)(XP(N,LLL),LLL=L1,L2)
95 CONTINUE
WRITE(3,211)
211 FORMAT('0', 'YPRIME VALUES')
DO 96 L=1,4
L1=((L-1)*12)+1
L2=L1+11
WRITE(3,205)(YP(N,LLL),LLL=L1,L2)
96 CONTINUE
3 CONTINUE
C
C   ALL DATA CARDS HAVE BEEN READ AND CONVERTED TO XPRIME AND YPRIME
C
C
C
C   WRITE A TAPE ON DRIVE 180 IF ITC1 IS NOT ZERO
IF(ITC1)20,21,20
20 DO 22 N=1,NS
WRITE(8)N,GMLAT(N),GMLONG(N),(XP(N,K),K=1,48),(YP(N,K),K=1,48)
22 CONTINUE
GO TO 21
C
C   READ A TAPE SECTION
500 DO 501 N=1,NS
READ(8)N,GMLAT(N),GMLONG(N),(XP(N,K),K=1,48),(YP(N,K),K=1,48)
501 CONTINUE

```

```
C
C      PLOT SECTION
      21 WRITE(3,203)
      203 FORMAT('1','TO BE CONTINUED AT A LATER DATE')
      STOP
      END
/*
// EXEC LNKEDT
// EXEC
```

```

// JOB POLAR 448 R PORTER PLOTS FOR C. MENG FEB. 68
* GEOPHYSICAL INSTITUTE COURIER SERVICE
// OPTION DECK
// EXEC FORTRAN
C
C
C ACCEPTS AS INPUT THE TAPE MADE BY PROGRAM ASA-PO WITH XPRIME AND
C YPRIME VALUES AND GENERATES A TAPE FOR POLAR PLOTS
C INPUT TAPE IS GIO11026 STORED IN SLOT NO. 267 -PUT ON DRIVE 180
C OUTPUT TAPE IS GIO11027-PUT ON DRIVE 181. STORED IN SLOT 262
C
C 3 INPUT CARDS ARE USED FOR PROGRAM CONTROL
C 1. CARD TO INDICATE NO. OF STATIONS ON INPUT TAPE TO BE READ
C   FORMAT =COL 1-2 = NO. OF STATIONS (NS) (NOT TO EXCEED 80)
C 2. CARD TO INDICATE WHICH TIMES ARE TO BE PLOTTED OF THE 48 AVAIL-
C   ABLE TIMES
C   FORMAT =COLS 1-48 PUT A ZERO IN ALL COLS CORRESPONDING TO TIMES
C   NOT TO BE PLOTTED. PUT A 1(OR ANY DIGIT) IN COLS WITH NUMBERS
C   CORRESPONDING TO TIMES TO BE PLOTTED. (KTIME(K),K=1,48)
C 3. CARD TO INDICATE WHICH STATIONS ARE TO BE PLOTTED.
C   FORMAT =COLS 1-80 PUT A ZERO IN ALL COLS CORRESPONDING TO
C   STATIONS NOT TO BE PLOTTED. PUT A 1(OR ANY DIGIT) IN COLS
C   WITH NUMBERS(FOR STATION NUMBERS SEE PRINTOUT OF ASA-PO OR
C   ASA-PT)CORRESPONDING TO THE STATIONS TO BE PLOTTED (KSTAT(K),
C   K=1,80)
C *****IF IT IS DESIRABLE TO LABEL THE STATION NUMBER BESIDE ITS
C   DATA POINT, PUT A 2 IN THE CORRESPONDING COLUMN.
C A 4TH CARD IS USED WITH THE ALPHA TITLES FOR THE PAGE AND TIME
C
C INPUT TAPE LAYOUT - FOR EACH STATION
C STATION NUMBER, GEOMAG. LAT,GEOMAG.LONG.,48 XPRIME VALUES AND THEN
C 48 Y PRIME VALUES.
C
C PLOTTING INSTRUCTIONS.
C A TAPE IS MADE ON DRIVE 181. THIS TAPE MAY BE USED FOR PLOTTING
C ON THE GEO.INST PLOTTER OR MAY BE CONVERTED TO CARDS USING THE
C 360 WITH STEVE GELLER'S PLOTTER SIMULATOR PROGRAM AND THE CARDS
C USED FOR PLOTTING ON THE 1620. IN EITHER CASE THE FOLLOWING
C INSTRUCTIONS APPLY.
C 1. USE BLANK PAPER
C 2. USE .4MM BLACK INK PEN
C 3. ZERO PLOTTER IN CENTER OF PAPER,THAT IS 6 INCHES IN FROM
C   EITHER SIDE. NOTE THE PLOTTER WILL MOVE 5INCHES IN NEG X
C   DIRECTION. THUS MAKE SURE THERE IS ABOUT 1FOOT OF PAPER
C   ON TAKE UP SPOOL BEFORE STARTING FIRST PLOT.
C
C
C DIMENSION ASIN(361),ACOS(361),GMLAT(80),GMLONG(80),XP(80,48),
C IYP(80,48),KTIME(48),KSTAT(80),ALAB1(17)
C
C READ HEADER CARDS
C READ(1,100)NS
C 100 FORMAT(12)

```

```

      READ(1,101)(KTIME(K),K=1,48)
101  FORMAT(48I1)
      READ(1,102)(KSTAT(K),K=1,80)
102  FORMAT(80I1)
      READ(1,103)(ALAB1(K),K=1,17),ALAB2
103  FORMAT(18A4)
C
C      MAKE SIN AND COSINE TABLE
      DO 2 N=1,361
      Z=N
      Z=Z*.01745329
      ASIN(N)=SIN(Z)
      ACOS(N)=COS(Z)
2  CONTINUE
C
C      READ DATA TAPE
      DO 3 N=1,NS
      READ(8)M,GMLAT(N),GPLONG(N),(XP(N,K),K=1,48),(YP(N,K),K=1,48)
3  CONTINUE
C
C      CALL PLOTS
      DO 48 L=1,48
      IF(KTIME(L))4,48,4
C
C
C      PUT IN A DELAY TO ALLOW OPERATOR TO MAKE ANY ADJUSTMENTS NECESSARY
C      THIS IS ACCOMPLISHED BY DRIVING PEN OFF SCALE TO THE RIGHT 20
C      INCHES, AND THEN MOVING NEW ZERO UP 5.5 INCHES.
4  CALL PLOT(0.0,-20.,3)
   CALL PLOT(0.0,-14.5,-3)
C
C      WRITE PLOT NUMBER ON PRINTER IN CASE A RESTART IS REQUIRED
      WRITE(3,200)L
200  FORMAT(' ', 'PLOT NUMBER NOW IN PROGRESS IS',I3)
C      PLOT AT POLE FOR CHECK
      CALL SYMBOL(0.0,0.0,.07,04,0.0,-1)
C
C      DRAW AXIS AND 45DEG LINES
      CALL PLOT(5.0,-5.0,2)
      CALL PLOT(5.0,5.0,2)
      CALL PLOT(-5.0,5.0,2)
      CALL PLOT(-5.0,-5.0,2)
      CALL PLOT(5.0,-5.0,2)
      CALL PLOT(5.0,0.0,2)
      CALL PLOT(-5.0,0.0,2)
      CALL PLOT(0.0,5.0,3)
      CALL PLOT(0.0,-5.0,2)
      CALL PLOT(-5.0,-5.0,2)
      CALL PLOT(5.0,5.0,2)
      CALL PLOT(-5.0,5.0,2)
      CALL PLOT(0.0,0.0,2)
C
C      DRAW CIRCLES AT 60 DEG, 30 DEG, AND 0 DEG LATITUDES
      CALL PLOT(1.5,0.0,3)

```

```

DO 5 N=1,361
X=ACOS(N)*1.5
Y=ASIN(N)*1.5
CALL PLOT(X,Y,2)
5 CONTINUE
CALL PLOT(3.0,0.0,3)
DO 6 N=1,361
X=ACOS(N)*3.0
Y=ASIN(N)*3.0
CALL PLOT(X,Y,2)
6 CONTINUE
CALL PLOT(4.5,0.0,3)
DO 7 N=1,361
X=ACOS(N)*4.5
Y=ASIN(N)*4.5
CALL PLOT(X,Y,2)
7 CONTINUE
C
C LABEL LONGITUDE LINES
CALL NUMBER(4.6,0.2,.14,0.0,0.0,-1)
CALL NUMBER(-.2,4.6,.14,90.,90.,-1)
CALL NUMBER(-5.0,0.2,.14,180.,0.0,-1)
CALL NUMBER(.2,-4.6,.14,270.,270.,-1)
C
C LABEL 30 DEG AND 60 DEG LATITUDE CIRCLES
C
CALL NUMBER(1.1,-2.9,.14,30.,5.0,-1)
CALL NUMBER(1.1,-1.3,.14,60.,5.0,-1)
C
C TITLE GRAPH AT BOTTOM
CALL SYMBOL(-4.6,-5.2,.14,ALAB1,0.0,69)
C
C COMPUTE AND LABEL TIME IN LOWER RIGHTHAND CORNER
HOUR=(L-1)/12+12
MIN1=(L-1)*5
MIN2=(L-1)/12
MIN3=MIN2*60
AIN=MIN1-MIN3
CALL SYMBOL(2.5,-4.9,.14,ALAB2,0.0,4)
CALL NUMBER(3.2,-4.9,.14,HOUR,0.0,-1)
CALL SYMBOL(3.4,-4.9,.14,122,0.0,-1)
CALL NUMBER(3.5,-4.9,.14,AIN,0.0,-1)
CALL SYMBOL(3.8,-4.9,.14,100,0.0,-1)
CALL SYMBOL(3.95,-4.9,.14,99,0.0,-1)
C
C NOW PLOT EACH STATION AS INDICATED BY KSTAT'S
DO 80 M=1,80
IF(KSTAT(M))8,80,8
C
C CALCULATE AND PLOT X AND Y VALUES FOR LOCATION OF STATION ON MAP
8 T=GMLUNG(M)*.01745329
X=((90.-GMLAT(M))*0.5)*COS(T)
Y=((90.-GMLAT(M))*0.5)*SIN(T)
IF(KSTAT(M)-2)13,12,13
12 X3=X+.07
Y3=Y-.02

```



```

      STANUM=M
      CALL NUMBER(X3,Y3,.07,STANUM,0.0,-1)
13  CALL SYMBOL(X,Y,.07,01,0.0,-1)
C
C      CALCULATE NEW X AND Y VALUES USING XPRIME AND YPRIME AND PLOT
      IF(GMLAT(M)-60.)9,10,10
      9  AULT=.005
      GO TO 11
10  AULT=.001
11  X2=X+((( -1.*COS(T)*XP(M,L))+(-1.*SIN(T)*YP(M,L)))*AULT)
      Y2=Y+((( -1.*SIN(T)*XP(M,L))+COS(T)*YP(M,L))*AULT)
      AL=2.
      CALL PLOT(X2,Y2,2)
80  CONTINUE
C
C      PLOT A CHECK POINT AT POLE
      CALL SYMBOL(0.0,0.0,.07,04,0.0,-1)
C
C      MOVE TO NEW ZERO
      CALL PLOT(15.,0.0,-3)
48  CONTINUE
C
C      END JOB
      CALL PLOT(0.0,0.0,99)
      STOP
      END
/*
/*

```

## REFERENCES

- Akasofu, S.-I., Large-scale auroral motions and polar magnetic disturbances - I., A polar disturbance at about 1100 hours on Sept. 23, 1957, *J. Atmosph. Terr. Phys.*, 19, 10-25, 1960.
- Akasofu, S.-I., A source of the energy for geomagnetic storms and auroras, *Planetary Space Sci.*, 12, 801-833, 1964.
- Akasofu, S.-I., The neutral hydrogen flux in the solar plasma flow, *Planetary Space Sci.*, 12, 905-913, 1964.
- Akasofu, S.-I., The development of the auroral substorm, *Planet. Space Sci.*, 12, 273-282, 1964.
- Akasofu, S.-I., Dynamical morphology of auroras, *Space Sci. Rev.*, 4, 498-540, 1965.
- Akasofu, S.-I., Electrodynamics of the magnetosphere: Geomagnetic Storms, *Space Sci. Rev.*, 6, 21-143, 1966.
- Akasofu, S.-I. and S. Chapman, The ring current geomagnetic disturbance, and the Van Allen Radiation belts, *J. Geophys. Res.*, 66, 1321-1350, 1961.
- Akasofu, S.-I. and S. Chapman, Magnetic Storms: Their geometrical and physical analysis, and their classifications, pp. 40, 12. Particular magnetic storms, *Studia. Geoph. et Geod.*, 5, 1961.
- Akasofu, S.-I. and S. Chapman, Large scale auroral motions and polar magnetic disturbances IV: The aurora and magnetic storm of 11 February, 1958, *J. Atmosph. Terr. Phys.*, 24, 735-796, 1962.
- Akasofu, S.-I. and S. Chapman, Magnetic storms: The simultaneous development of the main phase (DR) and of polar magnetic storms (DP). *J. Geophys. Res.*, 68, 3155-3158, 1963.
- Akasofu, S.-I. and S. Chapman, On the asymmetric development of magnetic storm fields in low and middle latitudes, *Planet. Space Sci.*, 12, 607-626, 1964.
- Akasofu, S.-I. and S. Yoshida, Growth and decay of the ring current and the polar electrojets, *J. Geophys. Res.*, 71, 231-240, 1966.
- Akasofu, S.-I. and S. Chapman, A systematic shift of the DS axis, *Planet. Space Sci.*, 15, 937-938, 1967.
- Akasofu, S.-I., S. Chapman and P. C. Kendall, The significance of the multiple structure of the auroral arc, *Aurora and Airglow*, Reinhold, New York, 1967.

- Akasofu, S.-I. and C. E. McIlwain, Energetic neutral hydrogen atoms as a source of the ring current particles, *Trans. Amer. Geophys. Union*, 44, 883, 1963.
- Akasofu, S.-I. and C.-I. Meng, The abnormally early appearance of active auroras, *J. Atmosph. Terr. Phys.*, 29, 601-602, 1967.
- Akasofu, S.-I., D. S. Kimball and C.-I. Meng, The dynamics of the aurora - Westward drifting loops, *J. Atmosph. Terr. Phys.*, 27, 189-196, 1965.
- Alfven, H., *Cosmical Electrodynamics*, Oxford Univ. Press, 1950.
- Alfven, H., On the electric field theory of magnetic storms and aurorae, *Tellus*, 1, 50-64, 1955.
- Axford, W. I., Magnetic storm effects associated with the tail of the magnetosphere, *Space Science Rev.*, 7, 149-157, 1967a.
- Axford, W. I., The interaction between the solar wind and the magnetosphere, *Aurora and Airglow*, ed. by McCormac, Reinhold, New York, 1967b.
- Axford, W. I. and C. O. Hines, A unifying theory of high latitude geophysical phenomena and geomagnetic storms, *Canadian J. Phys.*, 39, 1433-1464, 1961.
- Behannon, K. W. and N. F. Ness, Magnetic storms in the earth's magnetic tail, *J. Geophys. Res.*, 71, 2327-2351, 1966.
- Birkeland, K., *Norwegian Aurora Polaris Expedition 1902-03*, Vol. I and II. Christiania, H. Aschehong 1908, 1913.
- Birkeland, K., *Phenomenes celestes et analogies experimentales*, *Comptes. Rendus Acad. Sci. Paris*, 153, 938-940, 1911.
- Block, L. P., On the distribution of electric fields in the magnetosphere, *J. Geophys. Res.*, 71, 858-864, 1966.
- Brandt, J. C. and D. M. Hunten, On ejection of neutral hydrogen from the sun and the terrestrial consequences, *Planetary Space Sci.*, 14, 95-105, 1966.
- Burdo, O. A., USSR Academy of Sciences Press, Moscow, DRB Transl. T321R 1957.
- Cahill, L. J., Inflation of the inner magnetosphere during a magnetic storm, *J. Geophys. Res.*, 71, 4505-4519, 1966.
- Celsius, A., 'Bemerkungen uber der Magnetnadel stundliche Veranderungen in ihrer Abweichung', *Svensk. Vet. Acad. Handl.*, 1740, pp. 296-299.

- Chamberlain, J. W., J. Kern and E. H. Vestine, Some consequences of local acceleration, *J. Geophys. Res.*, 65, 2535-2537, 1960.
- Chamberlain, J. W., Theory of auroral bombardment, *Astrophys. J.*, 134, 401-424, 1961.
- Chapman, S., An outline of a theory of magnetic storms, *Proc. Roy. Soc. London A*, 95, 61-83, 1918.
- Chapman, S., 'The motion of a neutral ionized stream in the earth's magnetic field', *Proc. Phil. Soc. Cambridge*, 21, 577-594, 1923.
- Chapman, S., On certain average characteristics of world-wide magnetic disturbance, *Proc. Roy. Soc. London A*, 115, 242-267, 1927.
- Chapman, S., The electric current systems of magnetic storms, *Terr. Mag.*, 40, 349-370, 1935.
- Chapman, S. and J. Bartels, *Geomagnetism*, Oxford University Press, 1940.
- Chapman, S., The equatorial electrojet as detected from the abnormal electric current distribution above Huancayo, Peru and elsewhere, *Arch. fur Met. Geophys. U. Bioklim.*, 4, 368-390, 1951.
- Chapman, S., The morphology of geomagnetic storms: An extension of the analysis of DS, the disturbance local-time in equality, *Annali di Geofisica*, 5, 481-499, 1952.
- Chapman, S., Polar and tropical aurorae, and the iso-auroral diagram, *Proc. Indian Acad. Sci.*, 37, 175-188, 1953.
- Chapman, S. and V. C. A. Ferraro, 'A new theory of magnetic storms', *Nature*, 126, 129-130 (1930); *Terr. Magn.*, 36, 77-97, 171-186 (1931); 37, 147-156 (1932).
- Chapman, S. and V. C. A. Ferraro, The geomagnetic ring current: its radial stability, *Terr. Mag.*, 46, 1-6, 1941.
- Cloutier, P. A., A comment on the neutral hydrogen flux in the solar plasma flow by S.-I. Akasofu, *Planetary Space Sci.*, 14, 809-812, 1966.
- Cole, K. D., A dynamo theory of the aurora and magnetic disturbance, *Australian J. Phys.*, 13, 484-497, 1960.
- Cole, K. D., On solar wind generation of polar magnetic disturbance, *Geophys. J. Roy. Ast. Soc.*, 6, 103-114, 1961.
- Cole, K. D., On Chamberlain's theory of auroral rays, *Astrophys. J.*, 136, 677-678, 1962.

- Cole, K. D., Damping of a magnetospheric motion by the ionosphere, *J. Geophys. Res.*, 68, 3231-3236, 1963.
- Cole, K. D., Magnetic storms and associated phenomena, *Space Sci. Rev.*, 5, 699-770, 1966.
- Coppi, B., G. Laval and R. Pellat, A model for the influence of the earth's magnetic tail on geomagnetic phenomena, *Phys. Rev. Letters*, 16, 1207, 1966.
- Cummings, W. D., Asymmetric ring currents and the low-latitude disturbance daily variation, *J. Geophys. Res.*, 71, 4495-4503, 1966.
- Cummings, W. D. and P. J. Coleman, Jr., Simultaneous magnetic field variations at the earth's surface and at the synchronous, equatorial distance, *Radio Science*, July 1968.
- Davis, T. N., The morphology of the polar aurora, *J. Geophys. Res.*, 65, 3497-3500, 1960.
- Davis, T. N., The morphology of the auroral displays of 1957-1958, 1, Statistical analysis of Alaska data, *J. Geophys. Res.*, 67, 59-74, 1962.
- Davis, T. N., The morphology of the auroral displays of 1957-1958, 2, Detailed analysis of Alaska data and analysis of high-latitude data, *J. Geophys. Res.*, 67, 75-110, 1962.
- Davis, T. N., Negative correlation between polar cap visual aurora and magnetic activity, *J. Geophys. Res.*, 68, 4447-4453, 1963.
- Davis, T. N. and R. Parthasarathy, The relationship between polar magnetic activity DP and growth of the geomagnetic ring current, *J. Geophys. Res.*, 72, 5825-5836, 1967.
- Davis, T. N. and C. Echols and Y. S. Wong, Hourly values of the auroral electrojet activity under AE for July-December 1957, UAG-R-194, *Geophys. Inst. Sci. Rept.*, 1968.
- Davis, T. N. and M. Sugiura, Auroral electrojet activity index AE and its universal time variations, *J. Geophys. Res.*, 71, 785-801, 1966.
- Davis, T. N. and Y. S. Wong, Hourly values of the auroral electrojet activity index AE for 1964, Scientific Report, UAG R-198, *Geophys. Inst., Univ. of Alaska*, 1967.
- De Mairan, *Traite physique et historique de l'aurore boreale, Suite des Mem. Acad. Roy. Sci.*, 570 pp. Paris, 1733; 2nd ed., 1754.
- Denholm, J. V., Some auroral observations inside the southern auroral zone, *J. Geophys. Res.*, 66, 2105-2111, 1961.

- Dungey, J. W., Interplanetary magnetic fields and the auroral zones, *Phys. Rev. Letters*, 6, 47-48, 1961.
- Dungey, J. W., The structure of the exosphere or adventures in velocity space, *Geophysics, The Earth's Environment*, DeWitt, Hieblot, and Lebeau, Gordon and Breach, New York, 1963.
- Dungey, J. W., The length of the magnetospheric tail, *J. Geophys. Res.*, 70, 1753, 1965.
- Fairfield, D. H. and L. J. Cahill, Jr., Transition region magnetic field and polar magnetic disturbances, *J. Geophys. Res.*, 71, 155-169, 1966.
- Fejer, J. A., The effects of energetic trapped particles on magnetospheric motions and ionospheric currents, *Can. J. Phys.*, 39, 1409-1417, 1961.
- Fejer, J. A., Theory of auroral electrojets, *J. Geophys. Res.*, 68, 2147-2158, 1963.
- Fejer, J. A., Theory of the geomagnetic daily disturbance variations, *J. Geophys. Res.*, 69, 123-138, 1964.
- Fejer, J. A., Geometry of the magnetospheric tail and auroral current systems, *J. Geophys. Res.*, 70, 4972-4975, 1965.
- Feldstein, Y. I., The aurora australis during July 1959 at the geomagnetic pole, *IUGG Monograph No. 2, Symposium on July 1959, events and associated phenomena*, pp. 126-128, 1960.
- Feldstein, Y. I., Geographical distribution of aurora and azimuth of auroral arcs, *Investigations of Aurorae, Aurorae and Airglow*, No. 4, 61-78, *Publ. House Acad. Sci., USSR, Moscow*, 1960.
- Feldstein, Y. I., Some problems concerning the morphology of auroras and magnetic disturbances at high latitudes, *Geomag. and Aeronomy*, 3, 183-192, 1963.
- Feldstein, Y. I., Auroral morphology, II. Auroral and geomagnetic disturbances, *Tellus*, 14, 258-267, 1964.
- Feldstein, Y. I., Peculiarities in the auroral distribution and magnetic disturbance distribution in high latitudes caused by the asymmetrical form of the magnetosphere, *Planet. Space Sci.*, 14, 121-130, 1966.
- Feldstein, Y. I. and E. K. Solomatina, Some problems of the geographic distribution of aurorae in the northern hemisphere. Results of IGY researches, *Aurorae and Airglow*, No. 7, Sect. IV, IGY Program, 51-59, *Publishing House Acad. Sci. USSR, Moscow*, 1961.

- Foppl, H., G. Haerendel, L. Haser, R. Lust, F. Melzner, B. Meyer, H. Neuss, H.-H. Rabben, E. Riger, J. Stocker and W. Stoffregen, Preliminary results of electric field measurements in the auroral zone, *J. Geophys. Res.*, 73, 21-26, 1968.
- Frank, L. A., On the extraterrestrial ring current during geomagnetic storms, *J. Geophys. Res.*, 72, 3753-3767, 1967.
- Fritz, H., *Das Polarlicht*, 348 pages, Leipzig, 1881.
- Fritz, H., *Verzeichnis beobachteter polarlichter*, Wien (Akademie), 1873.
- Fukushima, N., Polar magnetic storms and geomagnetic bays, *J. Fac. Sci., Tokyo Univ.*, 8, 293-412, 1953.
- Fukushima, N. and T. Oguti, Polar magnetic storms and geomagnetic bays, a theory of SD field, *Rep. Ionosphere and Space Res. Japan*, 7, 137-146, 1953.
- Fukushima, N. and H. Ono, World wide character of the progressive change in the disturbance forces of geomagnetic bays, *J. Geomag. Geoelec.*, 4, 57-62, 1952.
- Gilbert, W., *De Magnete, magneticisque corporibus, et de magno magnete tellure physiologia nova*. London, English translation by P. Fleury Mattelay, 368 pp. New York, J. Wiley and Sons, 1893- G. Hellmann, 'Zur Bibliographie von W. Gilbert's "De Magneti"', *Terr. Magn.*, 7, 63-66, 1902.
- Gosling, J. T., J. R. Asbridge, S. J. Bame, A. J. Hundhausen, and I. B. Strong, Measurements of the interplanetary solar wind during the large geomagnetic storm of April 17-18, 1965, *J. Geophys. Res.*, 72, 1813-1821, 1967.
- Graham, G., *Phil. Trans. London*, No. 383, p. 96, 1724.
- Harang, L., The mean field of disturbance of polar geomagnetic storms, *Terr. Magn. Atmos. Elect.*, 51, 353-380, 1946.
- Heppner, J. T., Time sequences and spatial relations in auroral activity during magnetic bays at College, Alaska, *J. Geophys. Res.*, 59, 329-338, 1954.
- Heppner, J. P., *Goddard Spa. Flt. Center Pub.*, X-612-66-455, 1966.
- Heppner, J. P., *High latitude magnetic disturbances, Aurora & Airglow*, ed. by McCormac, Reinhold, New York, 1967.
- Hines, C. O., Hydromagnetic motions in the magnetosphere, *Space Sci. Review*, 3, 342-379, 1964.

- Hope, E. R., Low-latitude and high-latitude geomagnetic agitation, *J. Geophys. Res.*, 66, 747-776, 1961.
- Karlson, E. T., Motion of charged particles in an inhomogenous magnetic field, *Phys. Fluids*, 5, 476-486, 1962.
- Karlson, E. T., Streaming of a plasma through a magnetic dipole field, *Phys. Fluids*, 6, 708-722, 1963.
- Kern, J. W., A charge separation mechanism for the production of polar auroras and electrojets, *J. Geophys. Res.*, 67, 2649-2666, 1962.
- Kern, J. W. and E. H. Vestine, Theory of auroral morphology, *J. Geophys. Res.*, 66, 713-724, 1961.
- Khorosheva, O. V., The diurnal drift of the closed auroral ring, *Geomag. and Aeronomy* 2, 696-705, 1962.
- Knapp, D. G., *J. Geophys. Res.*, 66, 2053, 1961.
- Krassovsky, V. I., *Aurorae, Planet. Space Sci.*, 16, 47-59, 1968.
- Lassen, K., Daytime aurorae observed at Godhavn, 1954-56, *Det Danske Met. Inst. Medd. No. 15*, Charlottenlund, 1961.
- Levy, R. H., H. E. Petschek, and G. L. Siscoe, Aerodynamic aspects of the magnetospheric flow, *A.I.A.A.J.*, 2, 2065-2076, 1964.
- Lincoln, J. V., Geomagnetic and solar data, *J. Geophys. Res.*, 71, 1477-1479, 1966.
- Lindemann, F. A., 'Note on the theory of magnetic storms', *Phil. Mag.* 38, 669-684, 1919.
- Loomis, On the geographical distribution of auroras in the northern hemisphere, *Amer. J. Sci. and Arts*, 30, 89-94, 1860.
- Maris, H. B. and E. O. Hulburt, A theory of auroras and magnetic storms, *Phys. Rev.*, 33, 412-431, 1929.
- Martyn, D. F., The theory of magnetic storms and auroras, *Nature (London)*, 167, 92-94, 1951.
- Matsushita, S. and H. Maeda, On the geomagnetic solar quiet daily variation field during the IGY, *J. Geophys. Res.*, 70, 2535-2558, 1965.
- Mawson, D., Records of the aurora polaris Australasian Antarctic expedition 1911-1914, *Sci. Rept. B.*, 2, 1925.
- Mayaud, P.-N., *Terre Adelie 1951-1952, fasc. II, Expeditions polaires francaises, Resultats scientifiques IV*, 2, Paris, 1955.



- Mayaud, P.-N., Principes d'une discrimination entre Sq et SD sur les enregistrements individuels; et description d'un type special de perturbation magnetique, les oscillations lentes, *Ann de Geophys.*, 21, 121-142, 1965.
- Mead, G. D., Deformation of the geomagnetic field by the solar wind, *J. Geophys. Res.*, 68, 1181-1195, 1946.
- Meng, C.-I., Polar magnetic and auroral substorms M. Sc. Thesis, Geophys. Inst. Univ. of Alaska, 1965.
- Moos, N. A. F., Colaba Magnetic Data, 1846 to 1905, 782 pages, Bombay, 1910.
- Nagata, T. and S. Kokubun, Polar magnetic storms, with special reference to relation between geomagnetic disturbances, *Rep. Ionosph. Res. Japan*, 14, 273-290, 1960.
- Nikolsky, A. P., Dual laws of the course of magnetic disturbances and the nature of mean regular variations, *Terr. Magn. Atmos. Elec.*, 52, 147-173, 1947.
- Obayashi, T. and J. A. Jacobs, Sudden commencements of magnetic storms and atmospheric dynamo action, *J. Geophys. Res.*, 62, 589-616, 1957.
- Parker, E. N., Nonsymmetric inflation of a magnetic dipole, *J. Geophys. Res.*, 71, 4485-4494, 1966.
- Petschek, H. E., Magnetic field annihilation, AAS-NASA Symposium on the Physics of Solar Flares, NASA SP-50.
- Piddington, J. J., Geomagnetic storm theory, *J. Geophys. Res.*, 65, 93-106, 1960.
- Piddington, J. H., A hydromagnetic theory of geomagnetic storms, *Geophys. J.*, 7, 183-193, 1962a.
- Piddington, J. H., A hydromagnetic theory of geomagnetic storms and auroras, *Planet. Space Sci.*, 9, 947-960, 1962b.
- Piddington, J. H., Connections between geomagnetic and auroral activity and trapped ions, *Planet. Space Sci.*, 11, 451-462, 1963.
- Piddington, J. H., Geomagnetic storms, auroras and associated effects, *Space Sci. Rev.*, 3, 724-780, 1964.
- Piddington, J. H., A theory of auroras and the ring current, *J. of Atmosph. and Terr. Phys.*, 29, 87-105, 1967.
- Rikitake, T., *Rep. Ionosph. Res. Japan*, 2, 57, 1948.

- Rostoker, G., Midlatitude transition bays and their relation to the spatial movement of overhead current systems, *J. Geophys. Res.*, 71, #1, 79-95, 1966.
- Sabine, E., On periodical laws discoverable in the mean effects of the larger magnetic disturbances, *Phil. Trans. London*, 1851, pp. 123-139, 1852, pp. 103-124.
- Scruse, F. J., The electric current associated with polar magnetic substorms, *J. of Atmos. and Terr. Physics*, 20, 567-579, 1967.
- Shaw, J. E., Outline of a theory of magnetic separation of auroral particles and the origin of the SD field, *Planet. Space Sci.*, 2, 49-55, 1959.
- Silsbee, H. C. and E. H. Vestine, Geomagnetic bays, their frequency and current systems, *Terr. Mag.*, 47, 195-208, 1942.
- Singer, S. F., A new model of magnetic storms and aurorae, *Trans. Amer. Geophys. Un.*, 38, 175-190, 1957.
- Speiser, T. W. and N. F. Ness, The neutral sheet in the geomagnetic tail: its motion, equivalent currents, and field line connection through it, *J. Geophys. Res.*, 72, 131-141, 1967.
- Stagg, J. M., The diurnal variation of magnetic disturbance in the high latitudes, *Proc. Royal Soc., London*, A-149 (807), 298-311, 1935.
- Stormer, C., Sur les trajectoires des corpuscles electrises dans l'espace sous l'action du magnetisme terrestre avec application aux aurores boreales, *Arch. Sci. Phys. Nat. Geneve*, 117-123, 32, 1911, 51-69, 33, 1912.
- Stormer, C., *The Polar Auroras*, Oxford Univ. Press, 1955.
- Stringer, R. W., M.S. Thesis, *Geophys. Inst., University of Alaska*, 1966.
- Stringer, W. J., A. E. Belon and S.-I. Akasofu, The latitude of auroral activity during periods of zero and very weak magnetic disturbance, *J. Atmosph. Terr. Phys.*, 27, 1039-1044, 1965.
- Sugiura, M., The solar diurnal variation in the amplitude of sudden commencements of magnetic storms at the geomagnetic equator, *J. Geophys. Res.*, 58, 558-559, 1953.
- Sugiura, M., *Annals of the IGY*, 35, Part 1, pp. 1-45, 1963.
- Sugiura, M. and S. Chapman, The average morphology of geomagnetic storms with sudden commencement, *Abh. d. Akad. d. Wiss. Gottingen, Math-Phys., Klasse*, 1960.
- Swift, D. W., The generation and effect of electrostatic fields during an auroral disturbance, *J. Geophys. Res.*, 68, 2131-2140, 1963.

- Swift, D. W., The possible relationship between the auroral breakup and the interchange instability of the ring current, *Planet. Space Sci.*, 15, 1225-1237, 1967.
- Swift, D. W., Possible consequences of the asymmetric development of the ring current belt., *Planet. Space Sci.*, 15, 835-862, 1967.
- Swift, D. W., Possible consequences of Akasofu's neutral hydrogen hypothesis 73, 1847-1850, 1968.
- Swift, D. W., Possible consequences of the asymmetric development of the ring current belt, II. Effect of variations in ionospheric conductivity, *Planet. Space Sci.*, (in press) 1968.
- Ulwick, J. C., W. Pfister, O. C. Haycock and K. D. Baker, Rocket measurements with electron and ion probes in an aurora, *Space Research V*, 293-311, 1965.
- Vestine, E. H., Disturbance field of magnetic storms, *Trans. Wash. Assem.* 1939, Publ. IATME Bull. No. 11, 360, 1940.
- Vestine, E. H., The geographic incidence of aurora and magnetic disturbance, northern hemisphere, *Terr. Magn.*, 49, 77-102, 1944.
- Wescott, E. M., Magnetic variations at conjugate points, *J. Geophys. Res.*, 66, #6, 1789-1792, 1961.
- Wescott, E. M., Magneto conjugate phenomena, *Space Sci. Rev.*, 4, June Issue, 507-561, 1966.
- Wescott, E. M. and K. B. Mather, Magnetic conjugacy from L = 6 to L = 1.4, I. Auroral zone, *J. Geophys. Res.*, 70, 29-42, 1965a.
- Wescott, E. M. and K. B. Mather, Magnetic conjugacy from L = 6 to L = 1.4, II. Midlatitude conjugacy, *J. Geophys. Res.*, 70, 43-47, 1965b.
- Wescott, E. M. and K. B. Mather, Magnetic conjugacy from L = 6 to L = 1.4, III. Low latitude conjugacy, *J. Geophys. Res.*, 70, 49-51, 1965c.
- Wescott, E. M. and K. B. Mather, Magnetic conjugacy at very high latitude, Shepherd Bay-Scott Base relationship, *Planet. Space Sci.*, 13, April Issue, 303-324, 1965d.
- Wilcke, J. C., 'Von den gahrlichen und taglichen Bewegungen der Magnetnadel in Stockholm', *Svensk. Vet. Acad. Handl.*, 1777, pp. 273-300.
- Yoshida, S., The new classification of geomagnetic storms and their source flares, Scientific Report, UAG-R167, *Geophys. Inst.*, University of Alaska, 1965.
- Zelwer, R., P. C. B. Fernando, and S. H. Ward, Interplanetary magnetic field data and corresponding geomagnetic effects for the storm of October 7, 1962, *J. Geophys. Res.*, 72, 3471-3482, 1967.
- Zmuda, A. J., J. H. Martin and F. T. Heuring, Transverse magnetic disturbances at 1100 kilometers in the auroral region, *J. Geophys. Res.*, 71, 5033, 1966.